

Exploring the vinylogous conjugate-addition and radical reactions of *para*-quinone methides

Sonam Sharma

A thesis submitted for the partial fulfillment of

the degree of Doctor of Philosophy



Department of Chemical Sciences

Indian Institute of Science Education and Research (IISER) Mohali

Knowledge City, Sector 81, , S. A. S. Nagar, Manauli PO, Mohali, 140306 Punjab, India.

May 2023

Dedicated

To

My beloved parents

Declaration

The work presented in this thesis has been carried out by me under the guidance of **Prof. R. Vijaya Anand** at the Indian Institute of Science Education and Research Mohali.

This work has not been submitted in part or in full for a degree, diploma, or fellowship to any other university or institute. Whenever contributions of others are involved, every effort is made to indicate this clearly with due acknowledgment of collaborative research and discussions. This thesis is a bonafide record of original work done by me, and all sources listed within have been detailed in the bibliography.

Sonam Sharma

In my capacity as the supervisor of the candidate's thesis work, I certify that the above statements by the candidate are true to the best of my knowledge.

Prof. R. Vijaya Anand

Acknowledgment

It gives me great pleasure to convey my sincere gratitude to everyone who has contributed in some manner to making this journey successful and unforgettable.

I want to start by expressing my sincere gratitude to my supervisor, Professor R Vijaya Anand, for his superb direction, tremendous support, and insightful recommendations in order to successfully complete this work effort. He helped me with a lot of support, both personally and professionally. He gave me so much freedom to explore own ideas so, that I can think in a better way and I learnt many things from our cordial conversations. I will always be grateful of his insight, expertise, and genuine concern. His ability to think critically and logically, his never-say-impossible attitude, and his disciplined behaviour have all helped to my development both personally and professionally. The joy and enthusiasm he has for his research was a source of constant motivation for me, even during the tough times during this work.

I would like to thank my committee members, Prof. S. Arulananda Babu and Dr. Sripada S. V. Ramasastry, for their fruitful discussions and valuable suggestions and for evaluating my research improvement yearly by spending their valuable time. I am fortunate to have attended their highly beneficial courses during my study.

I wish to thank our former Director, Prof. N. Sathyamurthy, Prof. Debi P. Sarkar, and current Director, Prof. J. Gowrishankar, for providing world-class infrastructure and facilities. I would like to thank our former Head of Department (HOD), Prof. K. S. Viswanathan, Dr. S. Arulananda Babu, and current Head of Department (HOD), Dr. Sanjay Singh, for their valuable suggestions and for providing the facilities at the department of chemical sciences. I am also thankful to IISER Mohali for NMR, HRMS, IR, departmental X-Ray facilities, and other facilities.

I gratefully thank all the faculty members of the Department of Chemical Sciences for allowing me to use the departmental facilities.

Furthermore, I would like to express my heart full thanks to my brilliant labmates, Dr. Mahesh Sriram, Dr. Abhijeet Sahebrao Jadhav, Dr. Prithwish Goswami, Dr. Dilip Kumar, Dr. Priya Ghosh, Dr. Akshi Tyagi, Dr. Gurdeep Singh, Ms. Guddi Kant, Feroz Ahmad, Yogesh Pankhade, Pavit Kumar, Rekha, Rajat Pandey, Shaheen Fatma, Akshay, Shruthi, Arun, Athira, Rupali, Piyush Saini, Munnu Kumar for their valuable discussions, cooperation and for creating a healthy environment around me. I am grateful to Dr. Prithwish Goswami, Dr. Gurdeep Singh,

for their help and assistance during the projects. I am also obliged to Dr. Atanu Mondal, Dr. Sandeep Kumar Thakur, and Chandrakala Negi for their help in solving the crystal structure. I am very thankful to Dr. Gurdeep Singh for their generous support in correcting my thesis. I also acknowledge all the summer trainees who worked for a short time in our lab.

I am also thankful to Mr. Balbir and Mr. Triveni for their help. I would like to thank the chemistry teaching lab assistants for their cooperation during my research. I am also thankful to all my IISERM friends for their timely help.

I cannot complete my acknowledgment without thanking all my friends. So, I am pleased to acknowledge Lona Dutta, Chandrakala Negi, Dr. Gurdeep Singh, Pooja, Rekha, Nisha, Shruti, Dr Atanu Mondal, Rajat Pandey, Dr. Sandeep Kumar Thakur, Prateek, Himanshu, Prashant Kumar, and Suresh Kumar. They stood with me during tough times and shared my sorrow and joy on many occasions. I am fortunate to have these friends in my life. I am also grateful to all my teachers from the bottom of my heart for their guidance and inspiration

I must also acknowledge the IISER Mohali for fellowship during my doctoral study. I would also like to thank the Department of Science and Technology (DST), India, and IISER Mohali for funding and allowing me to complete my Ph.D.

Last but most significant, it gives me immense pleasure to express my gratitude to my beloved **parents** (Naresh Kumar Sharma and Kamlesh Sharma), **sister** (Shailja Sharma) and **brother** (Ankush Sharma). They have always believed in me and supported me with unconditional love.

Abstract

The research work performed in this thesis is based on the synthesis of oxygen, sulfur, and nitrogen-containing heterocycles from *para*-quinone methides under metal-free conditions. It also includes the C-C reductive dimerization *para*-quinone methides. The thesis is divided into four chapters. Chapter 1 describes the general introduction to *para*-quinone methides and the reactivity profile of structurally modified *para*-quinone methides. Chapter 2 describes an acid-mediated synthesis of 4H-chromen-4-ones from *para*-quinone methides and 2-hydroxyphenyl-substituted enaminones. Chapter 3 deals with the one-pot synthesis of xanthene, thioxanthene, and 10H-indolo[1,2-*a*]indole-based heterocycles using functionalized *para*-quinone methides. Chapter 4 deals with the SmI₂-catalyzed reductive dimerization of *para*-quinone methides.

Chapter 1: General introduction to *para*-quinone methides chemistry

In this chapter, a brief introduction on the reactions of *para*-quinone methides and structurally modified *para*-quinone methides leading to various classes of heterocycles, carbocycles and diaryl-/triarylmethanes has been included.

Chapter 2: Synthesis of 4H-chromen-4-one derivatives through an acid-mediated reaction of enaminones with *para*-quinone methides

This chapter describes the synthesis of 3-substituted chromone-based heterocycles from *para*-quinone methides under acidic conditions. 4H-chromen-4-one is a privileged class of oxygen-containing heterocycles, as many of their natural and unnatural derivatives are known

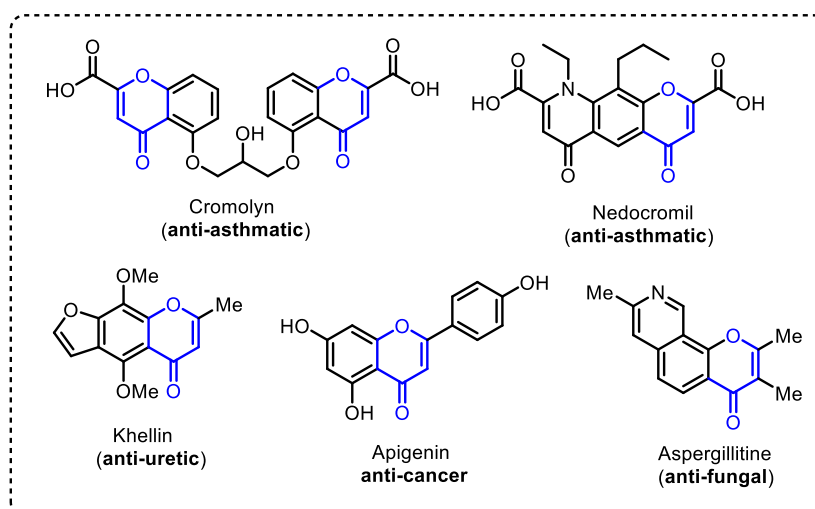
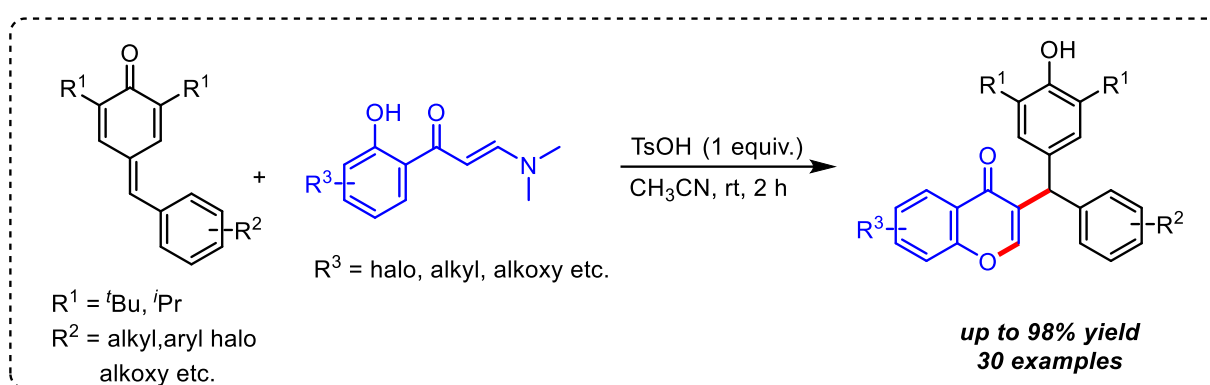


Figure 1. Chromenone-based biologically active molecules and natural products

to have pharmacological activities. Some of the 4H-chromen-4-ones with remarkable biological activities are shown in Figure 1. In recent years, significant developments in the synthetic elaborations of *para*-quinone methides to access heterocycles have been documented in the literature. While exploring the synthetic applications of *para*-quinone methides to the synthesis of oxygen-containing heterocycles, we have developed an unprecedented protocol to access chromone derivatives through a 1,6-conjugate addition of 2-hydroxyphenyl-substituted *N,N*-dimethyl enaminones to *para*-quinone methides followed by intramolecular cyclization (Scheme 1).



Scheme 1. Synthesis of chromone derivatives from *para*-quinone methides and enaminones

Chapter 3. TfOH-mediated one-pot approach to the synthesis of O-, S-, and N-based heterocycles from 2-hetero-atom functionalized *para*-quinone methides

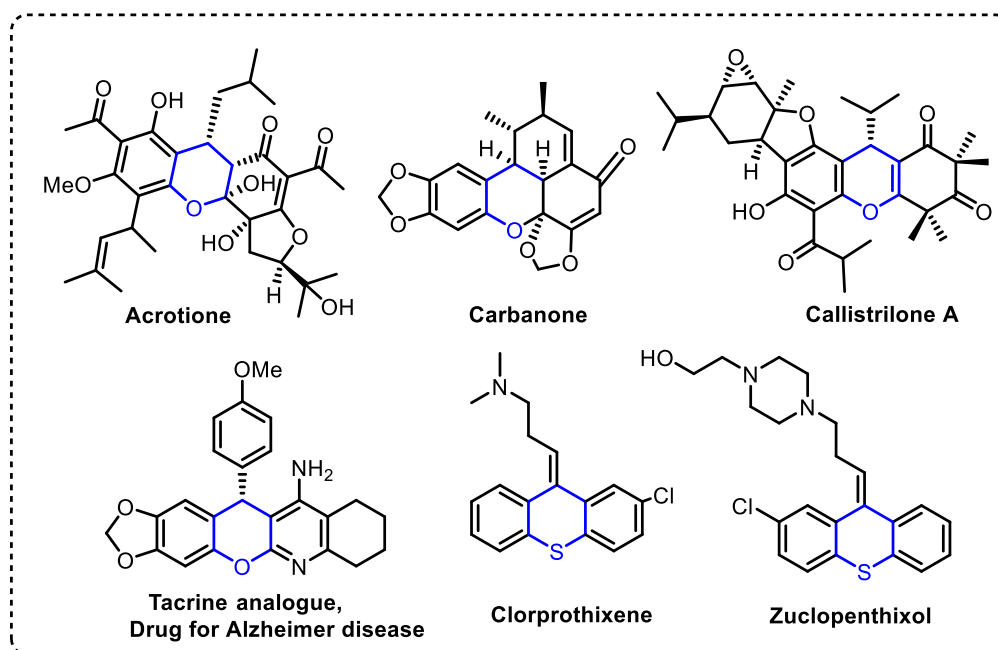
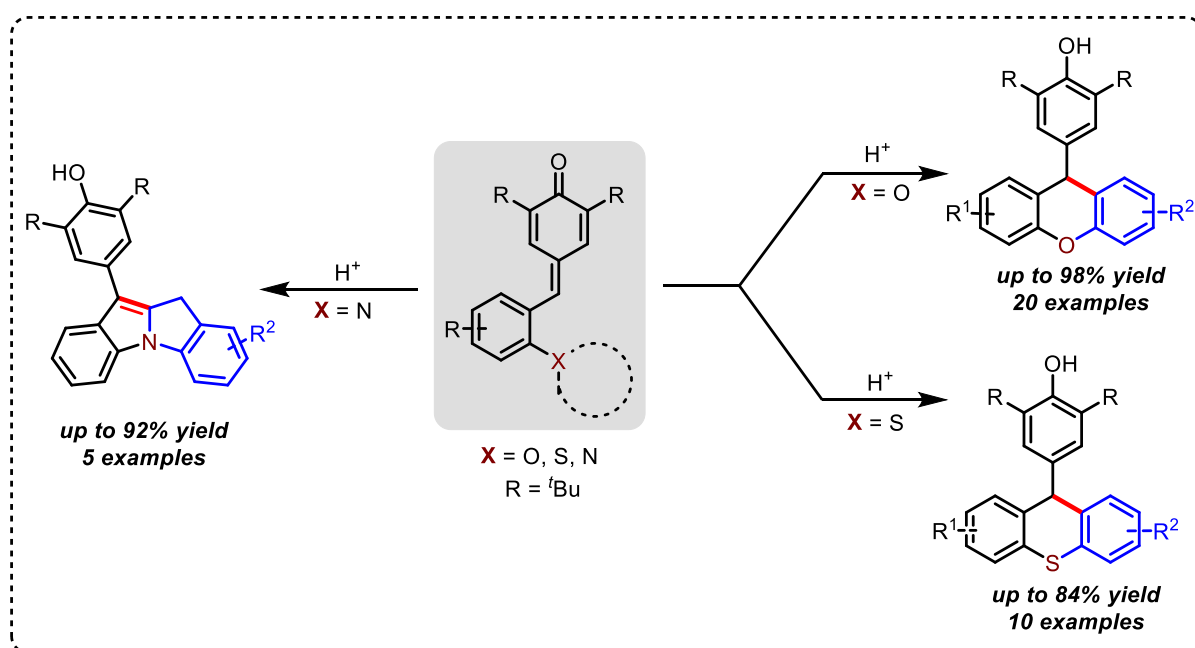


Figure 2. Biologically active xanthene and thioxanthene derivatives

In this chapter, we have described the synthesis of xanthene and thioxanthene-based heterocycles from 2-hetero-aryl-substituted *para* quinone methides under acidic conditions. Both xanthene and thioxanthenes are hetero-annulated aromatic condensed ring systems. These privileged scaffolds are known to have great pharmacological activities such as anticancer, antitumor, antioxidant, antifungal, etc. (Figure 2). In addition, xanthene derivatives are widely used as dyes and fluorescent materials. Because of their wide spread applications of xanthene derivatives in the area of medicinal and materials chemistry, various synthetic approaches have been developed for their syntheses.



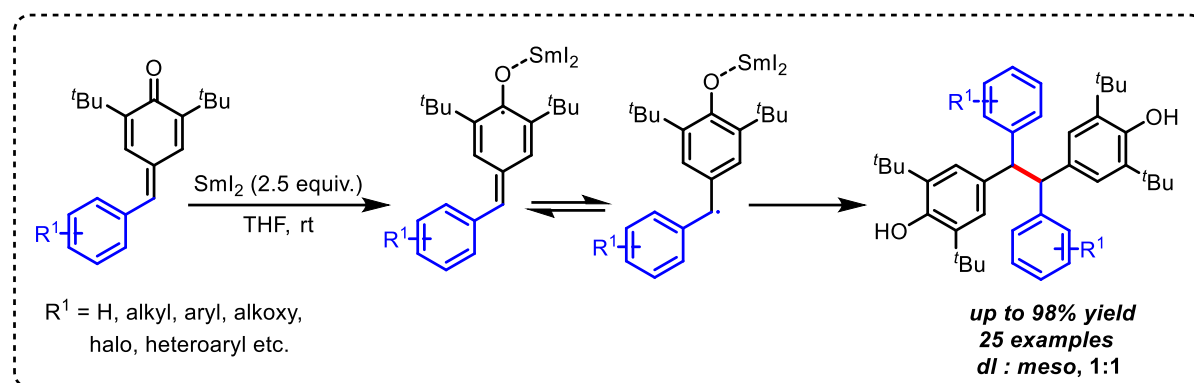
Scheme 2. Synthesis of xanthene, thioxanthene and 10H-indolo[1,2-*a*]indole derivatives

While exploring the synthesis of various heterocycles using *para*-quinone methides, we have developed a one-pot approach for the synthesis of xanthene and thioxanthene derivatives through an acid-mediated intramolecular Friedel-Crafts reaction of functionalized *para*-quinone methides (Scheme 2). This protocol was also found to be suitable for the synthesis of 10H-indolo[1,2-*a*]indole derivatives.

Chapter 4. SmI₂-mediated reductive coupling of *para*-quinone methides

Electron transfer reactions play a pivotal role in organic chemistry as well as in biological processes. This chapter deals with a SmI₂-mediated reductive dimerization of *para*-quinone methides leading to 1,1,2,2-tetraaryl ethane derivatives. The reaction proceeds through SmI₂-mediated single electron transfer to *p*-QM leading to diarylmethyl radical, which subsequently undergoes self-dimerization to produce 1,1,2,2-tetraaryl ethane derivatives.

Under optimal conditions, many substituted *p*-QMs underwent smooth conversion to the respective tetraarythane derivatives in moderate to good yields.



Scheme 3. Reductive dimerization of *para*-quinone methides

Abbreviations

ACN	Acetonitrile
AcOH	Acetic acid
Ac ₂ O	Acetic anhydride
Aq	Aqueous
B ₂ (pin) ₂	Bis(pinacolato)diboron
brs	Broad singlet
Bn	Benzyl
BPO	Benzoyl Peroxide
BQ	1,4-Benzoquinone
CHCl ₃	Chloroform
CCl ₄	Carbon tetrachloride
CSA	Camphorsulfonic acid
clcd	Calculated
Cy	Cyclohexyl
CO	Carbon monoxide
CsOAc	Caesium acetate
Cs ₂ CO ₃	Cesium carbonate
cm	Centimetre
δ	Chemical shift
CDCl ₃	Chloroform-D
<i>J</i>	Coupling constant
DCE	Dichloroethane
DCM	Dichloromethane
Et ₂ O	Diethyl ether
°C	Degree celsius
dr	Diastereomeric ratio
DMA	Dimethylacetamide
DMAP	4-Dimethylaminopyridine
DME	Dimethoxyethane
DMSO	Dimethyl sulfoxide
DBU	1,8-Diazabicyclo[5.4.0]undec-7-ene
DBN	1,5-Diazabicyclo[4.3.0]non-5-ene

d	Doublet
dd	Doublet of doublet
ddd	Doublet of doublet of doublet
dt	Doublet of triplets
EWG	Electron withdrawing
ESI	Electrospray ionization
<i>ee</i>	Enantiomeric excess
<i>er</i>	Enantiomeric ratio
EtOH	Ethanol
EtOAc	Ethylacetate
equiv	Equivalents
FT-IR	Fourier transform infrared spectroscopy
Hz	Hertz
HRMS	High-resolution Mass Spectrum
HPLC	High Performance Liquid Chromatography
h	Hour(s)
<i>i</i> -Pr	<i>iso</i> -Propyl
LED	Light-emitting diode
LHMDS	Lithium bis(trimethylsilyl)amide
LDA	Lithium diisopropylamide
^t BuOLi	Lithium- <i>tert</i> -butoxide
<i>m/z</i>	Mass/Charge
MHz	Megahertz
m.p.	Melting point
Mes	Mesityl
MeOH	Methanol
Mg	Milligram(s)
ml	Milliliter(s)
mmol	Millimole(s)
min	Minute(s)
μL	Microliter (s)
M.S.	Molecular sieves
m	Multiplet
DMF	<i>N,N'</i> -Dimethyl formamide

NHC	<i>N</i> -heterocyclic carbene
NMO	<i>N</i> -Methylmorpholine- <i>N</i> -oxide
NMR	Nuclear Magnetic Resonance
<i>n</i> -Pr	Propyl
^t BuOK	Potassium- <i>tert</i> -butoxide
POCl ₃	Phosphoryl chloride
<i>P</i> -TSA	<i>p</i> -Toluene sulfonic acid
q	Quartet
R _f	Retention factor
rt	Room temperature
sept	Septet
s	Singlet
NaH	Sodium hydride
^t Bu	<i>tert</i> -Butyl
<i>tert</i>	Tertiary
Boc	<i>tert</i> -Butyloxycarbonyl
TBAB	Tetrabutylammonium bromide
TPAP	Tetrapropylammonium perruthenate
THF	Tetrahydrofuran
TMS	Tetramethylsilane
TBS	<i>tert</i> -Butyldimethylsilane
TFA	Trifluoroacetic acid
TFE	2,2,2-Trifluoroethanol
t	Triplet
td	Triplet of doublets
tt	Triplet of triplet
UV	Ultraviolet
Vis	Visible

Contents

Declaration	i
Acknowledgements	ii
Abstract	iv
Abbreviations	viii

The thesis work is divided into **four** chapters

Chapter 1: General introduction to para-quinone methides chemistry and reactivity profile of structurally modified para-quinone methides

1.1 Introduction	3
1.2 Literature reports on the synthesis of oxygen-containing heterocycles	8
1.3 Literature reports on the synthesis of nitrogen-containing heterocycles	13
1.4 Literature reports on the synthesis of carbocycles	16
1.5 Literature reports on radical reactions of <i>p</i> -QMs	18
1.6 References	20

Chapter 2: Reaction of 2-hydroxy phenyl substituted N, N-dimethyl enamines with p-quinone methides: Access to chromone derivatives

2.1 Introduction	24
2.2 Literature reports on the synthesis synthesis of chromone derivatives	25
2.3 Literature reports on enaminone for the synthesis of 4H-chromenone	30
2.4 Background	35
2.5 Result and discussion	36
2.6 Conclusion	40
2.7 Experimental Section	40
2.8 References	60

<i>Chapter 3: TfOH acid-mediated one-pot synthesis of O, S, and N-based heterocycles from 2-hetero atom functionalized para-quinone methides</i>	
3.1 Introduction	62
3.2 Literature reports on the synthesis of 9H-xanthene and 9H-thioxanthene derivatives	63
3.3 Background	70
3.4 Results and Discussions	71
3.5 Conclusion	78
3.6 Experimental Section	78
3.7 References	115
4 Chapter 4: SmI₂-mediated reductive coupling of para-quinone methides	
4.1 Introduction	118
4.2 Literature reports on SmI ₂ -mediated transformations	119
4.3 Background	122
4.4 Results and Discussions	124
4.5 Control Experiment	127
4.6 Conclusion	128
4.7 Experimental Section	128
4.8 References	145
Curriculum Vitae	147

1. General introduction to the synthesis of different classes of heterocycles from *para*-quinone methides.

1.1 Introduction

Quinone methides (QMs) are a significant class of synthetically active substances that function as intermediates in many biological and chemical processes.¹ They were found naturally, and isolated from wood, insect pigments and fungal metabolites. *p*-QMs, structurally similar to *p*-benzoquinone and *p*-quino-dimethanes, are identified as intermediates in the production of Elansolid biosynthesis, metabolites from gliding bacterium *Chitinophaga Sancti*.^{2,3} This class of organic compounds consists of cyclohexadiene moiety having a carbonyl and an exocyclic methyldene unit. The carbonyl and methyldene moiety can be positioned in 1,2 and 1,4 fashion leading to *ortho*-quinone methides and *para*-quinone methides, respectively.⁴ This unique structural assembly changes the reactivity of quinone methide, which leads to a polarization of the molecule, owing to resonance between neutral and zwitterionic intermediates (Figure 1).^{5,6}

Interestingly, this resonance stabilization makes the *p*-QM interact with various nucleophiles to reach a more stable aromatic neutral state. Aromatization of the cyclohexadiene ring is the driving force for the unique reactivity of *p*-QMs. This phenomenon makes the nucleophilic attack at the benzylic carbon with high regioselectivity.

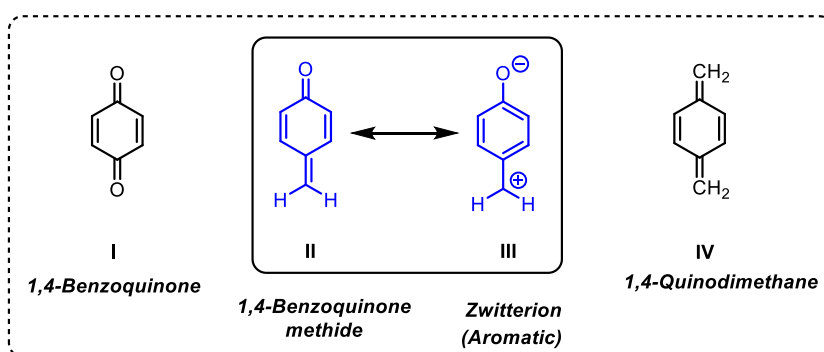


Figure 1. Zwitterionic form of *para*-quinone methide

Though unsubstituted *p*-QMs are considered unstable intermediates and can be stabilized by introducing bulky alkyl or aryl substituents at C-2 and C-6 positions. The presence of bulky substituents not only increases the stability but also hinders the attack of nucleophiles

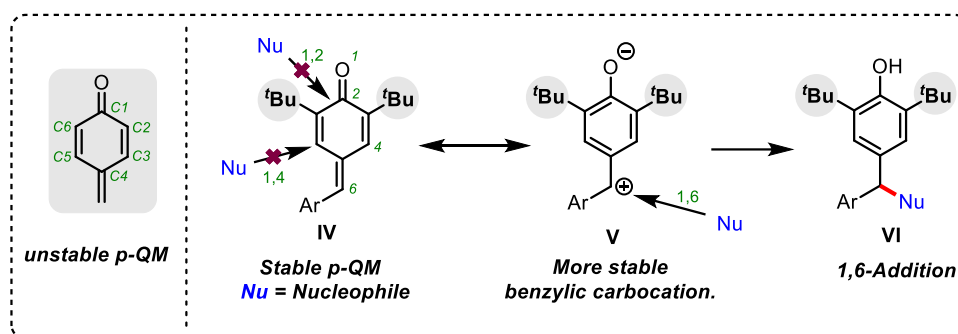


Figure 2. Reactivity of *p*-QM

at the C-1 and C-2 positions and directs the nucleophile to attack at the exocyclic methylene part. Therefore, *p*-QMs are recognized as important synthetic precursors for regiospecific 1,6-conjugate addition reactions to access structurally diverse diaryl- and triaryl methane derivatives (Figure 2).

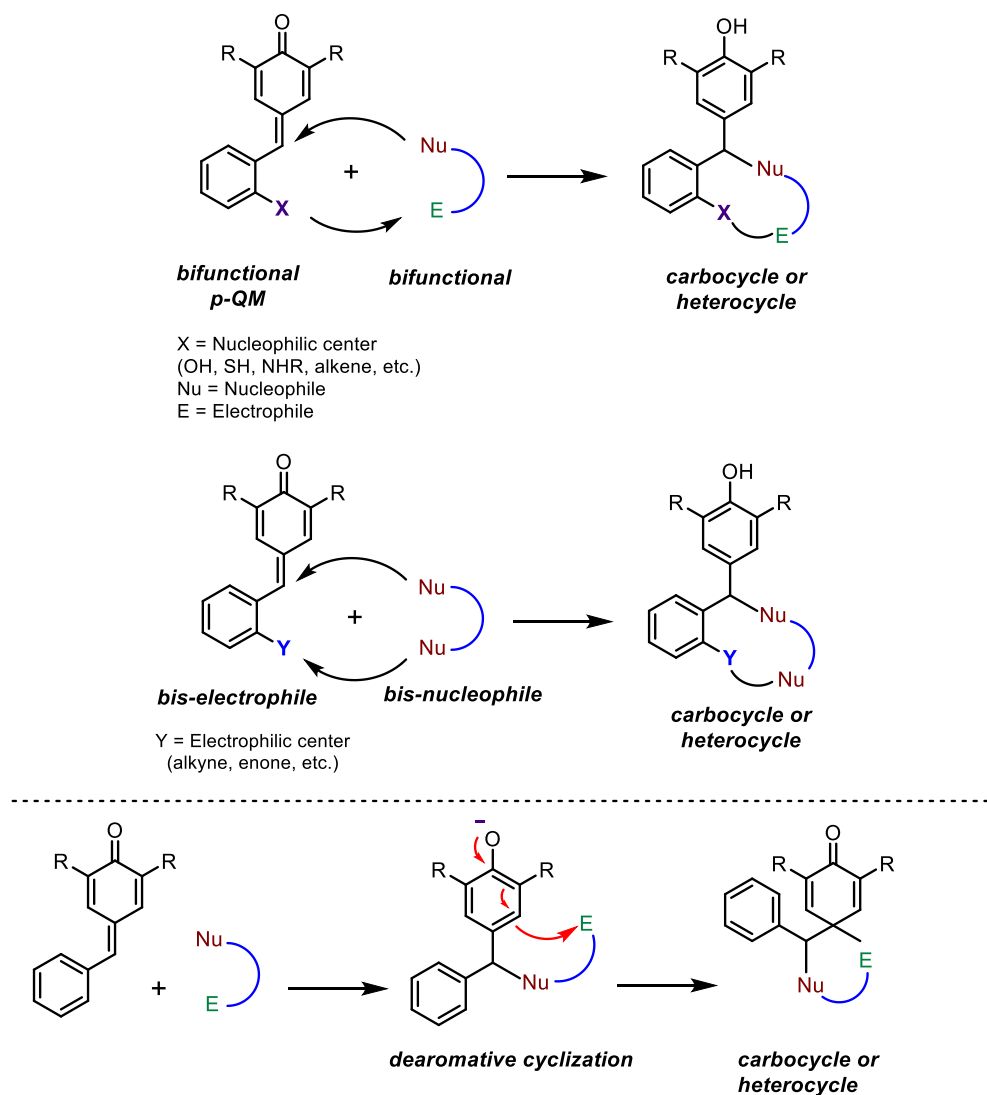
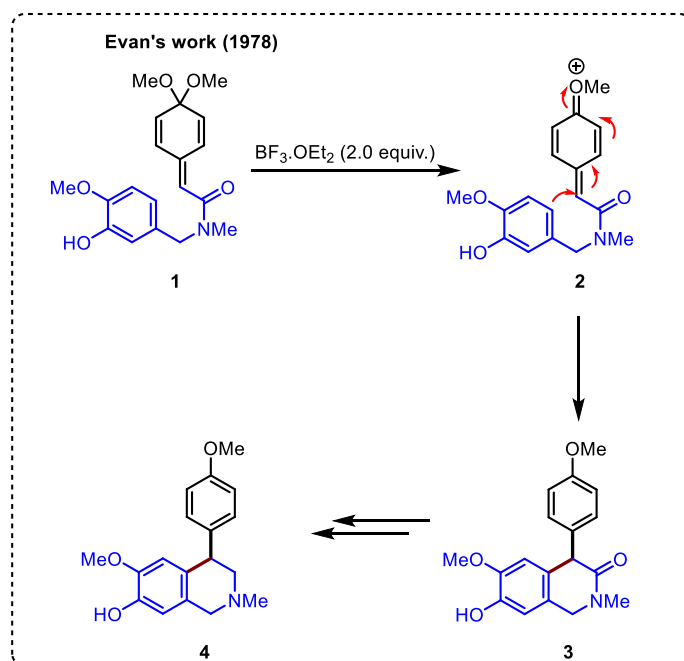


Figure 3. Proposed strategies for the synthesis of carbocycles/heterocycles from *p*QM

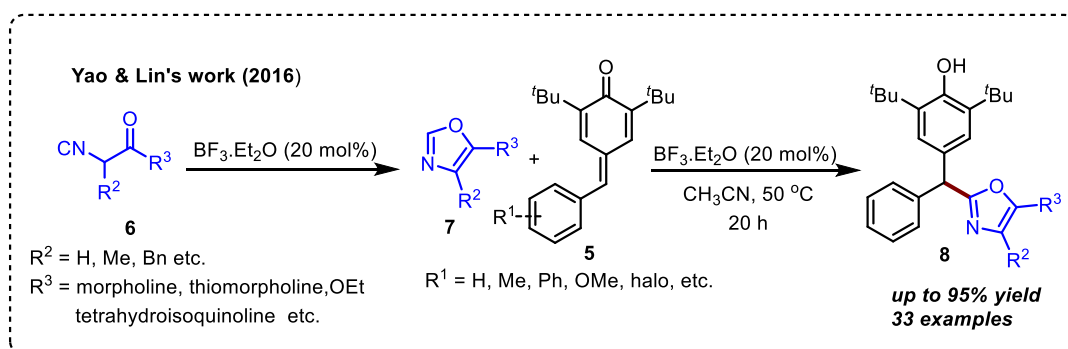
Despite their intrinsic instability, chemists worldwide have paid much attention to preparing *p*-QMs and have used them as synthons in many organic transformations.⁷ Very recently, chemists have tried to tune the reactivity of *p*-QM so that it can act as a bifunctional molecule. In this regard, some structural modifications in the basic skeleton of *p*-QM have been done so that it can be used as a valuable synthon for constructing fused heterocycles, carbocycles, etc. Moreover, simple aryl-substituted *p*-QM with bifunctional molecules undergo dearomative cyclization to afford *spiro*-carbocycles/heterocycles. So far, many reports have appeared in the literature for the construction of fused carbocycles/heterocycles by following this reaction pathway (Figure 3).

In 1978, Evan and co-workers reported the synthesis of (\pm)-Cherylline (**4**) by utilizing *p*-QM as an intermediate. This reaction proceeds through a Lewis acid-mediated intramolecular cyclization of *p*-QM **1** (Scheme 1).⁸



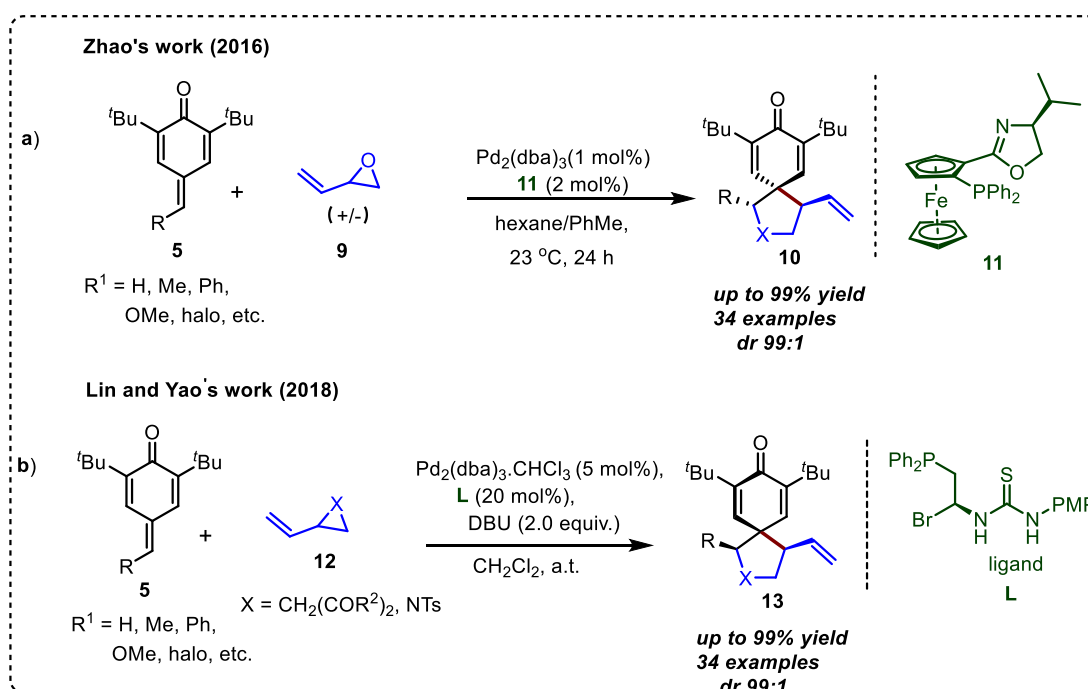
Scheme 1. Evans's approach for the synthesis of (\pm)-Cherylline (**4**) by using *p*-QM

Later in 2016, Yao and Lin's group disclosed a $\text{BF}_3 \cdot \text{Et}_2\text{O}$ -catalyzed methodology for the 1,6-arylation of *p*-QMs **5** using α -cyanoacetamides **6** as a nucleophilic source (Scheme 2).⁹ According to the proposed reaction mechanism, the transformation of α -cyanoacetamides **6** to oxazole **7** is favored by the catalyst followed by 1,6-addition to *p*-QMs to produce the expected product **8**. The reported approach enabled the first-ever easy synthesis of a variety of unsymmetrical triarylmethanes having oxazole and phenol groups in moderate to good yields (46-95%) under mild reaction conditions.⁹



Scheme 2. Synthesis of unsymmetrical triarylmethanes

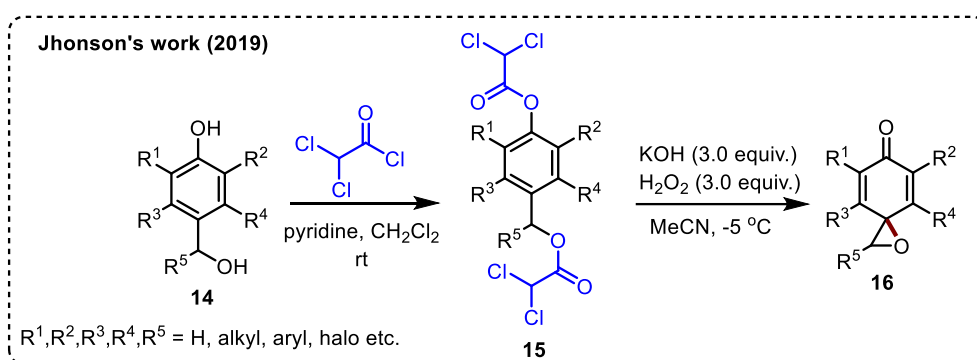
Zhao and co-workers demonstrated a Pd-catalyzed enantioselective formal [3+2] cycloaddition reaction between *para*-quinone methides **5** and vinyl epoxides **9**, to access a wide range of chiral *spiro*-cyclic tetrahydrofuran derivatives **10**. According to the proposed reaction mechanism, initially, ring opening of epoxide takes place followed by chiral Pd-catalyzed enantioselective formal [3+2]-cycloaddition between the coupling reactants to afford the product **10** (a, Scheme 3).¹⁰



Scheme 3. Five-membered spirocyclic tetrahydrofuran derivatives

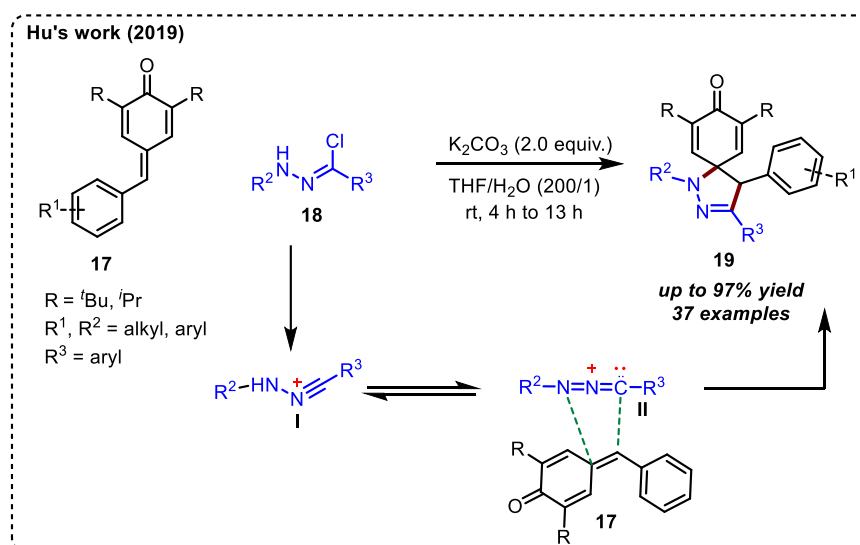
Lin, Yao, and co-workers, in 2018, developed a novel [3+2]-annulation approach involving *p*-QMs (**5**) and vinyl cyclopropanes (**12**). This transformation provides *spiro*-[4.5]-deca-6,9-diene-8-ones (**13**) in high yield with good diastereoselectivity using palladium and phosphine-thiourea co-operative catalysis. A mechanistic study reveals that palladium and

phosphine-thiourea (**L**) activate both *p*-QM and vinyl cyclopropane simultaneously (**b**, Scheme 3).¹¹ Recently, the Johnson group disclosed the synthesis of *para*-spiro-epoxydienones *via* in situ generated *p*-QM through phenolic oxidation in the presence of H₂O₂. They have prepared a series of 4-(hydroxymethyl) phenols **14** and treated them with 2,2-dichloroacetyl chloride using pyridine as a base to form their respective bis(dichloroacetate) derivatives **15** in high yields. Bis(dichloroacetate) derivatives **15**, under the optimized basic reaction conditions, generate *para*-quinone methide followed by oxidation with H₂O₂ to furnish the corresponding *para*-spiro-epoxy-dienones **16** (Scheme 4).¹²



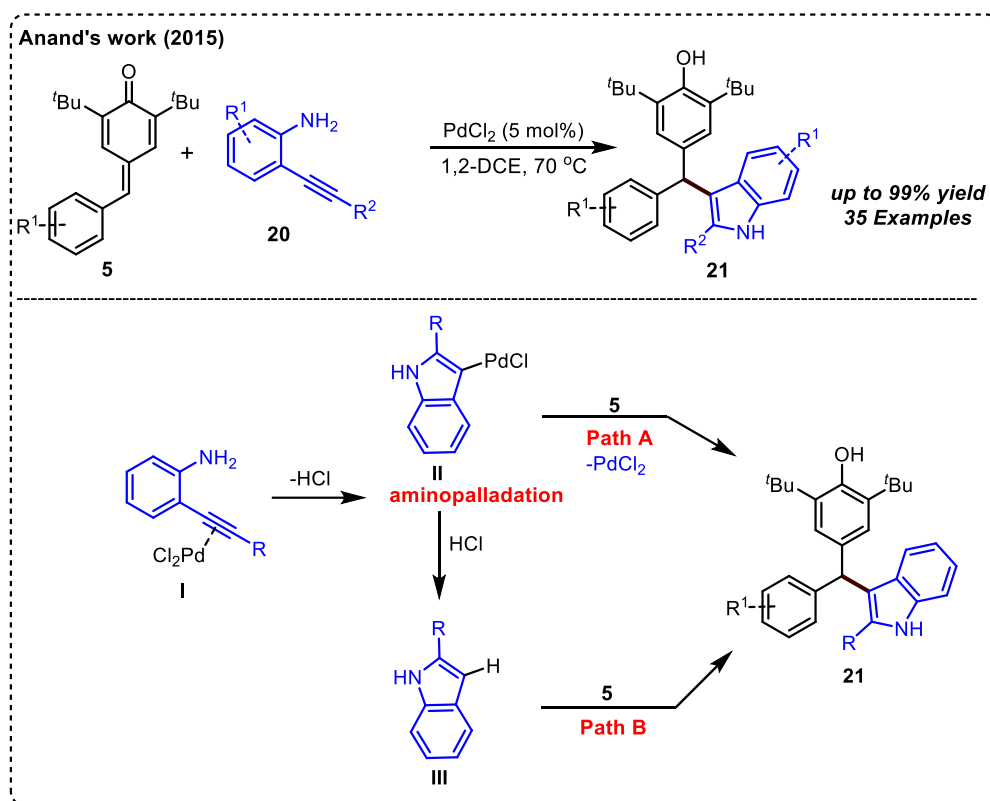
Scheme 4. Synthesis of *spiro*-epoxy-dienones.

In the same year, Hu's group described a [3+2]-cycloaddition between nitrile imine and *para*-quinone methide **17** for the synthesis of *spiro*-pyrazoline-cyclohexadienones **19**. The reaction proceeds through the dehydrochlorination of hydrazonoyl chloride **18** to form nitrile imine in the presence of K₂CO₃. The nitrile imine can exist in two resonating forms, **I** and **II**,



Scheme 5. Approach towards *spiro*-pyrazoline-cyclohexadienones derivatives

out of which **II** reacts with *p*-QM **17** to furnish the desired product **19**. A variety of *p*-QMs responded efficiently with **18** under the standard reaction conditions to afford their respective *spiro*-pyrazoline-cyclohexadienone derivatives **19** in excellent yields. (Scheme 5).¹³



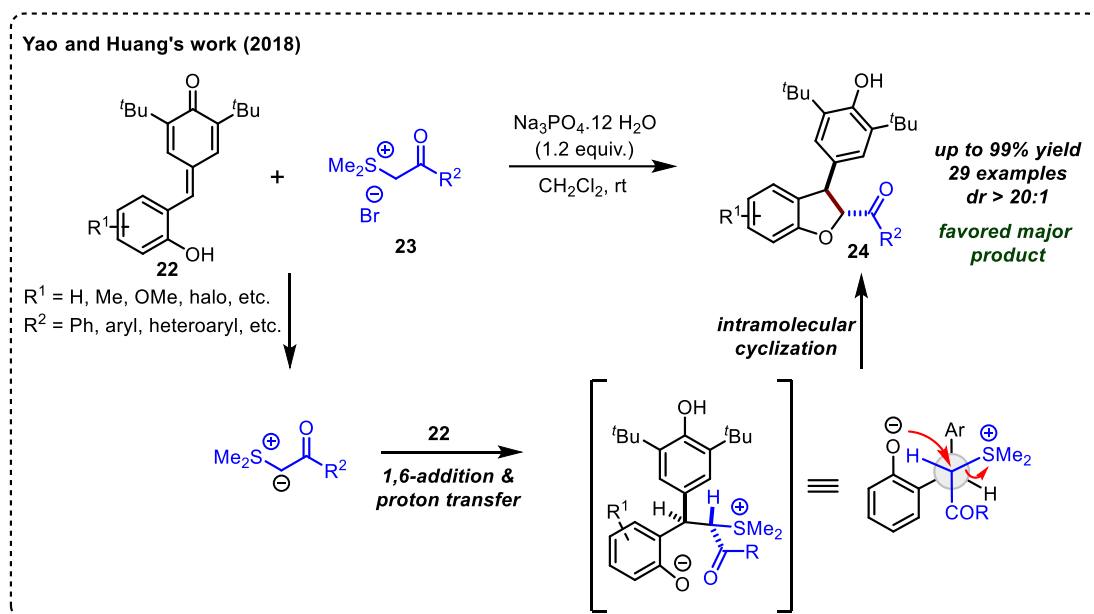
Scheme 6. Anand's approach towards unsymmetrical triarylmethanes

In 2015, Anand & co-workers established a palladium-catalyzed synthesis of unsymmetrical triarylmethanes through the reaction of *p*-QMs with *in-situ* generated 2-substituted indoles (from *o*-alkynyl aniline) [Scheme 6]. According to the proposed mechanism, PdCl₂ activated the alkyne, and as a result, **20** undergoes 5-*endo-dig* cyclization to form an intermediate **II**, which may directly attack the *p*-QM in a 1,6-conjugate fashion to produce the product **21** (path A). There is also another possibility in which intermediate **II** gets converted in to intermediate **III** followed by 1,6-conjugate addition (path B) to give desired product **21** as shown in (Scheme 6).¹⁴

1.2 Literature reports on the synthesis of oxygen-containing heterocycles

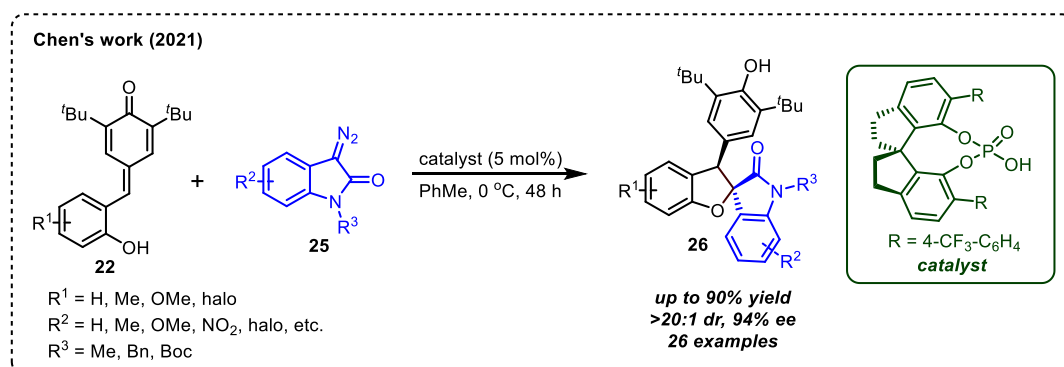
Oxygen-based heterocycles are necessary scaffolds in various natural products and bioactive molecule classes.¹⁵ So far, many research groups have developed synthetic routes in this area, and a few of them are discussed in this section. Many reports are known in the

literature on the synthesis of various classes of six-membered oxygen-containing heterocycles such as chromenes, xanthenes, chroman, etc. In this section, a few of them are discussed.



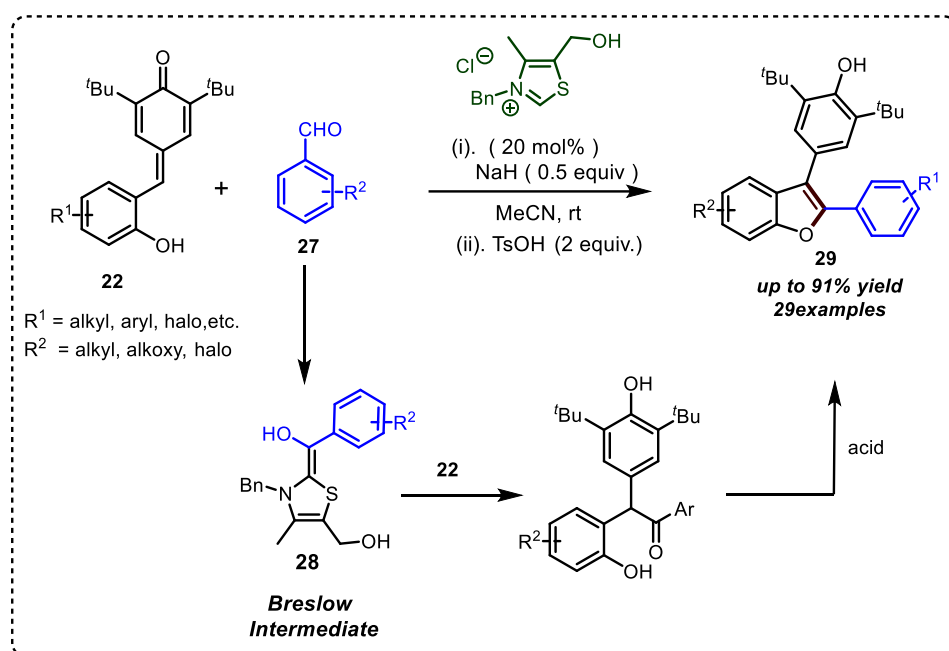
Scheme 7. Synthesis of 2,3-dihydrobenzofurans using sulfonium salts

In 2018, Yao and Huang reported the synthesis of 2,3-dihydrobenzofuran derivatives **24** via [4+1]-cycloaddition reaction of 2-hydroxyphenyl substituted *p*-QMs **22** and sulfonium salts **23**. The product **24** was obtained with good yield and excellent diastereoselectivity. According to the proposed reaction mechanism, $\text{Na}_3\text{PO}_4 \cdot 12\text{H}_2\text{O}$ abstracts the proton from the sulfonium salt, followed by 1,6-conjugate addition and subsequent proton exchange, generating an intermediate, which subsequently undergoes intramolecular nucleophilic substitution reaction to furnish the desired 2,3-dihydrobenzofurans derivatives **24** (Scheme 7).¹⁶



Scheme 8. Synthesis of *spiro*-dihydro benzofuran derivatives

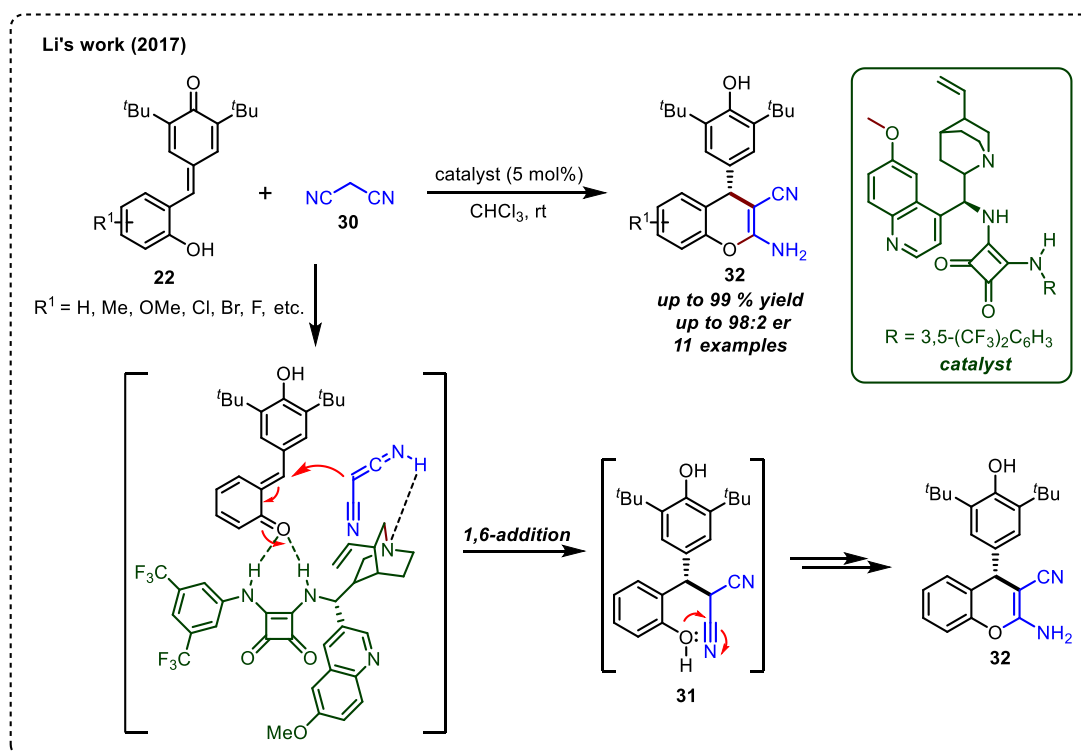
In 2021, Chen's and co-workers developed a chiral phosphoric acid-promoted asymmetric synthesis of *spiro*-dihydrobenzofuran derivatives (**26**) using 2-hydroxyphenyl substituted *p*-QMs (**22**) and 3-diazo oxindoles (**25**). The reaction happens through the isomerization of **22** to *ortho*-quinone methide *via* a proton transfer step followed by 1,4-conjugate-addition of 3-diazo oxindoles and subsequent intramolecular nucleophilic substitution to form the product **26** with the release of nitrogen gas (Scheme 8).¹⁷



Scheme 9. Synthesis of diarylbenzo[*b*]furan derivatives

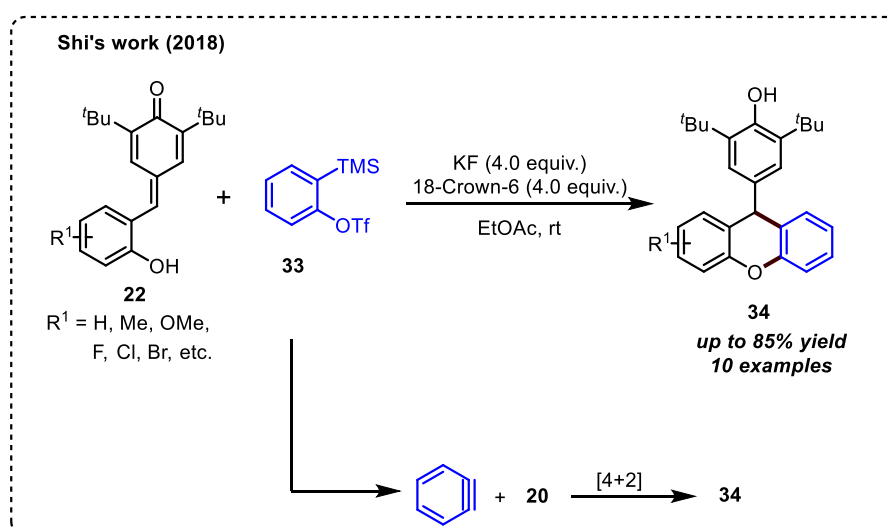
In 2018, Anand and co-workers established a one-pot protocol for the synthesis of 2,3-diarylbenzo[*b*]furan derivatives (**29**) using *N*-heterocyclic carbene (NHC) by the reaction 2-hydroxyphenyl substituted *p*-QMs (**22**) and aromatic aldehydes (**27**). The reaction proceeds through the formation of Breslow intermediate **28**, which then undergoes 1,6-conjugate addition followed by acid-mediated intramolecular cyclization and dehydration to afford the desired diarylbenzo[*b*]furan derivatives **29** (Scheme 9).¹⁸

The enantioselective synthesis of 4H-chromene derivatives by the reaction of 2-hydroxyphenyl substituted *para*-quinone methide **22**, and malononitrile **30** has been reported by Li and co-workers (2017) using a chiral squaramide-based bifunctional catalyst. It was proposed that the reaction proceeds through the *insitu* generation of *o*-QM from *p*-QM in the presence of a catalyst followed by enantioselective addition to form adduct **31**, which then undergo intramolecular cyclization and isomerization to develop their respective 4H-chromene derivatives **32** in good yield with excellent enantioselectivity. (Scheme 10).¹⁹

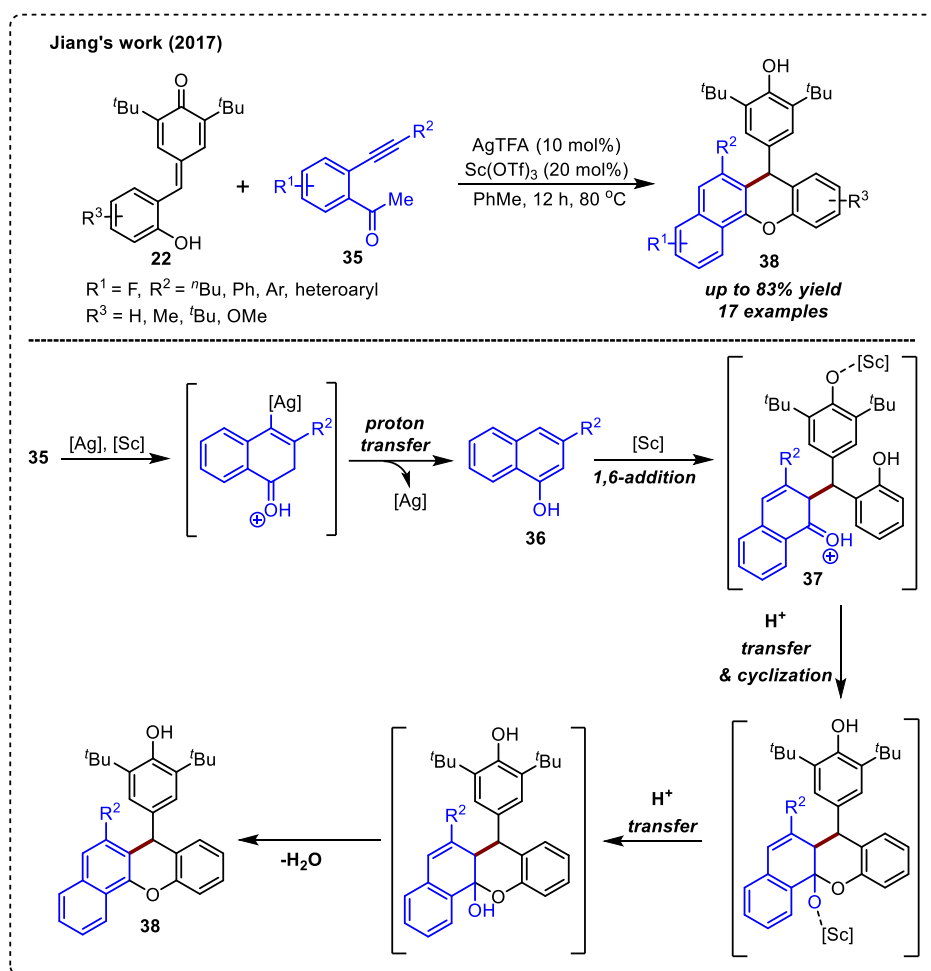


Scheme 10. Synthesis of 4H-chromenes using malononitriles

Shi's²⁰ and He's²¹ research groups independently demonstrated a [4+2]-cycloaddition reaction between 2-hydroxyphenyl substituted *p*-QMs (**22**) and arynes for the synthesis of xanthene derivatives (**34**). This methodology provides a wide range of xanthene derivatives in good to excellent yields. The reaction proceeds through *in situ*-generated benzyne from **33**, which then undergoes cycloaddition to furnish the product **34** (Scheme 11).^{20,21}



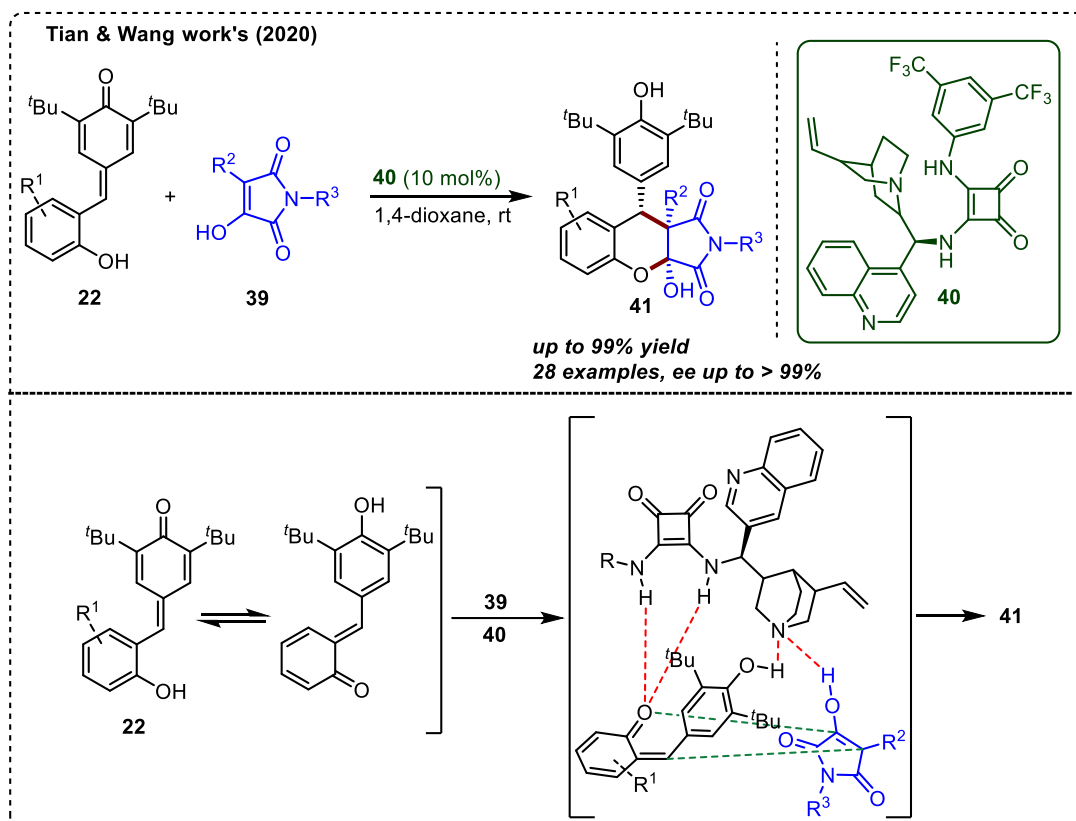
Scheme 11. Synthesis of xanthenes using arynes



Scheme 12. Jiang's approach towards benzo[*c*]xanthene derivatives

In 2017, Jiang and co-workers reported a AgTFA and Sc(OTf)₃-catalyzed synthesis of benzo[*c*]xanthene derivatives **38** using β -alkynyl acetophenones (**35**) and 2-hydroxyphenyl substituted *p*-QMs (**22**). The reaction occurs through Ag/Sc catalyzed *6-endo-dig* cyclization followed by proton transfer and 1,6-conjugate addition with **22** to generate another intermediate **37**. Then, intermediate **37** undergoes proton transfer followed by an intramolecular cyclization and dehydration sequence to yield benzo[*c*]xanthene **38** in excellent yields (Scheme 12).²²

Very recently, Tian and Wang established the synthesis of chiral fused-chromane derivatives *via* [4+2]-annulation reaction between 2-hydroxyphenyl substituted *p*-QMs (**22**) and hydroxy-maleimides **39**. They have used chiral squaramide **40** as a catalyst and used this approach to prepare a wide range of fused-chromane derivatives in good yield with excellent enantioselectivity (Scheme 13).²³

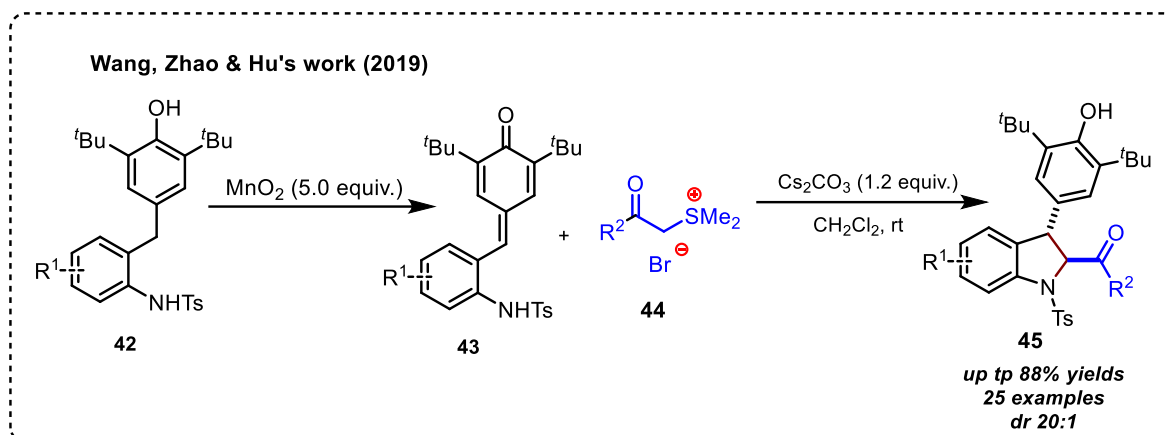


Scheme 13. Tian and Wang's approach to accessing chiral chromane

1.3 Synthesis of Nitrogen-containing heterocycles

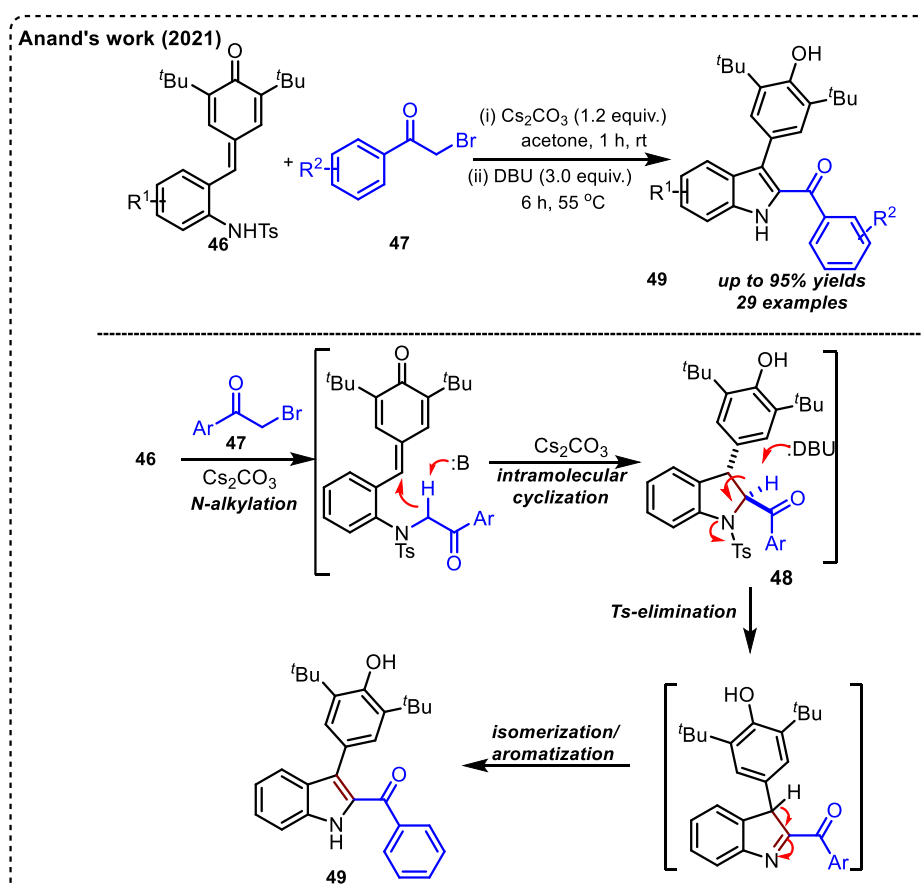
Nitrogen-based heterocycles such as indole, quinoline, isoquinoline, pyrrole, and pyrazole are regarded as the most important class of organic molecules as they are extensively used in various biological processes and discovered as integral components in many naturally occurring and artificial biologically relevant compounds.²⁴ This section will discuss the literature reports on synthesizing *N*-heterocycles using the *p*-QMs.

In 2019, Wang, Zhao, Hu, and co-workers reported a base-mediated [4+1]-annulation reaction between *o*-tosylaminophenyl-substituted *p*-QMs **43** and sulfonium ylides **44** to access



Scheme 14. Base-mediated synthesis of 2,3-dihydroindoles

a wide range of 2,3-dihydroindoles derivatives **45** in good yield and excellent diastereoselectivities (Scheme 14).²⁵

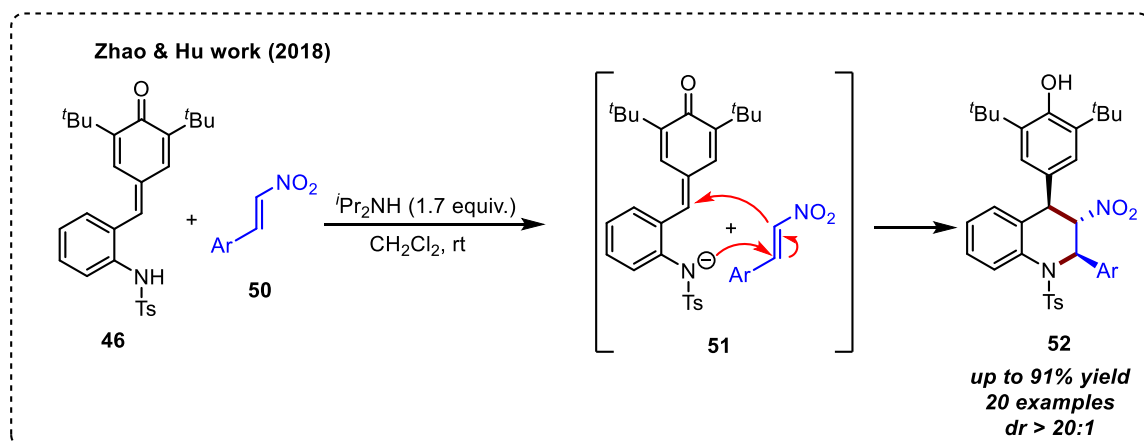


Scheme 15. Synthesis of 2,3-dihydroindoles

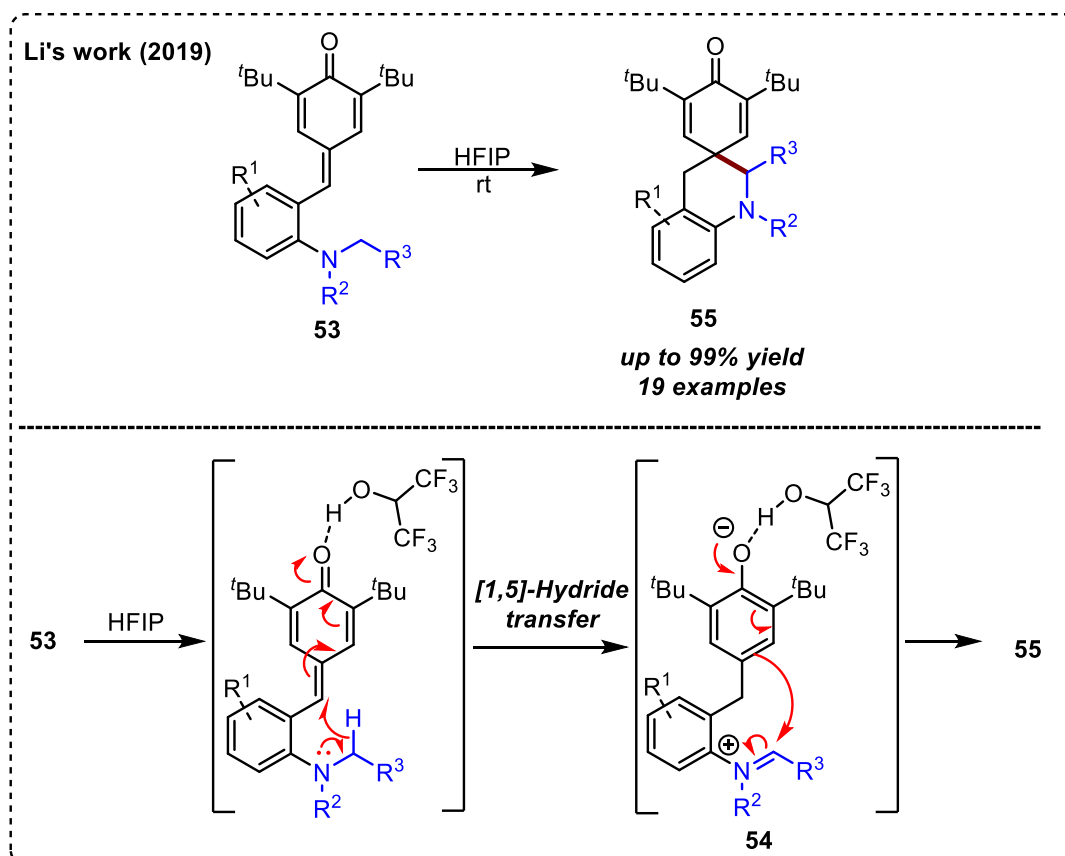
Similarly, Anand & co-workers disclosed the inorganic and organic base-promoted synthesis of 2,3-disubstituted indole derivatives **49** using *o*-tosylaminophenyl-substituted *p*-QMs **46** and substituted-phenacyl bromides **47** as precursors. (Scheme 19). The reaction proceeds through *N*-alkylation in the presence of an inorganic base followed by intramolecular

cyclization to produce intermediate **48**, which then undergoes DBU-mediated removal of tosyl group and isomerization/aromatization to furnish the final product **49** in good yields (Scheme 15).²⁶

In 2018, Zhao, Hu, and co-workers demonstrated a base-mediated *aza*-Michael addition of nitrostyrene **50** with *in situ* generated *o*-tosylaminophenyl-substituted *p*-QMs to access 4-aryl-substituted tetrahydroquinolines derivatives **52** in good yield and high diastereoselectivity (Scheme 16).²⁷



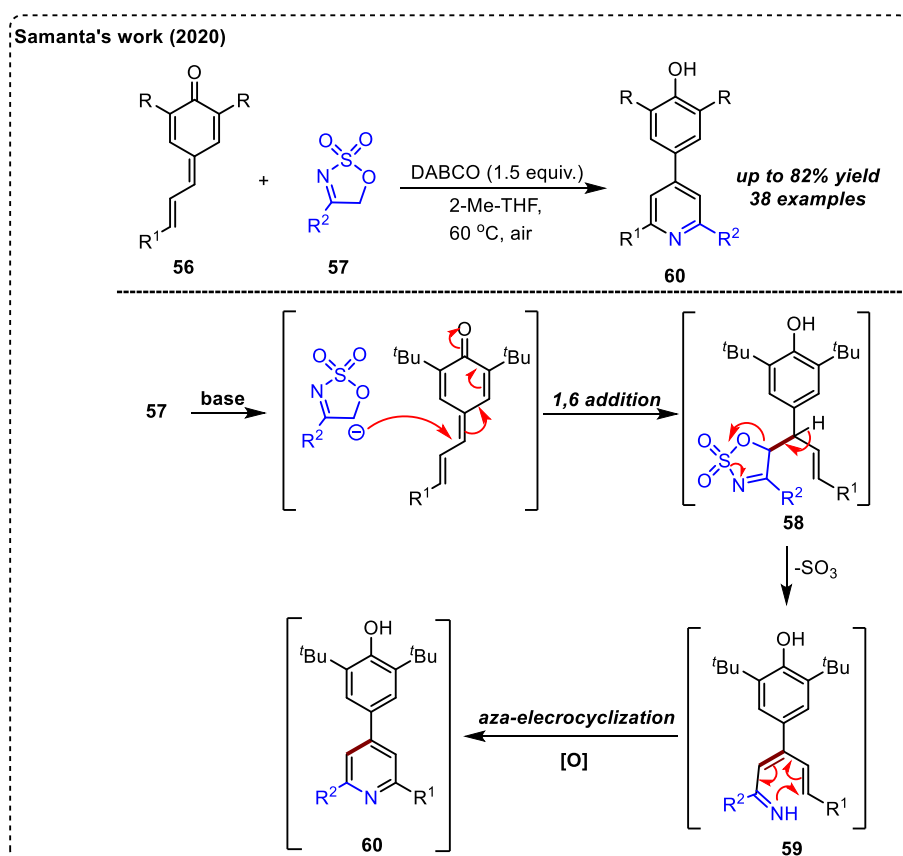
Scheme 16. Synthesis of 4-aryl-substituted tetrahydroquinolines



Scheme 17. HFIP-mediated synthesis of spirocyclic tetrahydroquinolines

Recently Li and Xiao reported the synthesis of *spiro*-cyclic tetrahydroquinolines from 2-aminophenyl-substituted *p*-QMs **53**. The reaction proceeds through HFIP-mediated activation of **53** followed by HFIP induced 1,5-hydride shift to generate an iminium intermediate **54**, which transforms into the *spiro*-cyclic tetrahydroquinolines derivatives **55** via a dearomative cyclization process (Scheme 17).²⁸

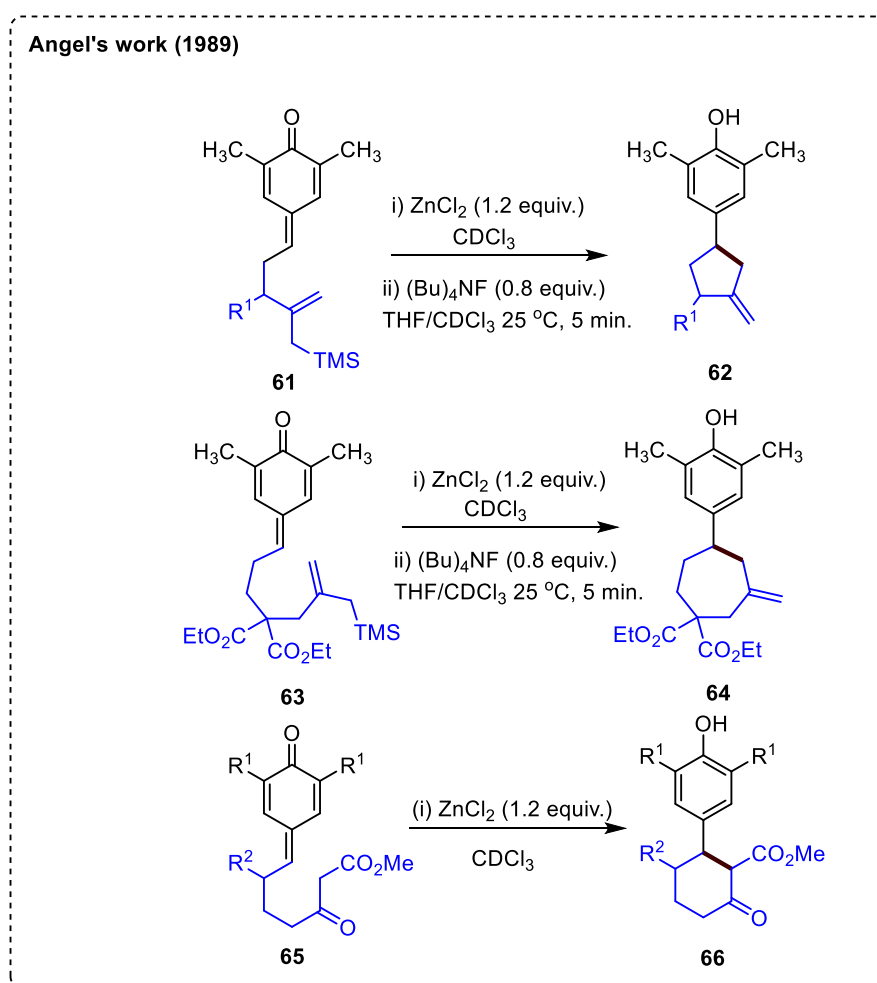
In 2020, Samanta's group described the synthesis of substituted pyridines from vinyl-substituted *p*-QMs **56** and cyclic sulfamidate-imines **57** as the precursors. They have used DABCO as a base to promote this methodology. As proposed by the authors, the base (DABCO) abstracts a proton from sulfamidate-imines **57** to generate the corresponding anion, which undergoes 1,6-conjugate addition followed by SO₃ removal to generate intermediate **59**. The intermediate **59** then undergoes *aza*-electrocyclization and aerobic oxidation to furnish the product **60** (Scheme 18).²⁹



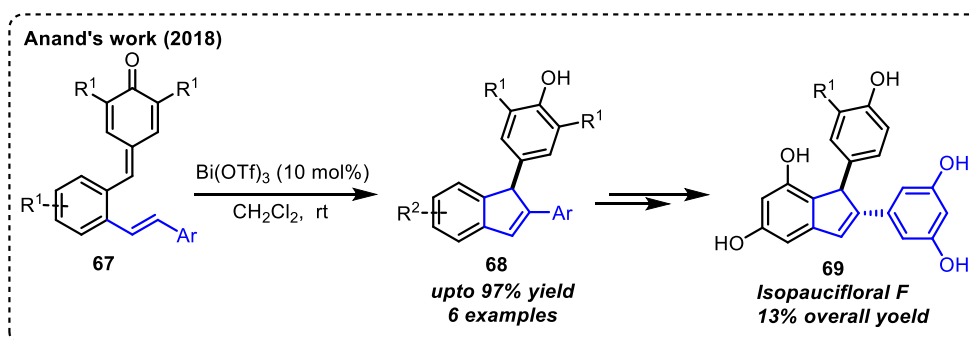
Scheme 18. Synthesis of substituted pyridines from *p*-QMs

1.4 Literature reports on the synthesis of carbocycles

Angle and co-workers, in 1989, for the first time, exploited *para*-quinone methide chemistry to synthesize five, six, and seven-membered carbocycles through intramolecular cyclization. They have utilized β -keto esters functionalized *p*-QMs (**61**, **63** & **65**) as starting materials. According to the proposed reaction mechanism, ZnCl_2 activates the *para*-quinone methide followed by intramolecular 1,6-cyclization to furnish its respective products (**62**, **64** & **66**) [Scheme 19].³⁰

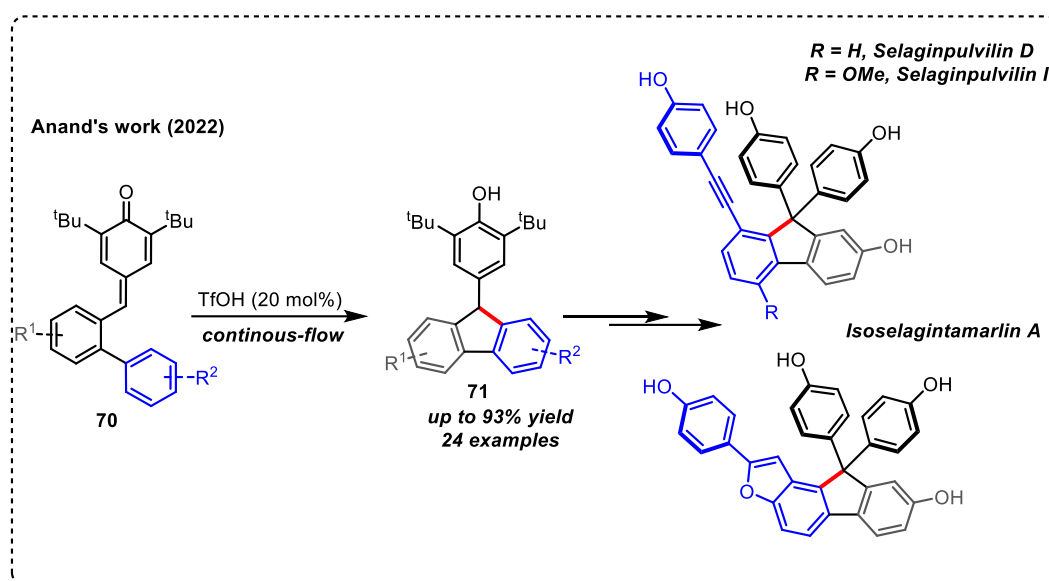


Scheme 19. Angel's approach towards carbocycles



Scheme 20. 1,6-Hydro-olefination of 2-alkenyl phenyl substituted *p*-QM

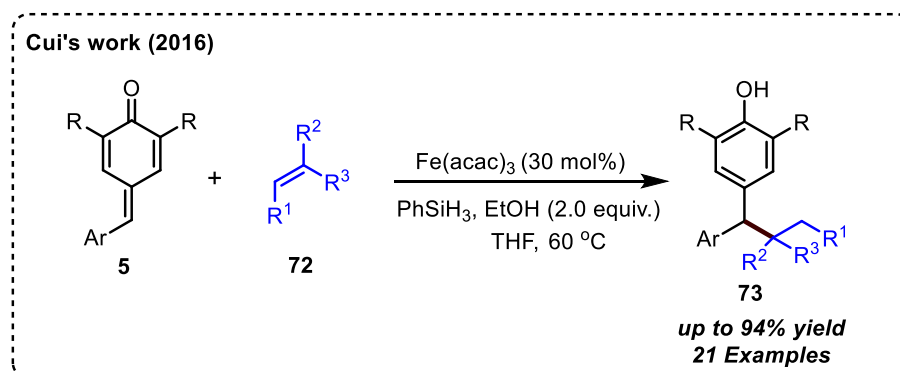
Later, Anand and co-workers, in 2018, reported a 1,6-hydro-olefination reaction of 2-alkenyl phenyl substituted *para*-quinone methides **67** using bismuth triflate as a catalyst. Further, they have elaborated the same methodology for synthesizing the natural product Isopaucifloral F **69** in 13% overall yield in nine consecutive steps (Scheme 20).³¹ Very recently (2022), the same group has established a methodology for synthesizing fluorene derivatives **71** in excellent yields under continuous-flow using triflic acid as a catalyst. Using the same approach, they have synthesized Selaginpulvin I and Isoselagintamarlin, fluorene-based natural products (Scheme 21).³²



Scheme 21. Synthesis of fluorene derivative under continuous-flow

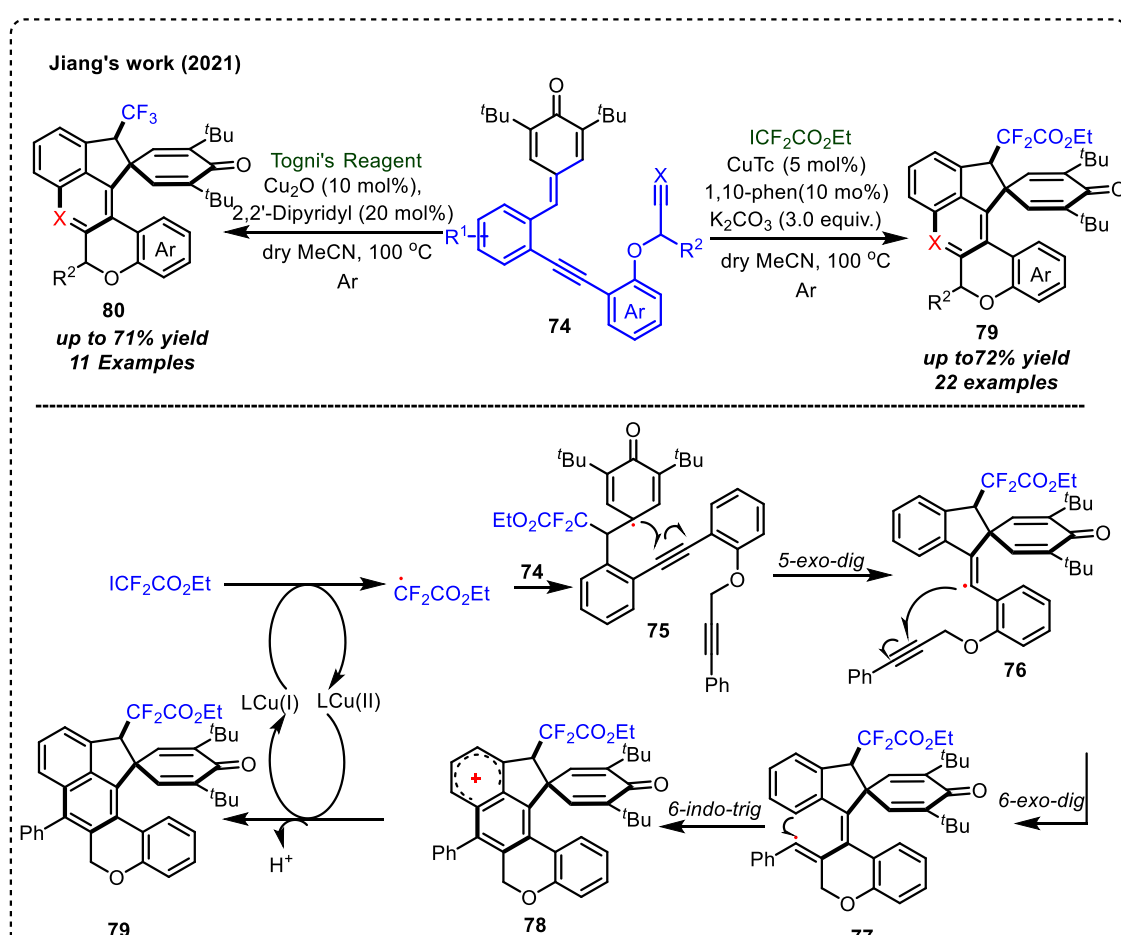
1.5 Literature reports on the radical reactions of *p*-QMs

In 2016, Cui and co-workers reported the hydro-alkylation of olefins **72** with *p*-QMs **5** in the presence of ferric acetylacetonate [Fe(acac)₃] as catalyst and PhSiH₃ as a reductant in EtOH, which led to the phenolic products **73** (scheme 22)³³



Scheme 22. Hydroalkylation of *p*-QM under the radical condition

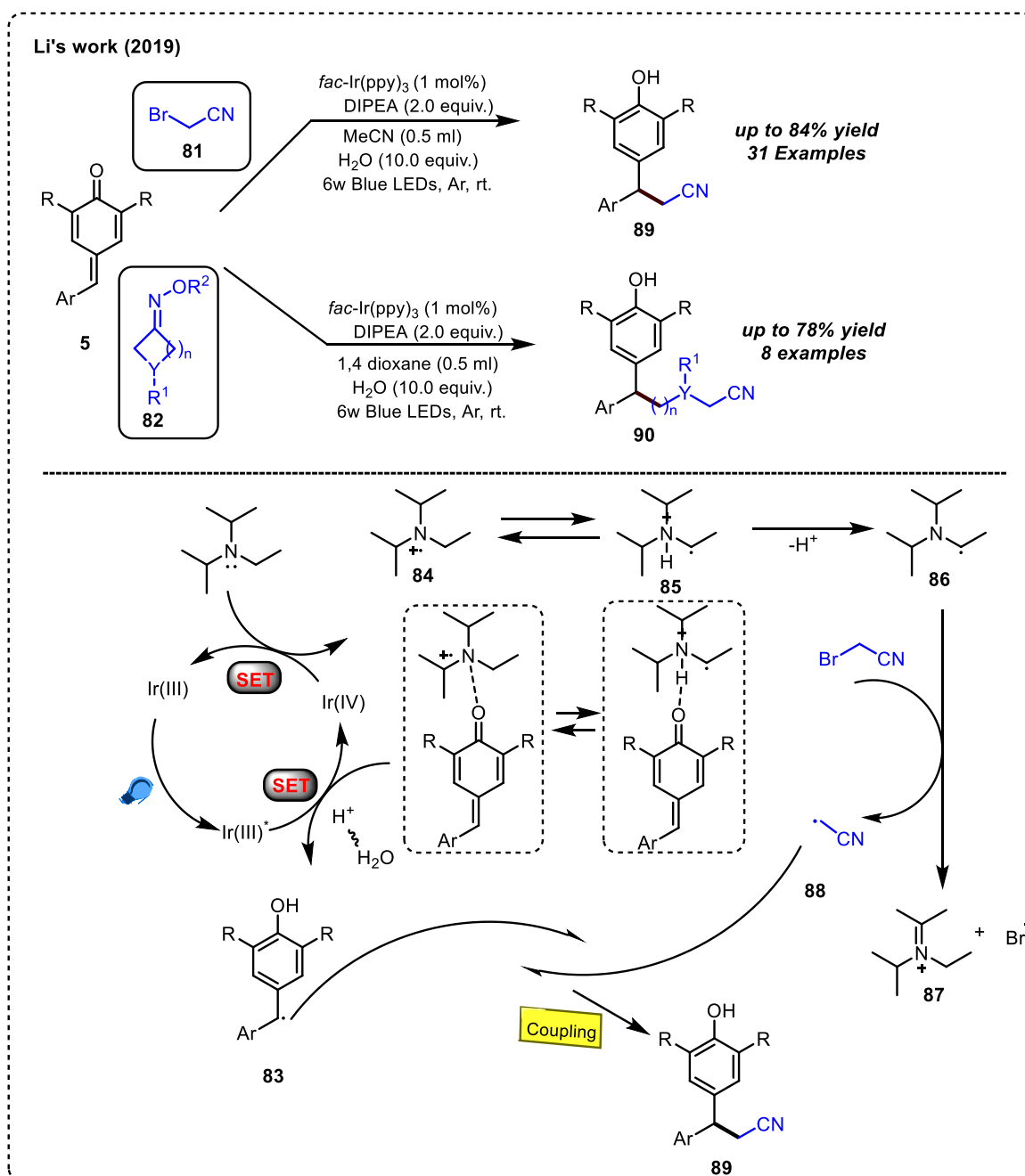
Very recently, a Cu-catalyzed method has been used by Guo, Hao, and Jiang's group to synthesize pentacyclic *spiro*-indenes (**80**). Fluoromethylation of enediyne/enyne-nitrile containing *p*-QMs with Togni's reagent and ethyl iodo-difluoroacetate to afford *spiro*-indenes **80** and **81** in moderate to good yields. In the proposed mechanism, the reduction of ethyl iodo-difluoroacetate affords difluoroacetate radical, which on 1,6-addition, formed another radical species **75**. After that, the radical intermediate **75** undergoes intramolecular *5-exo-dig* cyclization to give **76**, which further experiences *6-exo-dig* cyclization to give **77**. Radical species **77** further undergoes *6-endo-trig* cyclization to form **78**, followed by deprotonation to furnish the desired product **79** (Scheme 23).³⁴



Scheme 23. Synthesis of pentacyclic spiroindenes

In 2019, Li and co-worker used *fac*-Ir(ppy)₃ to synthesize cyano-alkylated diarylmethane from *p*-QMs (**5**) and bromoacetonitrile **81**. The reaction proceeds through the irradiation of Ir(III) by blue light to form Ir(III)* complex, which immediately transfers a single electron to *p*-QM to generate **84**, and itself gets oxidized to Ir(IV) species. Subsequently, DIPEA transfers an electron to Ir(IV) and forms a radical cation, which immediately rearranges to another

radical cation intermediate **85**, which, on deprotonation, gives another radical species **86**. The reduction of bromoacetonitrile by **86** generates **88**. The cross-coupling between **83** and **88** leads to the desired product **89** (Scheme 24).³⁵



Scheme 24. Visible light-mediated cyanoalkylation of *p*-QMs

1.6 References:

- (a) Larsen, A. A. *Nature* **1969**, 224, 25. (b) Hamels, D.; Dansette, P. M.; Hillard, E. A.; Top, S.; Vessieres, A.; Herson, P.; Jaouen, G.; Mansuy, D. *Angew. Chem. Int. Ed.* **2009**,

- 121, 9288. (c) Messiano, G. B.; da Silva, T.; Nascimento, I. R.; Lopes, L. M. X. *Phytochemistry* **2009**, *70*, 590. (d) Dehn, R.; Katsuyama, Y.; Weber, A.; Gerth, K.; Jansen, R.; Steinmetz, H.; Hçfle, G.; Müller, R.; Kirschning, A. *Angew. Chem. Int. Ed.* **2011**, *123*, 3968. (e) C. Sridar, C.; D'Agostino, J.; Hollenberg, P. F. *Drug Metab Dispos.* **2012**, *40*, 2280.
2. Dehn, R.; Katsuyama, Y.; Weber, A.; Gerth, K.; Jansen, R.; Steinmetz, H.; Hçfle, G.; Müller, R.; Kirschning, A. *Angew. Chem. Int. Ed.* **2011**, *123*, 3968.
 3. Wang, L. L.; Candito, D.; Dräger, G.; Herrmann, J.; Müller, R.; Kirschning, A. *Chem. Eur. J.* **2017**, *23*, 5291.
 4. Rokita, S. E. *Quinone Methides*, Wiley, Hoboken, **2009**.
 5. Koutek, B.; Pířová, M.; Souček, M.; Exner, O. *Collect. Czech. Chem. Commun.* **1976**, *41*, 1676.
 6. (a) Toteva, M. M.; Richard, J. P. *J. Am. Chem. Soc.* **2000**, *122*, 11073. (b) Richard, J. P.; Toteva, M. M.; Crugeiras, J. *J. Am. Chem. Soc.* **2000**, *122*, 1664. (c) Toteva, M. M.; Moran, M.; Amyes, T. L.; Richard, J. P. *J. Am. Chem. Soc.* **2003**, *125*, 8814. (d) Toteva, M. M.; Richard, J. P. *The Generation and Reactions of Quinone Methides. In Advances in Physical Organic Chemistry*; Academic Press, Elsevier, **2011**; *45*, 39.
 7. (a) Pospisek, J.; Pisova, M.; Soucek, M. *Collect. Czech. Chem. Commun.* **1975**, *40*, 142. (b) Koutek, B.; Pavlickova, L.; Soucek, M. *Synth. Commun.* **1976**, *6*, 305. (c) Richter, D.; Hampel, N.; Singer, T.; Ofial, A. R.; Mayr, H. *Eur. J. Org. Chem.* **2009**, 3203. (d) Reddy, V.; Anand, R. V. *Org. Lett.* **2015**, *17*, 3390. (e) Fan, Y. –J.; Zhou, L.; Li. S. *Org. Chem. Front.* **2018**, *5*, 1820. (f) Liu, Z. –Q.; You, P. –S.; Wu, C. –H.; Han, Y. –H. *J. Saudi Chem. Soc.* **2020**, *24*, 120.
 8. Hart, D. J.; Cain, P. A.; Evans, D. A. *J. Am. Chem. Soc.* **1978**, *100*, 1548.
 9. S. Gao, X. Xu, Z. Yuan, H. Zhou, H. Yao, A. Lin, *Eur. J. Org. Chem.* **2016**, 3006.
 10. Ma, C.; Huang, Y.; Zhao, Y. *ACS Catal.* **2016**, *6*, 6408.
 11. Yuan, Z.; Wei, W.; Lin, A.; Yao, H. *Org. Lett.* **2016**, *18*, 3370.
 12. McLaughlin, M. F.; Massolo, Elisabetta.; Cope, T. A.; Johnson, J. S. *Org. Lett.* **2019**, *21*, 6604.
 13. Su, Yingpeng.; Zhao, Yanan.; Chang, Bingbing.; Zhao, Xiaolong.; Zhang Rong.; Liu, Xuan.; Huang, Danfeng.; Wang, Ke-Hu.; Huo, Congde.; Hu, Yulai. *J. Org. Chem.* **2019**, *84*, 6719.
 14. Reddy, V.; Anand, R. V. *Org. Lett.* **2015**, *17*, 3390.
 15. For recent reviews, See: (a) Radadiya, A.; Shah, A. *Eur. J. Med. Chem.* **2015**, *97*, 356.

- (b) Stefanachi, A.; Leonetti, F.; Pisani, L.; Catto, M.; Carotti, A. *Molecules* **2018**, *23*, 250. (c) Saleeb, M.; Mojica, S.; Eriksson, A. U.; Anderson, C. D.; Gylfe, Å.; Elofsson, M. *Eur. J. Med. Chem.* **2018**, *143*, 1077.
16. Liu, L.; Yuan, Z.; Pan, R.; Zeng, Y.; Lin, A.; Yao, H.; Huang, Y. *Org. Chem. Front.* **2018**, *5*, 623.
17. Wu, Y. C.; Cui, B. D.; Long, Y.; Han, W. Y.; Wan, N. W.; Yuan, W. C.; Chen, Y. Z. *Adv. Synth. Catal.* **2021**, *363*, 1702.
18. Singh, G.; Goswami, P.; Sharma, S.; Anand, R. V. *J. Org. Chem.* **2018**, *83*, 10546–10554.
19. Duan, C.; Ye, L.; Xu, W.; Li, X.; Chen, F.; Zhao, Z.; Li, X. *Chinese Chem. Lett.* **2018**, *29*, 1273.
20. Mei, G. J.; Xu, S. L.; Zheng, W. Q.; Bian, C. Y.; Shi, F. *J. Org. Chem.* **2018**, *83*, 1414.
21. Li, Z.; Wang, W.; Jian, H.; Li, W.; Dai, B.; He, L. *Chinese Chem. Lett.* **2019**, *30*, 386.
22. Chen, K.; Liu, S.; Wang, D.; Hao, W. J.; Zhou, P.; Tu, S. J.; Jiang, B. *J. Org. Chem.* **2017**, *82*, 11524.
23. Xiang, M.; Li, C. –Y.; Song, X. –J.; Zou, Y.; Huang, Z. –C.; Li, X.; Tian, F.; Wang, L. –X. *Chem. Commun.* **2020**, *56*, 14825.
24. For selected references: (a) Noolvi, M. N.; Patel, H. M.; Bhardwaj, V.; Chauhan, A. *Eur. J. Med. Chem.* **2011**, *45*, 2327. (b) Verma, V.; Singh, K.; Kumar, D.; Klapotke, T. M.; Stierstorfer, J.; Narasimhan, B.; Qazi, A. K.; Hamid, A.; Jaglan, S. *Eur. J. Med. Chem.* **2012**, *56*, 195. (c) Yu, B.; Yu, D. –Q.; Liu, H. –M. *Eur. J. Med. Chem.* **2015**, *97*, 673. (d) Baumann, M.; Baxendale, I. R.; *Beilstein J. Org. Chem.* **2013**, *9*, 2265. (e) Agalave, S. G.; Maujan, S. R.; Pore, V. S. *Chem. Asian J.* **2011**, *6*, 2696. (f) Sridharan, V.; Suryavanshi, P. A.; Menendez, J. C. *Chem. Rev.* **2011**, *111*, 7157. (g) Thirumurugan, P.; Matosiuk, D.; Jozwiak, K. *Chem. Rev.* **2013**, *113*, 4905. (h) Hobson, L. A.; Nugent, W. A.; Anderson, S. R.; Deshmukh, S. S.; Haley, J. J.; Liu, P.; Magnus, N. A.; Sheeran, P.; Sherbine, J. P.; Stone, B. R. P. Zhu, J. *J. Org. Process Res. Dev.* **2007**, *11*, 985.
25. Wang, J.; Pan, X.; Zhao, L.; Zhao, L.; Liu, J.; Zhi, Y.; Wang, A.; Zhao, K.; Hu, L. *Org. Biomol. Chem.* **2019**, *17*, 10158.
26. Pandey, R.; Singh, G.; Gour, V.; Anand, R. V. *Tetrahedron* **2021**, *82*, 131950.
27. Wang, J.; Rong, Q.; Zhao, L.; Pan, X.; Zhao, L.; Zhao, K.; Hu, L. *J. Org. Chem.* **2020**, *85*, 11240.

28. Lv, X.; Hu, F.; Duan, K.; Li, S. -S.; Liu, Q.; Xiao, J. *J. Org. Chem.* **2019**, *84*, 1833. (b)
Li, S. -S.; Lv, X.; Ren, D.; Shao, C. -L Liuc, Q.; Xiao, J. *Chem. Sci.* **2018**, *9*, 8253.
29. Guin, S.; Gudimella, S. K.; Samanta, S. *Org. Biomol. Chem.* **2020**, *18*, 1337.
30. Angle, S. R.; Turnbull, K. D. *J. Am. Chem. Soc.* **1989**, *111*, 1136
31. Jadhav, A. S.; Pankhade, Y. A.; Hazra, R.; Anand, R. V. *J. Org. Chem.* **2018**, *83*, 10107
32. Pankhade, Y. A.; Pandey, R.; Fatma, S.; Ahmad, F.; Anand, R. V. *J. Org. Chem.* **2022**, *87*, 3363.
33. Shen, Y.; Qi, J.; Mao, Z.; Cui, S. *Org. Lett.* **2016**, *18*, 2722.
34. Zuo, H. D.; Ji, X. S.; Guo, C.; Tu, S. J.; Hao, W. J.; Jiang, B. *Org. Chem. Front.*, **2021**, *8*, 1496.
35. Zhang, W.; Yang, Chen.; Zhang, Z. P.; Li. X.; Cheng, J. P.; *Org. Lett.* **2019**, *21*, 4137-4142.

2. Reaction of 2-hydroxyphenyl substituted *N,N*-dimethyl enamines with *p*-quinone methides: Access to chromone derivatives

2.1. Introduction

Chromones are naturally occurring compounds abundant in nature, particularly in plants. The term chromone came from the Greek word *chroma*, which means “color,” indicating that many chromone derivatives can show a wide range of colors.¹ Chromones, flavones, and isoflavones are a privileged class of oxygen-containing heterocycles often found in numerous natural products, medical drug treatments, and lead compounds.² In addition to this, they are also found to have great pharmacological activities such as anticancer, antioxidant, antifungal, antiuretic, etc.³

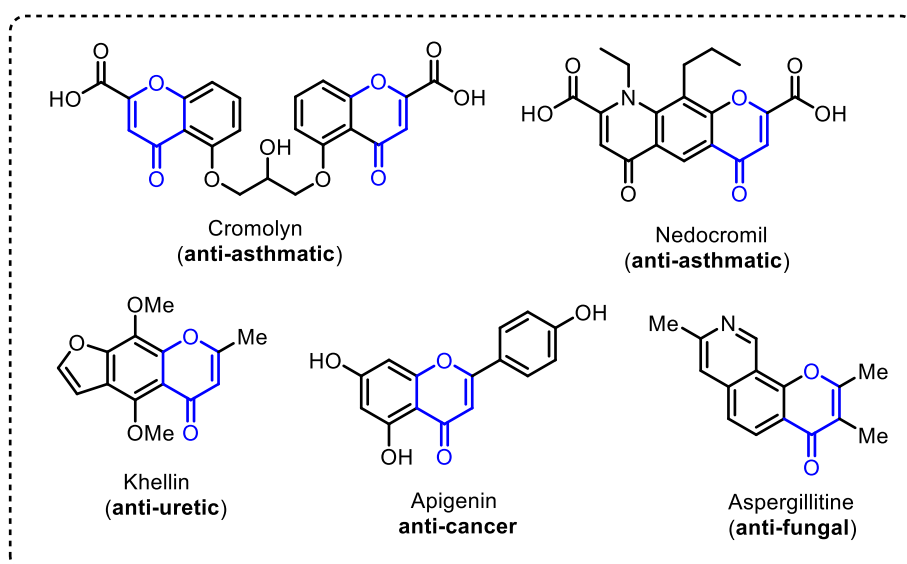


Figure 1. Some 4H-chromenone-based biological active molecules

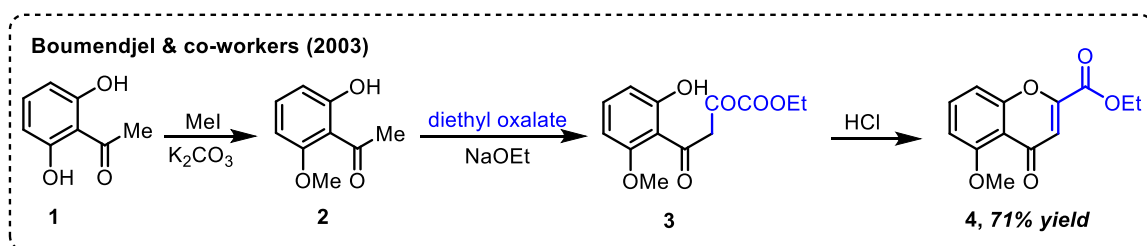
For example, cromolyn sodium has been found to have anti-asthmatic properties. This drug appears to be more effective in young asthmatics with low bronchial infection and mild pulmonary hyperinflation.^{3a} Khellinoflavanone, a semisynthetic derivative of Khellin, reduces benzo[*a*]pyrene toxicity in humans and cancer cells expressed with CYP1A1.^{3b} Apigenin has been shown to suppress various human cancers *in-vitro* and *in-vivo* through a variety of biological effects, including cell apoptosis and autophagy, cell cycle arrest, suppression of cell migration and invasion, and stimulation of an immune response.^{3c,d} Due to their widespread

use so far, many synthetic approaches have been developed to construct the heterocyclic core of these derivatives. A few of them are discussed below.

2.2 Literature reports on the synthesis of chromone derivatives

The most common methods reported for synthesizing 4H-chromenone (4-chromone) derivatives are based on annulation reactions of acetophenone derivatives under acidic and basic conditions.⁴

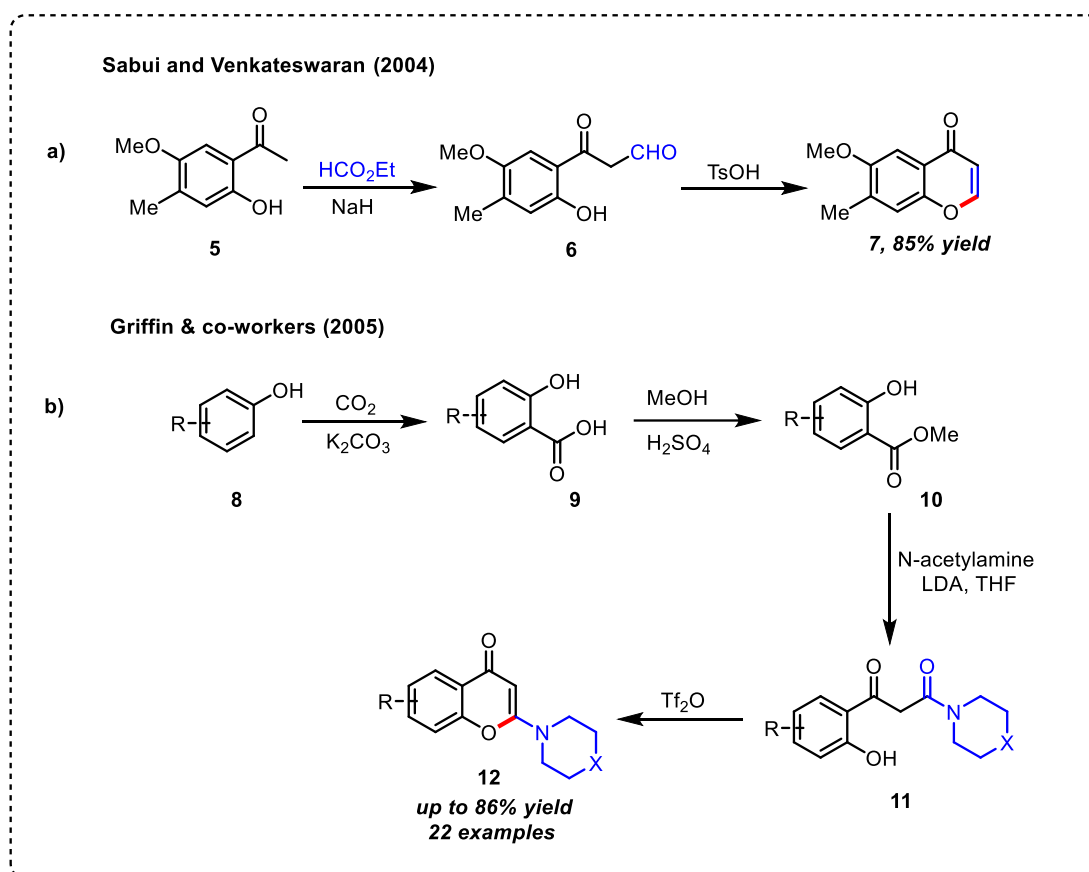
2.2.1 Through condensation of acetophenone derivatives.



Scheme 1. Hydrochloric acid-catalyzed ring closure for the synthesis of chromones

In 2003, Boumendjel and co-workers reported three-step protocol for the synthesis of chromone derivatives (**4**) using 2,6-dihydroxy acetophenone derivatives (**1**) as a starting material. Concentrated hydrochloric acid was used as a catalyst to carry out the ring closure. In the first step, reaction between 2,6-dihydroxy acetophenone **1** and methyl iodide gave 2-hydroxy-6-methoxy acetophenone **2**, which was further subjected to condensation with diethyl oxalate in the presence of sodium ethoxide in EtOH followed by concentrated HCl-catalyzed cyclization triggered the desired product **4** in good yield. (Scheme 1).⁴

In 2004, Sabui and Venkateswaran developed the synthesis of chromone derivatives using *p*-toluenesulfonic acid as a catalyst through a ring-closure reaction. The 6-methoxy-7-methyl chromone **7** was obtained in an overall yield of 85% by condensing the acetophenone **5** with ethyl formate in the presence of sodium hydride, followed by dehydration of the resulting chromanol (Scheme 2, **a**).⁵ Later on, Griffin & co-workers reported the synthesis of chromone derivatives (**12**) using triflic anhydride as a catalyst for the cyclization of β -keto amides (**11**). 2-hydroxy aryl carboxylate esters (**10**) were prepared by carboxylation and esterification reaction of appropriate phenol derivatives (**8**) using general methods. After that the resulting 2-hydroxy aryl carboxylate esters (**11**) were treated with *N*-acetyl amines to afford β -ketoamides (**11**), which were further subjected to ring-closure with triflic anhydride yielding the respective chromone derivatives (**12**) in good yields (Scheme 2, **b**).⁶

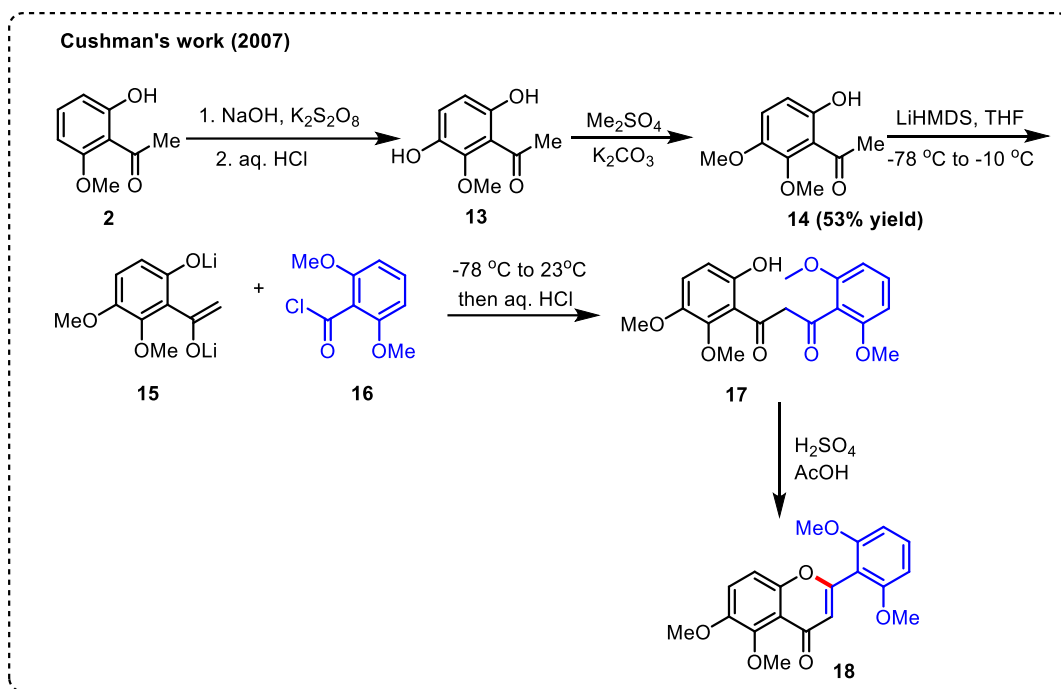


Scheme 2. (a) TsOH-catalyzed synthesis of chromones. (b) Tf₂O-catalyzed the synthesis of chromone derivatives

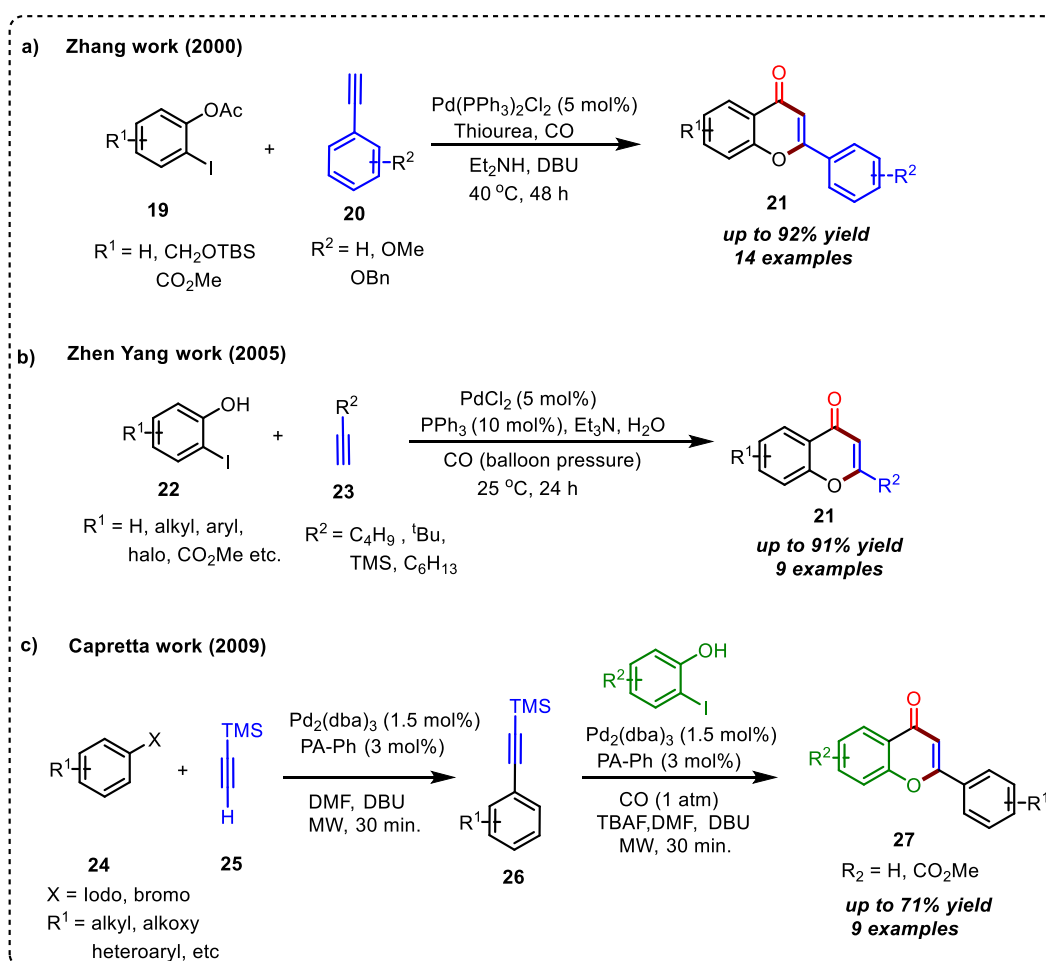
Cushman & co-workers, in 2007, used H₂SO₄ as a catalyst for chromone synthesis. 2-hydroxy-6-methoxyacetophenone **2** underwent Elbs oxidation with sodium persulfate and aqueous sodium hydroxide to give substituted acetophenone **13**, which was further subjected to regioselective methylation using anhydrous potassium carbonate and dimethyl sulfate in acetone to afford 6-hydroxy-2,3-dimethoxy acetophenone **14** in 53% yield. Treatment with four equivalents of lithium hexamethyl disilylazide in THF ensured the generation of the dilithium dianion **15** of the acetophenone **14**. The β -diketone intermediate **17** was obtained by treating dilithium dianion **15** with commercially available 2,6-dimethoxy-benzoyl chloride, followed by acidification. The resulting β -diketone intermediate **17** was used without purification for the cyclization to zapotin **18** under acidic conditions (Scheme 3).⁷

2.2.2. Metal-catalyzed approaches

In 2000, Zang & co-workers reported a palladium-thiourea-dppp complex mediated regioselective carbonylative-annulation reaction between iodophenol acetates (**19**) and phenylacetylenes (**20**) to construct chromone derivatives (**21**) in good yields (Scheme 4, a).⁸



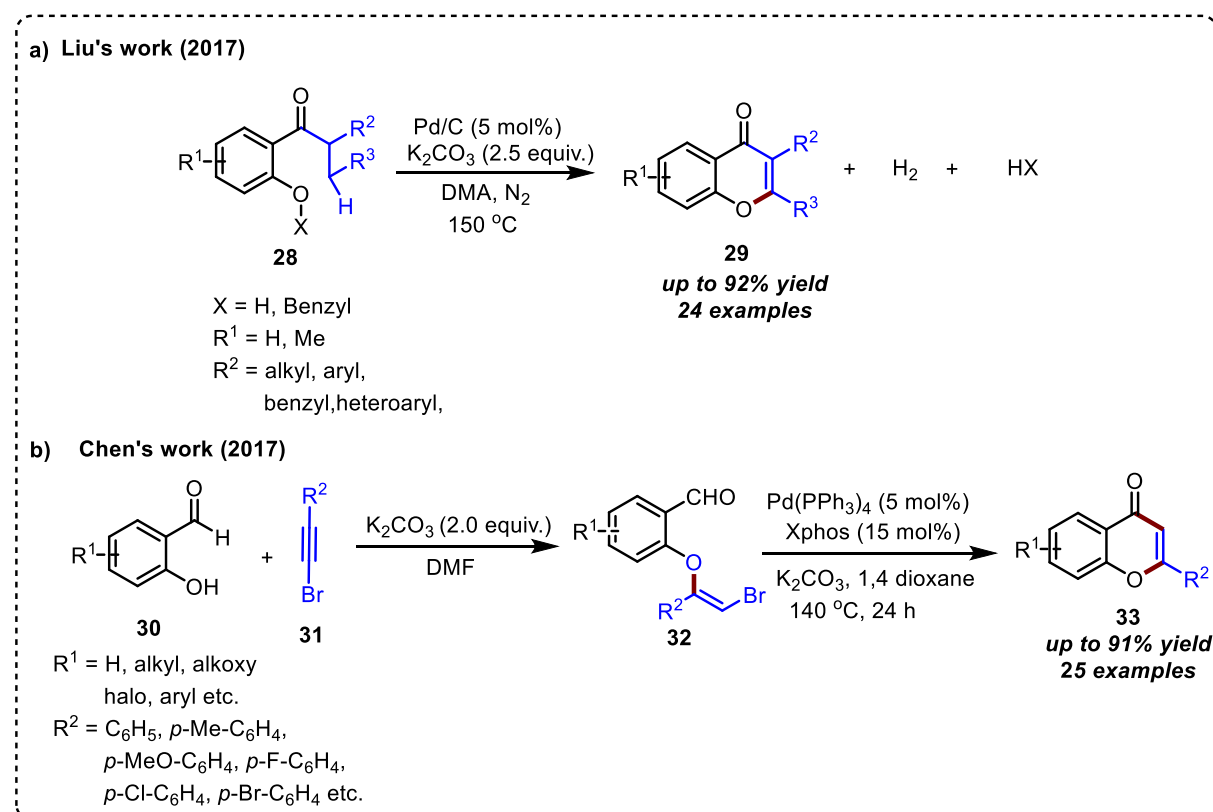
Scheme 3. H₂SO₄-mediated synthesis of chromone



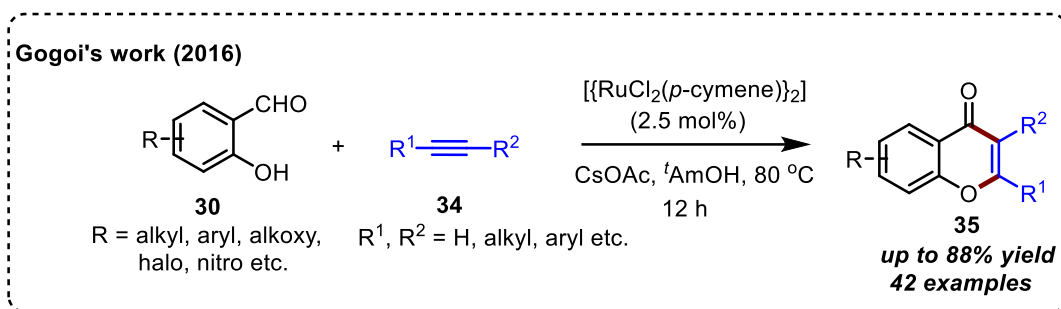
Scheme 4. Pd-catalyzed approaches toward flavones

Later on, Yang & co-workers established the synthesis of chromone derivatives using water as a solvent. They have used PdCl₂ as a catalyst for the copper-free carbonylative Sonagashira reaction of aryl iodides with alkynes. The reaction proceeds through the oxidative addition of aryl iodides to Pd-complex followed by alkyne coordination and intramolecular cyclization to furnish the desired product **21** in moderate to good yields (Scheme 4, **b**).⁹ In 2009, the Capretta group developed Microwave-assisted one-pot Sonagashira carbonylative-annulation reaction between iodophenols and alkynes to access a wide range of flavone derivatives **27** (Scheme 4, **c**).¹⁰

Recently, In 2017, Liu & co-workers disclosed a Pd-catalyzed dehydrogenation of *ortho*-acyl phenols **28** to flavonoid derivatives **29**. They have proposed that in the presence of Pd/C, carbonyl β -C(sp³)-H bond hydrogen of *ortho*-acyl phenols **28** undergoes an intramolecular substitution with phenolic hydroxyls to form *O*-heterocycles, followed by dehydrogenation to generate flavonoids **29** (Scheme 5, **a**).¹¹ In the same year, Chen & co-workers reported a Pd-catalyzed intramolecular acylation reaction of alkenyl bromides **32** with aldehydes to produce a wide range of 4H-chromen-4-one derivatives **33** (Scheme 5, **b**).¹²

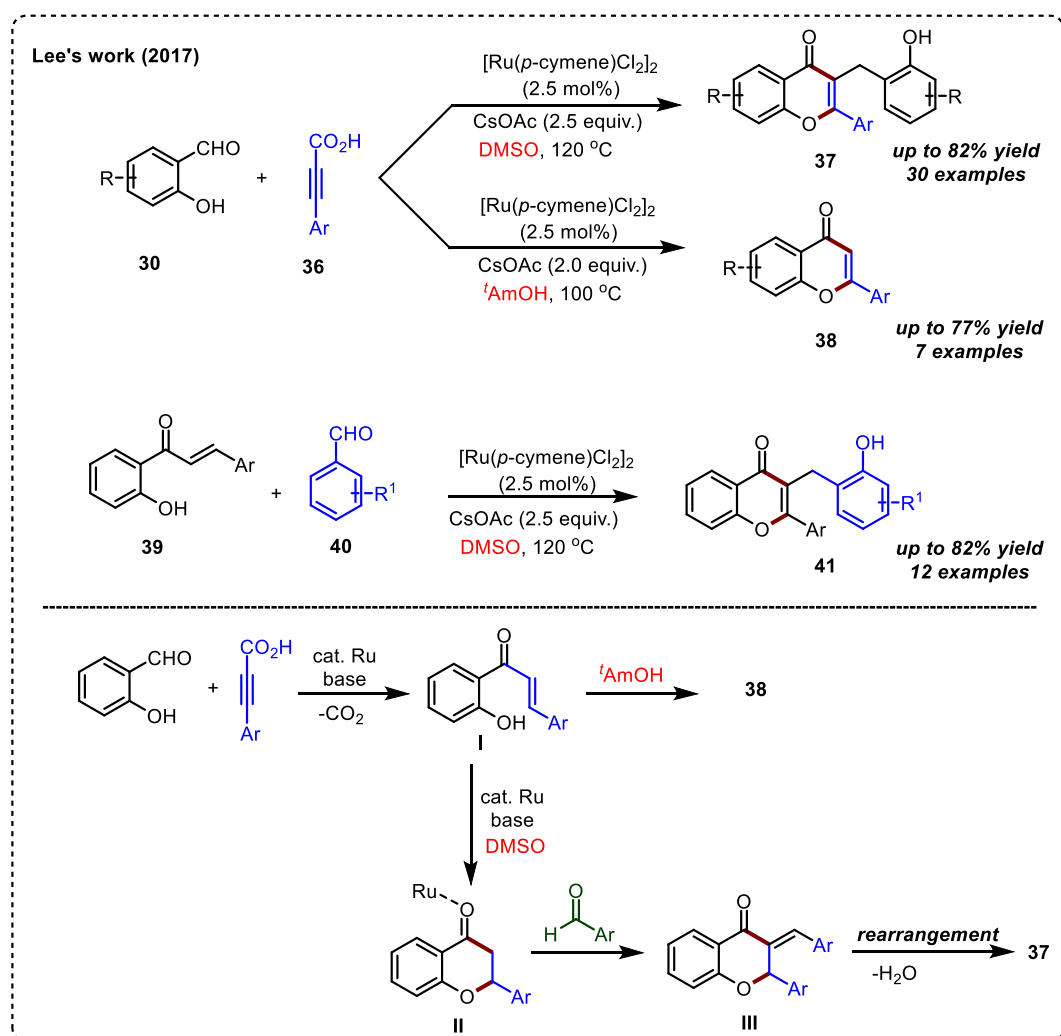


Scheme 5. Synthesis of chromones *via* intramolecular-annulation reactions



Scheme 6. Ru-catalyzed approaches toward flavones

The research group of Gogoi in 2016 reported the Ru-catalyzed C–H activation and annulation reaction between salicylaldehyde derivatives **30** and alkynes **34** to furnish their respective chromone derivatives **35** in good yields. (Scheme 6).¹³

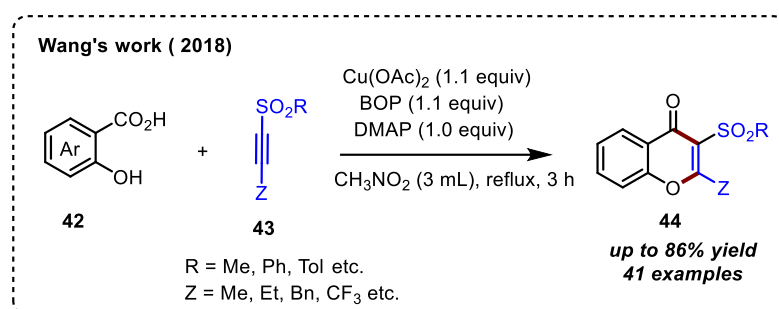


Scheme 7. Lee's approach towards chromone synthesis

In 2017, Lee & co-workers reported the synthesis of homo-isoflavanoids and flavonoids using alkyne acid **36** and salicylaldehydes **30**. They proposed that when DMSO was the

solvent of choice, they got homo-isoflavanoids derivatives (**37**) exclusively in good yields, but when they changed the solvent to *t*-AmOH, they observed the formation of flavone derivatives (**38**) under identical reaction conditions. According to the proposed reaction mechanism, in the presence of base and Ru, decarboxylation of alkynoic acid occurs, followed by addition to salicylaldehyde to form corresponding chalcone intermediate **I**, which gets converted into flavone **38** in *t*-AmOH. However, chromanone **II** was produced in DMSO under the given reaction condition. Chromanone **II** with aldehyde undergoes a Ru-catalyzed aldol reaction to give intermediate **III**, which experiences dehydration followed by rearrangement in DMSO to furnish the desired product **37** (Scheme 7).¹⁴

Wang's research group, in 2018, established a Cu-mediated [4+2]-annulation reaction between salicylic acids (**42**) and sulfonyl acetylenes (**43**) to access a wide range of sulfonyl chromen-4-ones (**44**) in good yields. This methodology was further elaborated to synthesize pyrazole derivatives in excellent yield by treatment of **44** with N₂H₄ via [3+2]-annulation approach (Scheme 8).¹⁵

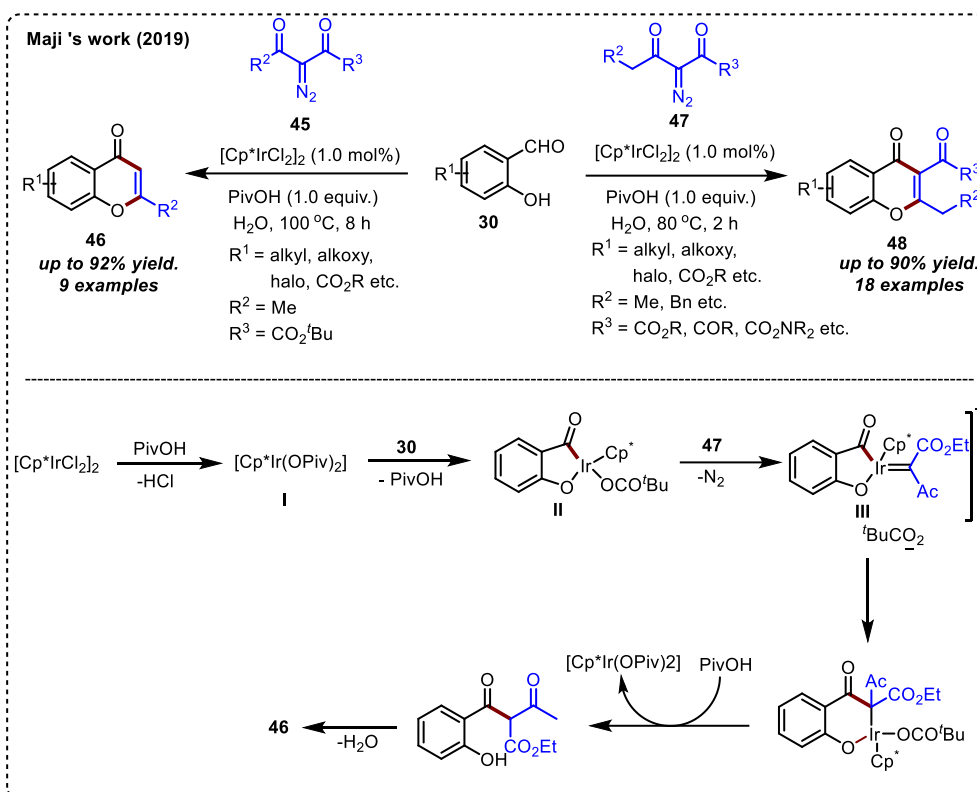


Scheme 8. Synthesis of sulfonyl chromen-4-ones

The research group of Maji in 2019 reported a Ir(III)-catalyzed C–H functionalization reaction in the water to synthesize chromone derivatives (**46/48**) via annulation between salicylaldehydes (**30**) and diazo compounds (**45/47**). According to the authors, [Cp*IrCl₂] gets activated by pivalic acid to form active catalyst **I**, which then interacts with aldehyde C–H and hydroxyl group to form intermediate **II**. The intermediate **II** reacts with diazo-compound to give iridium-carbenoid species **III**, which undergoes migratory insertion and delivers the product **46/48** along with the regeneration of the catalyst (Scheme 9).¹⁶

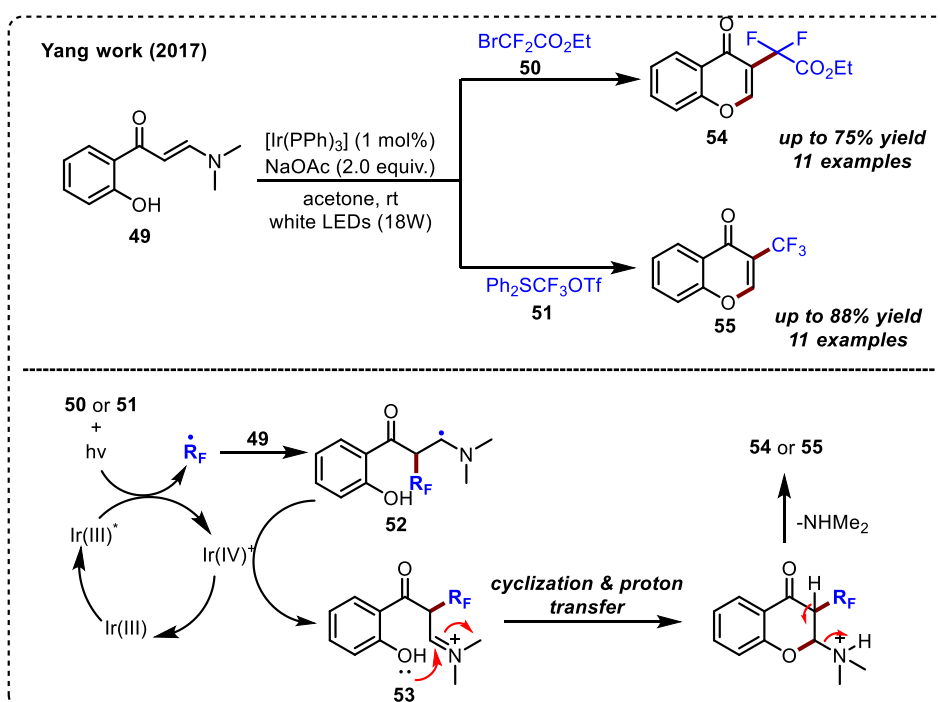
2.3 Literature reports on enaminone for the synthesis of C-3 functionalized chromone

In 2017, Chen, Yang's and co-workers established a visible light-driven synthesis of C-3 functionalized chromones using 2-hydroxy *N,N*-dimethyl enaminones (**49**). They have prepared a wide range of perfluoroalkyl-substituted chromones (**54/55**) in moderate to good



Scheme 9. Ir-catalyzed synthesis chromen-4-ones

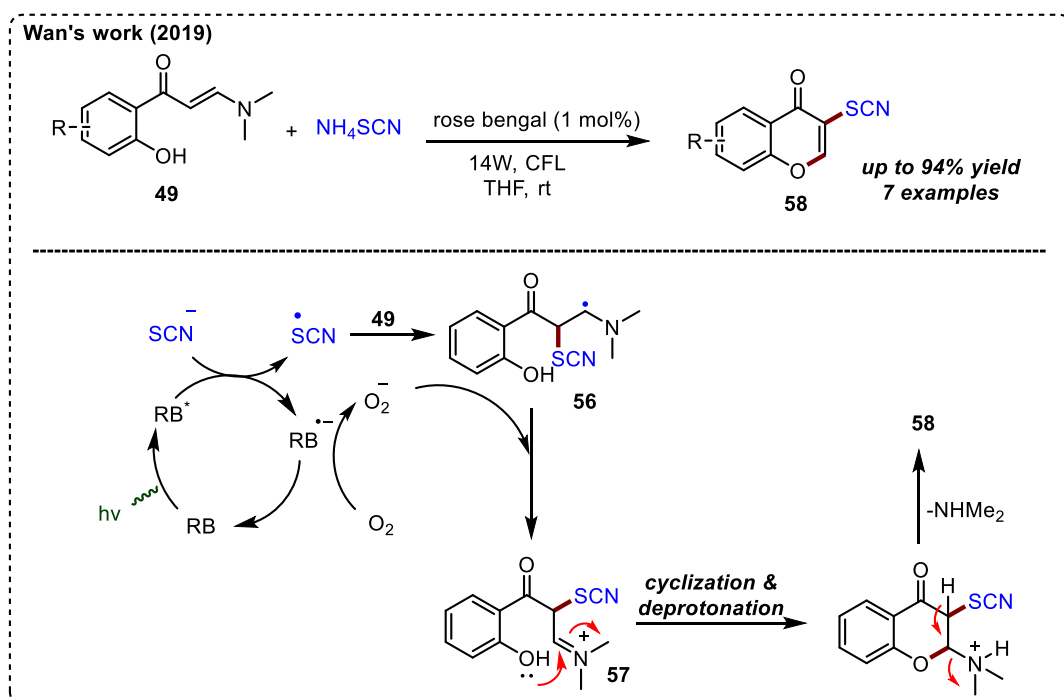
yields. Under the optimized reaction conditions with BrCF₂CO₂Et, difluoroalkyl chromones (**54**) were obtained. However, when Ph₂SCF₃OTf was used as a coupling partner, trifluoroalkyl



Scheme 10. Synthesis of perfluoroalkyl chromones

chromones (**55**) were produced in good yield. According to the proposed reaction mechanism, Ir(III) gets activated under white LED to Ir(III)*. The excited Ir(III)* species reacts with fluorinating agent to generate $\cdot R_F$, which then incorporates into enaminone **49** to yield radical intermediate **52**. The radical intermediate **52** further undergoes oxidation with Ir(IV)⁺ to regenerate the Ir(III) along with the generation of iminium ion intermediate **53**, which experiences cyclization & proton transfer along with the elimination of $-NHMe_2$ group to furnish the products (Scheme 10).¹⁷

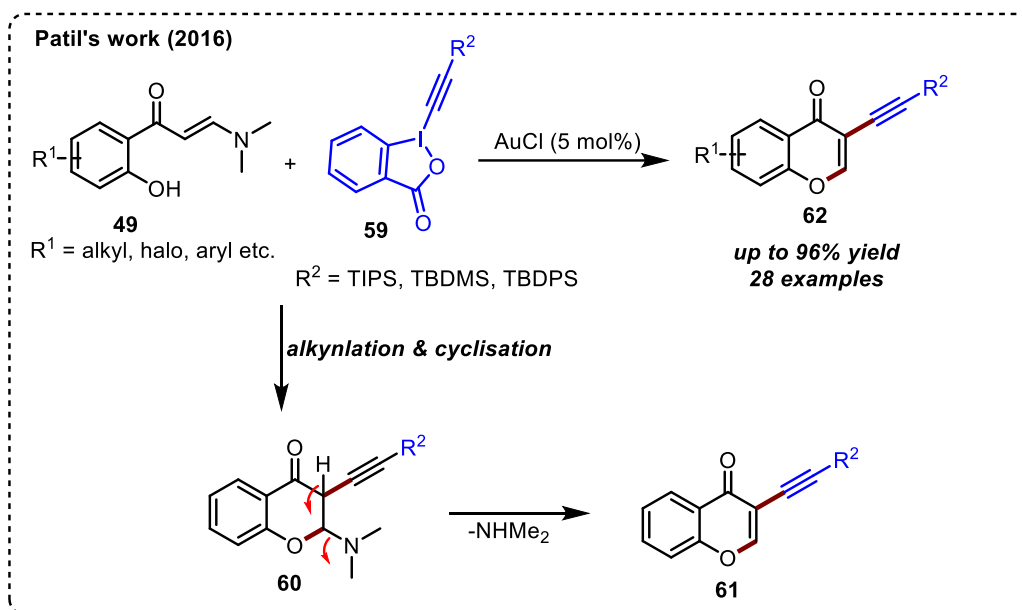
Wan research group, in 2019, successfully produced 3-thiocyanochromones (**58**) by irradiating enaminones (**49**) and NH_4SCN with constant visible light. This approach only needed 1 mol% of Rose Bengal (RB) as the photo-redox catalyst and air oxygen as the oxidant. In the presence of visible light, the RB catalyst converts to an excited state (RB*) which allows the formation of the SCN free radical through a single electron transfer. The SCN free radical adds to the C=C bond of the enaminone to generate **56**, along with the simultaneous oxidation of molecular oxygen to regenerate the catalyst (RB). The radical intermediate **56** transforms into iminium ion intermediate **57**, which then gets converted into product **58** via subsequent cyclization and deprotonation (Scheme 11).¹⁸



Scheme 11. Visible-light-driven synthesis of thiocyanated chromones

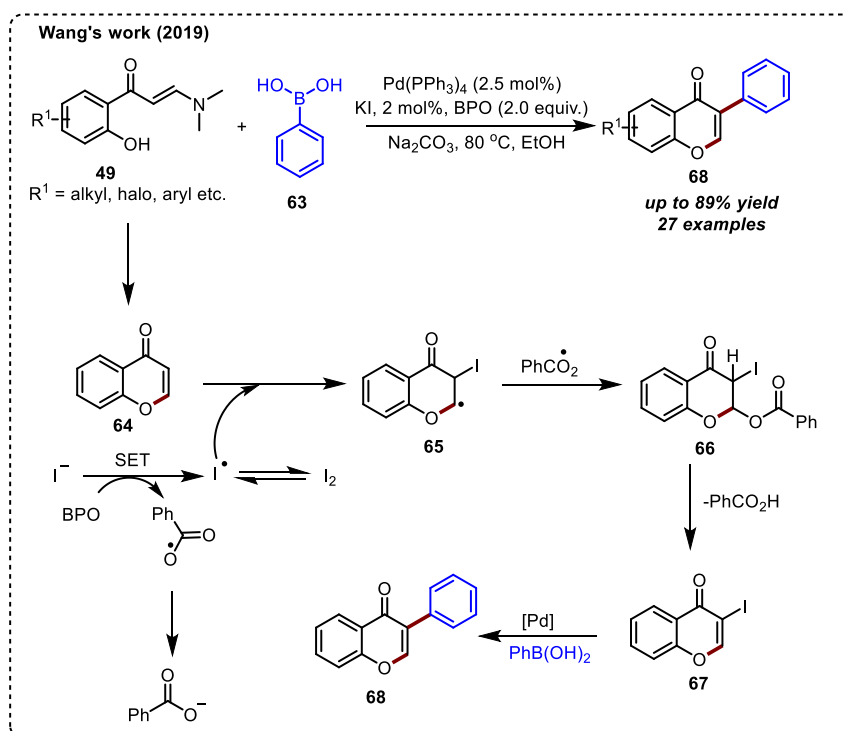
In 2016, Patil & co-workers disclosed a gold-mediated synthesis of 3-alkynyl chromones using 2-hydroxy *N,N*-dimethyl enaminones (**49**). The reaction proceeds through

the tandem alkylation of enaminone **49** followed by intramolecular cyclization to furnish the desired 3-alkynyl chromone derivatives **62** in excellent yields (Scheme 12).¹⁹



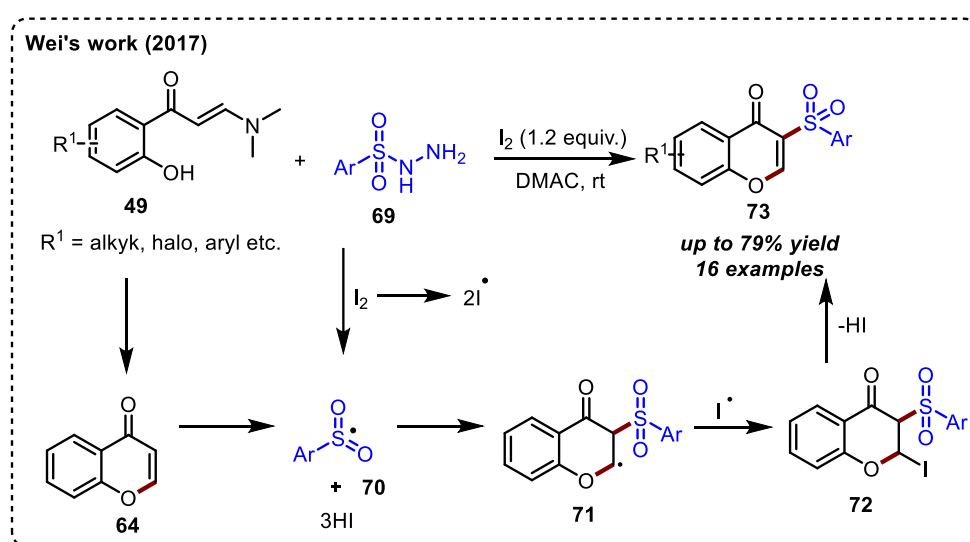
Scheme 12. Gold-mediated synthesis of alkylation chromones

Very recently, Wang's research group has established an exciting and fascinating approach based on transient and recyclable halogenation coupling (TRHC) between 2-hydroxy phenyl substituted enaminones (**49**) and aryl boronic acids (**63**) [Scheme 13]. This approach



Scheme 13. Wang's approach towards 3-aryl substituted chromones.

employs a new coupling protocol in constructing C-C bonds. In addition to being free of substrate pre-functionalization and stoichiometric hydrogen waste, the current coupling strategy drives unusual site selectivity to the chromone C-3 position instead of the C-2 position. According to the proposed reaction mechanism, thermo-induced homo-cleavage of benzoyl peroxide (BPO) will generate benzoyloxy radical, which experiences SET with iodide anion to afford iodine radical which incorporates into *in-situ* generated chromone **64** to provide **65** by radical addition. The radical intermediate **65** immediately interacts with another benzoyloxy radical molecule, leading to intermediate **66**. This intermediate endures β -elimination of benzoic acid to produce 3-iodo-chromones **67**, which subsequently undergoes Pd-catalyzed Suzuki cross-coupling between aryl boronic acid and C(sp²-I) to furnish the 3-aryl substituted chromones **68** in good yields (Scheme 13).²⁰

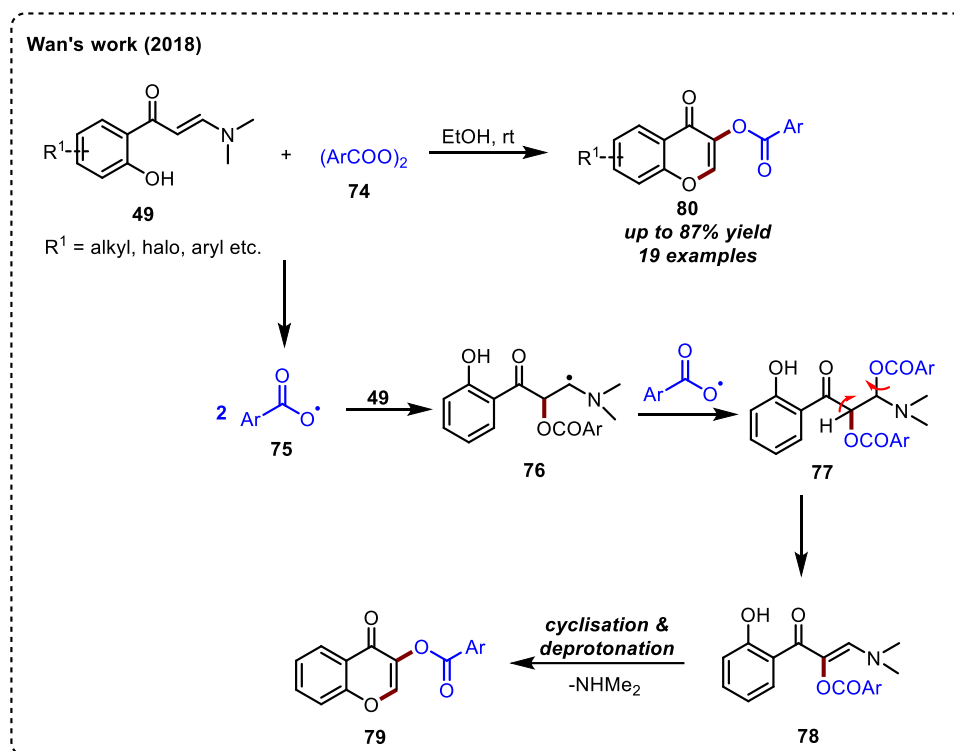


Scheme 14. I₂-mediated synthesis of 3-sulfonyl chromones

In 2017 Wei and co-workers utilized enaminones and sulfonyl hydrazines for constructing 3-sulfonyl chromones derivatives in moderate to good yields. The reaction occurs through the homolytic cleavage of molecular iodine to form an iodine-free radical, which reacts with sulfonyl hydrazine **69** to provide sulfonyl free radical **70** by extrusion of nitrogen from the molecule. The free radical **70** then reacts with the C=C bond of chromone **64** to generate another radical species **71**, which again traps iodine to produce **72**, which finally undergoes elimination to give desired 3-sulfonyl chromone derivatives **73** (Scheme 14).²¹

Later, in 2018, Wan's group developed a catalyst-free protocol for synthesizing acyloxy chromones using enaminone **49** and aroyl peroxides **74** as coupling partners. Simple

stirring of the coupling partners at room temperature provided the desired acyloxyl chromones **80** in excellent yields (Scheme 15).²²



Scheme 15. Synthesis of 3-acyloxyl chromones

2.4 Background

Although most of the approaches discussed above offer a wide range of substrates, the challenging reaction conditions and the costly metal catalysts or ligands required to carry out these transformations make them unattractive. Additionally, their practical applicability is constrained by the need to synthesize pre-functionalized starting materials, tedious workup processes, or the employment of stoichiometric activation agents. Therefore, it would be more appealing and highly desired to create an alternate and more effective approach for synthesizing 4H-Chromen-4-one, especially under organocatalytic circumstances.

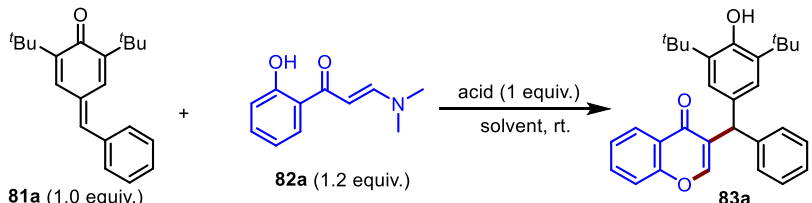
In recent years, significant progress has been made in the synthetic elaboration of *p*-quinone methides (*p*-QMs).¹⁵ Our research group also contributed in this area, focusing mainly on the synthetic uses of *p*-QMs to obtain heterocycles¹⁶ carbocycles¹⁷ and triaryl- and diarylmethanes.¹⁸ While exploring *p*-QMs as synthons in the synthesis of oxygen-containing heterocycles,¹⁹ we discovered that it is feasible to access 4H-chromen-4-one through an acid-mediated reaction between enaminones²⁰ and *p*-QMs. To the best of our knowledge, the

reaction between *p*-QMs and enaminones leads to 4H-chromen-4-one has not been reported so far, prompting us to work on this specific transformation.

2.5. Result and discussion

To find out the optimal reaction conditions for the synthesis of 4H-chromen-4-ones, the reaction between *p*-QM (**81a**, 1.0 equiv.) and 2-hydroxy phenyl substituted *N,N*-dimethyl enaminone (**82a**, 1.2 equiv) was examined under different acidic conditions, and the results are

Table 1. Optimization study^a



Entry	Acid	Solvent	Time [h]	Yield [%] 83a
1	CSA	CH ₃ CN	2	80
2	TFA	CH ₃ CN	2	85
3	TsOH	CH₃CN	2	95
4	TsOH	1,2-DCE	2	92
5	TsOH	DMF	2	86
6	TsOH	PhMe	5	72
7	TsOH	THF	5	68
8	TsOH	Et ₂ O	5	50

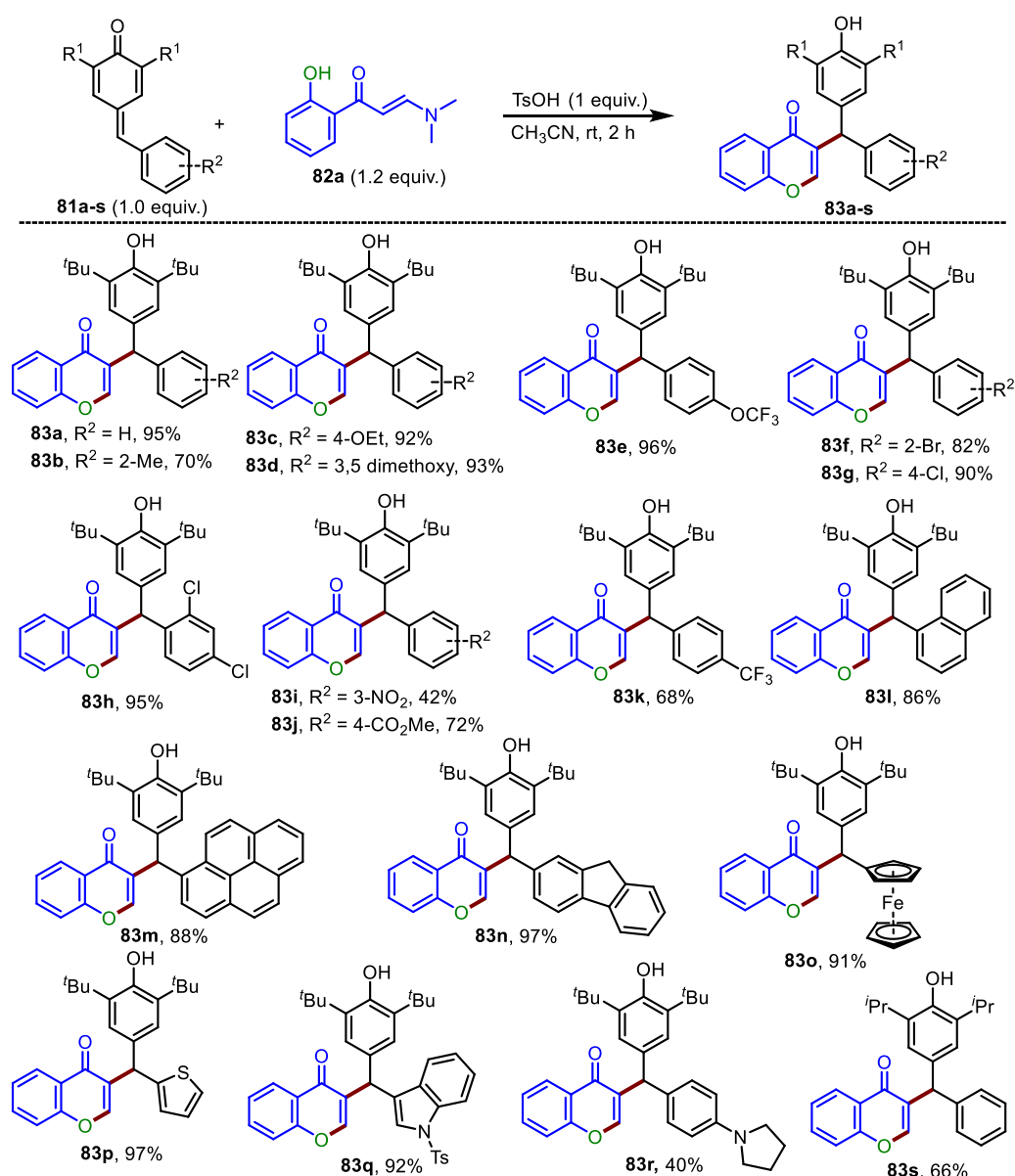
All reactions were carried out with **81a** (0.136 mmol), **82a** (0.1632 mmol) and TsOH (1.0 equiv.) in 1.5 mL of solvent. The yields reported are isolated yields.

summarized in Table 1. An extensive catalyst screening diagnostics have been performed with acid catalysts in CH₃CN medium. With CSA and TFA, the respective 4H-chromenones derivative **83a** was obtained in 80% and 85% isolated yields, respectively (entries 1 & 2). To our delight, in the experiment with TsOH (1 equiv.), the desired 4H-chromen-4-ones derivative **83a** was obtained in 95% yield within 2h at room temperature (entry 3). Further, to investigate the role of solvent few experiments have been carried out using different solvents (entries 4-8). Solvents such as 1,2 DCE and DMF were found to be effective for this transformation and the respective product **83a** was obtained in excellent yields (entries 4 & 5). Toluene and THF were also found to be suitable under the standard reaction condition, however, the reaction took

longer time to complete (entries 6 & 7). Et₂O was found to be less effective to drive this transformation (entry 8).

While evaluating the scope and limitation of this transformation, the optimal condition (entry 3, Table 1) was employed for the reaction between various *p*-QMs **81a-s** and *N,N*-dimethyl enaminones **82a**, and the results are summarized in Scheme 16. Electron-rich aryl-

Scheme 16. Substrate Scope with 2-Hydroxyphenyl-substituted Enaminone **82a** and various *p*-QMs (**81a-s**).

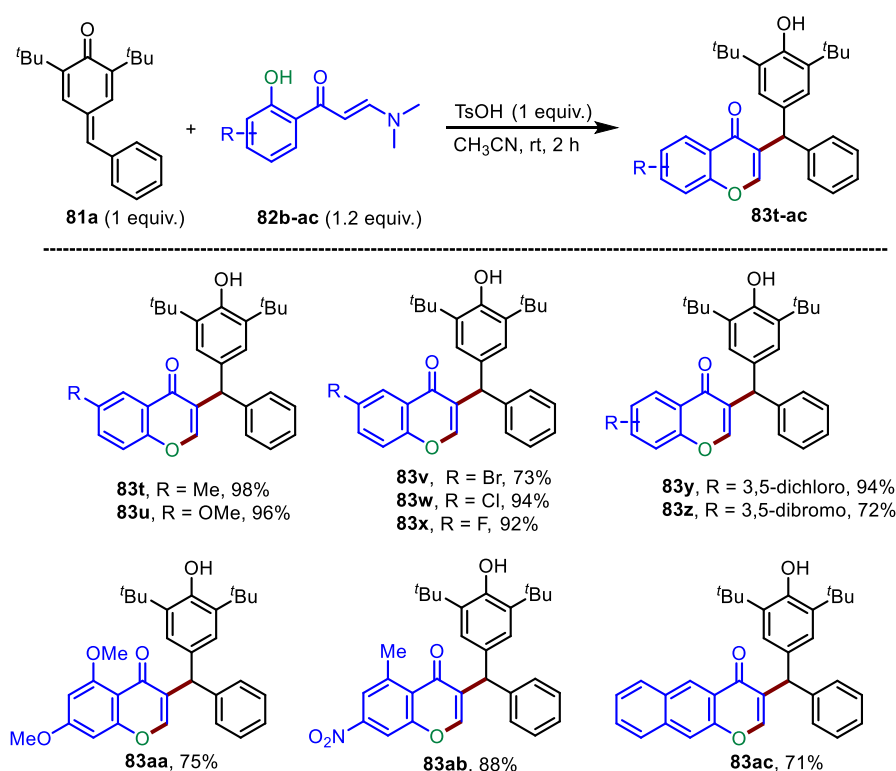


^aAll reactions were carried out with 40 mg scale of **81a-s** in 1.5 mL of MeCN. Yields reported are isolated yields.

substituted *p*-QMs (**81b-e**) furnished the respective 4H-chromen-4-ones **83b-e** in the range of 70-96% yields. Similarly, halo-substituted *p*-QMs (**81f-h**) reacted with **82a** under optimal

conditions and gave the corresponding products **83f-h** in good yields (82-95%). However, this protocol was found to be a bit less effective for the reactions between electron-poor *p*-QMs (**81i-k**) and **82a** and the respective products **83i-k** were obtained in relative lesser yields (42-72%). This approach was also found to be operative for *p*-QMs (**81l-q**), substituted with various higher order aromatic hydrocarbons and heteroarenes and, in all those cases, the corresponding 4H-chromones **83l-q** were isolated in good to excellent yields (86-97%). However, 4-(pyrrolidinyl)aryl-substituted *p*-QM **81r** reacted with **82a** to give the respective product **83r** only in 40% yield. The *p*-QM (**81s**), derived from 2,6-diisopropyl-phenol and benzaldehyde, also underwent reaction with **82a** and provided **83s** in 66% yield.

Scheme 17. Elaboration of Substrate Scope using different 2-Hydroxyphenyl-substituted *N,N*-dimethyl enaminones (**82b-ac**).^a

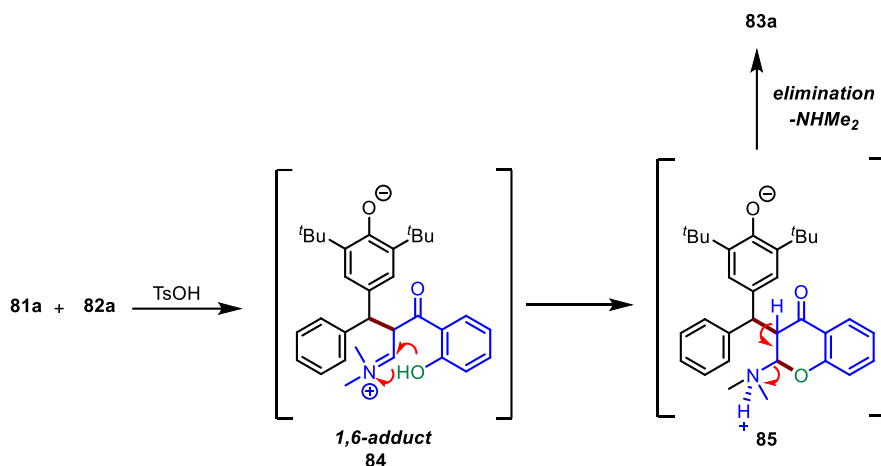


^aAll reactions were carried out with 40 mg scale of **81a** in 1.5 mL of MeCN. Yields reported are isolated yields.

Similarly, other 2-hydroxyphenyl-substituted *N,N*-dimethyl enaminones **82b-j** were also subjected to the reaction with **81a** under standard conditions to give their respective 4H-chrome-4-none derivatives **83t-ac** in excellent yields (72-98%) (Scheme 17). *N,N*-dimethyl enaminones (**82b-h**) derived from 2-hydroxy acetophenone derivatives having alkyl and halo substituent on the aryl ring react well with *p*-QM under the standard reaction condition to yield their respective chromone derivatives (**83t-z**) in good to excellent yields. It has been found that

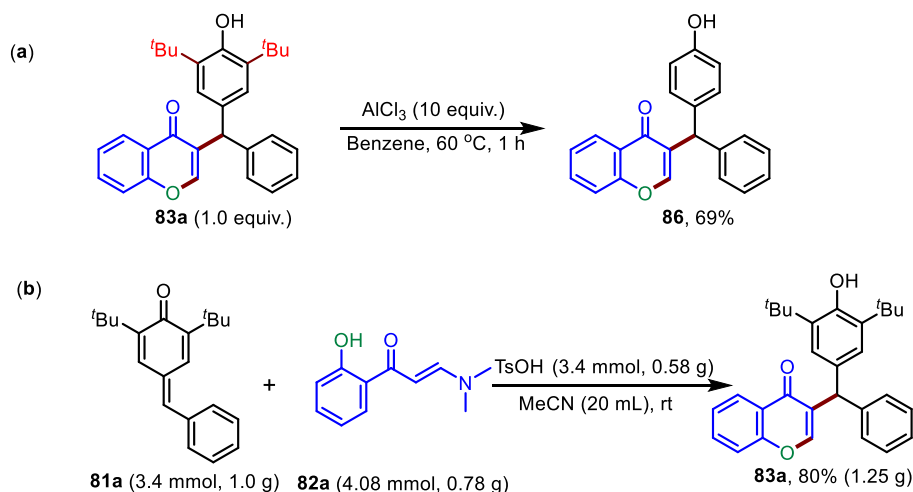
other enaminones such as (**82aa-ac**) irrespective of the electronic nature of group attached furnish their desired products (**83aa-ac**) in moderate to good yields.

Based on the above-mentioned observations and control experiments, a plausible mechanism for the formation of 4H-chromen-4-one **83a** has been proposed (Scheme 18).



Scheme 18. Proposed mechanism of formation of 4H-chromen-4-one

Initially, *p*-QM **81a** gets activated by TsOH acid, which then undergoes 1,6-conjugate addition with enaminone **82a** to generate an 1,6-conjugate adduct **84**. Then adduct **84** undergoes an intramolecular cyclization to form the cyclized intermediate **85** which subsequently undergoes acid-mediated elimination of -NHMe_2 group to give the product **83a**.



Scheme 19. Synthetic elaboration and gram-scale reaction

Next, to show the practical applications of this transformation, one of the 4H-chromen-4-one derivatives, **81a** was subjected to de-*tert*-butylation reaction with excess of AlCl_3 to produce the respective de-*tert*-butylated product **86** in 69% yield (**a**, Scheme 19). To show the scalability of this transformation, a relatively larger scale reaction (1.0 g scale) was performed

using **81a** and, in this case, the desired 4H-chromen-one derivative **83a** was obtained in 80% yield (**b**, Scheme 19).

2.6 Conclusion

In conclusion, we have successfully demonstrated a Brønsted acid-mediated approach for the synthesis of 4H-chromen-4-ones through a 1,6-conjugate addition of *N,N*-dimethyl enaminones to *p*-QMs followed by intramolecular cyclization/elimination sequence. A wide range of 4H-chromen-4-ones could be accessed in good to excellent yields by treating 2-hydroxyphenyl-substituted enaminones and simple *p*-QMs. Since 4H-chromen-4-ones are considered as one of the privileged class of compounds in drug discovery, we believe the developed methodology would definitely be useful for the synthesis of those drugs and related natural products.

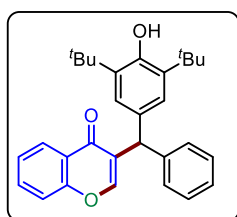
2.7 Experimental Section

General Information. All reactions were carried out under an argon atmosphere in an oven dried round bottom flask. All the solvents were distilled before use and stored under argon atmosphere. Most of the reagents and starting materials were purchased from commercial sources and used as such. 2-hydroxyphenyl-substituted *N,N*-Dimethyl enaminones were prepared according to the literature procedure.²⁷ *para*-quinone methides were prepared by following a literature procedure.²³ Melting points were recorded on SMP20 melting point apparatus and are uncorrected. ¹H, ¹³C and ¹⁹F spectra were recorded in CDCl₃ and DMSO (400, 100 and 376 MHz respectively) on Bruker FT-NMR spectrometer. Chemical shift (δ) values are reported in parts per million relative to TMS and the coupling constants (*J*) are reported in Hz. High resolution mass spectra were recorded on Waters Q-TOF Premier-HAB213 spectrometer. FT-IR spectra were recorded on a Perkin-Elmer FTIR spectrometer. Thin layer chromatography was performed on Merck silica gel 60 F₂₅₄ TLC pellets and visualized by UV irradiation and KMnO₄ stain. Column chromatography was carried out through silica gel (100–200 mesh) using EtOAc/hexane as an eluent.

General procedure for the synthesis of 4H-Chromen-4-one derivatives (83a-y) from *para*-Quinone Methides (81a-s) and 2-hydroxy *N,N*-dimethyl phenyl substituted enaminones (82a-j):

TsOH (1 equiv.) was added to a mixture of *para*-quinone methide (40 mg, 1.0 equiv., 0.136 mmol) and 2-hydroxy *N,N*-dimethyl phenyl substituted enaminones (1.2 equiv., 0.163 mmol) dissolved in Acetonitrile (1.5 mL). Then resulting reaction mixture was stirred at room temperature. After the reaction was complete (based on TLC analysis), residue was then concentrated under reduced pressure and the residue was then purified through a silica gel column using EtOAc/Hexane mixture as an eluent to get the pure product.

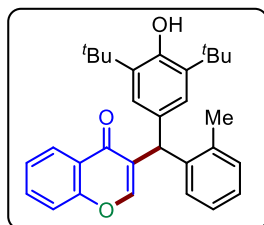
3-((3,5-di-*tert*-butyl-4-hydroxyphenyl)(phenyl)methyl)-4H-chromen-4-one (83a): The



reaction was performed at 0.136 mmol scale of **81a**; white solid (57.1 mg, 95% yield); m. p. = 178–180 °C; R_f = 0.4 (10% EtOAc in hexane); ^1H NMR (400 MHz, CDCl_3) δ 8.24 (dd, J = 8.0, 1.4 Hz, 1H), 7.68 – 7.63 (m, 1H), 7.45 – 7.43 (m, 2H), 7.41 – 7.37 (m, 1H), 7.34 – 7.30 (m, 2H), 7.26 – 7.18 (m, 3H), 6.99 (s, 2H), 5.74 (s, 1H), 5.16 (s, 1H), 1.40 (s, 18H);

$^{13}\text{C}\{^1\text{H}\}$ NMR (100 MHz, CDCl_3) δ 176.8, 156.3, 155.4, 152.5, 142.2, 135.9, 133.5, 131.7, 128.9, 128.6, 128.5, 126.5, 126.3, 125.7, 125.0, 124.0, 118.1, 47.0, 34.5, 30.4; FT-IR (thin film, neat): 3637, 2957, 1644, 1349, 783 cm^{-1} ; HRMS (ESI): m/z calcd for $\text{C}_{30}\text{H}_{33}\text{O}_3$ $[\text{M}+\text{H}]^+$: 441.2430; found : 441.2427.

3-((3,5-di-*tert*-butyl-4-hydroxyphenyl)(*o*-tolyl)methyl)-4H-chromen-4-one (83b): The

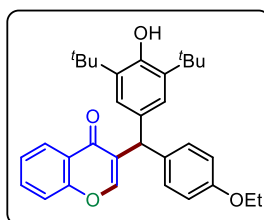


reaction was performed at 0.129 mmol scale of **81b**; white solid (40.0 mg, 70% yield); m. p. = 187–189 °C; R_f = 0.4 (10% EtOAc in hexane); ^1H NMR (400 MHz, CDCl_3) δ 8.22 (dd, J = 8.0, 1.5 Hz, 1H), 7.67 – 7.63 (m, 1H), 7.43 (d, J = 8.1 Hz, 1H), 7.40 – 7.36 (m, 1H), 7.35 (d, J = 0.8 Hz, 1H), 7.19 – 7.17 (m, 1H), 7.15 – 7.07 (m, 2H), 6.97 – 6.95 (m,

1H), 6.93 (s, 2H), 5.79 (s, 1H), 5.10 (s, 1H), 2.34 (s, 3H), 1.37 (s, 18H); $^{13}\text{C}\{^1\text{H}\}$ NMR (100 MHz, CDCl_3) δ 176.9, 156.4, 155.2, 152.5, 140.6, 136.7, 135.9, 133.5, 130.8, 130.7, 128.3, 127.7, 126.6, 126.3, 125.8, 125.7, 125.1, 123.9, 118.2, 43.6, 34.5, 30.4, 19.9; FT-IR (thin film, neat): 3636, 2956, 1642, 1182, 780 cm^{-1} ; HRMS (ESI): m/z calcd for $\text{C}_{31}\text{H}_{35}\text{O}_3$ $[\text{M}+\text{H}]^+$: 455.2586; found : 455.2594.

3-((3,5-di-*tert*-butyl-4-hydroxyphenyl)(4-ethoxyphenyl)methyl)-4H-chromen-4-one

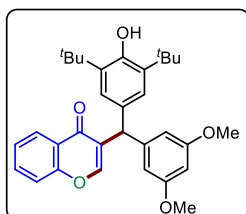
(83c): The reaction was performed at 0.110 mmol scale of **81c**; pale yellow solid (49.0 mg,



92% yield); m. p. = 88–90 °C; R_f = 0.4 (10% EtOAc in hexane); δ 8.22 (dd, J = 8.0, 1.4 Hz, 1H), 7.67 – 7.62 (m, 1H), 7.43–7.41 (m, 2H), 7.37 (t, J = 7.8, 1H), 7.12 (d, J = 8.6 Hz, 2H), 6.96 (s, 2H), 6.83 (d, J = 8.6 Hz, 2H), 5.65 (s, 1H), 5.11 (s, 1H), 4.00 (q, J = 6.9 Hz, 2H), 1.40 (t, J

= 7.0 Hz, 3H), 1.38 (s, 18H); $^{13}\text{C}\{^1\text{H}\}$ NMR (100 MHz, CDCl_3) δ 176.9, 157.6, 156.4, 155.3, 152.5, 135.8, 134.1, 133.5, 132.1, 129.9, 128.9, 126.4, 125.7, 125.0, 124.0, 118.1, 114.5, 63.5, 46.2, 34.5, 30.4, 15.0; FT-IR (thin film, neat): 3637, 2958, 1644, 1574, 762 cm^{-1} ; HRMS (ESI): m/z calcd for $\text{C}_{32}\text{H}_{37}\text{O}_4$ $[\text{M}+\text{H}]^+$: 485.2692; found : 485.2696.

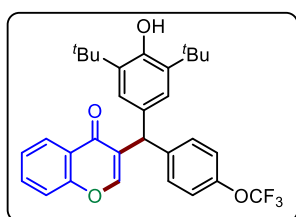
3-((3,5-di-*tert*-butyl-4-hydroxyphenyl)(3,5-dimethoxyphenyl)methyl)-4H-chromen-4-one (83d): The reaction was performed at 0.112 mmol scale of **81d**; pale yellow solid (51.1 mg,



93% yield); m. p. = 90–92 °C; R_f = 0.4 (10% EtOAc in hexane); ^1H NMR (400 MHz, CDCl_3) δ 8.21 (dd, J = 8.0, 1.4 Hz, 1H), 7.66 – 7.62 (m, 1H), 7.42 (t, J = 4.1 Hz, 2H), 7.37 (t, J = 7.9 Hz, 1H), 6.99 (s, 2H), 6.38 (d, J = 2.3 Hz, 2H), 6.33 (t, J = 2.2 Hz, 1H), 5.63 (s, 1H), 5.13 (s, 1H), 3.74 (s, 6H), 1.38 (s, 18H); $^{13}\text{C}\{^1\text{H}\}$ NMR (100 MHz, CDCl_3) δ 176.9, 160.8, 156.4, 155.4, 152.6, 144.8, 135.9, 133.6, 131.3, 128.4, 126.3, 125.6, 125.1, 124.0, 118.1, 107.4, 98.4, 55.4, 55.3, 47.1, 34.5, 30.4; FT-IR (thin film, neat): 3636, 2957, 1642, 1466, 761 cm^{-1} ; HRMS (ESI): m/z calcd for $\text{C}_{32}\text{H}_{37}\text{O}_5$ $[\text{M}+\text{H}]^+$: 501.2641; found : 501.2646.

3-((3,5-di-*tert*-butyl-4-hydroxyphenyl)(4-(trifluoromethoxy)phenyl)methyl)-4H-

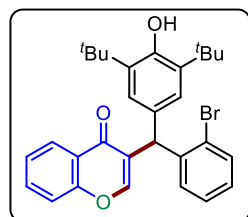
chromen-4-one (83e): The reaction was performed at 0.105 mmol scale of **81e**; white solid



(55.0 mg, 96% yield); m. p. = 138–140 °C; R_f = 0.6 (10% EtOAc in hexane); ^1H NMR (400 MHz, CDCl_3) δ 8.22 (dd, J = 8.0, 1.4 Hz, 1H), 7.69 – 7.65 (m, 1H), 7.42 (d, J = 8.4 Hz, 1H), 7.42 – 7.38 (m, 2H), 7.27 – 7.25 (m, 2H), 7.15 (d, J = 8.2 Hz, 2H), 6.92 (s, 2H) 5.70 (s, 1H), 5.17 (s, 1H), 1.38 (s, 18H); $^{13}\text{C}\{^1\text{H}\}$ NMR (100 MHz, CDCl_3) δ 176.8, 156.4, 155.5, 152.8, 147.9 (q, $J_{\text{C-F}}$ = 1.73 Hz), 141.0, 136.2, 133.8, 131.2, 130.1, 128.2, 126.3, 125.7, 125.2, 124.0, 121.0 (q, $J_{\text{C-F}}$ = 255.3 Hz), 120.9, 118.2, 46.5, 34.5, 30.4; $^{19}\text{F}\{^1\text{H}\}$ NMR (376 MHz, CDCl_3) δ – 57.85; FT-IR (thin film, neat): 3639, 2997, 1645, 1507, 728 cm^{-1} ; HRMS (ESI): m/z calcd for $\text{C}_{31}\text{H}_{32}\text{F}_3\text{O}_4$ $[\text{M}+\text{H}]^+$: 525.2253; found : 525.2261.

3-((2-bromophenyl)(3,5-di-*tert*-butyl-4-hydroxyphenyl)methyl)-4H-chromen-4-one (83f):

The reaction was performed at 0.107 mmol scale of **81f**; yellow solid (45.0 mg, 82% yield); m.

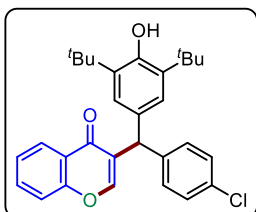


p. = 216–218 °C; R_f = 0.4 (10% EtOAc in hexane); ^1H NMR (400 MHz, CDCl_3) δ 8.22 (dd, J = 8.0, 1.3 Hz, 1H), 7.67 – 7.63 (m, 1H), 7.59 (d, J = 7.7 Hz, 1H), 7.43 (d, J = 8.4 Hz, 1H), 7.38 (t, J = 7.6 Hz, 1H), 7.34 (s, 1H), 7.21 (t, J = 7.5 Hz, 1H), 7.10 (td, J = 6.3, 1.4 Hz, 1H), 7.04 (d, J = 7.7, 1H), 6.97 (s, 2H), 5.97 (s, 1H), 5.14 (s, 1H), 1.38 (s, 18H); $^{13}\text{C}\{^1\text{H}\}$ NMR (100 MHz, CDCl_3) δ 176.6, 156.4, 155.0, 152.7, 141.9, 135.9, 133.6, 133.5, 129.8, 129.6, 128.2, 127.5,

127.2, 126.3, 125.9, 125.6, 125.1, 123.9, 118.1, 47.0, 34.5, 30.4; FT-IR (thin film, neat): 3635, 3065, 2958, 1646, 1466, 760 cm^{-1} ; HRMS (ESI): m/z calcd for $\text{C}_{30}\text{H}_{32}\text{BrO}_3$ $[\text{M}+\text{H}]^+$: 519.1535; found : 519.1540.

3-((4-chlorophenyl)(3,5-di-*tert*-butyl-4-hydroxyphenyl)methyl)-4H-chromen-4-one (83g):

The reaction was performed at 0.121 mmol scale of **81g**; white solid (51.0 mg, 90% yield); m.

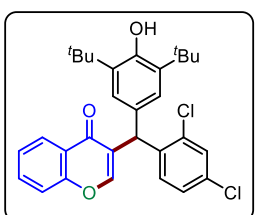


p. = 167–169 °C; R_f = 0.4 (10% EtOAc in hexane); ^1H NMR (400 MHz, CDCl_3) δ 8.22 (dd, J = 8.0, 1.3 Hz, 1H), 7.68 – 7.64 (m, 1H), 7.44 (d, J = 8.4 Hz, 1H), 7.41 – 7.37 (m, 2H), 7.27 (d, J = 8.5 Hz, 2H), 7.18 (d, J = 8.4 Hz, 2H), 6.93 (s, 2H), 5.66 (s, 1H), 5.17 (s, 1H), 1.38 (s, 18H);

$^{13}\text{C}\{^1\text{H}\}$ NMR (100 MHz, CDCl_3) δ 176.8, 156.3, 155.4, 152.7, 140.8, 136.1, 133.7, 132.3, 131.2, 130.2, 128.6, 128.2, 126.3, 125.7, 125.2, 123.9, 118.1, 46.6, 34.5, 30.4; FT-IR (thin film, neat): 3636, 2960, 1644, 1466, 1276, 750 cm^{-1} ; HRMS (ESI): m/z calcd for $\text{C}_{30}\text{H}_{32}\text{ClO}_3$ $[\text{M}+\text{H}]^+$: 475.2040; found : 475.2052.

3-((3,5-di-*tert*-butyl-4-hydroxyphenyl)(2,4-dichlorophenyl)methyl)-4H-chromen-4-one (83h):

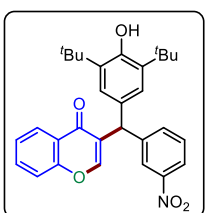
The reaction was performed at 0.110 mmol scale of **81h**; white solid (69.0 mg, 95%



yield); m. p. = 86–88 °C; R_f = 0.6 (10% EtOAc in hexane); ^1H NMR (400 MHz, CDCl_3) δ 8.20 (dd, J = 8.0, 1.5 Hz, 1H), 7.68 – 7.64 (m, 1H), 7.45 – 7.41 (m, 2H), 7.38 (d, J = 7.4 Hz, 1H), 7.35 (s, 1H), 7.15 (dd, J = 8.4, 2.0 Hz, 1H), 7.0 (d, J = 8.4 Hz, 1H), 6.93 (s, 2H), 5.92 (s, 1H), 5.17 (s, 1H), 1.38 (s, 18H);

$^{13}\text{C}\{^1\text{H}\}$ NMR (100 MHz, CDCl_3) δ 176.6, 156.4, 155.1, 152.9, 139.0, 136.2, 135.3, 133.8, 132.9, 130.2, 129.9, 129.0, 127.1, 126.8, 126.3, 125.7, 125.2, 123.9, 118.2, 44.1, 34.5, 30.4; FT-IR (thin film, neat): 3634, 2966, 1648, 1467, 1347, 763 cm^{-1} ; HRMS (ESI): m/z calcd for $\text{C}_{30}\text{H}_{31}\text{ClO}_3$ $[\text{M}+\text{H}]$: 509.1650; found : 509.1645.

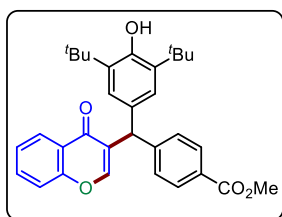
3-((3,5-di-*tert*-butyl-4-hydroxyphenyl)(3-nitrophenyl)methyl)-4H-chromen-4-one (83i):



The reaction was performed at 0.110 mmol scale of **81i**; white solid (22.0 mg, 42% yield); m. p. = 84–86 °C; R_f = 0.4 (10% EtOAc in hexane); ^1H NMR (400 MHz, CDCl_3) δ 8.18 (dd, J = 8.0, 1.4 Hz, 1H), 8.10 – 8.09 (m, 2H), 7.71 – 7.66 (m, 1H), 7.61 (d, J = 7.7 Hz, 1H), 7.50 – 7.45 (m, 2H); 7.44 –

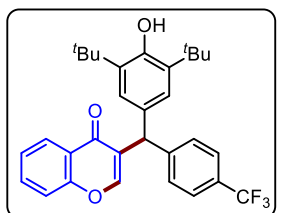
7.39 (m, 2H), 6.90 (s, 2H), 5.72 (s, 1H), 5.19 (s, 1H), 1.37 (s, 18H); $^{13}\text{C}\{^1\text{H}\}$ NMR (100 MHz, CDCl_3) δ 176.8, 156.4, 155.7, 153.0, 148.5, 144.6, 136.5, 135.2, 134.0, 130.2, 129.4, 127.4, 126.3, 125.7, 125.4, 123.9, 123.4, 121.9, 118.3, 47.2, 34.5, 30.3; FT-IR (thin film, neat): 3636, 3005, 2964, 1640, 1466, 1348, 746 cm^{-1} ; HRMS (ESI): m/z calcd for $\text{C}_{30}\text{H}_{32}\text{NO}_5$ $[\text{M}+\text{H}]^+$: 486.2280; found : 486.2274.

4-((3,5-di-*tert*-butyl-4-hydroxyphenyl)(4-oxo-4H-chromen-3-yl)methyl)benzoate (**83j**):



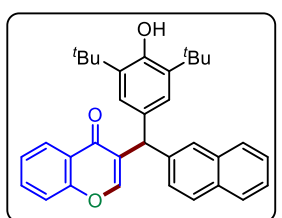
The reaction was performed at 0.113 mmol scale of **81j**; white solid (39.1 mg, 72% yield); m. p. = 142–144 °C; R_f = 0.6 (10% EtOAc in hexane); ^1H NMR (400 MHz, CDCl_3) δ 8.20 (d, J = 7.8 Hz, 1H), 7.97 (d, J = 7.5 Hz, 2H), 7.66 (t, J = 7.7 Hz, 1H), 7.45 – 7.37 (m, 3H), 7.31 (d, J = 7.5, Hz, 2H), 6.92 (s, 2H), 5.72 (s, 1H), 5.17 (s, 1H), 3.89 (s, 3H), 1.36 (s, 18H); $^{13}\text{C}\{^1\text{H}\}$ NMR (100 MHz, CDCl_3) δ 176.8, 167.2, 156.4, 155.5, 152.8, 147.7, 136.2, 133.7, 130.9, 129.9, 128.9, 128.4, 128.0, 126.3, 125.8, 125.2, 123.9, 118.2, 52.15, 52.12, 47.2, 34.5, 30.3; FT-IR (thin film, neat): , 3630, 2956, 1721, 1182, 755 cm^{-1} ; HRMS (ESI): m/z calcd for $\text{C}_{32}\text{H}_{35}\text{O}_5$ $[\text{M}+\text{H}]^+$: 499.2484; found : 499.2486.

3-((3,5-di-*tert*-butyl-4-hydroxyphenyl)(4-(trifluoromethyl)phenyl)methyl)-4H-chromen-4-one (**83k**):



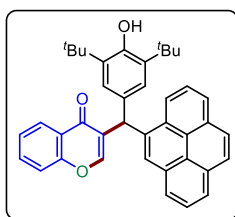
The reaction was performed at 0.110 mmol scale of **81k**; white solid (38.0 mg, 68% yield); m. p. = 196–198 °C; R_f = 0.5 (10% EtOAc in hexane); ^1H NMR (400 MHz, CDCl_3) δ 8.20 (dd, J = 7.9, 1.2 Hz, 1H), 7.69 – 7.65 (m, 1H), 7.55 (d, J = 8.12 Hz, 2H), 7.45 (d, J = 8.4 Hz, 1H), 7.42 – 7.35 (m, 4H), 6.92 (s, 2H), 5.71 (s, 1H), 5.17 (s, 1H), 1.37 (s, 18H); $^{13}\text{C}\{^1\text{H}\}$ NMR (100 MHz, CDCl_3) δ 176.8, 156.4, 155.5, 152.9, 146.5 (q, $J_{\text{C-F}}$ = 1.2 Hz), 136.2, 133.82, 133.8, 130.7, 129.1, 127.9, 126.6 (q, $J_{\text{C-F}}$ = 272.1 Hz), 126.3, 125.7, 125.5 (q, $J_{\text{C-F}}$ = 3.7 Hz), 125.3, 123.9, 118.2, 47.1, 34.5, 30.4; $^{19}\text{F}\{^1\text{H}\}$ NMR (376 MHz, CDCl_3) δ – 62.31; FT-IR (thin film, neat): 3639, 2988, 1645, 1476, 1326, 758 cm^{-1} ; HRMS (ESI): m/z calcd for $\text{C}_{31}\text{H}_{32}\text{F}_3\text{O}_3$ $[\text{M}+\text{H}]^+$: 509.2304; found : 509.2302.

3-((3,5-di-*tert*-butyl-4-hydroxyphenyl)(naphthalen-2-yl)methyl)-4H-chromen-4-one (**83l**):



The reaction was performed at 0.116 mmol scale of **81l**; white solid (57.5 mg, 86% yield); m. p. = 216–218 °C; R_f = 0.4 (10% EtOAc in hexane); ^1H NMR (400 MHz, CDCl_3) δ 8.26 (dd, J = 8.3, 1.7 Hz, 1H), 8.08 – 8.06 (m, 1H), 7.87 – 7.85 (m, 1H), 7.75 (d, J = 8.2 Hz, 1H), 7.67 – 7.63 (m, 1H), 7.48 – 7.43 (m, 2H), 7.42 – 7.34 (m, 4H), 7.08 – 7.05 (m, 3H), 6.48 (s, 1H) 5.12 (s, 1H), 1.37 (s, 18H); $^{13}\text{C}\{^1\text{H}\}$ NMR (100 MHz, CDCl_3) δ 176.7, 156.4, 155.5, 152.7, 139.1, 135.9, 134.2, 133.6, 131.7, 130.9, 128.8, 128.1, 127.6, 126.44, 126.4, 126.3, 125.9, 125.7, 125.2, 125.1, 124.3, 124.0, 118.2, 42.8, 34.5, 30.4; FT-IR (thin film, neat FT-IR (thin film, neat): 3632, 2958, 1639, 1467, 1349, 750 cm^{-1} ; HRMS (ESI): m/z calcd for $\text{C}_{34}\text{H}_{35}\text{O}_3$ $[\text{M}+\text{H}]^+$: 491.2586; found : 491.2587.

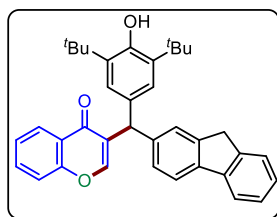
3-((3,5-di-*tert*-butyl-4-hydroxyphenyl)(pyren-4-yl)methyl)-4H-chromen-4-one (83m):



The reaction was performed at 0.118 mmol scale of **81m**; white solid (47.0 mg, 88% yield); m. p. = 241 – 243 °C; R_f = 0.4 (10% EtOAc in hexane); ^1H NMR (400 MHz, CDCl_3) δ 8.38 (d, J = 9.3 Hz, 1H), 8.30 – 8.28 (m, 1H), 8.17 (dd, J = 7.5, 2.8 Hz, 2H), 8.10 – 8.08 (m, 2H), 8.04 (s, 2H), 7.99 (t, J = 7.6 Hz, 1H), 7.68 (d, J = 8.0 Hz, 1H), 7.67 – 7.62 (m, 1H), 7.42 – 7.39 (m, 2H), 7.36 (s, 1H), 7.13 (s, 2H), 6.82 (s, 1H), 5.16 (s, 1H), 1.39 (s, 18H); $^{13}\text{C}\{^1\text{H}\}$ NMR (100 MHz, CDCl_3) δ 176.7, 156.4, 155.8, 152.7, 136.7, 136.0, 133.6, 131.5, 131.3, 130.9, 130.3, 128.9, 128.8, 128.0, 127.6, 127.2, 126.4, 126.3, 126.0, 125.9, 125.4, 125.2, 125.1 (2C), 124.9, 124.6, 124.0, 123.7, 118.2, 43.3, 34.5, 30.4; FT-IR (thin film, neat): 3636, 2957, 1643, 1476, 1391, 751 cm^{-1} ; HRMS (ESI): m/z calcd for $\text{C}_{40}\text{H}_{37}\text{O}_3$ $[\text{M}+\text{H}]^+$: 565.2743; found : 565.2722.

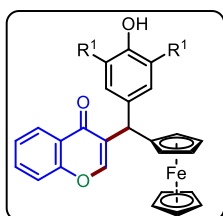
3-((3,5-di-*tert*-butyl-4-hydroxyphenyl)(9H-fluoren-2-yl)methyl)-4H-chromen-4-one (83n):

The reaction was performed at 0.104 mmol scale of **81n**; pale yellow solid (59.0 mg,



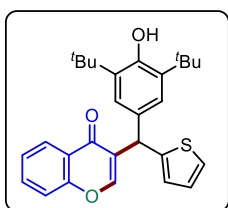
97% yield); m. p. = 122–124 °C; R_f = 0.4 (10% EtOAc in hexane); ^1H NMR (400 MHz, CDCl_3) δ 8.23 (dd, J = 7.9, 1.3 Hz, 1H), 7.76 (d, J = 7.5 Hz, 1H), 7.72 (d, J = 7.9 Hz, 1H), 7.68 – 7.64 (m, 1H), 7.52 (d, J = 7.4 Hz, 1H), 7.46 – 7.44 (m, 3H), 7.40 (d, J = 7.8 Hz, 1H), 7.37 – 7.34 (m, 1H), 7.30 – 7.24 (m, 2H), 7.01 (s, 2H) 5.79 (s, 1H), 5.15 (s, 1H), 3.86 (d, J = 4.1 Hz, 2H), 1.38 (s, 18H); $^{13}\text{C}\{^1\text{H}\}$ NMR (100 MHz, CDCl_3) δ 177.0, 156.4, 155.4, 152.6, 143.7, 143.5, 141.8, 140.9, 140.3, 136.0, 133.6, 132.0, 128.8, 127.4, 126.8, 126.5, 126.4, 125.8, 125.7, 125.11, 125.1, 124.1, 119.85, 119.81, 118.1, 47.2, 37.0, 34.5, 30.4; FT-IR (thin film, neat): FT-IR (thin film, neat): 3634, 2963, 1643, 1466, 1348, 766 cm^{-1} ; cm^{-1} ; HRMS (ESI): m/z calcd for $\text{C}_{37}\text{H}_{37}\text{O}_3$ $[\text{M}+\text{H}]^+$: 529.2743; found : 529.2728.

3-((3,5-di-*tert*-butyl-4-hydroxyphenyl)(ferrocenyl)methyl)-4H-chromen-4-one (83o):



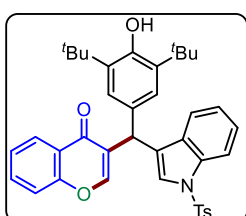
The reaction was performed at 0.124 mmol scale of **81o**; brown solid (60.7 mg, 91% yield); R_f = 0.5 (10% EtOAc in hexane); ^1H NMR (400 MHz, CDCl_3) δ 8.22 (dd, J = 7.9, 1.1 Hz, 1H), 7.64 – 7.59 (m, 1H), 7.58 (s, 1H), 7.39 (d, J = 8.4 Hz, 1H), 7.35 (t, J = 7.9 Hz, 1H), 7.17 (s, 2H), 5.38 (s, 1H), 5.09 (s, 1H), 4.15 – 4.12 (m, 2H), 4.08 (s, 1H), 4.02 (s, 5H), 3.85 (s, 1H), 1.44 (s, 18H); $^{13}\text{C}\{^1\text{H}\}$ NMR (100 MHz, CDCl_3) δ 176.5, 156.2, 154.2, 152.4, 135.3, 133.4, 132.4, 129.7, 126.3, 125.4, 124.9, 124.1, 118.1, 91.5, 68.9, 68.2, 68.1, 67.6, 41.1, 34.5, 30.5; FT-IR (thin film, neat): FT-IR (thin film, neat): 3637, 2958, 1643, 1466, 1318, 750 cm^{-1} ; cm^{-1} ; HRMS (ESI): m/z calcd for $\text{C}_{34}\text{H}_{37}\text{FeO}_3$ $[\text{M}+\text{H}]^+$: 549.2092; found : 549.2086.

3-((3,5-di-*tert*-butyl-4-hydroxyphenyl)(thiophen-2-yl)methyl)-4H-chromen-4-one (83p):



The reaction was performed at 0.133 mmol scale of **81p**; pale yellow solid (55.5 mg, 97% yield); m. p. = 169–170 °C; R_f = 0.6 (10% EtOAc in hexane); ^1H NMR (400 MHz, CDCl_3) δ 8.25 (dd, J = 8.0, 1.4 Hz, 1H), 7.67 – 7.63 (m, 1H), 7.62 (d, J = 0.9 Hz, 1H), 7.45 – 7.43 (m, 1H), 7.41 – 7.37 (m, 1H), 7.19 (dd, J = 5.1, 1.2 Hz, 1H), 7.10 (s, 2H), 6.94 (dd, J = 5.1, 3.5 Hz, 1H), 6.81 (dt, J = 3.4, 1.0 Hz, 1H), 5.93 (s, 1H), 5.17 (s, 1H), 1.41 (s, 18H); $^{13}\text{C}\{^1\text{H}\}$ NMR (100 MHz, CDCl_3) δ 176.5, 156.3, 155.0, 152.8, 146.7, 135.9, 133.6, 131.8, 128.8, 126.8, 126.3, 126.1, 125.2, 125.1, 124.4, 124.0, 118.2, 42.0, 34.5, 30.4; FT-IR (thin film, neat): 3636, 2957, 1643, 1467, 1348 cm^{-1} ; HRMS (ESI): m/z calcd for $\text{C}_{28}\text{H}_{31}\text{O}_3\text{S}$ $[\text{M}+\text{H}]^+$: 447.1994; found : 447.1984.

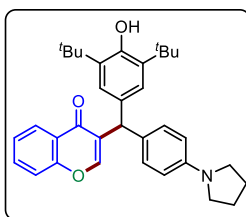
3-((3,5-di-*tert*-butyl-4-hydroxyphenyl)(1H-indol-3-yl)methyl)-4H-chromen-4-one (83q):



The reaction was performed at 0.102 mmol scale of **81q**; white solid (49.5 mg, 92% yield); m. p. = 75–77 °C; R_f = 0.6 (10% EtOAc in hexane) ^1H NMR (400 MHz, CDCl_3) δ 8.25 (d, J = 7.8 Hz, 1H), 7.98 (d, J = 8.2 Hz, 1H), 7.67 – 7.65 (m, 3H), 7.44 – 7.42 (m, 2H), 7.40 – 7.39 (m, 1H), 7.30 – 7.25 (m, 2H), 7.20 (d, J = 8.2 Hz, 2H), 7.13 (t, J = 7.1 Hz, 1H), 7.01 (brs, 3H), 5.78 (s, 1H), 5.15 (s, 1H), 2.36 (s, 3H), 1.36 (s, 18H); $^{13}\text{C}\{^1\text{H}\}$ NMR (100 MHz, CDCl_3) δ 176.6, 156.4, 154.9, 152.9, 145.0, 136.0, 135.1, 133.7, 130.2, 130.0, 129.9, 126.8 (2C), 126.3, 126.0, 125.41, 125.4, 125.2, 125.05, 125.0, 124.0, 123.4, 120.6, 118.3, 114.0, 37.9, 34.5, 30.4, 21.7; FT-IR (thin film, neat): 3635, 2958, 1644, 1466, 1349, 752 cm^{-1} ; NHRMS (ESI): m/z calcd for $\text{C}_{39}\text{H}_{39}\text{NNaO}_5\text{S}$ $[\text{M}+\text{Na}]^+$: 656.2447; found : 656.2432.

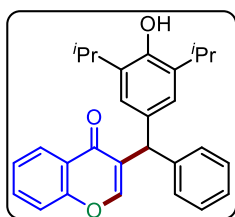
3-((3,5-di-*tert*-butyl-4-hydroxyphenyl)(4-(pyrrolidin-1-yl)phenyl)methyl)-4H-chromen-

4-one (83r): The reaction was performed at 0.110 mmol scale of **81r**; orange solid (22.0 mg,



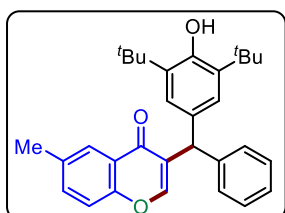
40% yield); m. p. = 218–220 °C; R_f = 0.4 (10% EtOAc in hexane); ^1H NMR (400 MHz, CDCl_3) δ 8.21 (dd, J = 8.0, 1.4 Hz, 1H), 7.65 – 7.61 (m, 1H), 7.43 – 7.40 (m, 2H), 7.38 – 7.34 (m, 1H), 7.04 (d, J = 8.5 Hz, 2H), 7.01 (s, 2H), 6.50 (d, J = 8.4 Hz, 2H), 5.61 (s, 1H), 5.07 (s, 1H), 3.25 (t, J = 6.4 Hz, 4H), 1.98 (t, J = 6.4 Hz, 4H), 1.37 (s, 18H); $^{13}\text{C}\{^1\text{H}\}$ NMR (100 MHz, CDCl_3) δ 176.9, 156.3, 155.1, 152.2, 146.6, 135.5, 133.2, 132.4, 129.6, 129.3, 128.8, 126.3, 125.5, 124.8, 124.0, 118.0, 111.6, 47.7, 45.9, 34.4, 30.4, 25.5, FT-IR (thin film, neat): 3637, 2961, 1643, 1465, 1275, 749 cm^{-1} ; HRMS (ESI): m/z calcd for $\text{C}_{34}\text{H}_{40}\text{NO}_3$ $[\text{M}+\text{H}]^+$: 510.3008; found : 510.3026.

3-((4-hydroxy-3,5-diisopropylphenyl)(phenyl)methyl)-4H-chromen-4-one (83s):



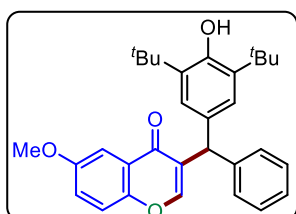
The reaction was performed at 0.150 mmol scale of **81s**; white solid (41.0 mg, 66% yield); m. p. = 148–150 °C; R_f = 0.4 (10% EtOAc in hexane); ^1H NMR (400 MHz, CDCl_3) δ 8.23 (dd, J = 8.0, 1.5 Hz, 1H), 7.67 – 7.63 (m, 1H), 7.45 – 7.43 (m, 2H), 7.40 – 7.36 (m, 1H), 7.32 – 7.29 (m, 2H), 7.24–7.20 (m, 3H), 6.86 (s, 2H), 5.75 (s, 1H), 5.00 (s, 1H), 3.14 (sept, J = 6.8 Hz, 2H), 1.20 (d, J = 6.8 Hz, 6H), 1.19 (d, J = 6.8 Hz, 6H); $^{13}\text{C}\{^1\text{H}\}$ NMR (100 MHz, CDCl_3) δ 176.9, 156.4, 155.4, 148.9, 142.1, 133.9, 133.6, 133.1, 128.9, 128.53, 128.5, 126.6, 126.4, 125.1, 124.3, 124.0, 118.1, 46.8, 27.4, 22.81, 22.8; FT-IR (thin film, neat): 3637, 2948, 1644, 1476, 755 cm^{-1} ; HRMS (ESI): m/z calcd for $\text{C}_{28}\text{H}_{29}\text{O}_3$ $[\text{M}+\text{H}]^+$: 413.2117; found : 413.2122.

3-((3,5-di-tert-butyl-4-hydroxyphenyl)(phenyl)methyl)-6-methyl-4H-chromen-4-one (83t):



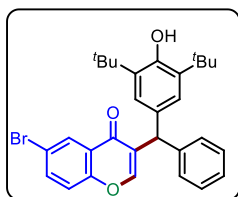
The reaction was performed at 0.140 mmol scale of **81a**; yellow gummy solid (63.0 mg, 98% yield); m. p. = 191–193 °C; R_f = 0.7 (10% EtOAc in hexane); ^1H NMR (400 MHz, CDCl_3) δ 8.00 (d, J = 1.08 Hz, 1H), 7.46 (dd, J = 8.6, 2.1 Hz, 1H), 7.40 (d, J = 1.0 Hz, 1H), 7.34 – 7.32 (m, 1H), 7.31 – 7.28 (m, 2H), 7.23 – 7.21 (m, 3H), 6.96 (s, 2H), 5.71 (s, 1H), 5.13 (s, 1H), 2.44 (s, 3H), 1.38 (s, 18H); $^{13}\text{C}\{^1\text{H}\}$ NMR (100 MHz, CDCl_3) δ 176.9, 155.3, 154.6, 152.5, 142.3, 135.8, 134.9, 134.8, 131.9, 128.9, 128.4, 128.3, 126.5, 125.8, 125.6, 123.7, 117.9, 46.93, 46.9, 34.5, 30.4, 21.1, 21.0; FT-IR (thin film, neat): 3637, 2958, 1644, 1434, 1138, 701 cm^{-1} ; HRMS (ESI): m/z calcd for $\text{C}_{31}\text{H}_{35}\text{O}_3$ $[\text{M}+\text{H}]^+$: 455.2586; found : 455.2578.

3-((3,5-di-tert-butyl-4-hydroxyphenyl)(phenyl)methyl)-6-methoxy-4H-chromen-4-one (83u):



The reaction was performed at 0.140 mmol scale of **81a**; white solid (63.0 mg, 96% yield); m. p. = 189–191 °C; R_f = 0.7 (10% EtOAc in hexane); ^1H NMR (400 MHz, CDCl_3) δ 7.53 (d, J = 3.04 Hz, 1H), 7.35 (s, 1H), 7.32 – 7.30 (m, 1H), 7.26 – 7.22 (m, 2H), 7.20 – 7.13 (m, 4H), 6.91 (s, 2H), 5.66 (s, 1H), 5.07 (s, 1H), 3.81 (s, 3H), 1.32 (s, 18H); $^{13}\text{C}\{^1\text{H}\}$ NMR (100 MHz, CDCl_3) δ 176.7, 156.8, 155.2, 152.5, 151.2, 142.3, 135.9, 131.8, 128.9, 128.4, 127.8, 126.5, 125.7, 124.5, 123.8, 119.5, 105.2, 55.93, 55.9, 47.0, 34.5, 30.4; FT-IR (thin film, neat): 3636, 2957, 1642, 1467, 1329, 800 cm^{-1} ; HRMS (ESI): m/z calcd for $\text{C}_{31}\text{H}_{35}\text{O}_4$ $[\text{M}+\text{H}]^+$: 471.2535; found : 471.2526.

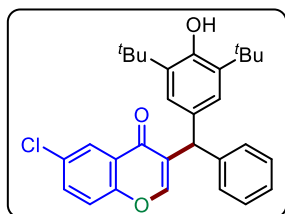
6-bromo-3-((3,5-di-*tert*-butyl-4-hydroxyphenyl)(phenyl)methyl)-4H-chromen-4-one



(**83v**): The reaction was performed at 0.136 mmol scale of **81a** pale yellow solid (51.0 mg, 73% yield); m. p. = 173–175 °C; R_f = 0.7 (10% EtOAc in hexane); ^1H NMR (400 MHz, CDCl_3) δ 8.33 (d, J = 2.4 Hz, 1H), 7.72 (dd, J = 8.9, 2.5 Hz, 1H), 7.42 (s, 1H), 7.34 – 7.29 (m, 3H), 7.24 – 7.20 (m, 3H), 6.97 (s, 2H), 5.68 (s, 1H), 5.15 (s, 1H), 1.38 (s, 18H); $^{13}\text{C}\{^1\text{H}\}$ NMR (100 MHz, CDCl_3) δ 175.6, 155.5, 155.1, 152.6, 141.8, 136.5, 137.0, 131.4, 128.91, 128.9 (2C), 128.5, 126.7, 125.7, 125.3, 120.1, 118.4, 47.0, 34.5, 30.4; FT-IR (thin film, neat): 3636, 2955, 1642, 1466, 1143, 762 cm^{-1} ; HRMS (ESI): m/z calcd for $\text{C}_{30}\text{H}_{32}\text{BrO}_3$ $[\text{M}+\text{H}]^+$: 519.1535; found : 519.1540.

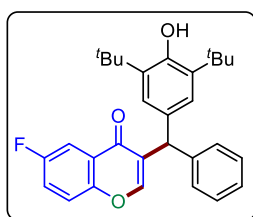
6-chloro-3-((3,5-di-*tert*-butyl-4-hydroxyphenyl)(phenyl)methyl)-4H-chromen-4-one

(**83w**): The reaction was performed at 0.140 mmol scale of **81a**; pale yellow solid (62.0 mg, 94% yield); m. p. = 211–213 °C; R_f = 0.7 (10% EtOAc in hexane); ^1H NMR (400 MHz, CDCl_3) δ 8.17(d, J = 2.5 Hz, 1H), 7.58 (dd, J = 8.9, 2.6 Hz, 1H), 7.42 (d, J = 1.0 Hz, 1H), 7.39 (d, J = 8.9 Hz, 1H), 7.33 – 7.29 (m, 2H), 7.24 – 7.21 (m, 3H), 6.96 (s, 2H), 5.69 (s, 1H), 5.15 (s, 1H), 1.38 (s, 18H); $^{13}\text{C}\{^1\text{H}\}$ NMR (100 MHz, CDCl_3) δ 175.7, 155.5, 154.7, 152.6, 141.8, 135.9, 133.8, 131.4, 130.9, 128.8, 128.7, 128.5, 126.7, 125.7, 125.6, 124.9, 119.9, 47.0, 46.96, 34.5, 30.4; FT-IR (thin film, neat): 3636, 2958, 1645, 1466, 1141, 762 cm^{-1} ; HRMS (ESI): m/z calcd for $\text{C}_{30}\text{H}_{32}\text{ClO}_3$ $[\text{M}+\text{H}]^+$: 475.2040; found : 475.2047.



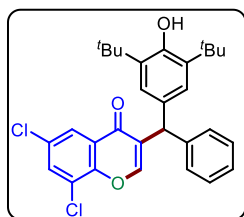
3-((3,5-di-*tert*-butyl-4-hydroxyphenyl)(phenyl)methyl)-6-fluoro-4H-chromen-4-one

(**83x**): The reaction was performed at 0.136 mmol scale of **81a**; pale yellow solid (57.0 mg, 92% yield); m. p. = 151–153 °C; R_f = 0.7 (10% EtOAc in hexane); ^1H NMR (400 MHz, CDCl_3) δ 8.26 – 8.22 (m, 1H), 7.41 (s, 1H), 7.33 – 7.30 (m, 2H), 7.26 – 7.21 (m, 3H), 7.13 – 7.09 (m, 2H), 6.98 (s, 2H), 5.71 (s, 1H), 5.17 (s, 1H), 1.39 (s, 18H); $^{13}\text{C}\{^1\text{H}\}$ NMR (100 MHz, CDCl_3) δ 176.0, 165.6 (d, $J_{\text{C-F}}$ = 253.2 Hz), 157.3 (d, $J_{\text{C-F}}$ = 13.3 Hz), 155.5, 152.6, 142.0, 136.0, 131.5, 129.0, 128.9, 128.8, 128.5, 126.6, 125.7, 120.9 (d, $J_{\text{C-F}}$ = 2.2 Hz), 114.1 (d, $J_{\text{C-F}}$ = 22.7 Hz), 104.8 (d, $J_{\text{C-F}}$ = 25.1 Hz), 46.9 (d, $J_{\text{C-F}}$ = 1.7 Hz), 34.5, 30.4; $^{19}\text{F}\{^1\text{H}\}$ NMR (376 MHz, CDCl_3) δ –103.18; FT-IR (thin film, neat): 3635, 2959, 1647, 1438, 1182, 701 cm^{-1} ; HRMS (ESI): m/z calcd for $\text{C}_{30}\text{H}_{32}\text{FO}_3$ $[\text{M}+\text{H}]^+$: 459.2335; found : 459.2335.



6,8-dichloro-3-((3,5-di-*tert*-butyl-4-hydroxyphenyl)(phenyl)methyl)-4H-chromen-4-one

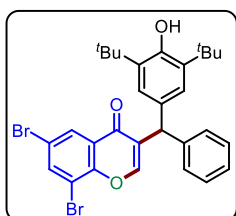
(83y): The reaction was performed at 0.135 mmol scale of **81a**; pale yellow solid (63.0 mg,



94% yield); m. p. = 144–146 °C; R_f = 0.6 (10% EtOAc in hexane); ^1H NMR (400 MHz, CDCl_3) δ 8.07 (d, J = 2.5 Hz, 1H), 7.70 (d, J = 2.5 Hz, 1H), 7.48 (d, J = 1.0 Hz, 1H), 7.32 – 7.28 (m, 2H), 7.24 – 7.19 (m, 3H), 6.93 (s, 2H), 5.64 (s, 1H), 5.14 (s, 1H), 1.37 (s, 18H); $^{13}\text{C}\{^1\text{H}\}$ NMR (100 MHz, CDCl_3) δ 175.1, 155.5, 152.7, 150.7, 141.4, 136.1, 133.7, 131.1, 130.7, 129.2, 128.8, 128.6, 126.8, 125.73, 125.7, 124.5, 124.3, 47.1, 34.5, 30.4; FT-IR (thin film, neat): 3562, 2957, 1647, 1447, 1114, 704 cm^{-1} ; HRMS (ESI): m/z calcd for $\text{C}_{30}\text{H}_{31}\text{Cl}_2\text{O}_3$ $[\text{M}+\text{H}]^+$: 509.1650; found : 509.1638.

6,8-dibromo-3-((3,5-di-*tert*-butyl-4-hydroxyphenyl)(phenyl)methyl)-4H-chromen-4-one

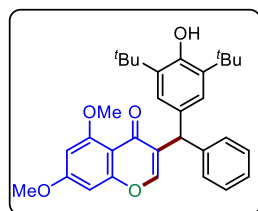
(83z): The reaction was performed at 0.135 mmol scale of **81a**; pale yellow solid (58.0 mg,



72% yield); m. p. = 171–173 °C; R_f = 0.6 (10% EtOAc in hexane); ^1H NMR (400 MHz, CDCl_3) δ 8.27 (d, J = 2.2 Hz, 1H), 8.00 (d, J = 2.2 Hz, 1H), 7.49 (s, 1H), 7.32 – 7.28 (m, 2H), 7.24 – 7.20 (m, 3H), 6.93 (s, 2H), 5.64 (s, 1H), 5.14 (s, 1H), 1.38 (s, 18H); $^{13}\text{C}\{^1\text{H}\}$ NMR (100 MHz, CDCl_3) δ 175.0, 155.6, 152.7, 152.0, 141.4, 139.3, 136.1, 131.1, 129.1, 128.8, 128.6, 128.4, 126.8, 126.0, 125.7, 118.3, 112.9, 47.13, 47.12, 34.5, 30.4; FT-IR (thin film, neat): 3562, 2958, 1649, 1440, 1145, 740 cm^{-1} ; HRMS (ESI): m/z calcd for $\text{C}_{30}\text{H}_{31}\text{Br}_2\text{O}_3$ $[\text{M}+\text{H}]^+$: 597.0640; found : 597.0630.

3-((3,5-di-*tert*-butyl-4-hydroxyphenyl)(phenyl)methyl)-5,7-dimethoxy-4H-chromen-4-one

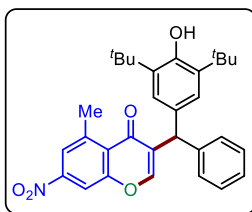
(83aa): The reaction was performed at 0.135 mmol scale of **81a**; pale yellow solid (51.0



mg, 75% yield); m. p. = 211–213 °C; R_f = 0.7 (10% EtOAc in hexane); ^1H NMR (400 MHz, CDCl_3) 7.28 – 7.24 (m, 2H), 7.20 – 7.17 (m, 4H), 6.92 (s, 2H), 6.38 (d, J = 2.3 Hz, 1H), 6.32 (d, J = 2.4 Hz, 1H), 5.67 (s, 1H), 5.06 (s, 1H), 1.37 (s, 18H); $^{13}\text{C}\{^1\text{H}\}$ NMR (100 MHz, CDCl_3) δ 175.6, 163.9, 161.4, 160.0, 153.1, 152.4, 142.6, 136.7, 132.2, 129.6, 129.0, 128.3, 126.3, 125.7, 109.5, 96.0, 92.5, 55.84, 55.8, 46.5, 34.4, 30.4; FT-IR (thin film, neat): 3636, 2959, 1648, 1465, 1142, 760 cm^{-1} ; HRMS (ESI): m/z calcd for $\text{C}_{30}\text{H}_{32}\text{ClO}_3$ $[\text{M}+\text{H}]^+$: 501.2641; found : 501.2647.

3-((3,5-di-*tert*-butyl-4-hydroxyphenyl)(phenyl)methyl)-5-methyl-7-nitro-4H-chromen-4-one

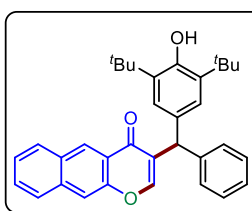
(83ab): The reaction was performed at 0.135 mmol scale of **81a**; pale yellow solid (57.0 mg, 88% yield); m. p. = 195–197 °C; R_f = 0.7 (10% EtOAc in hexane); ^1H NMR (400 MHz, CDCl_3) δ 8.28 (dd, J = 2.2, 0.7 Hz, 1H), 8.15 (d, J = 1.9, 2.5 Hz, 1H), 7.48 (d, J = 1.0 Hz, 1H),



7.33 – 7.29 (m, 2H), 7.24 – 7.21 (m, 3H), 6.94 (s, 2H), 5.65 (s, 1H), 5.15 (s, 1H), 2.15 (s, 3H), 1.37 (s, 18H); $^{13}\text{C}\{^1\text{H}\}$ NMR (100 MHz, CDCl_3) δ 175.0, 155.3, 152.8, 147.0, 141.3, 138.5, 136.1, 134.9, 132.0, 130.9, 130.7, 129.5, 128.8, 128.6, 126.8, 125.7, 125.4, 47.1, 34.5, 30.4, 20.9; FT-IR (thin film, neat): 3635, 2956, 1645, 1462, 1147, 762 cm^{-1} ; HRMS (ESI): m/z calcd for $\text{C}_{31}\text{H}_{34}\text{NO}_5$ $[\text{M}+\text{H}]^+$: 500.2437; found : 500.2440.

3-((3,5-di-tert-butyl-4-hydroxyphenyl)(phenyl)methyl)-4H-benzo[g]chromen-4-one

(**83ac**): The reaction was performed at 0.135 mmol scale of **81a**; pale yellow solid (45.0 mg,

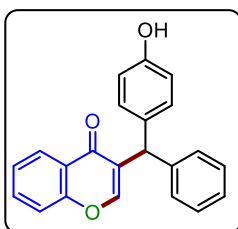


71% yield); m. p. = 140–142 °C; R_f = 0.7 (10% EtOAc in hexane); ^1H NMR (400 MHz, CDCl_3) δ 10.07 (d, J = 8.6 Hz, 1H), 8.06 (d, J = 9.0 Hz, 1H), 7.89 (d, J = 7.5 Hz, 1H), 7.72 – 7.68 (m, 1H), 7.61 – 7.57 (m, 1H), 7.49 – 7.46 (m, 2H), 7.33 – 7.20 (m, 5H), 7.00 (s, 2H), 5.84 (s, 1H), 5.13 (s, 1H), 1.39 (s, 18H); $^{13}\text{C}\{^1\text{H}\}$ NMR (100 MHz, CDCl_3) δ 178.4, 157.5, 153.2, 152.5, 142.4, 135.9, 135.4, 132.1, 131.1, 130.8, 130.7, 129.3, 128.9, 128.5, 128.3, 127.5, 126.6, 126.5, 125.8, 117.8, 117.2, 47.1, 34.5, 30.4; FT-IR (thin film, neat): 3636, 2954, 1644, 1468, 1142, 76 cm^{-1} ; HRMS (ESI): m/z calcd for $\text{C}_{34}\text{H}_{35}\text{O}_3$ $[\text{M}+\text{H}]^+$: 491.2586; found : 491.2596.

General Procedure for Gram Scale Synthesis of **83a**.

In a 100 mL round bottom flask, *p*-QM **81a** (1g, 3.40 mmol), 2-hydroxy *N,N*-dimethyl phenyl substituted enaminones **82a** (0.78 g, 4.08 mmol), TsOH (0.58 g, 3.40 mmol) were dissolved in 20 mL of MeCN. The resulting reaction mixture was stirred at room temperature for 6 h, after that the organic layer was concentrated under reduced pressure. The resulting residue was then purified through silica gel chromatography using EtOAc/Hexane mixture as an eluent to get the pure product **83a** in 80% isolated yield.

General Procedure for De-tert-butylation of **86**

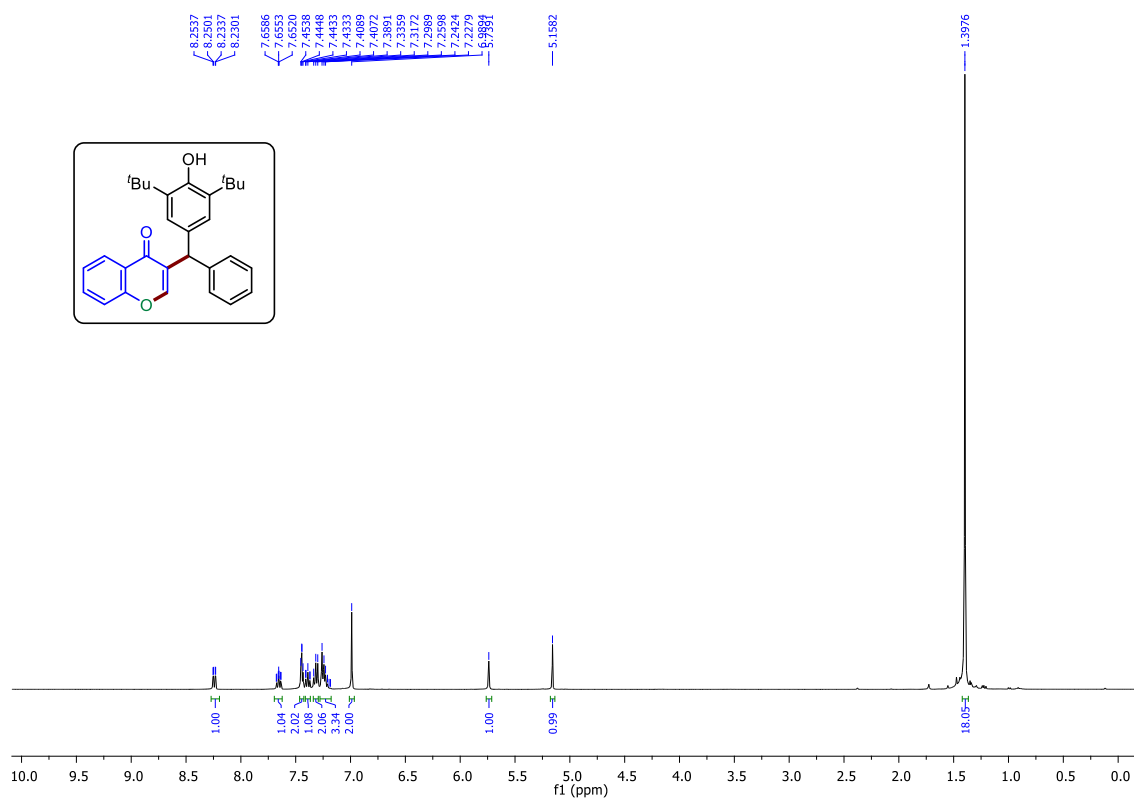


AlCl_3 (151 mg, 10 equiv., 1.13 mmol) was added to a solution of **83a** (50 mg, 1.0 equiv., 0.113 mmol) in benzene (2.0 mL). The resulting reaction mixture was stirred at 60 °C for 1 h and then quenched with 5 mL of cold ice water. It was extracted with EtOAc (3x10 mL), and the combined organic layer was dried over anhydrous sodium sulfate and concentrated

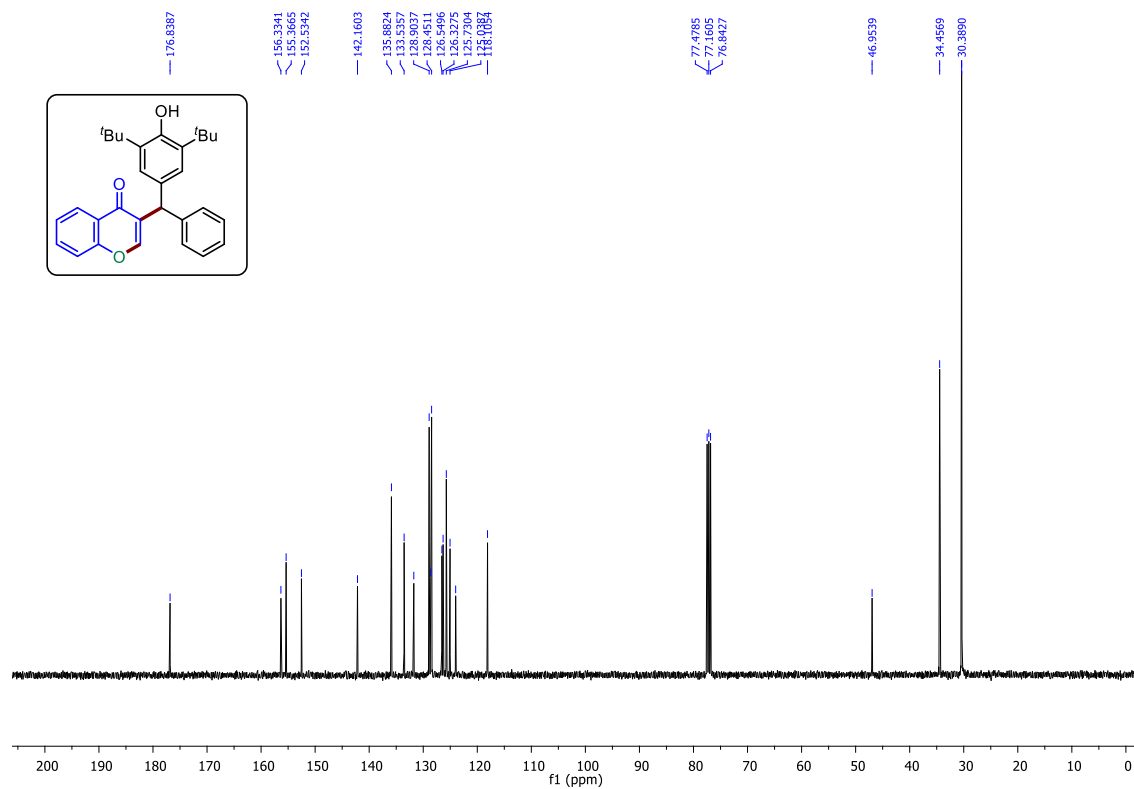
under reduced pressure. The residue was then purified through silica gel chromatography using EtOAc/Hexane mixture as an eluent to get the pure product **86**. Gummy solid (26.0 mg, 69%

yield); $R_f = 0.2$ (10% EtOAc in hexane); ^1H NMR (400 MHz, DMSO- d_6) δ 9.33 (s, 1H), 8.01 (dd, $J = 8.0, 1.5$ Hz, 1H), 7.81 – 7.77 (m, 1H), 7.66 (d, $J = 0.6$ Hz, 1H), 7.61 (d, $J = 8.2$ Hz, 1H), 7.49 – 7.45 (m, 1H), 7.31 – 7.27 (m, 2H), 7.22 – 7.17 (m, 3H), 7.00 (d, $J = 8.5$ Hz, 2H), 6.70 (d, $J = 8.5$ Hz, 2H), 5.52 (s, 1H); $^{13}\text{C}\{^1\text{H}\}$ NMR (100 MHz, DMSO- d_6) δ 175.5, 155.9, 155.7, 155.4, 142.2, 134.2, 131.6, 129.8, 128.6, 128.3, 127.2, 126.3, 125.4, 125.2, 123.2, 118.4, 115.2, 45.8; FT-IR (thin film, neat): 3637, 2957, 1644, 1349, 783 cm^{-1} ; HRMS (ESI): m/z calcd for $\text{C}_{22}\text{H}_{17}\text{O}_3$ $[\text{M}+\text{H}]^+$: 329.1178; found : 329.1174.

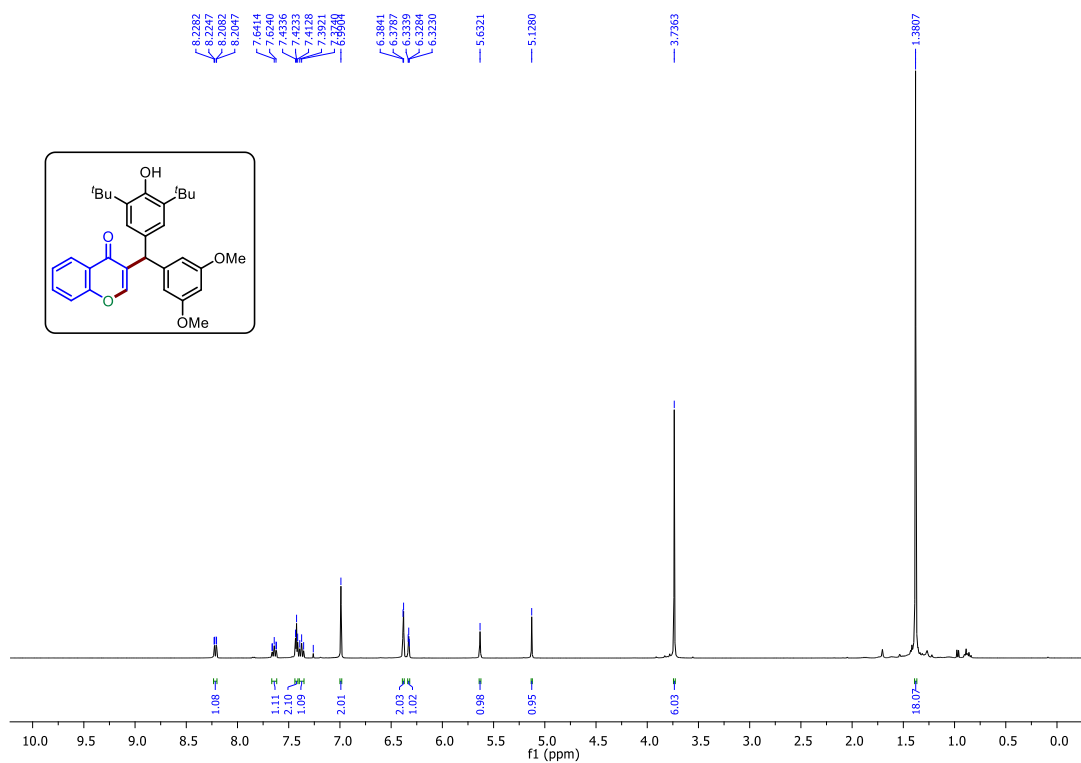
^1H NMR (400 MHz, CDCl_3) Spectrum of **83a**



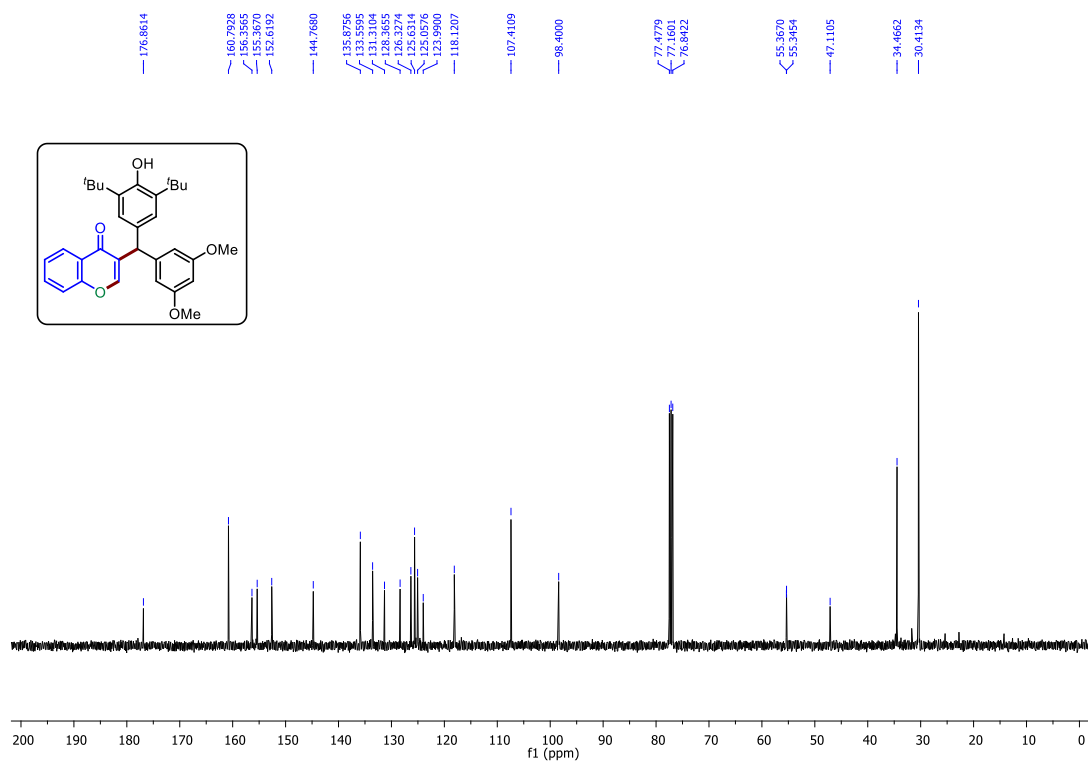
^{13}C [^1H] NMR (100 MHz, CDCl_3) Spectrum of **83a**



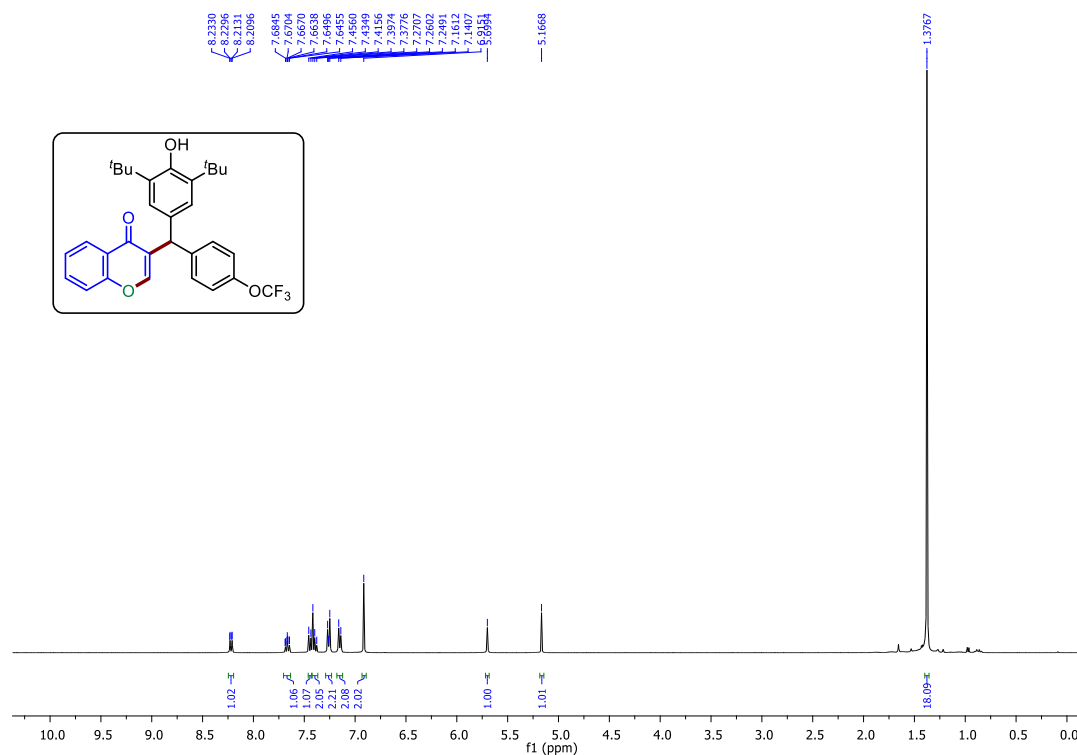
^1H NMR (400 MHz, CDCl_3) Spectrum of **83d**



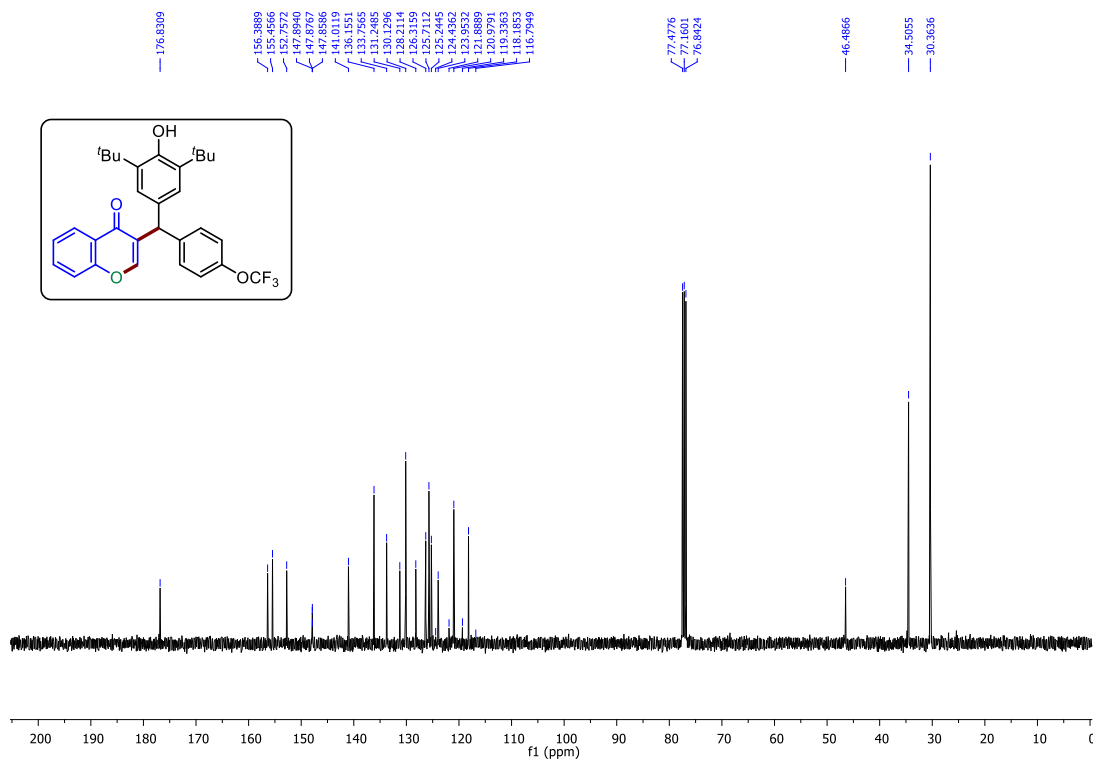
^{13}C { ^1H } NMR (100 MHz, CDCl_3) Spectrum of **83d**



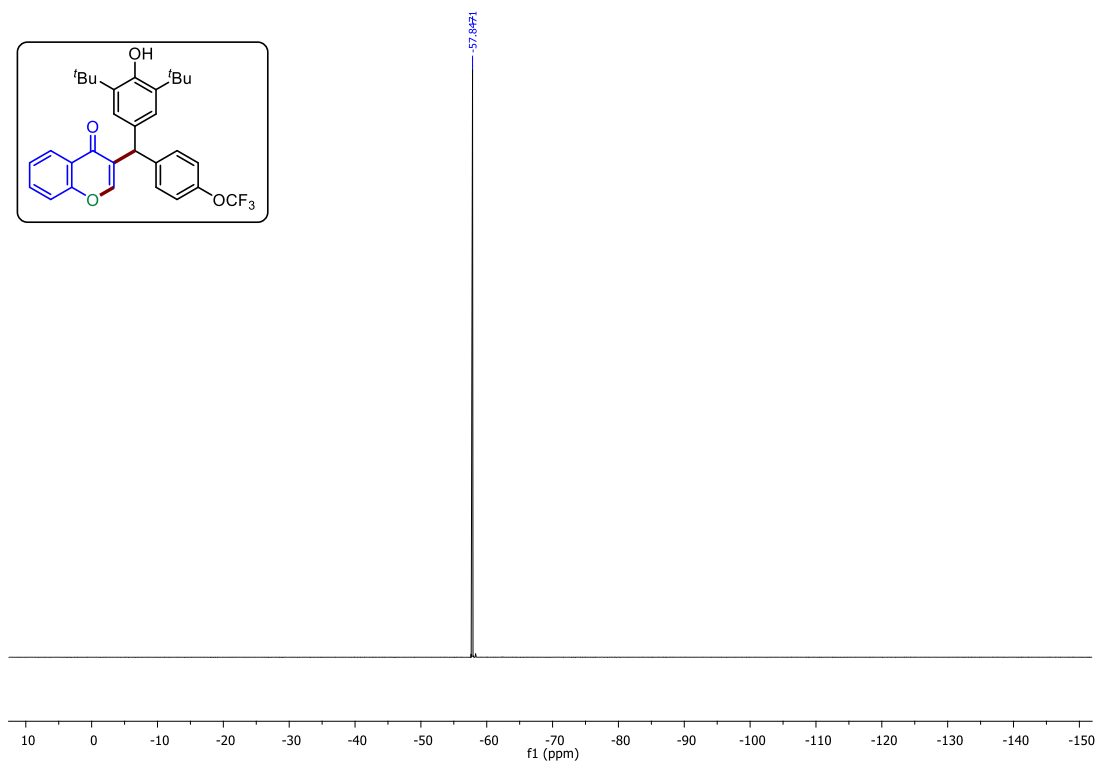
^1H NMR (400 MHz, CDCl_3) Spectrum of **83e**



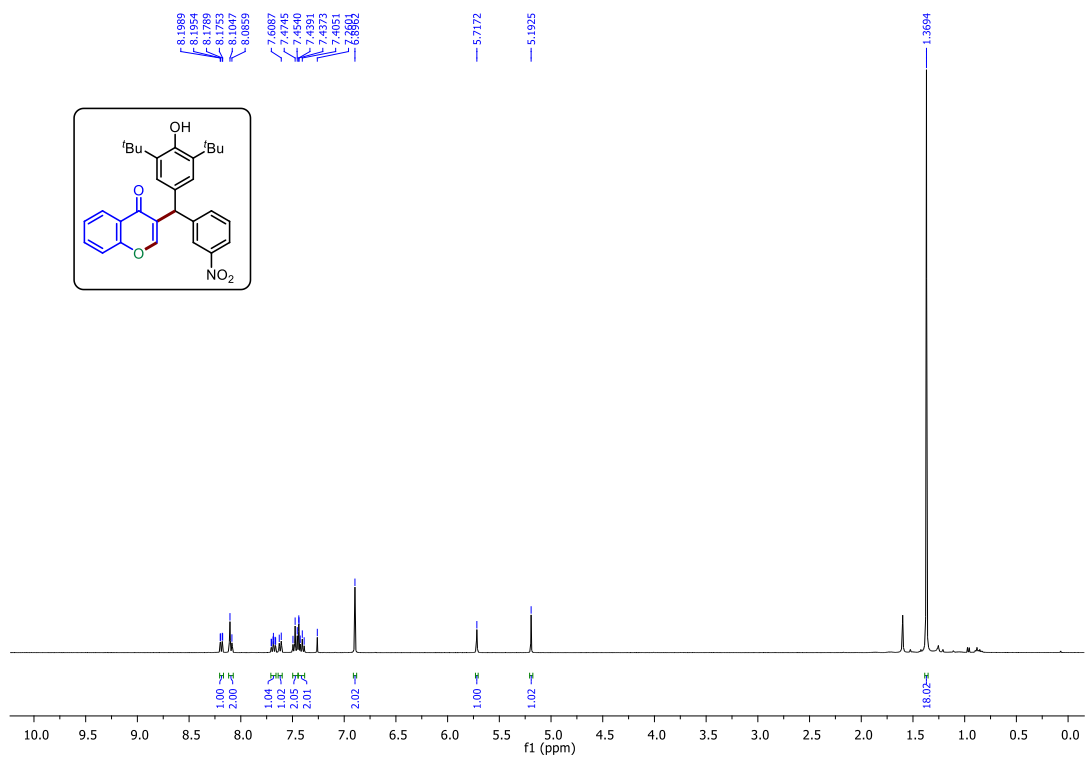
^{13}C { ^1H } NMR (100 MHz, CDCl_3) Spectrum of **83e**



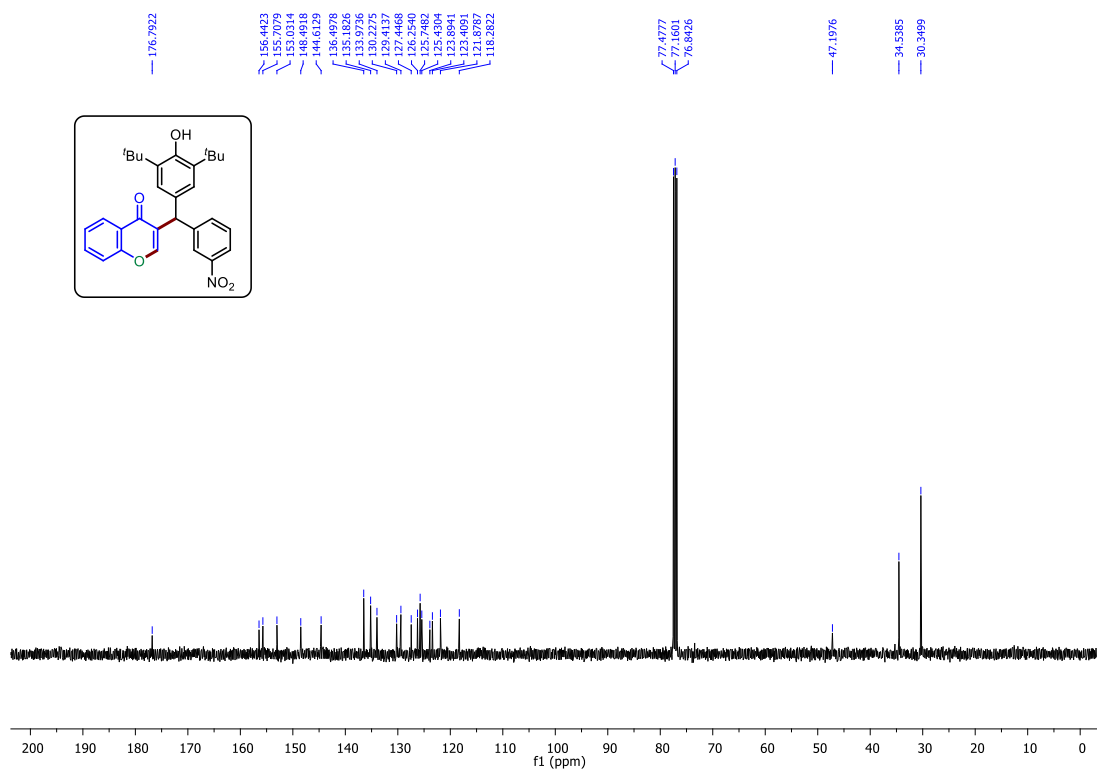
^{19}F $\{^1\text{H}\}$ NMR (376 MHz, CDCl_3) Spectrum of **83e**



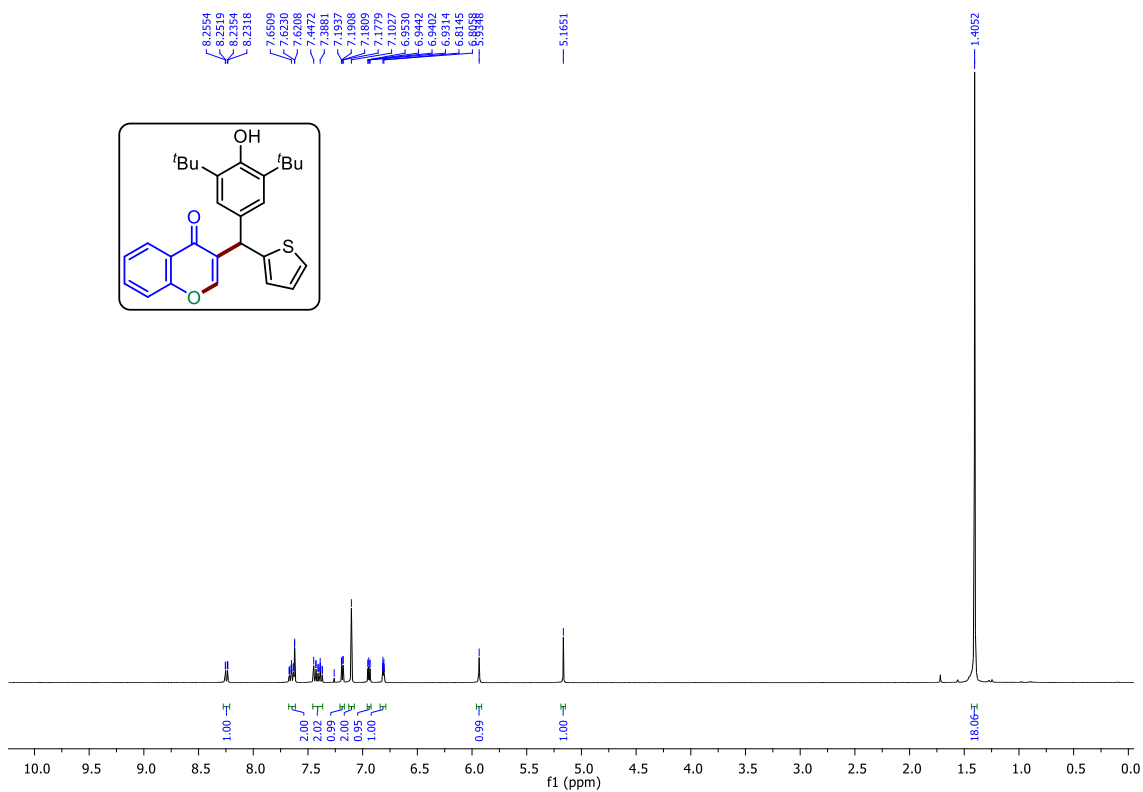
^1H NMR (400 MHz, CDCl_3) Spectrum of **83i**



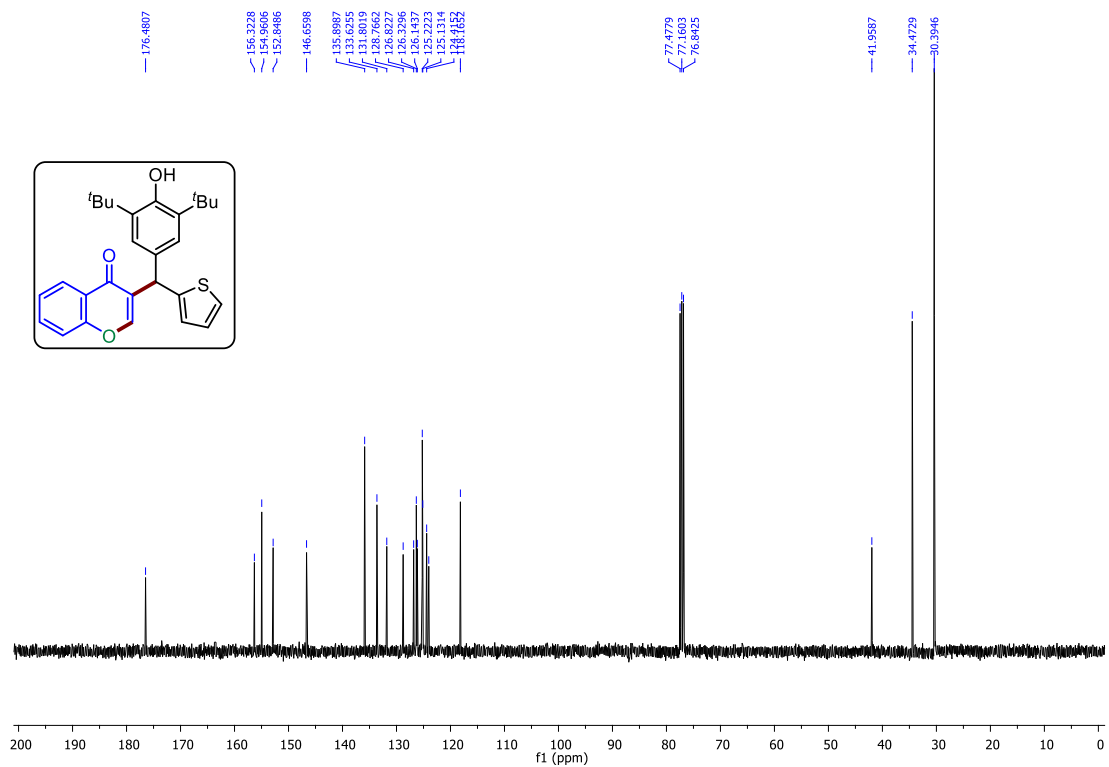
^{13}C $\{^1\text{H}\}$ NMR (100 MHz, CDCl_3) Spectrum of **83i**



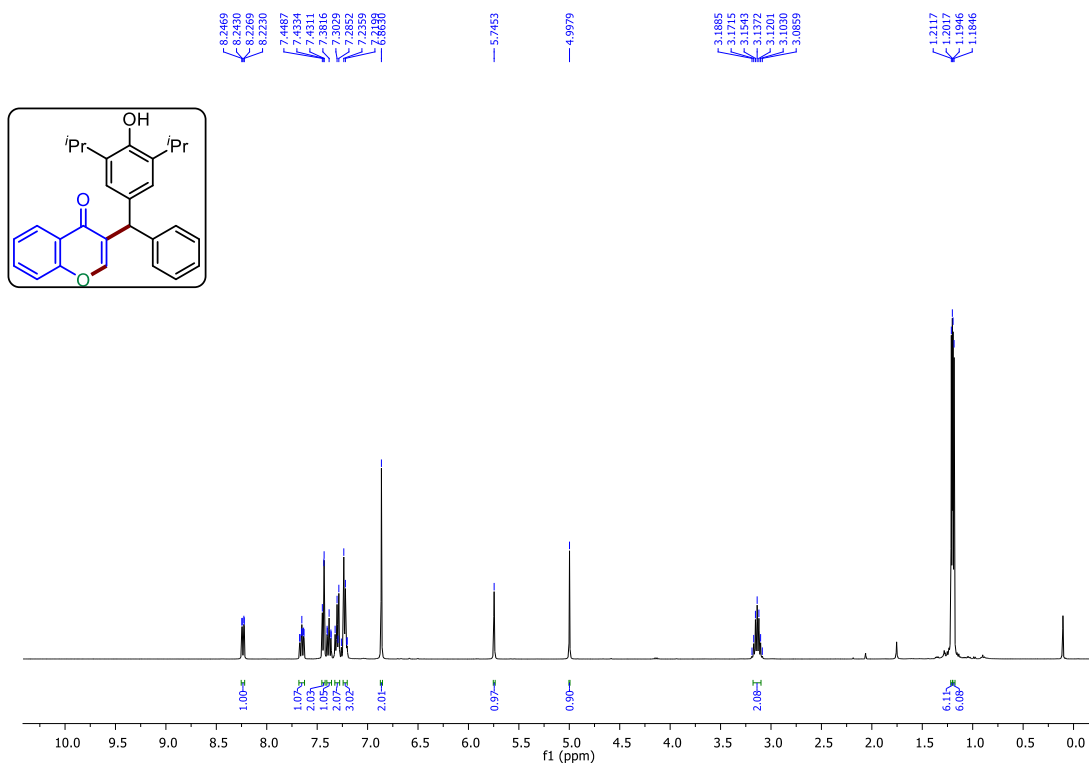
^1H NMR (400 MHz, CDCl_3) Spectrum of **83p**



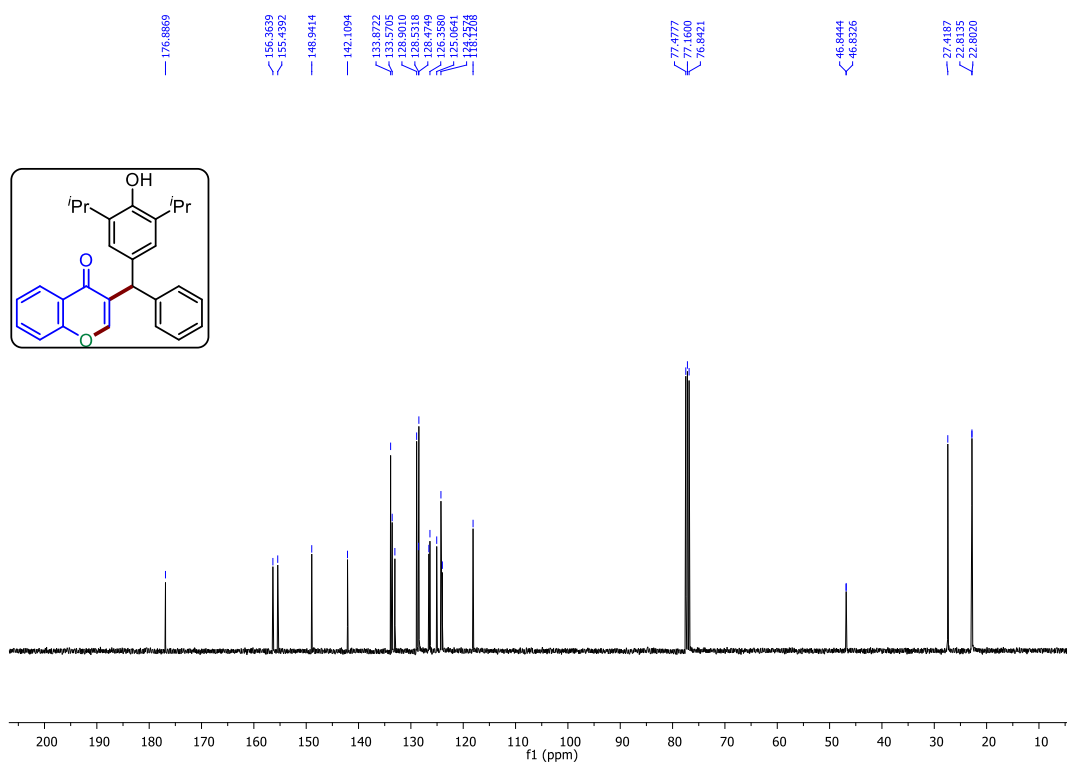
^{13}C $\{^1\text{H}\}$ NMR (100 MHz, CDCl_3) Spectrum of **83p**



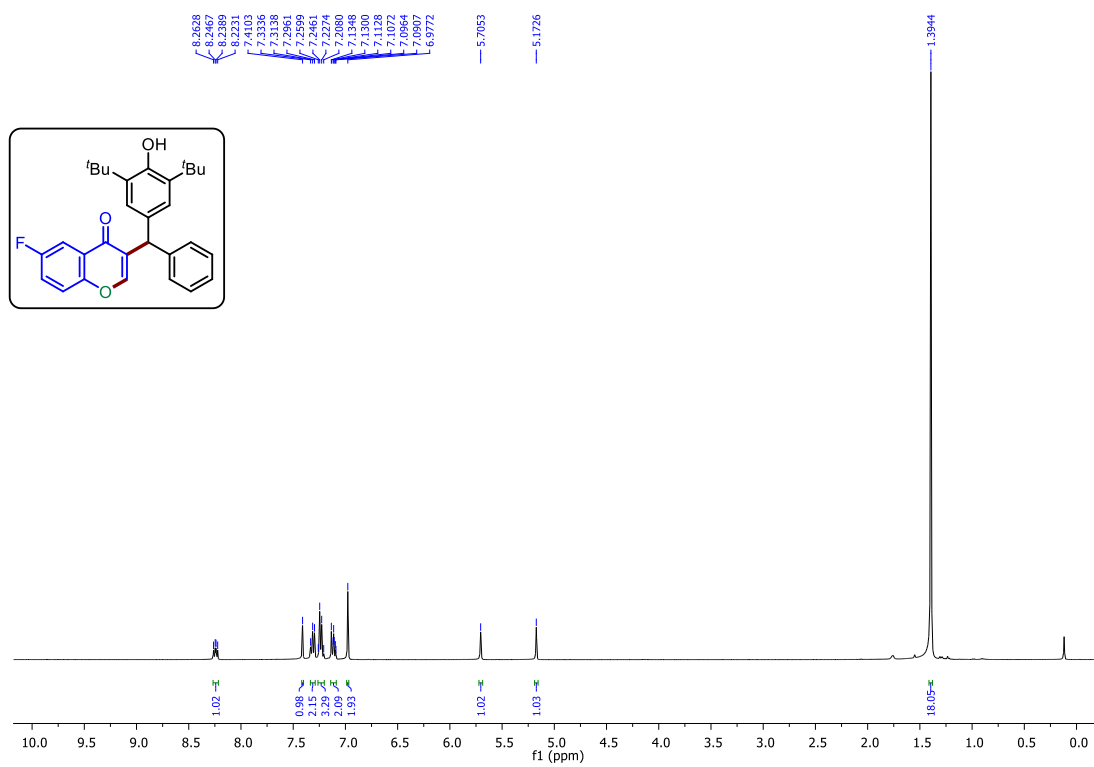
^1H NMR (400 MHz, CDCl_3) Spectrum of **83s**



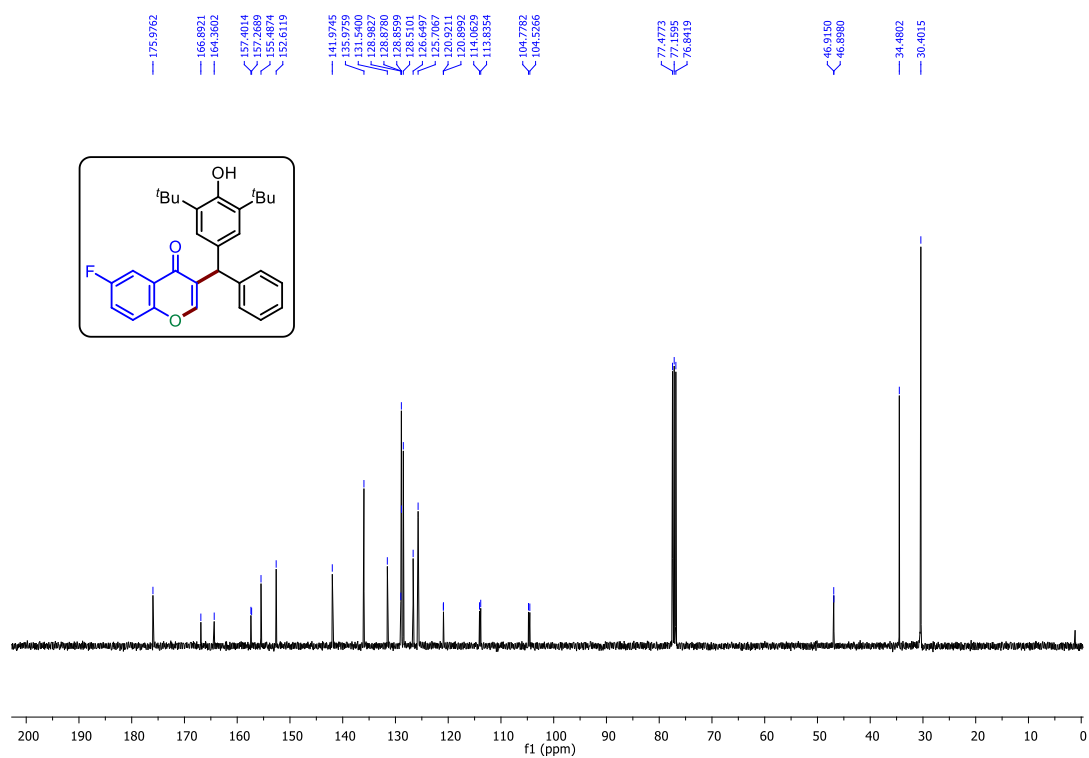
^{13}C $\{^1\text{H}\}$ NMR (100 MHz, CDCl_3) Spectrum of **83s**



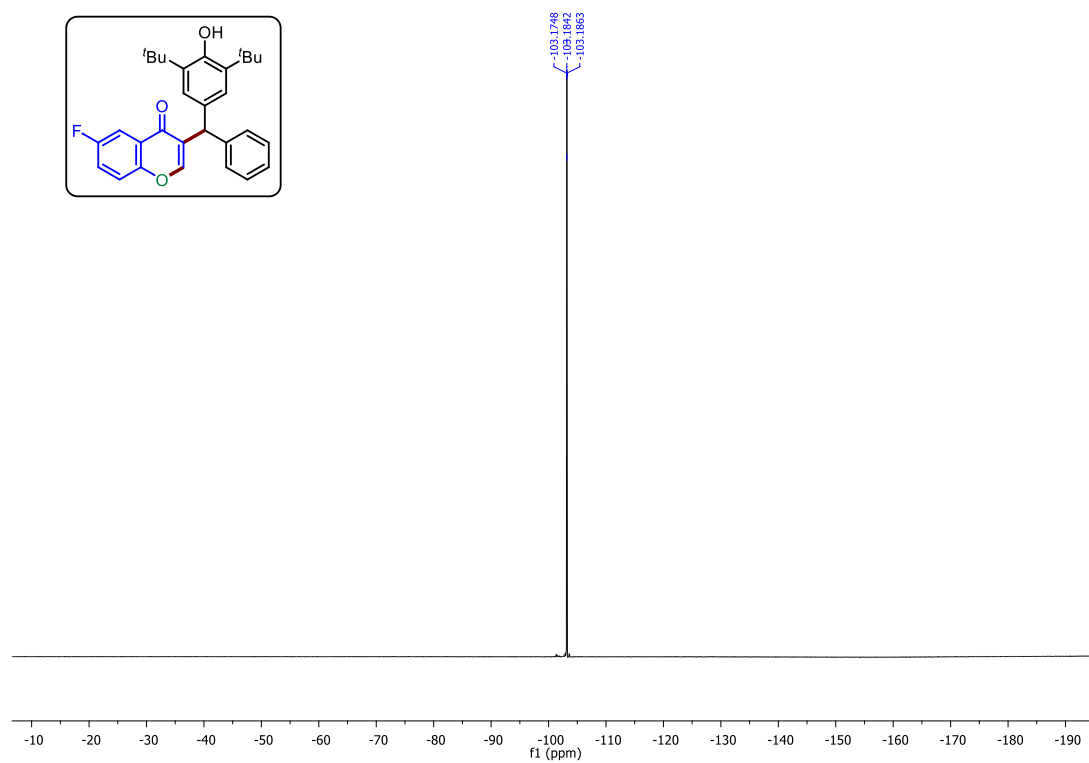
^1H NMR (400 MHz, CDCl_3) Spectrum of **83x**



^{13}C $\{^1\text{H}\}$ NMR (100 MHz, CDCl_3) Spectrum of **83x**



^{19}F $\{^1\text{H}\}$ NMR (376 MHz, CDCl_3) Spectrum of **83x**



2.8 References:

1. Ellis, G. P. In *Chromenes, Chromanones, and Chromones: The Chemistry of Heterocyclic Compounds*; Ellis, G. P., Ed.; John Wiley & Sons, Inc.: New York, 1977; Vol. 31, pp 1-10.
2. For recent reviews: (a) (a) Li, N. G.; Shi, Z. H.; Tang, Y. P.; Ma, H. Y.; Yang, J. P.; Li, B. Q.; Wang, Z. J.; Song, S. L.; Duana, J. A. Synthetic Strategies in the Construction of Chromones. *J. Heterocyclic Chem.*, **2010**, *47*, 785. (b) Gaspar, A.; Matos, M. J.; Garrido, J.; Uriarte, E.; Borges, F. Chromone: A Valid Scaffold in Medicinal Chemistry. *Chem. Rev.* **2014**, *114*, 4960. (c) Vanguru, M.; Merguru, R.; Garimella, S.; E. L.; A Review on The Synthetic Methodologies of Chromones. *Asian J Pharm Clin Res*, **2018**, *11*, 9.
3. (a) L. W. Burgher, R. M. Elliott and I. Kass, *Chest*, 1971, 60, 210. (b) Sharma, R.; Williams, I. S.; Gatchie, L.; Sonawane, V. R.; Chaudhuri, B.; Bharate, S. B. *ACS Omega* **2018**, *3* (8), 8553. (c) Yan, X.; Qi, M.; Li, P.; Zhan, Y.; Shao, H. of Action. *Cell Biosci.* **2017**, *7* (1), 1. (d) mran, M.; Aslam Gondal, T.; Atif, M.; Shahbaz, M.; Batool Qaisarani, T.; Hanif Mughal, M.; Salehi, B.; Martorell, M.; Sharifi-Rad, J. *Phyther. Res.* **2020**, *34* (8), 1812.
4. (a) Hadjeri, M.; Barbier, M.; Ronot, X.; Mariotte, A. M.; Boumendjel, A.; Boutonnat, J. *J. Med. Chem.* **2003**, *46* (11), 2125.
5. (a) Tawfik, H. A.; Ewies, E. F.; El-Hamouly, W. S. *Ijrpc* **2014**, *2014* (4), 1046. (b) Sabui, S. K.; Venkateswaran, R. V. *Tetrahedron Lett.* **2004**, *45* (5), 983.
6. Griffin, R. J.; Fontana, G.; Golding, B. T.; Guiard, S.; Hardcastle, I. R.; Leahy, J. J. J.; Martin, N.; Richardson, C.; Rigoreau, L.; Stockley, M.; Smith, G. C. M. *J. Med. Chem.* **2005**, *48* (2), 569.
7. Maiti, A.; Cuendet, M.; Kondratyuk, T.; Croy, V. L.; Pezzuto, J. M.; Cushman, M. *J. Med. Chem.* **2007**, *50* (2), 350.
8. Yang, Z.; Miao, H.; *Org. Lett.* **2000**, *12*, 1765.
9. Liang, Bo.; Huang, M.; You, Z.; Xiong, Z.; Lu, Kui.; Fathi, R.; Chen, J.; Yang, Z. *J. Org. Chem.* **2005**, *70*, 6097.
10. Awuah, E.; Capretta, A. *Org. Lett.* **2009**, *11*, 3210-3215.
11. Zhao, X.; Zhou, J.; Lin, S.; Jin, X.; Liu, R.; *Org. Lett.* **2017**, *19*, 976.
12. Yue, Yixia.; Peng, Jinsong.; Wang, Deqiang.; Bian, Yunyun.; Sun, Peng.; Chen, Chunxia. *J. Org. Chem.* **2017**, *82*, 5481.

13. Baruah, S.; Kaishap, P. P.; Gogoi, S. *Chem. Commun.*, **2016**, 52, 13004.
14. Raja, G. C. E.; Ryu, J. Y.; Lee, J.; Lee, S. *Org. Lett.* **2017**, 19, 6606.
15. Chang M. Y.; Chen, Y. H.; Wang, H. S. *J. Org. Chem.* **2018**, 83, 2361.
16. Debbarma, S.; Sk, M. R.; Modak, B.; Maji, M. S. *J. Org. Chem.* **2019**, 84, 6207.
17. Xiang, H.; Zhao, Q.; Tang, Z.; Xiao, J.; Xia, P.; Wang, C.; Yang, C.; Chen, X.; Yang, H.; *Org. Lett.* **2017**, 19, 146.
18. Gao, Y., Liu, Y., Wan, J.-P. *J. Org. Chem.* **2019**, 84, 2243.
19. Akram, M. O.; Bera, S.; Patil, N. T. *Chem. Commun.* **2016**, 52, 12306.
20. Wan, J.-P.; Tu, Z.; Wang, Y.; *Chem. Eur. J.* **2019**, 25, 6907-6910.
21. Wan, J.-P.; Zhong, S.; Guo, Y.; Wei, L.; *Eur. J. Org. Chem.* **2017**, 4401.
22. Guo, Y.; Xiang, Y.; Wei, L.; Wan, J.-P.; *Org. Lett.* **2018**, 20, 3971.
23. For recent reviews on *para*-quinone methides chemistry: (a) Li, W.; Xu, X.; Zhang, P.; Li, P. *Chem. Asian J.* **2018**, 17, 2350. (b) Lima, C. G. S.; Pauli, F. P.; Costa, D. C. S.; de Souza, A. S.; Forezi, L. S. M.; Ferriera, V. F.; de Carvalho da Silva. *Eur. J. Org. Chem.* **2020**, 18, 2650. (c) Wang, J. -Y.; Hao, W. -J.; Tu, S. -J.; Jiang, B. *Org. Chem. Front.* **2020**, 7, 1743.
24. For a recent review from our research group on *p*-QMs chemistry: Singh, G.; Pandey, R.; Pankhade, Y. A.; Fatma, S.; Anand, R. V. *Chem. Rec.* **2021**, 21, 4150.
25. (a) Jadhav, A. S.; Pankhade, Y. A.; Anand, R. V. *J. Org. Chem.* **2018**, 83, 8615. (b) Jadhav, A. S.; Pankhade, Y. A.; Hazra, R.; Anand, R. V. *J. Org. Chem.* **2018**, 83, 10107. (c) Pankhade, Y. A.; Pandey, R.; Fatma, S.; Ahmad, F.; Anand, R. V. *J. Org. Chem.* **2022**, 87, 3363.
26. (a) Singh, G.; Kumar, S.; Chowdhury, A; Anand, R. V. *J. Org. Chem.* **2019**, 84, 15978. (b) Singh, G.; Goswami, P.; Sharma, S.; Anand, R. V. *J. Org. Chem.* **2018**, 83, 10546.
27. For recent reviews on the synthetic applications of enamines: (a) Gaber, M.; Bagley, M. C.; Muhammad, Z. A.; Gomha, S. M. *RSC Adv.*, **2017**, 7, 14562. (b) Fu, L.; Wan, J. P. *Asian J. Org. Chem.* **2019**, 8, 767. (c) Huang, J.; Yu, F. *Synthesis* **2021**, 53, 587. (d) Chen, X. Y.; Zhang, X.; Wan, J. P. *Org. Biomol. Chem.* **2022**, 20, 2356.
28. (a) Duana, C.; Yeb, L.; Xua, W.; Lia, X.; Chena, F.; Zhaoa, Z.; Lia, X.. *Chin Chem Lett.* **2018**, 29, 1273. (b) Mei, G. J.; Xu, S. L.; Zheng, W. Q.; Bian, C. Y.; Shi, F. *J. Org. Chem.* **2018**, 83, 1414. (c) Satbhaiya, S.; Khonde, N. S.; Rathod, J.; Gonnade, R.; Kumar, P. *Eur. J. Org. Chem.* **2019**, 3127. (d) Song, Z.; Jia, Y.; Zhang, D.; Wang, D. *Eur. J. Org. Chem.* **2021**, 1942.

3. TfOH acid-mediated one-pot synthesis of *O*, *S*, and *N*-based heterocycles from 2-heteroatom functionalized *para*-quinone methides

3.1 Introduction

Xanthene and thioxanthenes are diaryl-annulated heterocyclic condensed aromatic systems often found in many natural products¹ and biologically active² compounds (Figure 1). Xanthene is the parent molecule, in which a pyran ring is fused with two benzene rings on both sides. Whereas in thioxanthene, the oxygen atom is replaced with a sulfur atom. Xanthene and thioxanthenes are privileged scaffolds known to have valuable biological properties such as anti-cancer,³ anti-microbial,⁴ anti-parasitic,⁵ anti-tumor,⁶ anti-proliferative,⁷ anti-inflammatory, antioxidant,⁸ etc. In addition to these properties, thioxanthene and its analogues are used for developing neuroleptic and anti-depressive drugs. For example, few thioxanthenes are used to treat Schizophrenia and other psychotic disorders.⁹ These compounds have also been used in material science as dyes and fluorescent molecules.¹⁰ For example, xanthene dyes, such as fluorescein, rhodamine, and rhodol have been utilized as fluorescent probes or imaging agents for small molecule targets, nucleic acids, proteins, lipid droplets, stem cells, and live animals.

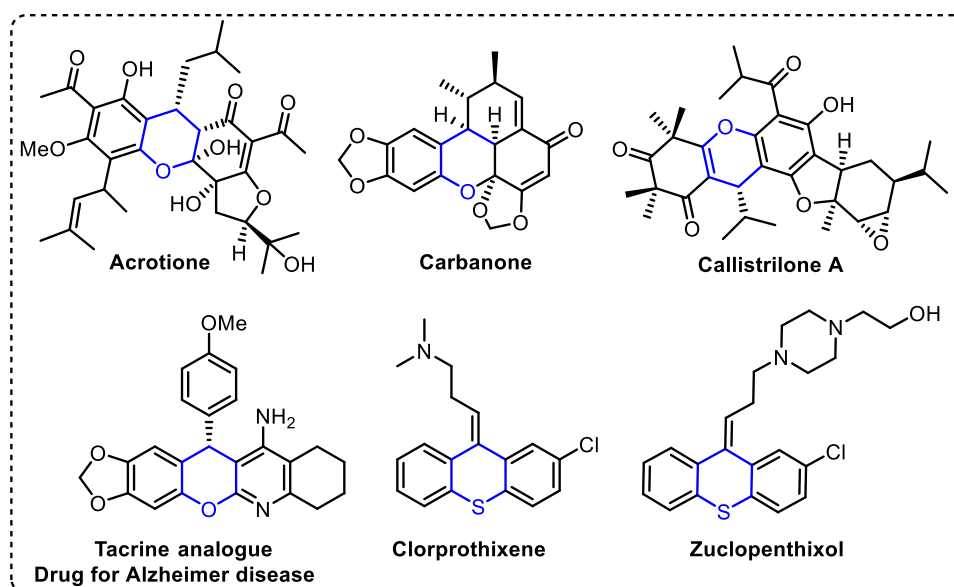


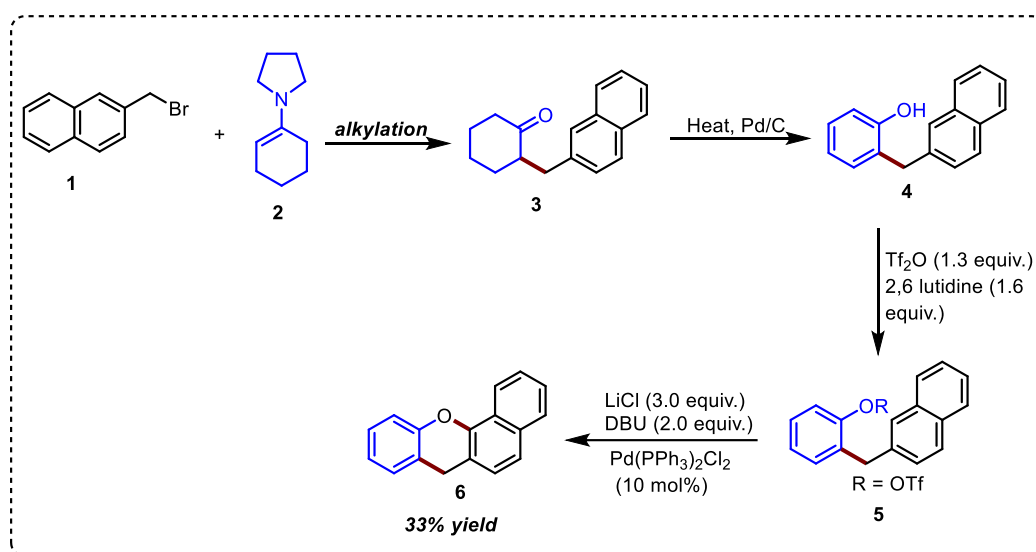
Figure 1. Some 9H-xanthene and 9H-thioxanthenes -based biologically active molecules

Due to such widespread applications in pharmaceutical chemistry and material science, organic chemists have paid much attention to their synthetic routes. Chemical synthesis of these

hetero-atom incorporating tricyclic compounds based on natural products and fluorescent molecules has been studied recently through various approaches. A few of them are discussed below.

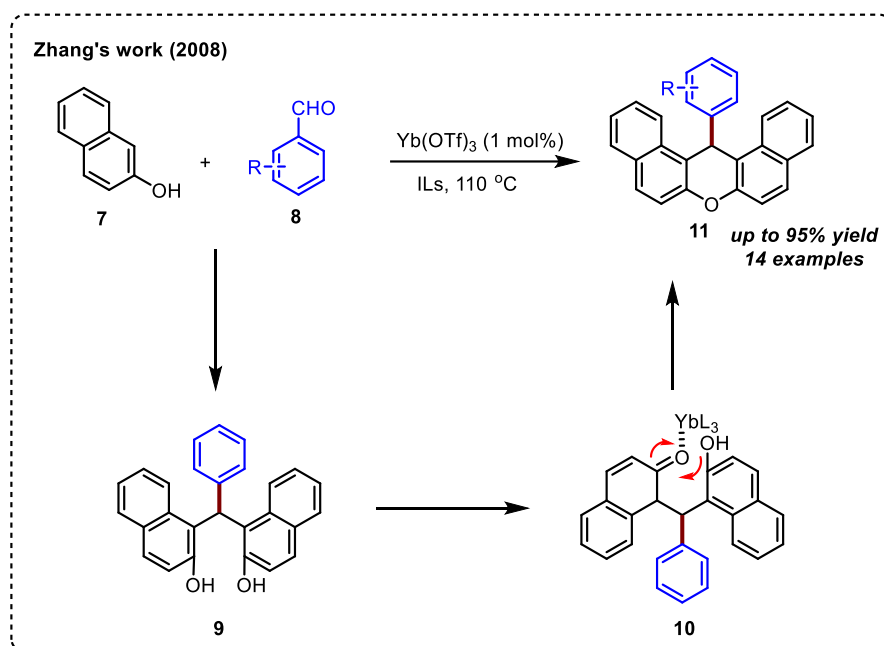
3.2. Literature reports on the synthesis of 9H-xanthene and 9H-thioxanthenes

In 2002, Harvey and co-workers reported a Pd-catalyzed cyclization of *O*-(aryl methyl)phenol triflate esters to polycyclic xanthene derivatives (Scheme 1). This reaction proceeds through an unexpected cleavage of the carbon-oxygen bond to furnish the desired product. This is the first example of a Pd-catalyzed cross-coupling reaction of aryl triflate esters with arenes to form diaryl ethers. The first step involves the alkylation of enamine **2** with **1** to produce 2-(naphthalene-2-ylmethyl)cyclohexane-1-one derivative **3**, which then undergoes a Pd-catalyzed dehydrogenation to give corresponding phenol derivative **4**. Compound **4** was then converted to an aryl triflate ester **5** by treatment with trifluoro methane sulfonic acid anhydride and lutidine. Finally, the last step involves the Pd-catalyzed cross-coupling to furnish the desired product **6** in 33% isolated yield (Scheme 1).¹¹

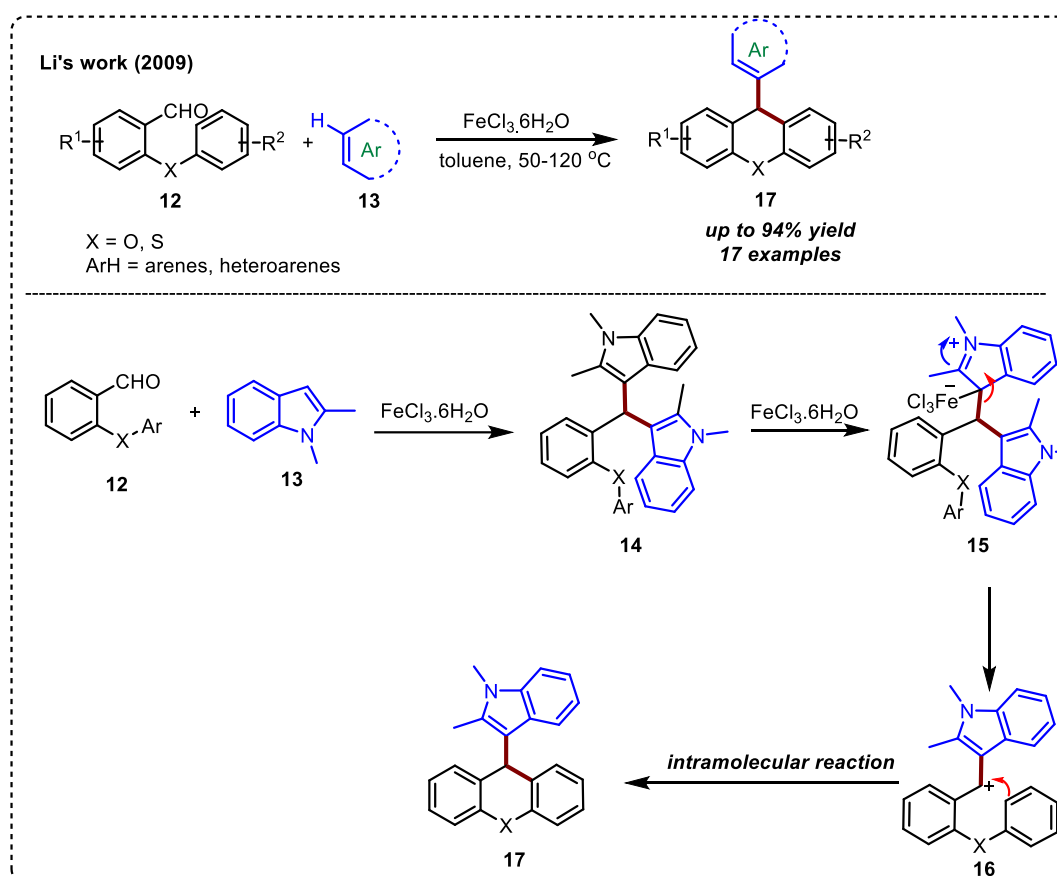


Scheme 1. Pd-catalyzed synthesis of polycyclic xanthenes

Later on, in 2008, Zhang's group developed a green approach for the synthesis of aryl-14H-dibenzo[*a,j*]xanthenes derivatives (**11**) via the condensation reaction of β -naphthol **7** with aldehydes (**8**) in ionic liquids using $\text{Yb}(\text{OTf})_3$ as a catalyst. $\text{Yb}(\text{OTf})_3$ has been used as a Lewis acid for several stages in this transformation. This transformation is beneficial for synthesizing ligands such as xantphos (Scheme 2).¹²



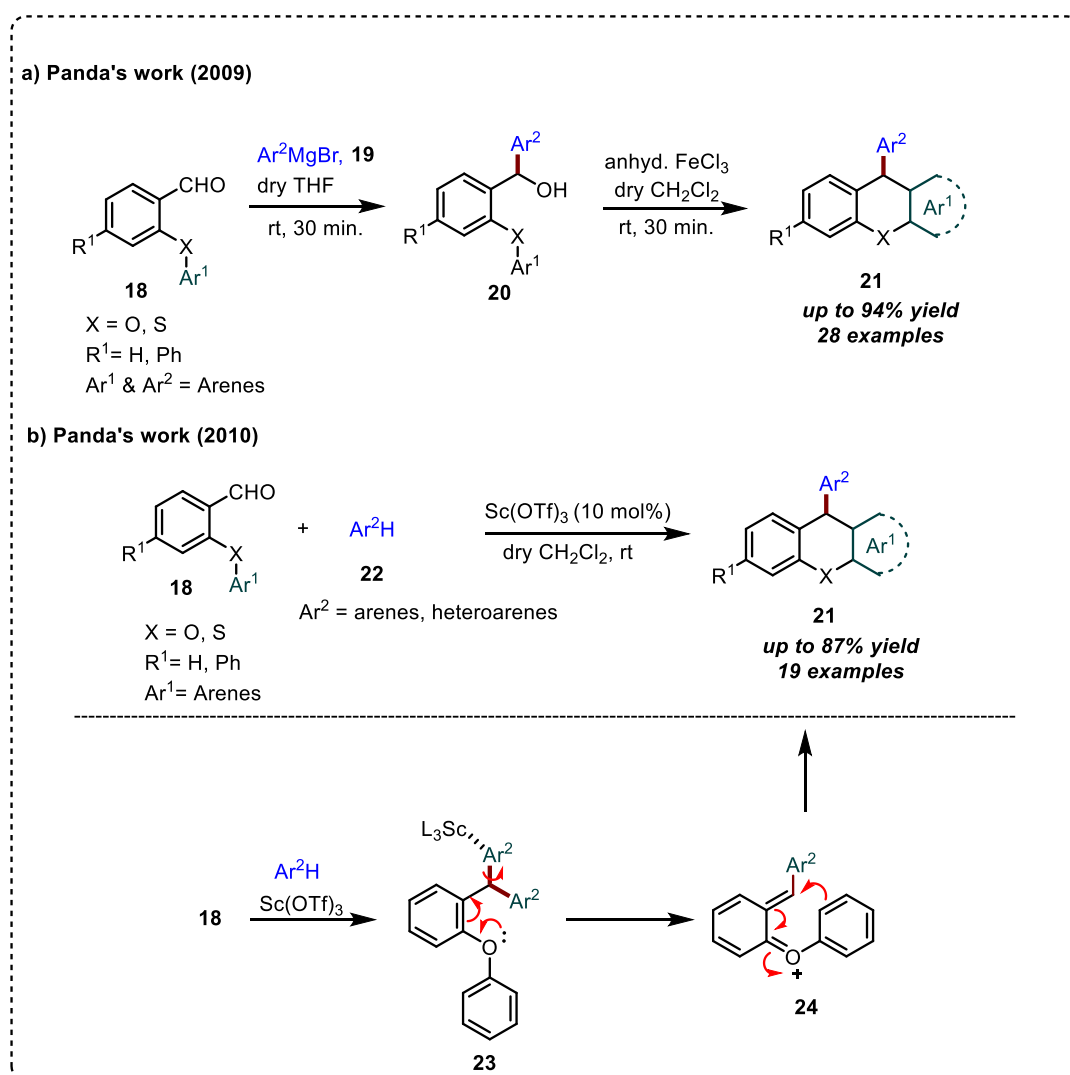
Scheme 2. Synthesis of aryl-14H-dibenzo[*a,j*]xanthenes derivatives in ionic liquids



Scheme 3. Fe(III)-catalyzed one-pot method to synthesize xanthene and thioxanthenes

In 2009, Li group established a Fe(III)-catalyzed one-pot method to synthesize xanthene and thioxanthene analogues (**17**) by annulation of 2-arenoxy and 2-arylsulfonyl

benzaldehyde **12** with electron-rich arenes. According to the proposed reaction mechanism, the reaction proceeds through a Fe(III)-assisted double Friedel-Craft alkylation of indole **13** to afford 1-aryl bis(1H-indol-3-yl) methane **14**, which further involves in electrophilic aromatic substitution on the indole-ring to generate intermediate **15**. Subsequently, intermediate **15** undergoes C-C bond cleavage to generate dibenzylic cation **16** followed by intramolecular Friedel-Craft reaction to furnish the desired product **17** in good yield (Scheme 3).¹³

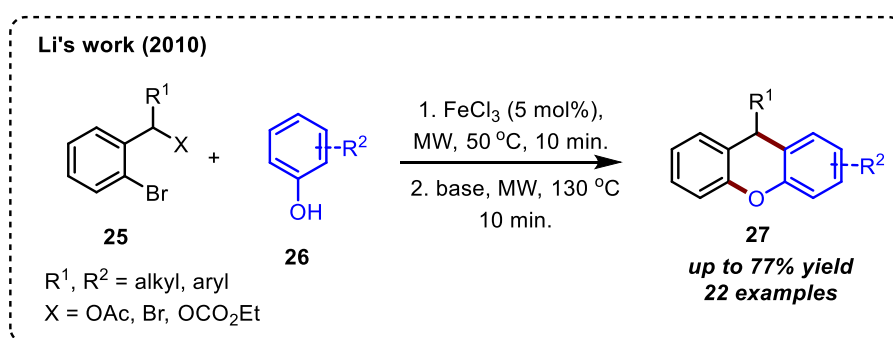


Scheme 4. Panda's approach towards xanthene derivatives.

In 2009, Panda & co-workers reported the synthesis of unsymmetrical 9-arylxanthenes (**21**) via FeCl₃-catalyzed intramolecular diaryl methylation of the carbinols. Carbinol **20** has been prepared in a two-step reaction sequence which involves the nucleophilic substitution of 2-fluoro benzaldehydes with arenoxides to form 2-arenoxy benzaldehydes **18** followed by Grignard reaction of the resulting 2-arenoxy benzaldehydes with aryl-magnesium bromide **19** (a, Scheme 4).¹⁴ Later, the same group in 2010, disclosed a Sc(OTf)₃-catalyzed one-pot

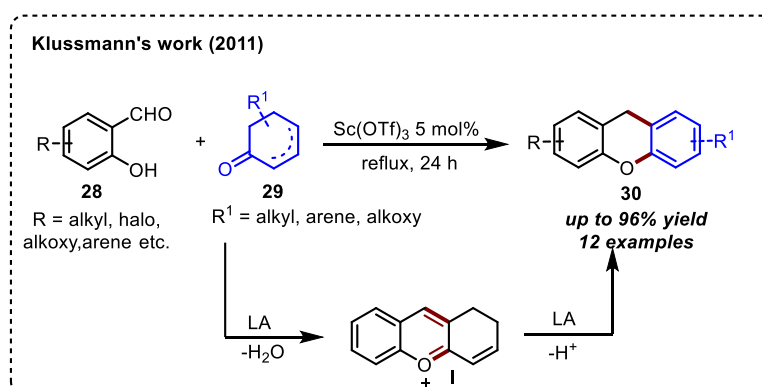
domino approach to synthesize xanthenes derivatives (**21**) under very mild conditions. They have prepared a variety of unsymmetrical 9-aryl/heteroaryl xanthenes **21** in moderate to good yields. This method has been further established to develop tandem carbon-sulfur (C-S) and carbon-carbon (C-C) bonds to create 9-(thioaryl) xanthenes (**b**, Scheme 4).¹⁵

Li & co-workers in 2010, disclosed an iron catalyzed, microwave-promoted, annulation reaction of phenols (**26**) with suitable benzylating agents such as benzyl acetates, benzyl bromides, and benzyl carbonates (**25**) to produce 9-substituted xanthenes (**27**) in good yields. Initially, the benzylation reaction between **25** and respective phenol derivative **26** occurs under microwave with 5 mol% of catalyst loading to give a benzylated product, which was further subjected to microwave irradiation after the addition of base to furnish the desired product **27** (Scheme 5).¹⁶



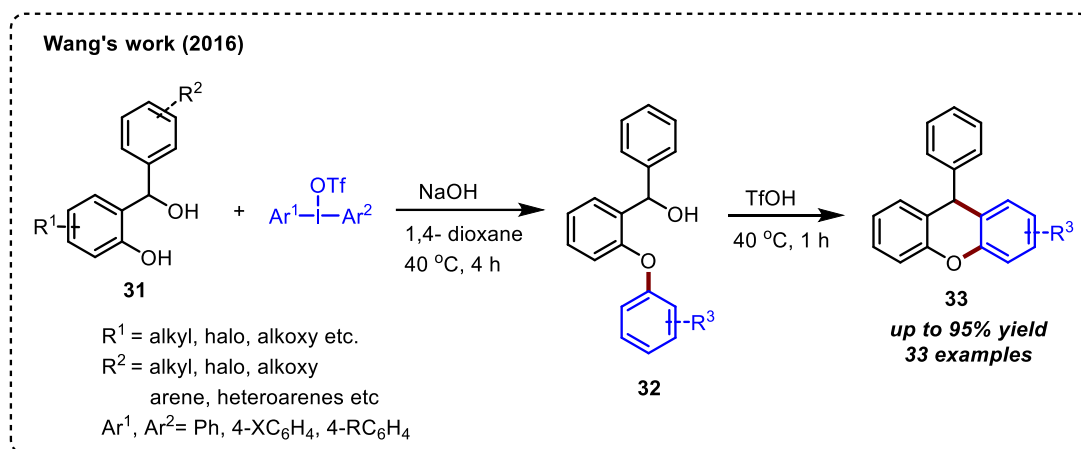
Scheme 5. Microwave-assisted synthesis of xanthenes

The research group of Klussmann in 2011, established a scandium triflate-mediated one-pot approach to synthesize substituted xanthenes (**30**) *via* an annulation reaction between salicylaldehyde **28** and cyclohexenones **29** in good to excellent yields. According to the proposed reaction mechanism, an acid-catalyzed condensation reaction between salicylaldehyde **28** and cyclohexenones **29** will produce benzopyrylium salt **I**, which



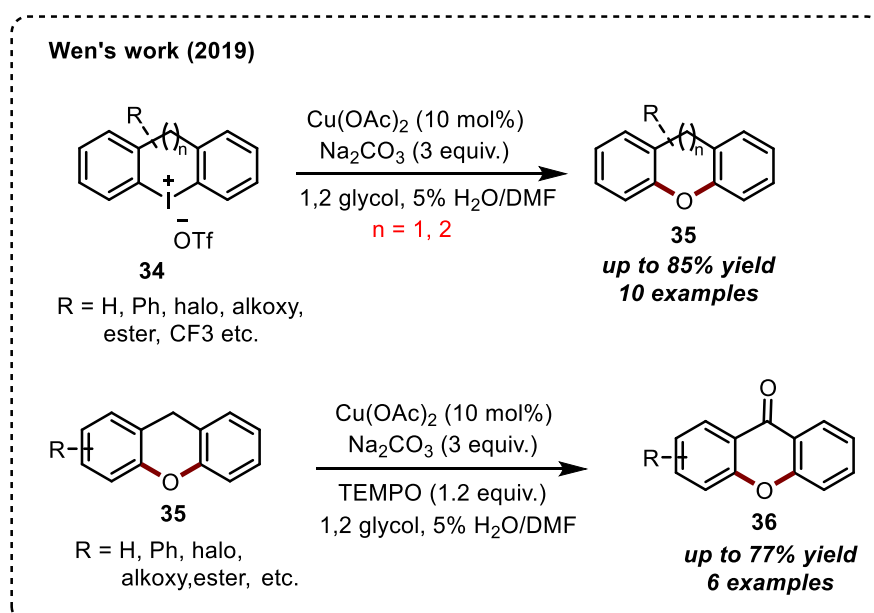
Scheme 6. Lewis acid-mediated approach

further undergoes subsequent sigmatropic hydrogen shift to afford the desired xanthene derivative **30** in excellent yields (Scheme 6).¹⁷



Scheme 7. Brønsted-acid catalyzed approach

In 2016, Wang & co-workers utilized readily available *o*-hydroxy bis-benzyl alcohols **31** and aryl diazonium salts for the one-pot synthesis of unsymmetrical 9-aryl xanthenes **33** in good yields. The reaction proceeds through the generation of carbinols **32** *in situ* using base-mediated annulation of *o*-hydroxy bis-benzyl alcohols **31** and aryl diazonium salts. The resulting carbinols are subjected to Brønsted-acid-enabled cyclization to furnish 9-aryl xanthene **33** (Scheme 7).¹⁸

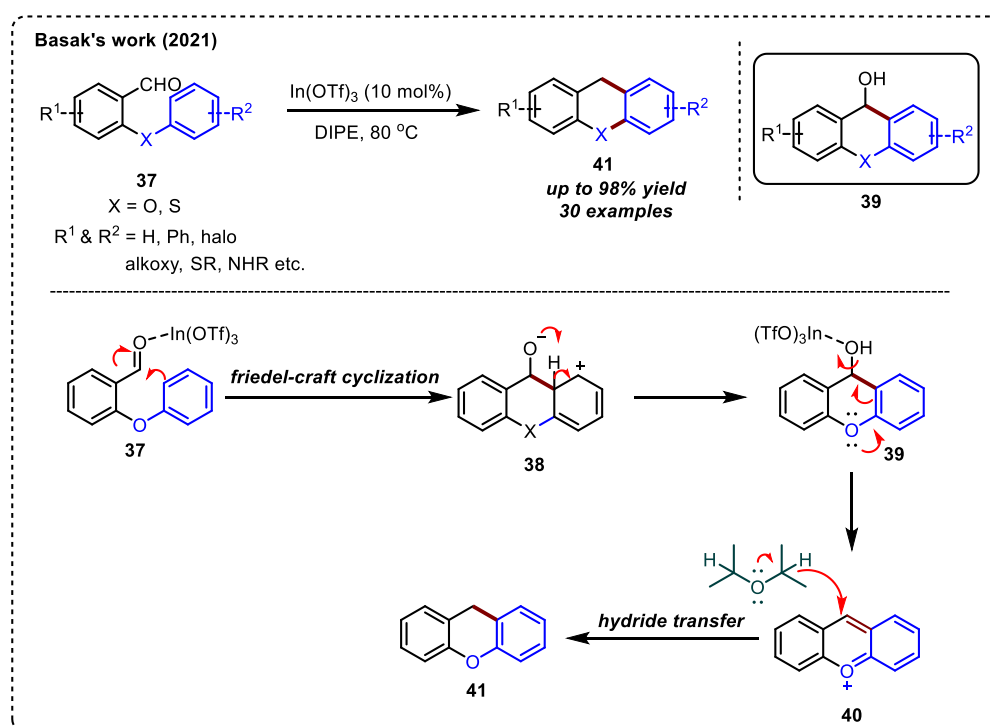


Scheme 8. Synthesis of xanthene and xanthenes from diphenyl iodonium

Very recently, Wen's group utilized diphenyl iodonium (CDPIs) salts as precursor for copper acetate catalyzed one-pot synthesis of xanthenes and xanthenes in good yields (Scheme

8). Numerous functionalized 6-membered CDPIs were made under the proposed reaction condition. However, the oxygenation of CDPIs with a seven-membered iodonium ring failed to yield the desired compounds. To rule out the possibility of radical pathways during the oxygenation of CDPIs with water, the controlled experiment has been done with TEMPO. It was found that oxygenation was not terminated after the addition of TEMPO; in fact, xanthenes **36** were produced with reasonably good yield. This result further ruled out a radical pathway, even though hypervalent iodonium might be able to produce radical intermediates. In this instance, TEMPO probably served as an oxidant to oxidize **35** (Scheme 8).¹⁹

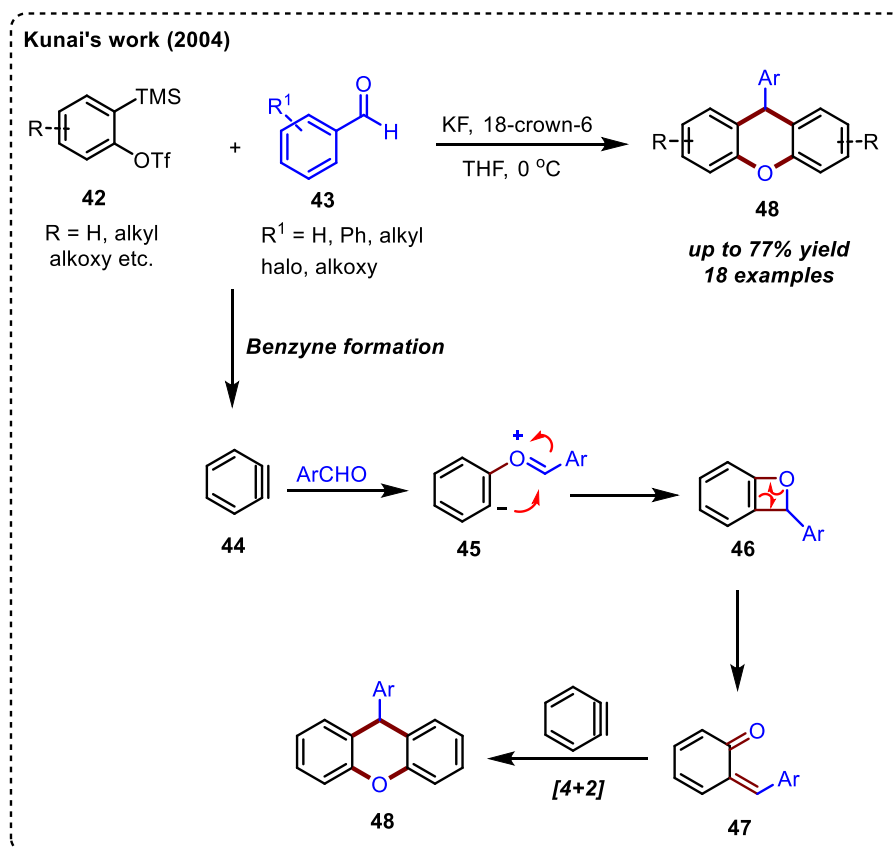
Very recently, Basak & co-workers in 2021, developed a reductive cyclization of 2-aryloxy benzaldehydes/2-(aryl thiol)benzaldehydes (**37**) in the presence of a Lewis acid such as indium triflate to access a wide range of unsubstituted 9H-xanthenes and thioxanthenes (**39**) using di-isopropyl ether as a solvent. Several significant functional groups are compatible with this reductive cyclization technique. Chemoselective reduction of transient xanthylum



Scheme 9. Synthesis of unsubstituted 9H-xanthenes and thioxanthenes

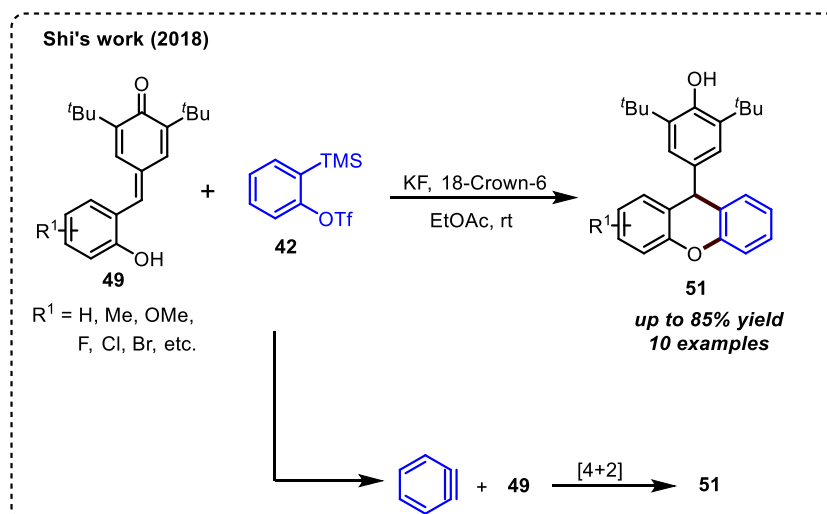
ion in the presence of an aldehydic group *via* intermolecular hydride transfer from the diisopropyl ether is crucial for this transformation (Scheme 9).²⁰

Kunai & co-workers, in 2004, reported the coupling of aldehydes (**43**) with arynes (**42**) to furnish 9-arylxanthenes derivatives (**48**) *via* the formation of *o*-quinone methide **47** as an intermediate. The reaction occurs through *in-situ* generation of benzyne intermediate **44** from



Scheme 10. Synthesis of 9-arylxanthenes *via* *o*-quinone methides

benzyne precursor **42**. The intermediate **42** then undergoes a [2+2]-cycloaddition with an aldehyde to form **46**, which subsequently experiences an electrocyclic ring opening to generate *o*-quinone methide **47**. Finally, the last step involves [4+2]-cyclization between *o*-quinone methide **47** and benzyne **44** to give the desired 9-arylxanthenes derivatives in good yield (Scheme 10).²¹

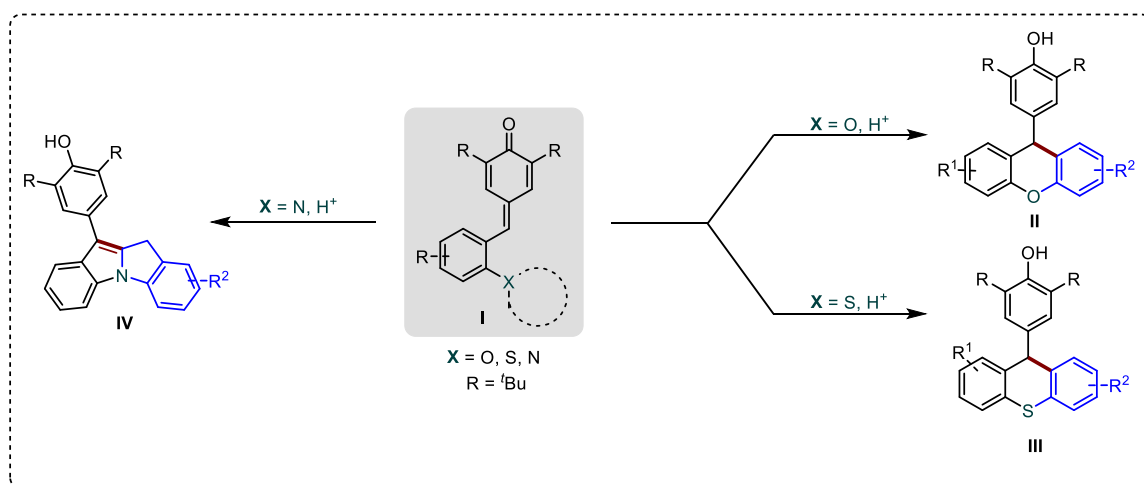


Scheme 11. Shi's approach towards xanthenes derivatives

In 2018, Shi's research group established the cyclization of *para*-quinone methide derivatives via a [4+2]-cycloaddition reaction of *ortho*-hydroxyphenyl-substituted *para*-quinone methides (**49**) and benzyne, which successfully built the xanthene scaffolds (**51**) in high yields (Scheme 11).²²

3.3 Background

Recently, the synthetic utility of functionally modified *p*-quinone methides has been revealed in the preparation of many heterocycles²⁴ and carbocycles²⁵, etc. In line with this, we have recently reported a one-pot protocol to access fluorene derivatives through triflic acid catalyzed 1,6-arylation of 2-aryl phenyl- substituted *p*-quinone methides under continuous flow. In continuation with our ongoing research in the area of *p*-QMs,²⁶ we believe that *ortho*-hetero-atom functionalized *p*-QMs could serve as a potential synthon for constructing xanthene and thioxanthene cores. Herein, we disclose an efficient one-pot method for synthesizing 9H-xanthene scaffolds using 2-hetero-atom functionalized *p*-quinone methides by intramolecular 1,6-conjugate addition strategy (Scheme 19). This method was also elaborated for the synthesis of 9H-thioxanthene derivatives. A similar protocol was also developed for the one-pot synthesis of 10H-indolo[1,2-*a*]indole-based heterocyclic systems through 1,6 intramolecular arylation of *ortho*-indol-phenyl substituted *para*-quinone methides (Scheme 12).



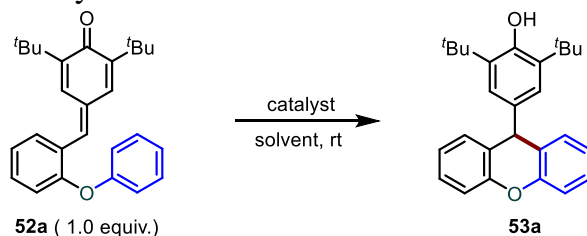
Scheme 12. Our Approach towards 9H-Xanthenes, 9H-thioxanthenes, and 10H-indolo[1,2-*a*]indoles from *p*-QMs

3.4 Results and discussion

We began the optimization experiments by employing *p*-QM **52a** under different reaction conditions, and the outcomes are summarized in Table 1. To our delight, the

result of our first attempt, utilizing TsOH as a catalyst in CH₂Cl₂, was delightful. The desired product **53a** was isolated in an 86% isolated yield within 30 min at room temperature (entry 1). In the case of other protic acids such as CSA, trifluoro acetic acid, and formic acid, **53a** was isolated in 68%, 85%, and 82% yields, respectively (entries 2-4).

Table 1. Optimization study^a



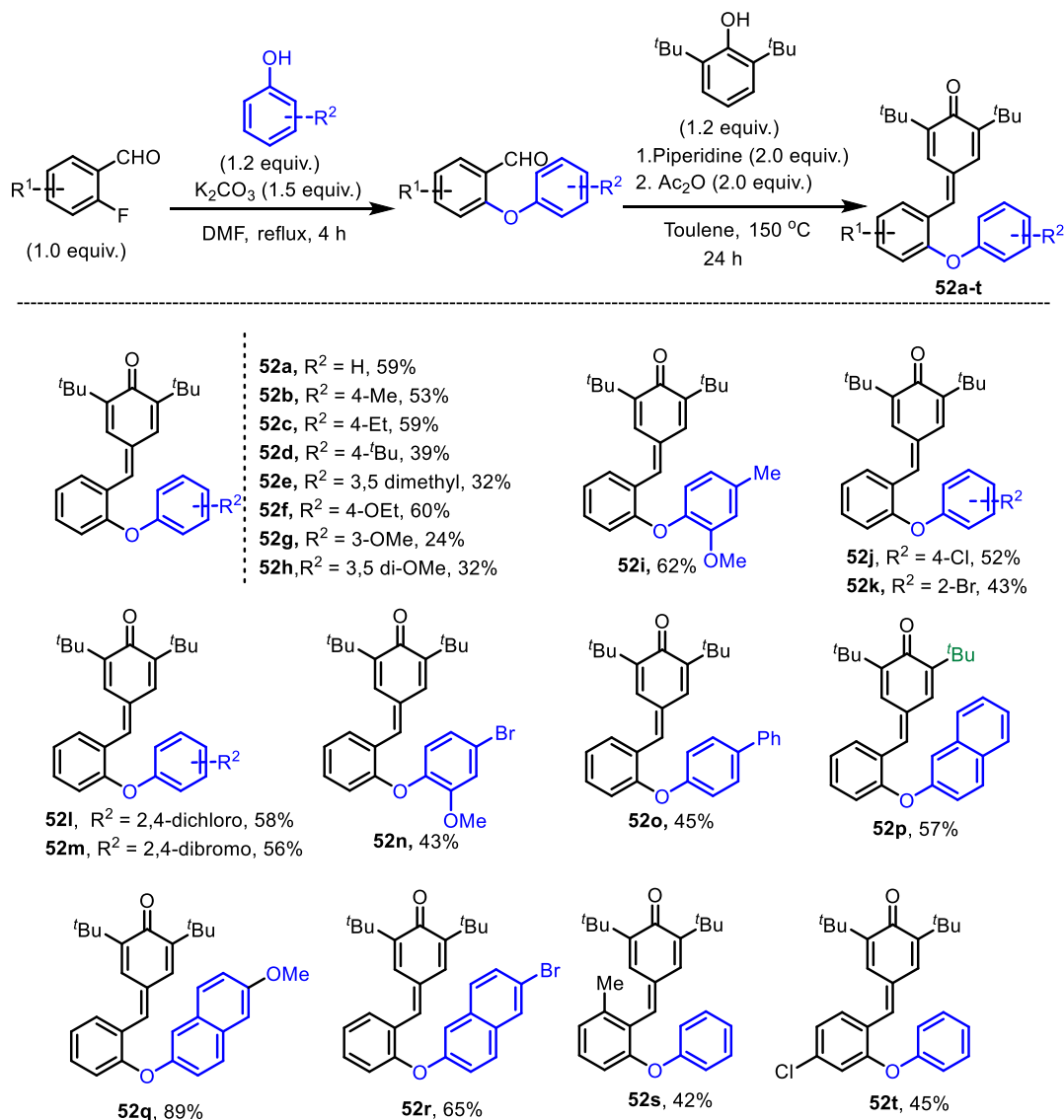
Entry	Acid [20 mol%]	Solvent	Time [min.]	Yield [%] ^b
1	TsOH	CH ₂ Cl ₂	30	86
2	CSA	CH ₂ Cl ₂	45	68
3	TFA	CH ₂ Cl ₂	30	85
4	HCOOH	CH ₂ Cl ₂	45	82
5	TfOH	CH₂Cl₂	30	96
6	TfOH	CH ₃ CN	30	85
7	TfOH	Acetone	45	80
8	TfOH	PhMe	30	76
9	TfOH	THF	45	nr
10	TfOH	DMF	30	65
11	TfOH	1,4-dioxane	45	72
12 ^c	Bi(OTf) ₃	CH ₂ Cl ₂	30	85
13 ^c	Cu(OTf) ₂	CH ₂ Cl ₂	30	75
14	--	CH ₂ Cl ₂	24 h	nr

^aAll reactions were carried out using **52a** (0.051mmol) in 1.5 mL of solvent. ^bIsolated yields. ^c10 mol% of the catalyst.

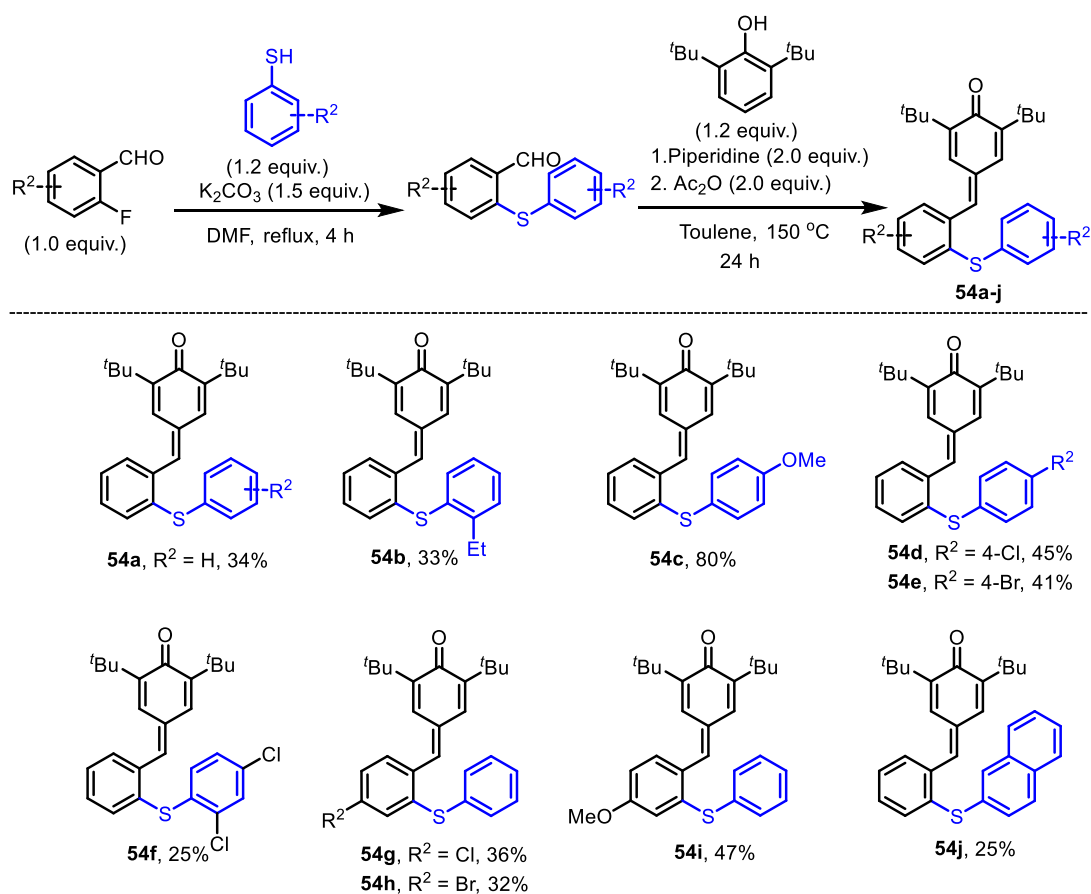
Interestingly, when TfOH in CH₂Cl₂ was used, the expected product **53a** was produced in 96% yield within 30 minutes (entry 5). Further optimization experiments were carried out using TfOH as a catalyst to screen the best solvent for this transformation. All the screened solvents worked efficiently to drive this transformation, and their respective yields are listed in Table 1 (entries 6-11). However, the reaction did not work when THF was used as a solvent. In the case of metal triflates, the yield of the product was found to be less as compared to TfOH acid (entries 12-13). No product formation was observed in the absence of a catalyst, clearly demonstrating the necessity of protic acid for this transformation (entry 14).

The hetero-atom-functionalized *p*-QMs (**52a-t**) and (**54a-j**) used in this study were prepared using hetero-atom-functionalized aldehydes and 2,6-di-*tert*-butylphenol according to the literature procedure²⁷ as shown in Table 2 and 3.

Table 2. Synthesis of 2-*O*- atom-functionalized *p*-QMs



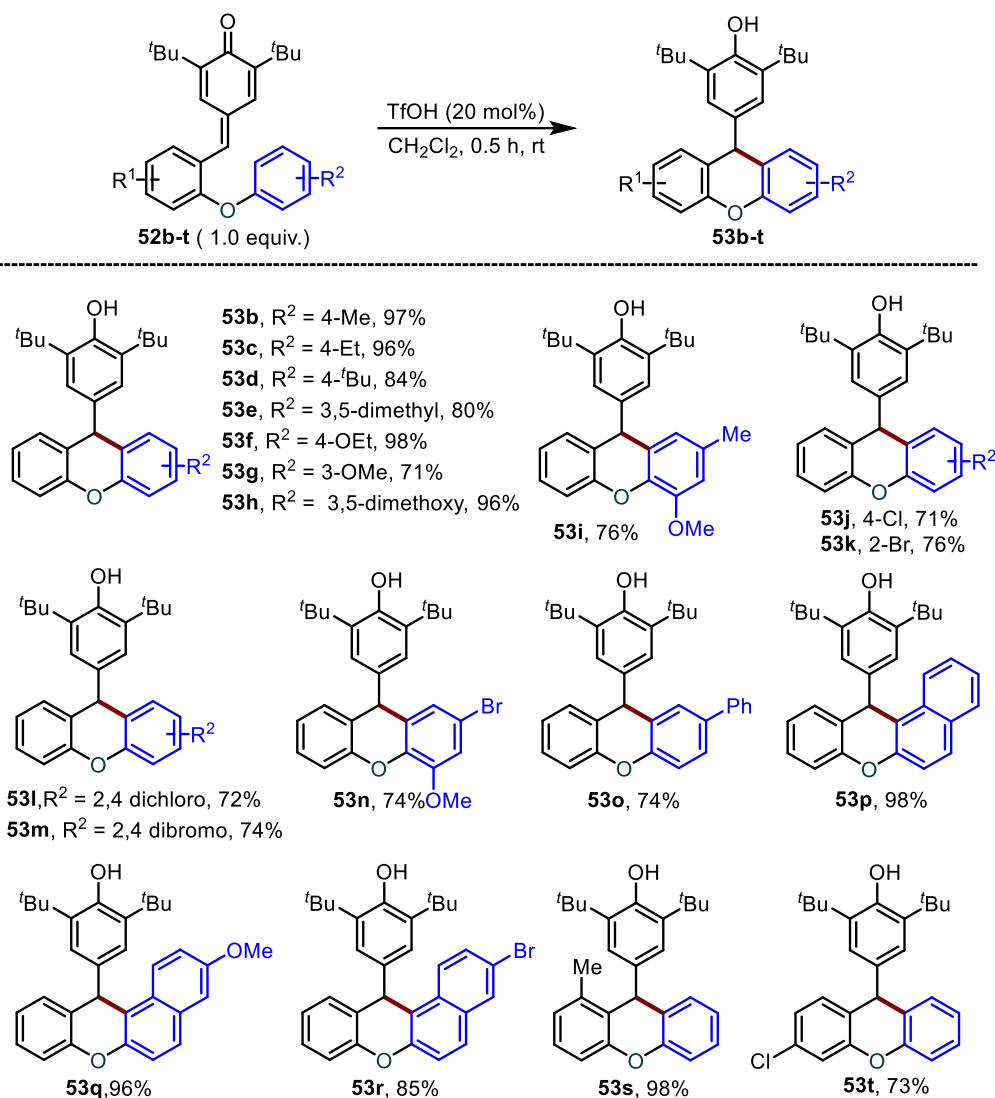
With the optimized reaction conditions in hand, the scope and limitations of this protocol were examined. The ideal conditions (entry 5, Table 1) were used for the reaction between several 2-*O*-aryl-substituted *p*-QMs, and the outcomes are summarized in Scheme 13. The standard reaction conditions were found to be appropriate for xanthenes derivatives (**53b-i**) derived from *p*-QMs (**52b-i**) having electron-rich substituents such as alkyl and alkoxy groups and, in all those cases, the expected products (**53b-i**) obtained in the range of 71-97%

Table 3. Synthesis of 2-*S*-atom-functionalized *p*-QMs

yields. Halo-substituted *p*-QMs **52j-m** also underwent cyclization under the standard condition to produce their respective products **53j-m** in moderate to good yields (71-76%). When the reaction was carried out with *p*-QM **52n** in which, halo and methoxy substituents were present, the respected xanthene derivative (**53n**) obtained in 74% yield. *p*-QMs substituted with various higher-order aromatic hydrocarbons such as **52o-r** worked well to generate the respective products **53o-r** in moderate to excellent yields (74-98%). Substrates such as **52s** and **52t** also reacted well under standard reaction conditions, and their corresponding products (**53s** and **53t**) are isolated in 73 & 98% yields, respectively.

Next, we turned our attention toward synthesizing thioxanthene derivatives using 2-*S*-atom functionalized *p*-QMs **54a** under the optimized reaction conditions, and the expected thioxanthene derivative **55a** was produced in 64% yield. Then the substrate scope was elaborated using a wide range of *p*-QMs (**54b-j**), and the results are shown in Scheme 3. Electron-rich aryl-substituted *p*-QMs **54b** & **54d** provided their corresponding products **55b** and **55d** in 66 & 84% isolated yields, respectively. Similarly, halo-substituted *p*-QMs (**54d-h**) reacted well under optimal conditions and

Scheme 13. Substrate scope with various *O*-atom functionalized *p*-QMs.^a

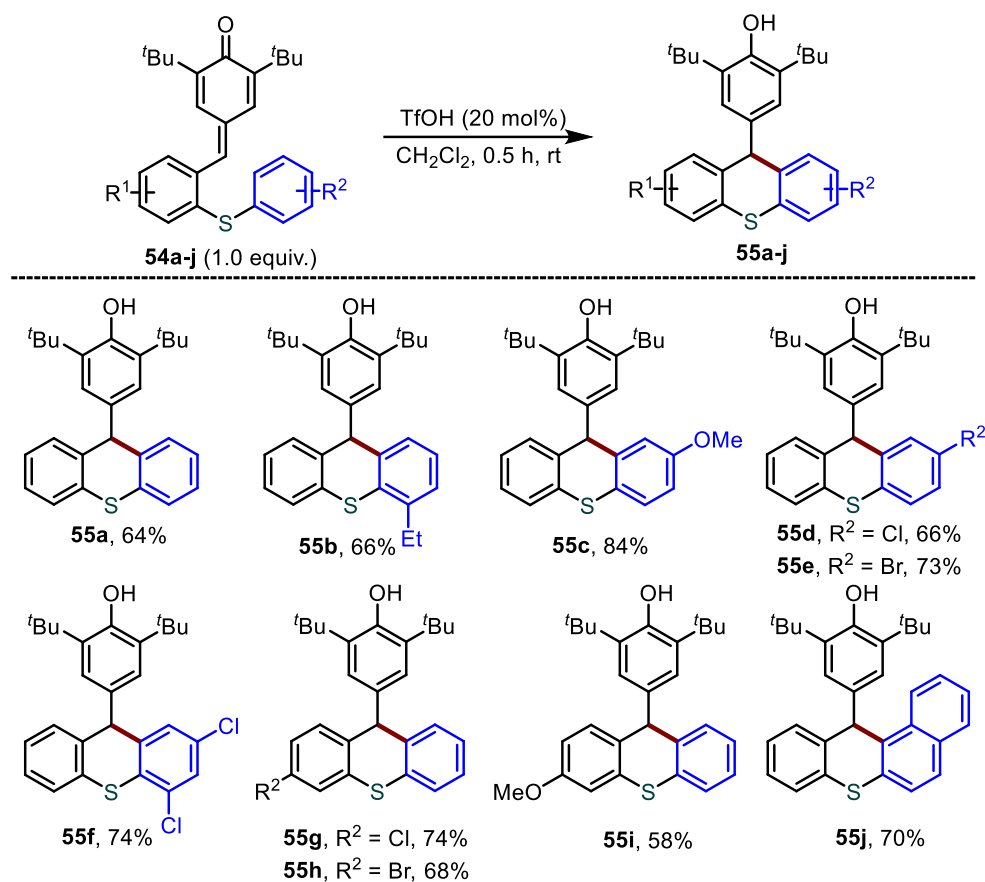


^aAll reactions were carried out using **52a-t** (40mg scale.) in 1.5 mL of CH₂Cl₂. Yields reported are isolated yields.

gave their desired products **55d-h** in good yields (68-74%). When the reaction was carried out with *p*-QM **54i**, the respective product **55i** was obtained with a relatively lesser yield (58%). This approach was also found to be operative for naphthyl-based *p*-QMs **54j**; in this case, we got the desired product **55j** in 70% isolated yield.

Polycyclic indoles have gained significant attention because of their frequent use in pharmaceutical and natural products.²⁸ Very recently, 10H-indolo[1,2-*a*]indole and its analogue have gained researcher's curiosity and become the gradually important heterocyclic framework in material science and medicinal chemistry.²⁹ Therefore, we became interested in the synthesis of these polycyclic indole derivatives. In this regard,

Scheme 14. Substrate scope with various *S*-atom functionalized *p*-QMs.^a



^aAll reactions were carried out using **54a-j** (40 mg scale.) in 1.5 mL of CH₂Cl₂. Yields reported are isolated yields.

Table 4. Synthesis of 2-*N*-atom functionalized *p*-QMs.

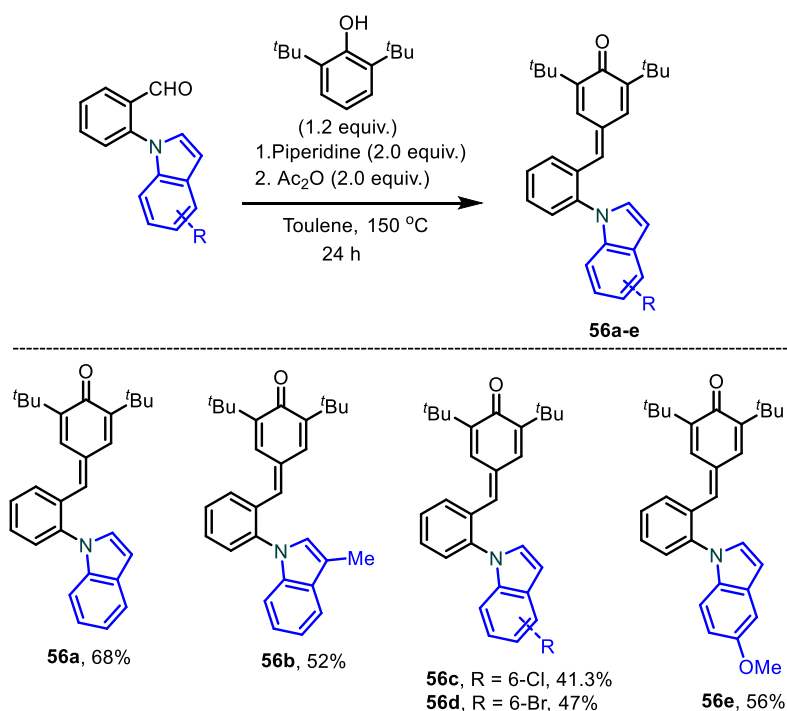
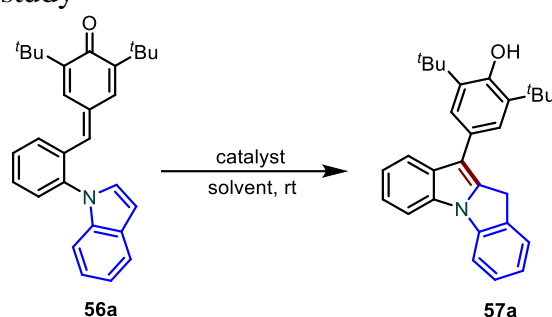
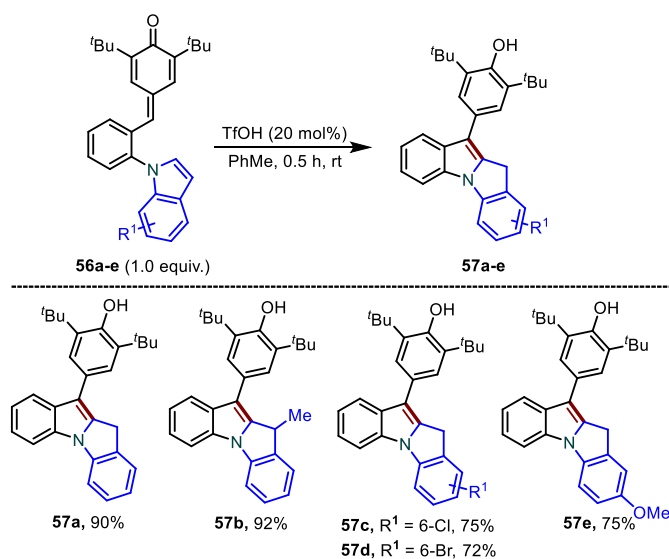


Table 5. Optimization study^a

Entry	Acid	Solvent	Time [min]	Yield [%] ^b
1	TfOH	CH ₂ Cl ₂	30	86
2	TfOH	CH ₃ CN	30	82
3	TfOH	Acetone	45	80
4	TfOH	PhMe	30	90
5	TfOH	THF	120	trace
6	TfOH	DMF	720	nr
7	TfOH	1,4-dioxane	120	50

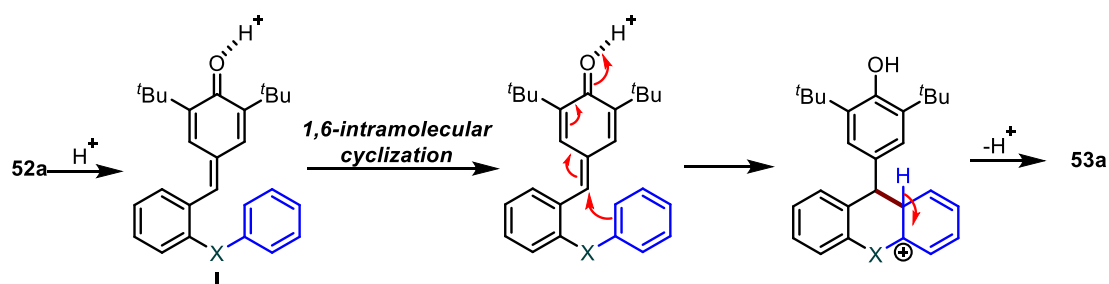
^aAll reactions were carried out using **56a** (0.098 mmol) in 1.5 mL of PhMe. Yields reported are isolated yields we extended the same protocol for synthesizing 10H-indolo[1,2-*a*]indole derivatives **57a-e** using *p*-QMs. Therefore, in this line we have prepared series of 2-indol-phenyl substituted *para*-quinone methides **56a-e** from 2-(1H-indol-1-yl)benzaldehyde derivatives and 2,6-di-tert-butylphenol using the literature procedure²⁷ and the results are summarized in Table 4.

Scheme 15. Substrate scope using different *N*-atom functionalized *p*-QMs.^a

^aAll reactions were carried out using **56a-e** (40 mg scale) in 1.5 mL of PhMe. Yields reported are isolated yields.

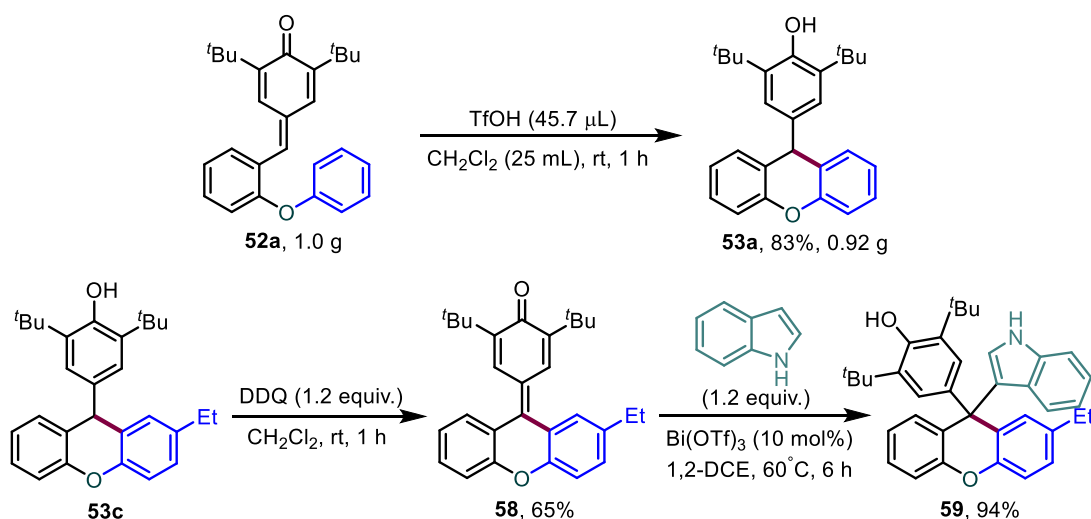
A short optimization study was carried out for this transformation using **56a**, and 20 mol% of triflic acid at room temperature under various reaction conditions and the results are summarized in Table 5. It was found that toluene is the best solvent for this transformation and the expected product **57a** was isolated in 90% yield within 0.5 h at room temperature.

Having the optimized reaction conditions in hand (Table 5), the substrate scope and boundaries were estimated using a wide range of 2-(1H-indol-1-yl) *p*-QMs (**56a-e**). All *p*-QMs reacted well to produce their respective 10H-indolo[1,2-*a*]indole derivatives (**57a-e**) in good yields and the results are summarized in Scheme 15.



Scheme 16. Proposed reaction mechanism

Based on the literature reports and the outcome of the reaction, a plausible reaction mechanism for this transformation has been proposed. Initially, triflic acid activates the *p*-QM to generate an intermediate (**I**) followed by 1,6 intramolecular arylation and aromatization to produce the product **53a** (Scheme 16).



Scheme 17. Gram scale reaction and synthetic elaboration

To show the practicality of this methodology, a relatively large-scale reaction was performed with **52a** under the standard reaction conditions and the product **53a** was obtained with an 83%

yield (Scheme 17). Further, one of the xanthene derivatives **53c** was subjected to DDQ oxidation to access the corresponding quinone product **58** in a 65% isolated yield. Since indole-containing diaryl- and triaryl methanes derivatives are very important scaffolds in many biologically active compounds.²⁰ So, we have converted **58** to indolyl methane analogue **59** by the reaction of indole in the presence of Bi(OTf)₃ (Scheme 17).

3.5 Conclusion

In conclusion, we have demonstrated a simple acid-catalyzed approach for the synthesis of xanthene derivatives under mild reaction conditions. A wide range of xanthene derivatives could be accessed using this protocol in moderate to good yields. We have also elaborated this methodology for the synthesis of thioxanthene and polycyclic indole derivatives. *N*, *O* and *S* containing compounds are present in many natural and pharmaceutically active molecules and these protocols provides the straightforward access to synthesize those biologically active molecules and related analogues.

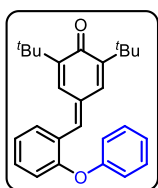
3.6 Experimental section

General methods: All reactions were carried out under an argon atmosphere in an oven-dried round bottom flask. All the solvents were distilled before use and stored under an argon atmosphere. Most of the reagents and starting materials were purchased from commercial sources and used as such. All *para*-quinone methides were prepared by following a literature procedure.¹ Melting points were recorded on the SMP20 melting point apparatus and are uncorrected. ¹H, and ¹³C spectra were recorded in CDCl₃ and DMSO (400, 100, and 376 MHz respectively) on Bruker FT-NMR spectrometer. Chemical shift (δ) values are reported in parts per million relatives to TMS and the coupling constants (*J*) are reported in Hz. High-resolution mass spectra were recorded on Waters Q-TOF Premier-HAB213 spectrometer. FT-IR spectra were recorded on a Perkin-Elmer FTIR spectrometer. Thin-layer chromatography was performed on Merck silica gel 60 F₂₅₄ TLC pellets and visualized by UV irradiation and KMnO₄ stain. Column chromatography was carried out through silica gel (100–200 mesh) using EtOAc/hexane as eluent.

General procedure for the synthesis of 2-heteroaryl-phenyl substituted *para*-quinone methides (52a-t), (54a-j) and (56a-e):): In a Dean-Stark apparatus, a solution of 2-heteroatom functionalized benzaldehyde (1.0 equiv.) and 2,6-di-*tert*-butyl phenol (1.2 equiv.) in toluene was heated to reflux for 30 min. To this solution, piperidine (3.0 equiv.) was added in

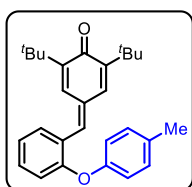
a drop-wise manner at 100 °C and, the resultant reaction mixture was stirred at 150 °C for 24 h. The reaction mixture was then cooled to room temperature; acetic anhydride (3.0 equiv.) was added at 100 °C and stirring was continued for additional 1 h. The reaction mixture was cooled to room temperature, poured on ice-cold water and extracted with dichloromethane. The combined organic layer was dried over sodium sulfate, filtered and concentrated under reduced pressure. The residue was then purified by neutral alumina chromatography using hexane/ethylacetate mixture to obtain pure 2-heteroaryl phenyl substituted *para*-quinone methides.

2,6-di-*tert*-butyl-4-(2-phenoxybenzylidene)cyclohexa-2,5-dien-1-one (52a): Yellow solid



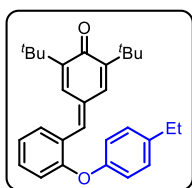
(1.00 g, 59% yield); m. p. = 130 –132 °C; R_f = 0.5 (5% EtOAc in hexane); ^1H NMR (400 MHz, CDCl_3) δ 7.52 – 7.49 (m, 2H), 7.42 (s, 1H), 7.40 – 7.31 (m, 3H), 7.21 – 7.13 (m, 2H), 7.05 – 7.02 (m, 3H), 6.92 (dd, J = 8.2, 0.8 Hz, 1H), 1.32 (s, 9H), 1.31 (s, 9H); $^{13}\text{C}\{^1\text{H}\}$ NMR (100 MHz, CDCl_3) δ 186.8, 156.7, 156.4, 149.4, 147.7, 137.8, 135.3, 132.4, 132.2, 130.8, 130.1, 128.2, 127.4, 124.0, 123.3, 119.3, 118.4, 35.6, 35.1, 29.7, 29.6; FT-IR (thin film, neat): 2954, 1613, 1575, 1475, 1301, 797 cm^{-1} ; HRMS (ESI): m/z calcd for $\text{C}_{27}\text{H}_{31}\text{O}_2$ $[\text{M}+\text{H}]^+$: 387.2324; found : 387.2326.

2,6-di-*tert*-butyl-4-(2-(*p*-tolylloxy)benzylidene)cyclohexa-2,5-dien-1-one (52b): Yellow



solid (1.12 g, 53% yield); m. p. = 120 – 122 °C; R_f = 0.5 (5% EtOAc in hexane); ^1H NMR (400 MHz, CDCl_3) 7.52 (d, J = 2.3 Hz, 1H), 7.49 (dd, J = 7.6 1.0 Hz, 1H), 7.45 (s, 1H), 7.33– 7.29 (m, 1H), 7.18 – 7.14 (m, 3H), 7.05 (d, J = 2.3 Hz, 1H), 6.96 – 6.92 (m, 2H), 6.87 (dd, J = 8.2, 0.8 Hz, 1H), 2.35 (s, 3H), 1.33 (s, 9H) 1.32 (s, 9H); $^{13}\text{C}\{^1\text{H}\}$ NMR (100 MHz, CDCl_3) δ 186.8, 157.0, 154.2, 149.3, 147.7, 138.0, 135.4, 133.7, 132.3, 132.1, 130.8, 130.6, 128.2, 127.0, 122.9, 119.4, 117.8, 35.6, 35.1, 29.7, 29.6, 20.9, 20.88; FT-IR (thin film, neat): 2954, 1613, 1575, 1475, 1301, 797 cm^{-1} ; HRMS (ESI): m/z calcd for $\text{C}_{28}\text{H}_{31}\text{O}_2$ $[\text{M}-\text{H}]^-$: 399.2324; found : 399.2327.

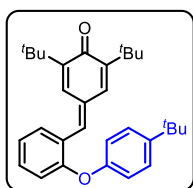
2,6-di-*tert*-butyl-4-(2-(4-ethylphenoxy)benzylidene)cyclohexa-2,5-dien-1-one (52c):



Yellow solid (1.20 g, 59% yield); m. p. = 140 – 142 °C; R_f = 0.5 (5% EtOAc in hexane); ^1H NMR (400 MHz, CDCl_3) 7.52 (d, J = 2.3 Hz, 1H), 7.48 (dd, J = 7.5, 0.7 Hz, 1H), 7.44 (s, 1H), 7.34– 7.29 (m, 1H), 7.20 – 7.14 (m, 3H), 7.04 (d, J = 2.3 Hz, 1H), 6.98 – 6.94 (m, 2H), 6.90 – 6.88 (m, 1H), 2.65 (q, J = 7.6 Hz, 2H), 1.32 (s, 9H), 1.31 (s, 9H), 1.25 (t, J = 7.6 Hz, 3H); $^{13}\text{C}\{^1\text{H}\}$ NMR (100 MHz, CDCl_3) δ 186.8, 157.0, 154.4, 149.3, 147.7, 140.1, 138.0, 135.4, 132.3, 132.1, 130.8, 129.4, 128.2, 127.1, 122.9, 119.4, 117.9, 35.6, 35.1, 29.7, 29.6, 28.3, 15.9; FT-IR (thin film, neat): 2956,

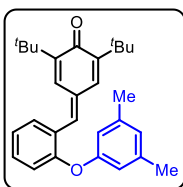
1613, 1451, 1359, 1236, 742 cm^{-1} ; HRMS (ESI): m/z calcd for $\text{C}_{29}\text{H}_{35}\text{O}_2$ $[\text{M}+\text{H}]^+$: 415.2637; found : 415.2633.

2,6-di-*tert*-butyl-4-(2-(4-(*tert*-butyl)phenoxy)benzylidene)cyclohexa-2,5-dien-1-one (52d):



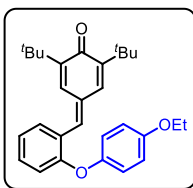
Yellow solid (0.35 g, 39% yield); m. p. = 137–138 °C; R_f = 0.5 (5% EtOAc in hexane); ^1H NMR (400 MHz, CDCl_3) δ 7.52 (d, J = 2.2 Hz, 1H), 7.49 (d, J = 7.6 Hz, 1H), 7.43 (s, 1H), 7.39 – 7.36 (m, 2H), 7.34 – 7.30 (m, 1H), 7.16 (t, J = 7.5 Hz, 1H), 7.03 (d, J = 2.3 Hz, 1H), 6.98 – 6.95 (m, 2H), 6.92 (d, J = 8.2 Hz, 1H), 1.33 (s, 9H), 1.32 (s, 9H), 1.31 (s, 9H); $^{13}\text{C}\{^1\text{H}\}$ NMR (100 MHz, CDCl_3) δ 186.8, 156.8, 154.2, 149.3, 147.7, 147.0, 138.0, 135.4, 132.3, 132.1, 130.8, 128.2, 127.2, 126.9, 123.0, 118.9, 118.1, 35.6, 35.1, 34.5, 31.6, 29.7, 29.6; FT-IR (thin film, neat): 2957, 1613, 1474, 1390, 1301, 755 cm^{-1} ; HRMS (ESI): m/z calcd for $\text{C}_{31}\text{H}_{39}\text{O}_2$ $[\text{M}+\text{H}]^+$: 443.2950; found : 443.2946.

2,6-di-*tert*-butyl-4-(2-(3,5-dimethylphenoxy)benzylidene)cyclohexa-2,5-dien-1-one (52e):



Yellow solid (0.70 g, 32% yield); m. p. = 123–125 °C; R_f = 0.5 (5% EtOAc in hexane); ^1H NMR (400 MHz, CDCl_3) δ 7.51 (d, J = 2.3 Hz, 1H), 7.48 (dd, J = 7.7, 1.2 Hz, 1H), 7.44 (s, 1H), 7.33 – 7.28 (m, 1H), 7.16 – 7.09 (m, 2H), 7.04 (d, J = 2.3 Hz, 1H), 6.87 (dd, J = 8.3, 0.9 Hz, 1H), 6.84 (d, J = 2.4 Hz, 1H), 6.77 (dd, J = 8.2, 2.6 Hz, 1H), 2.25 – 2.24 (m, 6H), 1.32 (s, 9H), 1.31 (s, 9H); $^{13}\text{C}\{^1\text{H}\}$ NMR (100 MHz, CDCl_3) δ 186.8, 157.0, 154.4, 149.3, 147.7, 138.6, 138.1, 135.4, 132.4, 132.3, 132.0, 130.9, 130.7, 128.3, 127.0, 122.8, 120.7, 117.8, 116.7, 35.6, 35.1, 29.7, 29.6, 20.1, 19.2; FT-IR (thin film, neat): 2921, 1740, 1616, 1457, 1251, 742 cm^{-1} ; HRMS (ESI): m/z calcd for $\text{C}_{29}\text{H}_{35}\text{O}_2$ $[\text{M}+\text{H}]^+$: 415.2637; found : 415.2622.

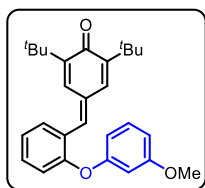
2,6-di-*tert*-butyl-4-(2-(4-ethoxyphenoxy)benzylidene)cyclohexa-2,5-dien-1-one (52f):



Yellow solid (0.95 g, 60% yield); m. p. = 140–142 °C R_f = 0.4 (5% EtOAc in hexane); ^1H NMR (400 MHz, CDCl_3) δ 7.52 (d, J = 2.2 Hz, 1H), 7.48 – 7.46 (m, 2H), 7.31 – 7.27 (m, 1H), 7.14 – 7.10 (m, 1H), 7.06 (d, J = 2.3 Hz, 1H), 7.00 – 6.96 (m, 2H), 6.92 – 6.88 (m, 2H), 6.80 (dd, J = 8.2, 0.7 Hz, 1H), 4.03 (q, J = 7.0 Hz, 2H), 1.43 (t, J = 7.0 Hz, 3H), 1.32 (s, 9H), 1.31 (s, 9H); $^{13}\text{C}\{^1\text{H}\}$ NMR (100 MHz, CDCl_3) δ 186.8, 157.7, 155.8, 149.5, 149.3, 147.7, 138.1, 135.4, 132.2, 132.1, 130.7, 128.3, 126.4, 122.5, 121.2, 116.8, 115.7, 64.0, 35.6, 35.2, 29.7, 29.6, 15.0; FT-IR (thin film, neat): 2923, 1614, 1503, 1360, 1228, 753 cm^{-1} ; HRMS (ESI): m/z calcd for $\text{C}_{29}\text{H}_{33}\text{O}_2$ $[\text{M}-\text{H}]^-$: 429.2430; found : 429.2433.

2,6-di-*tert*-butyl-4-(2-(3-methoxyphenoxy)benzylidene)cyclohexa-2,5-dien-1-one (52g):

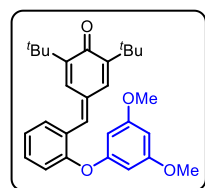
yellow solid (1.00 g, 24% yield); m. p. = 127– 129 °C; R_f = 0.4 (5% EtOAc in hexane); ^1H NMR (400 MHz, CDCl_3) δ 7.51 – 7.48 (m, 2H), 7.39 (s, 1H), 7.35 (td, J = 7.9, 1.5 Hz, 1H),



7.27 – 7.23 (m, 1H), 7.20 (t, $J = 7.4$ Hz, 1H), 7.03 (d, $J = 2.3$ Hz, 1H), 6.96 (dd, $J = 8.2, 0.8$ Hz, 1H), 6.71 – 6.68 (m, 1H), 6.61 – 6.58 (m, 2H), 3.78 (s, 3H), 1.32 (s, 9H), 1.31 (s, 9H); $^{13}\text{C}\{^1\text{H}\}$ NMR (100 MHz, CDCl_3) δ 186.8, 161.2, 158.0, 156.1, 149.4, 147.7, 137.7, 135.3, 132.5, 132.1, 130.8, 130.5, 128.2, 127.5, 123.5, 118.9, 111.2, 109.5, 105.2, 55.54, 55.5, 35.6, 35.1, 29.7, 29.6; FT-IR (thin film, neat): 2923, 1693, 1483, 1273, 1153, 754 cm^{-1} ; HRMS (ESI): m/z calcd for $\text{C}_{28}\text{H}_{33}\text{O}_3$ $[\text{M}+\text{H}]^+$ 417.2430; found : 417.2430.

2,6-di-tert-butyl-4-(2(3,5-dimethoxyphenoxy)benzylidene)cyclohexa-2,5-dien-1-one

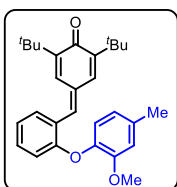
(52h): Yellow solid (0.26 g, 32% yield); m. p. = 132–134 °C; $R_f = 0.3$ (5% EtOAc in hexane);



^1H NMR (400 MHz, CDCl_3) δ 7.59 (d, $J = 2.2$ Hz, 1H), 7.36 – 7.32 (m, 2H), 7.29 (s, 1H), 7.12 – 7.07 (m, 2H), 6.98 – 6.96 (m, 3H), 6.57 (s, 1H), 3.93 (s, 3H), 3.81 (s, 3H), 1.33 (s, 9H), 1.30 (s, 9H); $^{13}\text{C}\{^1\text{H}\}$ NMR (100 MHz, CDCl_3) δ 186.5, 158.0, 151.5, 150.0, 149.1, 147.4, 145.7, 137.4, 135.6, 131.1, 130.1, 128.0, 123.2, 120.1, 117.6, 113.5, 104.4, 56.4, 56.32, 56.3, 35.6, 35.1, 29.8, 29.6; FT-IR (thin film, neat): 2956, 1456, 1229, 1143, 1091, 756 cm^{-1} ; HRMS (ESI): m/z calcd for $\text{C}_{29}\text{H}_{35}\text{O}_4$ $[\text{M}+\text{H}]^+$: 447.2535; found : 447.2536.

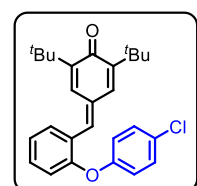
2,6-di-tert-butyl-4-(2-(2-methoxy-4-methylphenoxy)benzylidene)cyclohexa-2,5-dien-1-one

(52i): yellow solid (1.80 g, 62% yield); m. p. = 137–139 °C; $R_f = 0.4$ (5% EtOAc in



hexane); ^1H NMR (400 MHz, CDCl_3) δ 7.57 (s, 1H), 7.54 (d, $J = 2.3$ Hz, 1H), 7.45 (dd, $J = 7.6, 1.1$ Hz, 1H), 7.27 – 7.23 (m, 1H), 7.11 – 7.07 (m, 2H), 6.90 (d, $J = 8.0$ Hz, 1H), 6.83 (d, $J = 1.6$ Hz, 1H), 6.77 – 6.74 (m, 1H), 6.69 (dd, $J = 8.3, 0.9$ Hz, 1H), 3.79 (s, 3H), 2.37 (s, 3H), 1.32 (s, 9H), 1.31 (s, 9H); $^{13}\text{C}\{^1\text{H}\}$ NMR (100 MHz, CDCl_3) δ 186.9, 157.7, 151.3, 149.1, 147.5, 142.0, 138.5, 135.8, 135.6, 132.0, 131.9, 130.6, 128.5, 125.8, 122.1, 121.8, 121.7, 115.7, 113.9, 56.0, 55.99, 35.6, 35.1, 29.7, 29.6, 21.54, 21.5; FT-IR (thin film, neat): 2955, 1612, 1473, 1359, 1266, 747 cm^{-1} ; HRMS (ESI): m/z calcd for $\text{C}_{29}\text{H}_{35}\text{O}_3$ $[\text{M}+\text{H}]^+$: 431.2586; found : 431.2586.

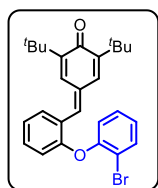
2,6-di-tert-butyl-4-(2-(4-chlorophenoxy)benzylidene)cyclohexa-2,5-dien-1-one (52j):



Yellow solid (0.28 g, 52% yield); m. p. = 131–133 °C; $R_f = 0.5$ (5% EtOAc in hexane); ^1H NMR (400 MHz, CDCl_3) δ 7.50 – 7.47 (m, 2H), 7.37 – 7.29 (m, 4H), 7.23 – 7.19 (m, 1H), 7.01 (d, $J = 2.3$ Hz, 1H), 6.97 – 6.93 (m, 2H), 6.91 (dd, $J = 8.0, 0.6$ Hz, 1H), 1.31 (s, 9H), 1.30 (s, 9H); $^{13}\text{C}\{^1\text{H}\}$ NMR (100 MHz, CDCl_3) δ 186.8, 155.9, 155.4, 149.5, 147.9, 137.2, 135.2, 132.6, 132.3, 130.9, 130.1, 129.0, 128.0, 127.5, 123.8, 120.4, 118.6, 35.6, 35.2, 29.7, 29.6; FT-IR (thin film, neat): 2955, 1692,

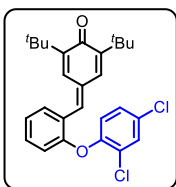
1612, 1479, 1234, 757 cm^{-1} ; HRMS (ESI): m/z calcd for $\text{C}_{27}\text{H}_{28}\text{ClO}_2$ $[\text{M}-\text{H}]^-$: 419.1778; found : 419.1763.

4-(2-(2-bromophenoxy)benzylidene)-2,6-di-*tert*-butylcyclohexa-2,5-dien-1-one (52k):



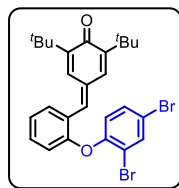
Yellow solid (0.76 g, 43% yield); m. p. = 122–124 °C; R_f = 0.5 (5% EtOAc in hexane); ^1H NMR (400 MHz, CDCl_3) δ 7.66 (d, J = 7.9 Hz, 1H), 7.51 – 7.48 (m, 3H), 7.33 – 7.28 (m, 2H), 7.19 (t, J = 7.5 Hz, 1H), 7.09 – 7.05 (m, 2H), 7.01 (d, J = 8.1 Hz, 1H), 6.75 (d, J = 8.2 Hz, 1H), 1.33 (s, 9H), 1.31 (s, 9H); $^{13}\text{C}\{^1\text{H}\}$ NMR (100 MHz, CDCl_3) δ 186.8, 156.1, 153.1, 149.4, 147.8, 137.5, 135.3, 134.2, 132.5, 132.2, 130.8, 129.0, 128.1, 126.8, 125.9, 123.4, 121.5, 117.1, 115.4, 35.6, 35.2, 29.7, 29.6; FT-IR (thin film, neat): 2921, 1616, 1464, 1360, 1237, 750 cm^{-1} ; HRMS (ESI): m/z calcd for $\text{C}_{27}\text{H}_{28}\text{BrO}_2$ $[\text{M}-\text{H}]^-$: 463.1273; found : 463.1268.

2,6-di-*tert*-butyl-4-(2-(2,4-dichlorophenoxy)benzylidene)cyclohexa-2,5-dien-1-one (52l):



Yellow solid (2.50 g, 58% yield); m. p. = 160–162 °C; R_f = 0.5 (5% EtOAc in hexane); ^1H NMR (400 MHz, CDCl_3) δ 7.50 – 7.47 (m, 3H), 7.41 (s, 1H), 7.33 (td, J = 7.8, 1.6 Hz, 1H), 7.24 – 7.19 (m, 2H), 7.04 (d, J = 2.3 Hz, 1H), 6.94 (d, J = 8.7 Hz, 1H), 6.75 (dd, J = 8.2, 0.8 Hz, 1H), 1.32 (s, 9H), 1.30 (s, 9H); $^{13}\text{C}\{^1\text{H}\}$ NMR (100 MHz, CDCl_3) δ 186.8, 155.7, 150.8, 149.5, 147.9, 136.9, 135.2, 132.7, 132.3, 130.82, 130.8, 130.1, 128.4, 128.0, 127.0, 126.8, 123.7, 122.2, 117.0, 35.6, 35.2, 29.7, 29.6; FT-IR (thin film, neat): 2955, 1774, 1470, 1253, 1100, 744 cm^{-1} ; HRMS (ESI): m/z calcd for $\text{C}_{27}\text{H}_{27}\text{Cl}_2\text{O}_2$ $[\text{M}-\text{H}]^-$: 453.1388; found : 453.1366.

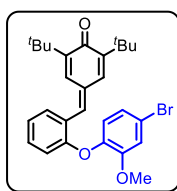
2,6-di-*tert*-butyl-4-(2-(2,4-dibromophenoxy)benzylidene)cyclohexa-2,5-dien-1-one (52m):



Yellow solid (1.55 g, 56% yield); m. p. = 145–147 °C; R_f = 0.5 (5% EtOAc in hexane) ^1H NMR (400 MHz, CDCl_3) δ 7.80 (d, J = 2.3 Hz, 1H), 7.51 – 7.49 (m, 1H), 7.47 (d, J = 2.2 Hz, 1H), 7.41 – 7.39 (m, 2H), 7.34 (td, J = 7.8, 1.5 Hz, 1H), 7.22 (t, J = 7.5 Hz, 1H), 7.04 (d, J = 2.3 Hz, 1H), 6.85 (d, J = 8.7 Hz, 1H), 6.78 – 6.76 (m, 1H), 1.32 (s, 9H), 1.30 (s, 9H); $^{13}\text{C}\{^1\text{H}\}$ NMR (100 MHz, CDCl_3) δ 186.8, 155.5, 152.7, 149.5, 148.0, 136.9, 136.4, 135.2, 132.7, 132.4, 132.0, 130.8, 128.0, 127.0, 123.9, 122.2, 117.4 (2C), 116.1, 35.6, 35.2, 29.7, 29.6; FT-IR (thin film, neat): 2921, 1616, 1462, 1360, 1238, 755 cm^{-1} ; HRMS (ESI): m/z calcd for $\text{C}_{27}\text{H}_{27}\text{Br}_2\text{O}_2$ $[\text{M}-\text{H}]^-$: 541.0378; found : 541.0381.

4-(2-(4-bromo-2-methoxyphenoxy)benzylidene)-2,6-di-*tert*-butylcyclohexa-2,5-dien-1-one (52n):

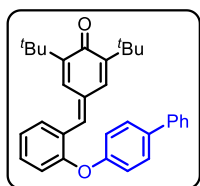
Yellow solid (1.20 g, 43% yield); m. p. = 139–141 °C; R_f = 0.4 (5% EtOAc in hexane); ^1H NMR (400 MHz, CDCl_3) δ 7.50 (d, J = 2.2 Hz, 1H), 7.48 – 7.45 (m, 2H), 7.30 – 7.26 (m, 1H), 7.15 – 7.12 (m, 2H), 7.09 – 7.06 (m, 2H), 6.87 (d, J = 8.5 Hz, 1H), 6.71 (dd, J =



8.2, 0.7 Hz, 1H), 3.80 (s 3H), 1.32 (s, 9H), 1.31 (s, 9H); $^{13}\text{C}\{^1\text{H}\}$ NMR (100 MHz, CDCl_3) δ 186.8, 156.8, 152.2, 149.3, 147.7, 143.9, 137.8, 135.4, 132.3, 132.1, 130.7, 128.3, 126.2, 124.2, 122.9, 122.8, 117.9, 116.5, 116.1, 56.32, 56.3, 35.6, 35.2; FT-IR (thin film, neat): 2955, 1612, 1452, 1359, 1230, 751 cm^{-1} ; HRMS (ESI): m/z calcd for $\text{C}_{28}\text{H}_{32}\text{BrO}_3$ $[\text{M}+\text{H}]^+$: 495.1535; found : 495.1522.

4-(2-([1,1'-biphenyl]-4-yloxy)benzylidene)-2,6-di-tert-butylcyclohexa-2,5-dien-1-one

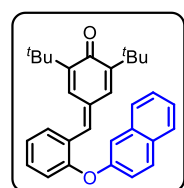
(52o): Yellow solid (0.80 g, 45% yield); m. p. = 183–185 °C; R_f = 0.5 (5% EtOAc in hexane);



^1H NMR (400 MHz, CDCl_3) δ 7.61 – 7.56 (m, 4H), 7.52 – 7.51 (m, 2H), 7.46 – 7.43 (m, 3H), 7.39 – 7.33 (m, 2H), 7.21 (t, J = 7.3 Hz, 1H), 7.12 – 7.08 (m, 2H), 7.04 (d, J = 2.3 Hz, 1H), 7.00 (dd, J = 8.2, 0.8 Hz, 1H), 1.32 (s, 18H); $^{13}\text{C}\{^1\text{H}\}$ NMR (100 MHz, CDCl_3) δ 186.8, 156.33, 156.3, 149.4, 147.8,

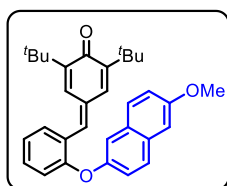
140.4, 137.7, 137.0, 135.3, 132.5, 132.2, 130.9, 129.0, 128.7, 128.1, 127.5, 127.3, 127.1, 123.5, 119.4, 118.7, 35.6, 35.2, 29.7, 29.6; FT-IR (thin film, neat): FT-IR (thin film, neat): 2955, 1614, 1459, 1360, 1228, 755 cm^{-1} ; HRMS (ESI): m/z calcd for $\text{C}_{33}\text{H}_{35}\text{O}_2$ $[\text{M}+\text{H}]^+$: 463.2637; found : 463.2654.

2,6-di-tert-butyl-4-(2-(naphthalen-2-yloxy)benzylidene)cyclohexa-2,5-dien-1-one (52p):



Yellow solid (1.55 g, 57% yield); m. p. = 127–129 °C; R_f = 0.4 (5% EtOAc in hexane); ^1H NMR (400 MHz, CDCl_3) δ 7.89 – 7.85 (m, 2H), 7.73 (d, J = 8.0 Hz, 1H), 7.59 – 7.57 (m, 2H), 7.51 – 7.43 (m, 3H), 7.40 – 7.36 (m, 2H), 7.32 – 7.22 (m, 2H), 7.06 (d, J = 8.0 Hz, 1H), 7.02 – 7.00 (m, 1H), 1.37 (s, 9H), 1.35 (s, 9H); $^{13}\text{C}\{^1\text{H}\}$ NMR (100 MHz, CDCl_3) δ 186.8, 156.2, 154.5, 143.4, 147.6, 137.7, 135.3, 134.4, 132.5, 132.2, 130.9, 130.5, 130.3, 128.1, 127.9, 127.6, 127.3, 126.8, 125.1, 123.6, 119.9, 118.9, 114.6, 35.6, 35.1, 29.7, 29.6; FT-IR (thin film, neat): 2954, 1614, 1493, 1360, 1261, 752 cm^{-1} ; HRMS (ESI): m/z calcd for $\text{C}_{31}\text{H}_{33}\text{O}_2$ $[\text{M}+\text{H}]^+$: 437.2481; found : 437.2471.

2,6-di-tert-butyl-4-(2-((6-methoxynaphthalen-2-yl)oxy)benzylidene)cyclohexa-2,5-dien-1-one (52q): yellow solid (1.00 g, 89% yield); m. p. = 98–100 °C; R_f = 0.3 (5% EtOAc in hexane);

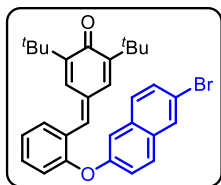


^1H NMR (400 MHz, CDCl_3) δ 7.76 (d, J = 8.9 Hz, 1H), 7.63 (d, J = 9.1 Hz, 1H), 7.56 – 7.53 (m, 2H), 7.49 (s, 1H), 7.38 – 7.32 (m, 2H), 7.26 – 7.14 (m, 4H), 7.05 (s, 1H), 6.94 (d, J = 8.2 Hz, 1H), 3.92 (s, 3H), 1.34 (s, 9H), 1.33 (s, 9H); $^{13}\text{C}\{^1\text{H}\}$ NMR (100 MHz, CDCl_3) δ 186.8, 157.3, 156.8,

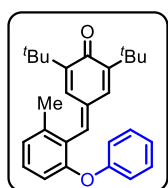
152.6, 149.3, 147.7, 137.9, 135.3, 132.4, 132.2, 131.6, 130.8, 129.6, 128.9, 128.7, 128.2, 127.2, 123.2, 120.5, 119.7, 118.2, 115.4, 106.0, 55.5, 55.4, 35.6, 35.1, 29.7, 29.6; FT-IR (thin film, neat): 2954, 1609, 1576, 1473, 1231, 739 cm^{-1} ; HRMS (ESI): m/z calcd for $\text{C}_{32}\text{H}_{35}\text{O}_3$ $[\text{M}+\text{H}]^+$: 467.2586; found : 467.2567.

4-(2-((6-bromonaphthalen-2-yl)oxy)benzylidene)-2,6-di-tert-butylcyclohexa-2,5-dien-1-one (**52r**):

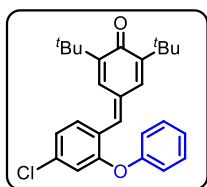
Yellow solid (0.95 g, 65% yield); m. p. = 127–129 °C; R_f = 0.4 (5% EtOAc in hexane); ^1H NMR (400 MHz, CDCl_3) δ 7.97 (d, J = 1.4 Hz, 1H), 7.75 – 7.68 (m, 1H), 7.56 – 7.48 (m, 4H), 7.37 – 7.33 (m, 2H), 7.28 – 7.23 (m, 3H), 6.98 – 6.96 (m, 2H), 1.29 (s, 9H), 1.27 (s, 9H); $^{13}\text{C}\{^1\text{H}\}$ NMR (100 MHz, CDCl_3) δ 186.8, 155.8, 155.1, 149.5, 147.9, 137.3, 135.2, 132.9, 132.7, 132.3, 131.4, 130.9, 130.2, 130.0, 129.4, 128.9, 128.1, 127.8, 124.0, 120.9, 119.2, 118.8, 114.2, 35.6, 35.2, 29.7, 29.6; FT-IR (thin film, neat): 2954, 1614, 1493, 1360, 1261, 752 cm^{-1} ; HRMS (ESI): m/z calcd for $\text{C}_{31}\text{H}_{30}\text{BrO}_2$ $[\text{M}-\text{H}]^-$: 523.1429; found : 523.1442.

**2,6-di-tert-butyl-4-(2-methyl-6-phenoxybenzylidene)cyclohexa-2,5-dien-1-one** (**52s**):

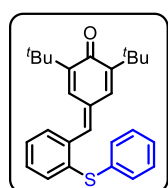
Yellow solid (0.21 g, 25% yield); m. p. = 116–118 °C; R_f = 0.4 (5% EtOAc in hexane); ^1H NMR (400 MHz, CDCl_3) δ 7.30 – 7.22 (m, 3H), 7.07 – 7.04 (m, 2H), 7.01 – 6.96 (m, 3H), 6.89 – 6.87 (m, 2H), 6.83 (d, J = 8.2 Hz, 1H), 2.30 (s, 3H), 1.31 (d, J = 1.0 Hz, 9H), 1.26 (d, J = 1.2 Hz, 9H); $^{13}\text{C}\{^1\text{H}\}$ NMR (100 MHz, CDCl_3) δ 186.9, 157.1, 154.7, 148.5, 147.5, 139.0, 137.5, 134.4, 134.0, 129.8, 129.6, 129.3, 126.9, 125.6, 123.3, 118.5, 116.6, 35.3, 35.1, 29.7, 29.6, 20.75, 20.7; FT-IR (thin film, neat): 2955, 1615, 1455, 1359, 1245, 742 cm^{-1} ; HRMS (ESI): m/z calcd for $\text{C}_{28}\text{H}_{33}\text{O}_2$ $[\text{M}+\text{H}]^+$: 401.2481; found : 401.2464.

**2,6-di-tert-butyl-4-(4-chloro-2-phenoxybenzylidene)cyclohexa-2,5-dien-1-one** (**52t**):

Yellow solid (0.36 g, 45% yield); m. p. = 140–142 °C; R_f = 0.4 (5% EtOAc in hexane); ^1H NMR (400 MHz, CDCl_3) δ 7.44 – 7.39 (m, 4H), 7.34 (s, 1H), 7.21 (t, J = 7.4 Hz, 1H), 7.15 (dd, J = 8.4, 1.9 Hz, 1H), 7.07 – 7.02 (m, 3H), 6.85 (d, J = 2.0 Hz, 1H), 1.32 (s, 9H), 1.31 (s, 9H); $^{13}\text{C}\{^1\text{H}\}$ NMR (100 MHz, CDCl_3) δ 186.8, 157.2, 155.8, 149.7, 148.0, 136.3, 136.2, 135.1, 132.7, 130.3, 127.7, 125.5, 124.8, 123.3, 119.8, 118.04, 118.0, 35.6, 35.2, 29.7, 29.6; FT-IR (thin film, neat): 2955, 1614, 1567, 1473, 1234, 918, 742 cm^{-1} ; HRMS (ESI): m/z calcd for $\text{C}_{27}\text{H}_{30}\text{ClO}_2$ $[\text{M}+\text{H}]^+$: 421.1934; found : 421.1947.

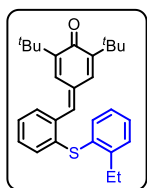
**2,6-di-tert-butyl-4-(2-(phenylthio)benzylidene)cyclohexa-2,5-dien-1-one** (**54a**):

Yellow solid (0.56 g, 34% yield); m. p. = 129–131 °C; R_f = 0.5 (5% EtOAc in hexane); ^1H NMR (400 MHz, CDCl_3) δ 7.42 (s, 1H), 7.40 – 7.37 (m, 1H), 7.35 – 7.30 (m, 6H), 7.29 – 7.26 (m, 3H), 7.02 (d, J = 2.3 Hz, 1H), 1.32 (s, 9H), 1.26 (s, 9H); $^{13}\text{C}\{^1\text{H}\}$ NMR (100 MHz, CDCl_3) δ 186.7, 149.4, 148.0, 140.2, 137.5, 136.4, 134.9, 134.6, 132.7, 131.8, 131.77, 131.7, 129.7, 129.5, 128.2, 127.8, 127.0, 35.5, 35.2,



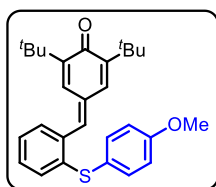
29.6; FT-IR (thin film, neat): 2954, 1613, 1563, 1359, 1254, 746 cm^{-1} ; HRMS (ESI): m/z calcd for $\text{C}_{27}\text{H}_{31}\text{OS}$ $[\text{M}+\text{H}]^+$: 403.2096; found : 403.2095.

2,6-di-*tert*-butyl-4-(2-((2-ethylphenyl)thio)benzylidene)cyclohexa-2,5-dien-1-one (54b):



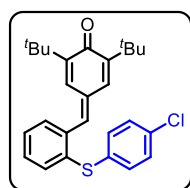
Yellow solid (0.15 g, 33% yield); m. p. = 143–145 $^{\circ}\text{C}$; R_f = 0.5 (5% EtOAc in hexane); ^1H NMR (400 MHz, CDCl_3) δ 7.45 (s, 1H), 7.40 – 7.37 (m, 1H), 7.34 – 7.335 (m, 1H), 7.32 – 7.30 (m, 2H), 7.29 – 7.23 (m, 3H), 7.17 – 7.13 (m, 1H), 7.08 – 7.05 (m, 2H), 2.82 (q, J = 7.6 Hz, 2H), 1.36 (s, 9H), 1.30 (s, 9H), 1.24 (t, J = 7.6 Hz, 3H); $^{13}\text{C}\{^1\text{H}\}$ NMR (100 MHz, CDCl_3) δ 186.6, 149.2, 147.9, 146.3, 140.1, 138.6, 135.3, 134.8, 134.2, 132.5, 132.2, 131.6, 130.0, 129.6, 129.3, 128.8, 128.2, 127.1, 126.1, 35.5, 35.1, 27.3, 15.15, 15.14; FT-IR (thin film, neat): 2954, 1613, 1563, 1359, 1254, 746 cm^{-1} ; HRMS (ESI): m/z calcd for $\text{C}_{29}\text{H}_{35}\text{OS}$ $[\text{M}+\text{H}]^+$: 431.2409; found : 431.2406.

2,6-di-*tert*-butyl-4-(2((4methoxyphenyl)thio)benzylidene)cyclohexa-2,5-dien-1-one (54c):



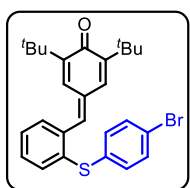
Yellow solid (2.00 g, 80% yield); m. p. = 165–167 $^{\circ}\text{C}$; R_f = 0.3 (5% EtOAc in hexane); ^1H NMR (400 MHz, CDCl_3) δ 7.43 (s, 1H), 7.42 – 7.38 (m, 2H), 7.34 – 7.30 (m, 2H), 7.25 – 7.20 (m, 2H), 7.07 (d, J = 2.2 Hz, 1H), 7.05 – 7.01 (m, 1H), 6.92 – 6.88 (m, 2H), 3.81 (s, 3H), 1.34 (s, 9H), 1.27 (s, 9H); $^{13}\text{C}\{^1\text{H}\}$ NMR (100 MHz, CDCl_3) δ 186.7, 160.3, 149.3, 147.9, 140.3, 140.0, 135.9, 134.9, 134.2, 132.6, 131.5, 129.5, 128.6, 128.3, 125.6, 123.3, 115.3, 55.5, 55.48, 35.5, 35.2, 29.6; FT-IR (thin film, neat): 2955, 1614, 1493, 1250, 1059, 742 cm^{-1} ; HRMS (ESI): m/z calcd for $\text{C}_{28}\text{H}_{33}\text{O}_2\text{S}$ $[\text{M}+\text{H}]^+$: 433.2201; found : 433.2214.

2,6-di-*tert*-butyl-4-(2-((4-chlorophenyl)thio)benzylidene)cyclohexa-2,5-dien-1-one (54d):



Yellow solid (0.20 g, 45% yield); m. p. = 122–124 $^{\circ}\text{C}$; R_f = 0.5 (5% EtOAc in hexane); ^1H NMR (400 MHz, CDCl_3) δ 7.40 – 7.34 (m, 3H), 7.33 – 7.29 (m, 2H), 7.27 – 7.21 (m, 5H), 6.99 (s, 1H), 1.32 (s, 9H), 1.26 (s, 9H); $^{13}\text{C}\{^1\text{H}\}$ NMR (100 MHz, CDCl_3) δ 186.6, 149.5, 148.2, 139.9, 136.7, 136.69, 134.7, 133.8, 133.6, 132.8, 132.7, 132.0, 131.9, 129.8, 129.7, 128.0, 127.4, 35.5, 35.2, 29.7; FT-IR (thin film, neat): 2955, 1615, 1475, 1360, 1091, 753 cm^{-1} ; HRMS (ESI): m/z calcd for $\text{C}_{30}\text{H}_{31}\text{Br}_2\text{O}_3$ $[\text{M}+\text{H}]^+$: 437.1706; found : 437.1705.

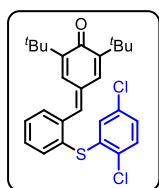
4-(2-((4-bromophenyl)thio)benzylidene)-2,6-di-*tert*-butylcyclohexa-2,5-dien-1-one (54e):



Yellow solid (1.00 g, 41% yield); m. p. = 125–127 $^{\circ}\text{C}$; R_f = 0.5 (5% EtOAc in hexane); ^1H NMR (400 MHz, CDCl_3) δ 7.40 – 7.38 (m, 3H), 7.37 – 7.32 (m, 4H), 7.23 (d, J = 2.2 Hz, 1H), 7.15 (d, J = 8.4 Hz, 2H), 6.98 (d, J = 2.2 Hz, 1H), 1.32 (s, 9H), 1.26 (s, 9H); $^{13}\text{C}\{^1\text{H}\}$ NMR (100 MHz, CDCl_3) δ 186.6, 149.5, 148.1, 139.9, 136.8, 136.4, 134.7, 134.4, 132.7 (2C), 132.6, 132.2, 131.9, 129.8, 127.9,

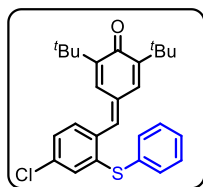
127.5, 121.6, 35.5, 35.2, 29.6; FT-IR (thin film, neat): 2955, 1613, 1468, 1359, 1254, 753 cm^{-1} ; HRMS (ESI): m/z calcd for $\text{C}_{27}\text{H}_{30}\text{BrOS}$ $[\text{M}+\text{H}]^+$: 481.1201; found: 481.1229.

2,6-di-*tert*-butyl-2((2,5-dichlorophenyl)thio)benzylidene)cyclohexa-2,5-dien-1-one (54f):



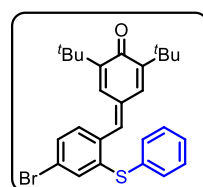
Yellow solid (0.15 g, 25% yield); m. p. = 121–122 °C; R_f = 0.5 (5% EtOAc in hexane); ^1H NMR (400 MHz, CDCl_3) 7.55 – 7.53 (m, 1H), 7.51 – 7.47 (m, 1H), 7.45 – 7.39 (m, 2H), 7.31 (s, 1H), 7.21 (d, J = 8.5 Hz, 1H), 7.18 (d, J = 2.0 Hz, 1H), 7.09 (dd, J = 8.5 2.4 Hz, 1H), 6.95 (d, J = 2.2 Hz, 1H), 6.76 (d, J = 2.4 Hz, 1H), 1.30 (s, 9H), 1.25 (s, 9H); $^{13}\text{C}\{^1\text{H}\}$ NMR (100 MHz, CDCl_3) δ 186.5, 149.6, 148.1, 139.7, 139.0, 137.7, 135.0, 134.4, 133.2, 132.9, 132.89, 132.8, 132.3, 131.6, 130.6, 130.1, 129.4, 129.2, 127.5, 35.5, 35.1, 29.6, 29.5; FT-IR (thin film, neat): 2921, 1616, 1458, 1360, 1091, 744 cm^{-1} ; HRMS (ESI): m/z calcd for $\text{C}_{30}\text{H}_{31}\text{Cl}_2\text{O}_3$ $[\text{M}-\text{H}]^-$: 469.1160; found: 469.1173.

2,6-di-*tert*-butyl-4-(4-chloro-2-(phenylthio)benzylidene)cyclohexa-2,5-dien-1-one (54g):



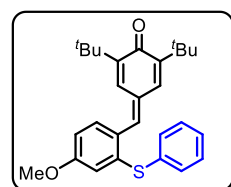
Yellow solid (0.25 g, 28% yield); m. p. = 110–112 °C; R_f = 0.4 (5% EtOAc in hexane); ^1H NMR (400 MHz, CDCl_3) δ 7.42 – 7.34 (m, 5H), 7.32 (s, 1H), 7.30 – 7.26 (m, 2H), 7.24 – 7.22 (m, 1H), 7.12 (d, J = 1.8 Hz, 1H) 7.04 (d, J = 2.2 Hz, 1H), 1.33 (s, 9H), 1.27 (s, 9H); $^{13}\text{C}\{^1\text{H}\}$ NMR (100 MHz, CDCl_3) δ 186.6, 149.7, 148.2, 140.4, 138.4, 135.6, 134.6, 133.7, 133.04, 133.0, 132.8, 132.5, 129.9, 129.7, 128.7, 127.7, 126.7, 35.6, 35.2, 29.6; FT-IR (thin film, neat): 2954, 1613, 1477, 1359, 1254, 739 cm^{-1} ; HRMS (ESI): m/z calcd for $\text{C}_{27}\text{H}_{30}\text{ClOS}$ $[\text{M}+\text{H}]^+$: 437.1706; found: 437.1725.

4-(4-bromo-2-(phenylthio)benzylidene)-2,6-di-*tert*-butylcyclohexa-2,5-dien-1-one (54h):



yellow solid (0.19 g 28% yield); m. p. = 108–110 °C; R_f = 0.4 (5% EtOAc in hexane); ^1H NMR (400 MHz, CDCl_3) δ 7.46 – 7.33 (m, 6H), 7.32 – 7.29 (m, 2H), 7.26 – 7.21 (m, 2H), 7.01 (d, J = 1.8 Hz, 1H), 1.32 (s, 9H), 1.27 (s, 9H); $^{13}\text{C}\{^1\text{H}\}$ NMR (100 MHz, CDCl_3) δ 186.6, 149.7, 148.3, 140.4, 138.5, 134.6, 134.3, 134.2, 133.0, 132.9, 132.8, 132.7, 129.9, 129.7, 128.6, 127.7, 123.8, 35.6, 35.2, 29.64, 29.6; FT-IR (thin film, neat): 2921, 1740, 1617, 1458, 1375, 740 cm^{-1} ; HRMS (ESI): m/z calcd for $\text{C}_{27}\text{H}_{30}\text{BrOS}$ $[\text{M}+\text{H}]^+$: 481.1201; found: 481.1213.

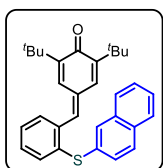
2,6-di-*tert*-butyl-4-(4-methoxy-2-(phenylthio)benzylidene)cyclohexa-2,5-dien-1-one (54i):



Yellow solid (0.30 g, 34% yield); m. p. = 171–173 °C; R_f = 0.3 (5% EtOAc in hexane); ^1H NMR (400 MHz, CDCl_3) δ 7.41 (s, 1H), 7.39 – 7.26 (m, 7H), 7.02 (d, J = 2.2 Hz, 1H) 6.86 (dd, J = 8.6, 2.5 Hz, 1H), 6.75 (d, J = 2.5 Hz, 1H) 3.74 (s, 3H), 1.33 (s, 9H), 1.28 (s, 9H); $^{13}\text{C}\{^1\text{H}\}$ NMR (100 MHz, CDCl_3) δ 186.7, 160.7, 149.0, 147.5, 140.1, 139.7, 135.1, 134.0, 133.1, 132.3, 131.7, 129.6, 128.6, 128.3, 128.1, 116.4, 112.7, 55.53, 55.5, 35.5, 35.1, 29.7, 29.6; FT-IR (thin film,

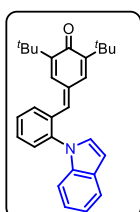
neat): 2954, 1610, 1589, 1359, 1252, 743 cm^{-1} ; HRMS (ESI): m/z calcd for $\text{C}_{28}\text{H}_{33}\text{O}_2\text{S}$ $[\text{M}+\text{H}]^+$: 433.2201; found : 433.2208.

2,6-di-*tert*-butyl-4-(2-(naphthalen-2-ylthio)benzylidene)cyclohexa-2,5-dien-1-one (54j):



Yellow solid (0.27 g, 32% yield); m. p. = 132–133 °C; R_f = 0.4 (5% EtOAc in hexane); ^1H NMR (400 MHz, CDCl_3) δ 7.82 (d, J = 1.2 Hz, 1H), 7.80 – 7.78 (m, 1H), 7.76 (d, J = 8.6 Hz, 1H), 7.73 – 7.71 (m, 1H), 7.50 – 7.45 (m, 2H), 7.44 (s, 1H), 7.41 – 7.35 (m, 3H), 7.33 – 7.28 (m, 2H), 7.27 – 7.26 (m, 1H), 6.98 (d, J = 2.3 Hz, 1H), 1.29 (s, 9H), 1.26 (s, 9H); $^{13}\text{C}\{^1\text{H}\}$ NMR (100 MHz, CDCl_3) δ 186.7, 149.4, 148.0, 140.2, 137.4, 136.5, 134.6, 133.9, 132.6, 132.5, 132.0, 131.8 (2C), 130.8, 129.7, 129.3, 129.0, 128.1, 127.9, 127.5, 127.1, 126.9, 126.7, 35.5, 35.1, 29.64, 29.60; FT-IR (thin film, neat): 2921, 1740, 1617, 1459, 1376, 743 cm^{-1} ; HRMS (ESI): m/z calcd for $\text{C}_{31}\text{H}_{33}\text{OS}$ $[\text{M}+\text{H}]^+$: 453.2252; found : 453.2259.

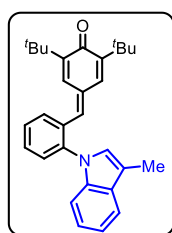
4-(2-(1H-indol-1-yl)benzylidene)-2,6-di-*tert*-butylcyclohexa-2,5-dien-1-one (56a):



Yellow solid (0.33 g 68% yield); m. p. = 141–143 °C; R_f = 0.5 (5% EtOAc in hexane); m. p. = 141–143 °C; R_f = 0.5 (5% EtOAc in hexane); ^1H NMR (400 MHz, CDCl_3) δ 7.74 – 7.73 (m, 1H), 7.65 – 7.63 (m, 1H), 7.56 – 7.51 (m, 4H), 7.29 – 7.26 (m, 1H), 7.23 – 7.19 (m, 3H), 6.78 (s, 1H), 6.73 – 6.71 (m, 2H), 1.35 (s, 9H), 1.27 (s, 9H); $^{13}\text{C}\{^1\text{H}\}$ NMR (100 MHz, CDCl_3) δ 186.7, 149.9, 148.0, 139.4, 138.3, 137.1, 134.8, 133.0, 132.9, 132.7, 130.1, 130.0, 128.9, 127.9, 127.7, 127.6, 122.7, 121.2, 120.7, 110.7, 103.8, 35.6, 35.2, 29.7, 29.6; FT-IR (thin film, neat): 2924, 1737, 1615, 1492, 1331, 743 cm^{-1} ; HRMS (ESI): m/z calcd for $\text{C}_{29}\text{H}_{32}\text{NO}$ $[\text{M}+\text{H}]^+$: 410.2484; found : 410.2479.

2,6-di-*tert*-butyl-4-(2-(3-methyl-1H-indol-1-yl)benzylidene)cyclohexa-2,5-dien-1-one (56b):

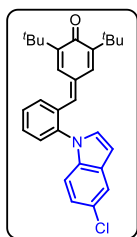
Yellow solid (0.30 g, 52% yield); m. p. = 179–181 °C; R_f = 0.5 (5% EtOAc in hexane);



^1H NMR (400 MHz, CDCl_3) δ 7.68 – 7.65 (m, 1H), 7.63 – 7.62 (m, 1H), 7.57 (d, J = 2.1 Hz, 1H), 7.55 – 7.47 (m, 3H), 7.21 – 7.20 (m, 3H), 6.98 (s, 1H), 6.80 – 6.79 (m, 2H), 2.40 (s, 3H), 1.35 (s, 9H), 1.27 (s, 9H); $^{13}\text{C}\{^1\text{H}\}$ NMR (100 MHz, CDCl_3) δ 186.7, 149.8, 147.9, 139.7, 138.7, 137.4, 134.9, 132.8, 132.68, 132.66, 130.1, 129.5, 127.8, 127.5, 127.4, 127.3, 122.7, 120.1, 119.2, 113.1, 110.7, 35.7, 35.2, 29.7, 29.6, 9.79, 9.76; FT-IR (thin film, neat): 2922, 1738, 1616, 1458, 1360, 741 cm^{-1} ; HRMS (ESI): m/z calcd for $\text{C}_{30}\text{H}_{34}\text{NO}$ $[\text{M}+\text{H}]^+$: 424.2640; found : 424.2620.

2,6-di-*tert*-butyl-4-(2-(5-chloro-1H-indol-1-yl)benzylidene)cyclohexa-2,5-dien-1-one (56c):

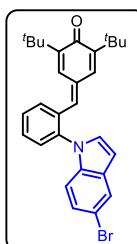
Yellow solid (0.066 g, 41.3% yield); m. p. = 132–134 °C; R_f = 0.4 (5% EtOAc in hexane); ^1H NMR (400 MHz, $\text{DMSO}-d_6$) δ 7.84 (d, J = 1.6 Hz, 1H), 7.69 – 7.62 (m, 3H), 7.61



– 7.57 (m, 1H), 7.49 (d, $J = 3.2$ Hz, 1H), 7.37 (d, $J = 1.2$ Hz, 1H), 7.24 (dd, $J = 8.7, 1.7$ Hz, 1H), 7.11 – 7.09 (m, 1H), 6.95 (brs, 2H), 6.67 (d, $J = 3.2$ Hz, 1H), 1.20 (s, 9H), 1.17 (s, 9H); $^{13}\text{C}\{^1\text{H}\}$ NMR (100 MHz, DMSO- d_6) δ 185.9, 148.2, 146.7, 139.6, 137.9, 135.2, 134.8, 132.5, 132.2, 132.1, 131.8, 130.6, 130.4, 128.2, 127.8, 127.7, 124.8, 123.1, 112.8, 112.4, 103.0, 35.0, 34.7, 29.24, 29.2; FT-IR (thin film, neat FT-IR (thin film, neat): 2925, 1740, 1607, 1459, 1362, 750 cm^{-1} ; HRMS (ESI): m/z calcd for $\text{C}_{29}\text{H}_{31}\text{ClNO}$ $[\text{M}+\text{H}]^+$: 444.2094; found : 444.2079.

4-(2-(5-bromo-1H-indol-1-yl)benzylidene)-2,6-di-tert-butylcyclohexa-2,5-dien-1-one

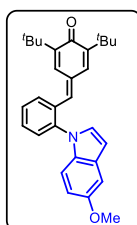
(56d): Yellow solid (0.134 g, 47% yield); m. p. = 134–136 °C; $R_f = 0.4$ (5% EtOAc in hexane);



^1H NMR (400 M DMSO- d_6) δ 7.68 – 7.62 (m, 4H), 7.60 – 7.58 (m, 1H), 7.48 (d, $J = 3.2$ Hz, 1H), 7.34 (d, $J = 1.8$ Hz, 1H), 7.12 – 7.09 (m, 1H), 7.08 (s, 1H), 6.96 (s, 1H), 6.94 (d, $J = 2.0$ Hz, 1H), 7.34 (dd, $J = 3.2, 0.6$ Hz, 1H), 1.19 (s, 9H), 1.16 (s, 9H); $^{13}\text{C}\{^1\text{H}\}$ NMR (100 MHz, DMSO- d_6) δ 185.9, 148.4, 146.8, 139.8, 137.7, 136.7, 134.7, 132.4, 132.3, 132.2, 131.3, 130.7, 128.3, 127.72, 127.7, 127.3, 127.1, 122.3, 120.6, 110.2, 103.6, 35.0, 34.7, 29.2, 29.1; FT-IR (thin film, neat FT-IR (thin film, neat): 2955, 1615 1483, 1458, 1360, 742 cm^{-1} ; HRMS (ESI): m/z calcd for $\text{C}_{29}\text{H}_{31}\text{BrNO}$ $[\text{M}+\text{H}]^+$: 488.1589; found : 488.1617.

2,6-di-tert-butyl-4-(2-(5-methoxy-1H-indol-1-yl)benzylidene)cyclohexa-2,5-dien-1-one

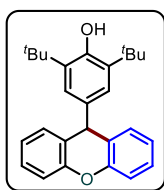
(56e): Yellow solid (0.15 g, 55.9% yield); m. p. = 143–145 °C; $R_f = 0.3$ (5% EtOAc in hexane);



^1H NMR (400 MHz, CDCl_3) δ 7.62 (d, $J = 7.1$ Hz, 1H), 7.54 – 7.52 (m, 3H), 7.51 – 7.48 (m, 1H), 7.17 – 7.15 (m, 3H), 6.87 (dd, $J = 9.0, 2.4$ Hz, 1H), 6.79 (d, $J = 2.2$ Hz, 1H), 6.73 (s, 1H), 6.63 (d, $J = 3.1$ Hz, 1H), 3.89 (s, 3H), 1.33 (s, 9H), 1.27 (s, 9H); $^{13}\text{C}\{^1\text{H}\}$ NMR (100 MHz, CDCl_3) δ 186.7, 154.9, 149.8, 148.0, 139.5, 138.5, 134.8, 132.9, 132.7, 132.6, 132.3, 130.6, 130.1, 129.5, 127.7, 127.6, 127.4, 112.9, 111.6, 103.5, 102.7, 56.0, 55.98, 35.6, 35.2, 29.7, 29.6; FT-IR (thin film, neat FT-IR (thin film, neat): 2954, 1614, 1578, 1483, 1256, 740 cm^{-1} ; HRMS (ESI): m/z calcd for $\text{C}_{30}\text{H}_{34}\text{NO}_2$ $[\text{M}+\text{H}]^+$: 440.2590; found : 440.2575.

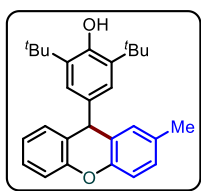
General procedure for the synthesis of xanthene (53a-t) and thioxanthene derivatives (55a-j): A stock solution of TfOH in CH_2Cl_2 [0.2 equiv.] was added to a solution of *ortho*-heteroaryl phenyl-substituted *para*-quinone methide (1.0 equiv.) in dichloromethane at room temperature, and the resulting reaction mixture was allowed to stir at room temperature until the starting material was completely consumed. Then, the excess solvent was removed under reduced pressure and the residue was directly loaded on a silica gel column and eluted using hexane/ethyl acetate to obtain the pure product.

2,6-di-tert-butyl-4-(9H-xanthen-9-yl)phenol (53a): The reaction was performed at 0.129



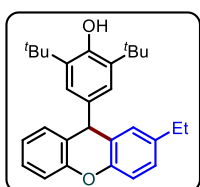
mmol scale of **52a**; pale yellow solid (48.0 mg, 96% yield); $R_f = 0.4$ (5% EtOAc in hexane); $^1\text{H NMR}$ (400 MHz, CDCl_3) δ 7.25 – 7.21 (m, 2H), 7.17 – 7.16 (m, 2H), 7.15 – 7.14 (m, 2H), 7.05 – 7.01 (m, 2H), 6.99 (s, 2H), 5.19 (s, 1H), 5.09 (s, 1H), 1.40 (s, 18H); ^{13}C $\{^1\text{H}\}$ NMR (100 MHz, CDCl_3) δ 152.5, 151.6, 136.9, 136.0, 129.7, 127.7, 125.6, 124.9, 123.3, 116.5, 44.6, 44.55, 34.4, 30.4; FT-IR (thin film, neat): 2957, 1600, 1574, 1477, 1316, 750 cm^{-1} ; HRMS (ESI): m/z calcd for $\text{C}_{27}\text{H}_{31}\text{O}_2$ $[\text{M}+\text{H}]^+$: 387.2324; found : 387.2326.

2,6-di-tert-butyl-4-(3-methyl-9H-xanthen-9-yl)phenol (53b): The reaction was performed at



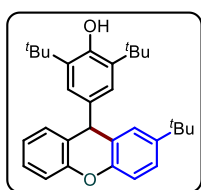
0.125 mmol scale of **52b**; pale yellow solid (48.5 mg, 97% yield); $R_f = 0.4$ (5% EtOAc in hexane); $^1\text{H NMR}$ (400 MHz, CDCl_3) δ 7.22 – 7.18 (m, 1H), 7.15 – 7.12 (m, 2H), 7.06 – 7.04 (m, 1H), 7.02 – 7.00 (m, 2H), 6.97 – 6.95 (m, 3H), 5.11 (s, 1H), 5.07 (s, 1H), 2.27 (s, 3H), 1.38 (s, 18H); ^{13}C $\{^1\text{H}\}$ NMR (100 MHz, CDCl_3) δ 152.5, 151.8, 149.6, 137.3, 135.9, 132.5, 129.9, 129.6, 128.4, 127.6, 125.7, 125.1, 124.7, 123.1, 116.5, 116.2, 44.8, 44.77, 34.4, 30.4, 21.91, 21.9; FT-IR (thin film, neat): 2956, 1599, 1480, 1454, 1313, 751 cm^{-1} ; HRMS (ESI): m/z calcd for $\text{C}_{28}\text{H}_{31}\text{O}_2$ $[\text{M}-\text{H}]^-$: 399.2324 found : 399.2339.

2,6-di-tert-butyl-4-(3-ethyl-9H-xanthen-9-yl)phenol (53c): The reaction was performed at



0.121 mmol scale of **52c**; pale yellow solid (48.0 mg, 96% yield); $R_f = 0.4$ (5% EtOAc in hexane); $^1\text{H NMR}$ (400 MHz, CDCl_3) δ 7.21 – 7.17 (m, 1H), 7.14 – 7.10 (m, 2H), 7.06 – 7.03 (m, 2H), 7.01 – 6.99 (m, 1H), 6.97 – 6.96 (m, 1H), 6.94 (s, 2H), 5.19 (s, 1H), 5.05 (s, 1H), 2.56 (q, $J = 7.6$ Hz, 2H), 1.36 (s, 18H), 1.17 (t, $J = 7.6$ Hz, 3H); ^{13}C $\{^1\text{H}\}$ NMR (100 MHz, CDCl_3) δ 152.4, 151.9, 149.8, 139.1, 136.9, 135.8, 129.6, 128.7, 127.6, 127.2, 125.7, 125.3, 124.8, 123.1, 116.5, 116.3, 44.7, 34.4, 30.4, 28.3, 16.0; FT-IR (thin film, neat): 2958, 16301, 1478, 1456, 1235, 754 cm^{-1} ; HRMS (ESI): m/z calcd for $\text{C}_{29}\text{H}_{33}\text{O}_2$ $[\text{M}-\text{H}]^-$: 413.2481; found : 413.2487.

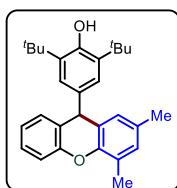
2,6-di-tert-butyl-4-(3-(tert-butyl)-9H-xanthen-9-yl)phenol (53d): The reaction was



performed at 0.110 mmol scale of **52d**; yellow gummy solid (42.0 mg, 84% yield); $R_f = 0.4$ (5% EtOAc in hexane); $^1\text{H NMR}$ (400 MHz, CDCl_3) δ 7.26 – 7.18 (m, 4H), 7.14 – 7.12 (m, 1H), 7.08 – 7.06 (m, 1H), 7.04 – 7.00 (m, 1H), 6.94 (s, 2H), 5.18 (s, 1H), 5.06 (s, 1H), 1.37 (s, 18H), 1.28 (s, 9H); ^{13}C $\{^1\text{H}\}$ NMR (100 MHz, CDCl_3) δ 152.4, 152.2, 149.7, 145.9, 136.3, 135.8, 129.6, 127.7, 126.2, 125.6, 125.0, 124.9, 124.7, 123.1, 116.5, 115.9, 44.63, 44.6, 34.6, 34.44, 34.4, 31.6, 30.4; FT-

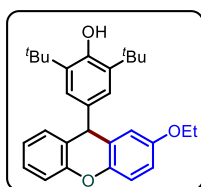
IR (thin film, neat): 2958, 1598, 1481, 1433, 1251, 753 cm^{-1} ; HRMS (ESI): m/z calcd for $\text{C}_{31}\text{H}_{37}\text{O}_2$ $[\text{M}-\text{H}]^-$: 441.2794; found : 441.2803.

2,6-di-tert-butyl-4-(2,4-dimethyl-9H-xanthen-9-yl)phenol (53e): The reaction was



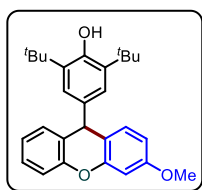
performed at 0.096 mmol scale of **52e**; white solid (41.0 mg, 80% yield); $R_f = 0.4$ (5% EtOAc in hexane); ^1H NMR (400 MHz, CDCl_3) δ 7.22 – 7.16 (m, 1H), 7.13 – 7.11 (m, 2H), 7.01 – 6.99 (m, 1H), 6.97 (s, 2H), 6.94 (s, 1H), 6.89 (s, 1H), 5.10 (s, 1H), 5.06 (s, 1H), 2.25 (s, 3H), 2.18 (s, 3H), 1.39 (s, 18H); ^{13}C $\{^1\text{H}\}$ NMR (100 MHz, CDCl_3) δ 152.4, 151.8, 149.5, 137.5, 136.1, 135.8, 131.3, 130.2, 129.7, 127.5, 125.8, 124.8, 123.0, 122.5, 117.3, 116.5, 44.4, 44.39, 34.4, 30.4, 19.74, 19.7, 19.2; FT-IR (thin film, neat): 2957, 1482, 1403, 1232, 753 cm^{-1} ; HRMS (APCI): m/z calcd for $\text{C}_{29}\text{H}_{33}\text{O}_2$ $[\text{M}-\text{H}]^-$: 413.2481; found : 413.2494.

2,6-di-tert-butyl-4-(2-ethoxy-9H-xanthen-9-yl)phenol (53f): The reaction was performed at



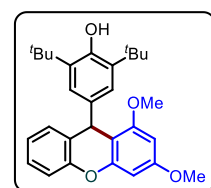
0.116 mmol scale of **52f**; white solid (49.1 mg, 98% yield); $R_f = 0.3$ (5% EtOAc in hexane); ^1H NMR (400 MHz, CDCl_3) δ 7.19 (t, $J = 7.6$ Hz, 1H), 7.10 (d, $J = 7.9$ Hz, 2H), 7.05 (d, $J = 8.8$ Hz, 1H), 7.00 – 6.96 (m, 1H), 6.95 (s, 2H), 6.76 (dd, $J = 8.8, 2.8$ Hz, 1H), 6.64 (d, $J = 2.6$ Hz, 1H), 5.10 (s, 1H), 5.05 (s, 1H), 3.95 (q, $J = 7.0$ Hz, 2H), 1.37 (s, 21H); ^{13}C $\{^1\text{H}\}$ NMR (100 MHz, CDCl_3) δ 154.7, 152.5, 151.9, 145.8, 136.8, 136.0, 129.6, 127.6, 126.3, 125.2, 124.8, 123.0, 117.1, 116.4, 114.9, 114.1, 64.0, 45.1, 45.0, 34.4, 30.4, 15.0; FT-IR (thin film, neat): 2959, 1478, 1434, 1252, 1223, 750 cm^{-1} ; HRMS (ESI): m/z calcd for $\text{C}_{29}\text{H}_{33}\text{O}_3$ $[\text{M}-\text{H}]^-$: 429.2430; found : 429.2441.

2,6-di-tert-butyl-4-(3-methoxy-9H-xanthen-9-yl)phenol (53g): The reaction was performed



at 0.120 mmol scale of **52g**; yellow gummy solid (36.5 mg, 71% yield); $R_f = 0.3$ (5% EtOAc in hexane); ^1H NMR (400 MHz, CDCl_3) δ 7.22 – 7.18 (m, 1H), 7.12 – 7.10 (m, 2H), 7.07 (d, $J = 8.9$ Hz, 1H), 7.01 – 6.97 (m, 1H), 6.95 (s, 2H), 6.78 (dd, $J = 8.9, 3.0$ Hz, 1H), 6.65 (d, $J = 2.9$ Hz, 1H), 5.11 (s, 1H), 5.06 (s, 1H), 3.74 (s, 3H), 1.37 (s, 18H); ^{13}C $\{^1\text{H}\}$ NMR (100 MHz, CDCl_3) δ 155.4, 152.5, 151.9, 145.8, 136.7, 135.9, 129.6, 127.7, 126.4, 125.1, 124.8, 123.0, 117.2, 116.4, 114.1, 113.4, 55.8, 55.7, 45.1, 34.4, 30.4; FT-IR (thin film, neat): 2959, 1624, 1481, 1433, 1238, 753 cm^{-1} ; HRMS (ESI): m/z calcd for $\text{C}_{28}\text{H}_{31}\text{O}_3$ $[\text{M}-\text{H}]^-$: 415.2273; found : 415.2294.

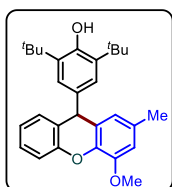
2,6-di-tert-butyl-4-(1,3-dimethoxy-9H-xanthen-9-yl)phenol (53h): The reaction was



performed at 0.112 mmol scale of **52h**; white solid (48.0 mg, 96% yield); $R_f = 0.2$ (5% EtOAc in hexane); ^1H NMR (400 MHz, CDCl_3) δ 7.26 – 7.23 (m, 1H), 7.21 – 7.19 (m, 1H), 7.16 – 7.14 (m, 1H), 7.05 (dd, $J = 7.4, 1.2$ Hz, 1H), 7.02 (s, 2H), 6.37 (d, $J = 2.4$ Hz, 1H), 6.21 (d, $J = 2.3$ Hz, 1H), 5.32 (s,

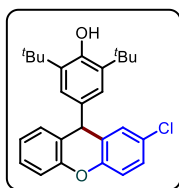
1H), 4.99 (s, 1H), 3.82 (s, 3H), 3.80 (s, 3H), 1.37 (s, 18H); ^{13}C $\{^1\text{H}\}$ NMR (100 MHz, CDCl_3) δ 159.7, 157.9, 153.3, 152.2, 152.0, 137.3, 135.3, 129.7, 127.4, 126.4, 124.3, 123.5, 116.3, 108.1, 94.1, 93.4, 55.70, 55.68, 55.54, 55.52, 38.95, 38.9, 34.4, 30.4; FT-IR (thin film, neat): 2956, 1603, 1454, 1229, 1143, 756 cm^{-1} ; HRMS (ESI): m/z calcd for $\text{C}_{29}\text{H}_{33}\text{O}_4$ $[\text{M}-\text{H}]^-$: 445.2379; found : 445.2382.

2,6-di-tert-butyl-4-(4-methoxy-2-methyl-9H-xanthen-9-yl)phenol (53i): The reaction was



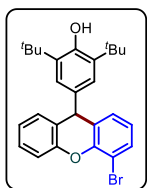
performed at 0.104 mmol scale of **52i**; white solid (38.0 mg, 76% yield); R_f = 0.3 (5% EtOAc in hexane); ^1H NMR (400 MHz, CDCl_3) δ 7.27 – 7.25 (m, 1H), 7.22 – 7.18 (m, 1H), 7.13 – 7.11 (m, 1H), 7.02 – 6.98 (m, 1H), 6.96 (s, 2H), 6.63 – 6.57 (m, 2H), 5.10 (s, 1H), 5.06 (s, 1H), 3.95 (s, 3H), 2.27 (s, 3H), 1.37 (s, 18H); ^{13}C $\{^1\text{H}\}$ NMR (100 MHz, CDCl_3) δ 152.4, 151.5, 147.7, 139.0, 137.2, 135.8, 132.4, 129.6, 127.6, 126.0, 125.3, 124.7, 123.3, 121.4, 116.8, 111.0, 56.3, 44.7, 34.4, 30.4, 21.4; FT-IR (thin film, neat): 2959, 1608, 1481, 1241, 1117, 753 cm^{-1} ; HRMS (ESI): m/z calcd for $\text{C}_{29}\text{H}_{33}\text{O}_3$ $[\text{M}-\text{H}]^-$: 429.2430; found : 429.2437.

2,6-di-tert-butyl-4-(2-chloro-9H-xanthen-9-yl)phenol (53j): The reaction was performed at



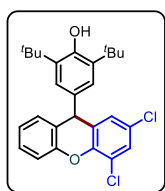
0.107 mmol scale of **52j**; yellow gummy solid (39.5 mg, 79% yield); R_f = 0.4 (5% EtOAc in hexane); ^1H NMR (400 MHz, CDCl_3) δ 7.23 – 7.12 (m, 3H), 7.10 – 7.05 (m, 3H), 7.03 – 6.98 (m, 1H), 6.92 (s, 2H), 5.10 (s, 1H), 5.09 (s, 1H), 1.37 (s, 18H); ^{13}C $\{^1\text{H}\}$ NMR (100 MHz, CDCl_3) δ 152.7, 151.2, 150.2, 136.4, 136.1, 129.7, 129.3, 127.9, 127.8, 127.2, 124.9, 124.8, 123.6, 118.9, 117.9, 116.5, 44.6, 34.4, 30.4; FT-IR (thin film, neat): 2956, 1598, 1474, 1434, 1254, 753 cm^{-1} ; HRMS (ESI): m/z calcd for $\text{C}_{27}\text{H}_{28}\text{ClO}_2$ $[\text{M}-\text{H}]^-$: 419.1778; found : 419.1784.

4-(1-bromo-9H-xanthen-9-yl)-2,6-di-tert-butylphenol (53k): The reaction was performed at



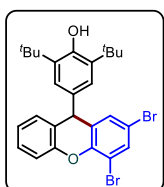
0.115 mmol scale of **52k**; yellow gummy solid (38.0 mg, 76% yield); R_f = 0.4 (5% EtOAc in hexane); ^1H NMR (400 MHz, CDCl_3) δ 7.40 (dd, J = 7.8, 1.4 Hz, 1H), 7.23 – 7.19 (m, 2H), 7.06 – 6.99 (m, 3H), 6.88 (s, 2H), 6.82 (t, J = 7.8 Hz, 1H), 5.11 (s, 1H), 5.05 (s, 1H), 1.32 (s, 18H); ^{13}C $\{^1\text{H}\}$ NMR (100 MHz, CDCl_3) δ 152.7, 152.6, 151.3, 148.4, 136.1, 136.08, 131.4, 129.5, 128.8, 127.9, 127.5, 125.3, 124.9, 123.9, 116.9, 110.7, 44.9, 44.8, 34.4, 30.4; FT-IR (thin film, neat): 2956, 1474, 1434, 1254, 754 cm^{-1} ; HRMS (ESI): m/z calcd for $\text{C}_{27}\text{H}_{28}\text{BrO}_2$ $[\text{M}-\text{H}]^-$: 463.1273; found : 463.1272.

2,6-di-tert-butyl-4-(1,3-dichloro-9H-xanthen-9-yl)phenol (53l): The reaction was performed at 0.109 mmol scale of **52l**; yellow gummy solid (36.0 mg, 72% yield); R_f = 0.4 (5% EtOAc in hexane); ^1H NMR (400 MHz, CDCl_3) δ 7.28 (d, J = 2.4 Hz, 1H), 7.25 – 7.23 (m, 2H), 7.08 – 7.02 (m, 2H), 7.00 (dd, J = 2.4, 0.6 Hz, 1H), 6.91 (s, 2H), 5.13 (s, 1H), 5.10 (s, 1H), 1.38 (s,



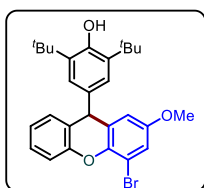
18H); ^{13}C $\{^1\text{H}\}$ NMR (100 MHz, CDCl_3) δ 152.9, 150.8, 146.3, 136.3, 135.7, 129.5, 128.6, 128.2, 128.1, 127.9, 127.6, 124.8, 124.5, 124.2, 122.5, 116.9, 44.76, 44.7, 34.5, 30.4; FT-IR (thin film, neat): 2959, 1595, 1449, 1264, 1183, 752 cm^{-1} ; HRMS (ESI): m/z calcd for $\text{C}_{27}\text{H}_{27}\text{ClO}_2[\text{M}-\text{H}]^-$: 453.1388; found : 453.1393.

2,6-di-tert-butyl-4-(1,3-dibromo-9H-xanthen-9-yl)phenol (53m): The reaction was



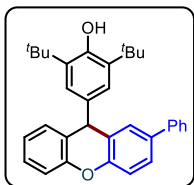
performed at 0.009 mmol scale of **52m**; yellow gummy solid (37.0 mg, 74% yield); $R_f = 0.4$ (5% EtOAc in hexane); ^1H NMR (400 MHz, CDCl_3) δ 7.58 (d, $J = 2.3$ Hz, 1H), 7.24 – 7.23 (m, 2H), 7.18 (dd, $J = 2.3, 0.6$ Hz, 1H), 7.08 – 7.02 (m, 2H), 6.90 (s, 2H), 5.13 (s, 1H), 5.10 (s, 1H), 1.37 (s, 18H); ^{13}C $\{^1\text{H}\}$ NMR (100 MHz, CDCl_3) δ 152.9, 151.0, 147.8, 136.3, 135.6, 133.7, 131.5, 129.5, 129.0, 128.1, 124.8, 124.7, 124.2, 116.9, 115.2, 111.6, 44.83, 44.8, 34.5, 30.4; FT-IR (thin film, neat): 2959, 1558, 1443, 1264, 1158, 753 cm^{-1} ; HRMS (ESI): m/z calcd for $\text{C}_{27}\text{H}_{27}\text{Br}_2\text{O}_2$ $[\text{M}-\text{H}]^-$: 541.0378; found : 541.0378.

4-(2-bromo-4-methoxy-9H-xanthen-9-yl)-2,6-di-tert-butylphenol (53n): The reaction was



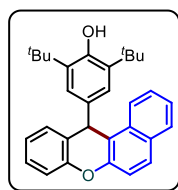
performed at 0.101 mmol scale of **52n**; white solid (37.0 mg, 74% yield); $R_f = 0.3$ (5% EtOAc in hexane); ^1H NMR (400 MHz, CDCl_3) δ 7.26 – 7.19 (m, 2H), 7.09 – 7.07 (m, 1H), 7.03 – 6.99 (m, 1H), 6.92 (s, 3H), 6.88 – 6.87 (m, 1H), 5.09 (s, 1H), 5.08 (s, 1H), 3.94 (s, 3H), 1.37 (s, 18H); ^{13}C $\{^1\text{H}\}$ NMR (100 MHz, CDCl_3) δ 152.7, 150.9, 148.8, 140.3, 136.4, 136.1, 129.6, 127.9 (2C), 124.8, 124.7, 123.9, 123.8, 116.8, 114.8, 113.4, 56.55, 56.5, 44.46, 44.4, 34.4, 30.4; FT-IR (thin film, neat): 2956, 1607, 1481, 1433, 1241, 752 cm^{-1} ; HRMS (ESI): m/z calcd for $\text{C}_{28}\text{H}_{30}\text{BrO}_3$ $[\text{M}-\text{H}]^-$: 493.1378; found : 493.1385.

2,6-di-tert-butyl-4-(2-phenyl-9H-xanthen-9-yl)phenol (53o): The reaction was performed at



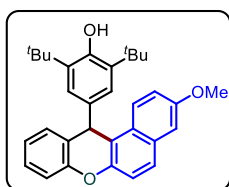
0.108 mmol scale of **52o**; yellow gummy solid (37.5 mg, 75% yield); $R_f = 0.4$ (5% EtOAc in hexane); ^1H NMR (400 MHz, CDCl_3) δ 7.53 (d, $J = 7.6$ Hz, 2H), 7.47 (dd, $J = 8.4, 2.0$ Hz, 1H), 7.44 – 7.39 (m, 3H), 7.35 – 7.30 (m, 1H), 7.26 – 7.22 (m, 2H), 7.19 – 7.17 (m, 2H), 7.06 (d, $J = 7.5$ Hz, 1H), 7.02 (s, 2H), 5.24 (s, 1H), 5.09 (s, 1H), 1.40 (s, 18H); ^{13}C NMR (100 MHz, CDCl_3) δ 152.6, 151.6, 151.3, 140.9, 136.9, 136.3, 136.0, 129.7, 128.8, 128.3, 127.7, 127.0, 126.9, 126.5, 125.8, 125.5, 124.8, 123.4, 116.9, 116.6, 44.8, 44.77, 34.4, 30.4; FT-IR (thin film, neat): 2958, 1601, 1478, 1434, 1235, 754 cm^{-1} ; HRMS (ESI): m/z calcd for $\text{C}_{29}\text{H}_{33}\text{O}_4$ $[\text{M}-\text{H}]^-$: 461.2481; found : 461.2494.

4-(12H-benzo[a]xanthen-12-yl)-2,6-di-*tert*-butylphenol (53p): The reaction was performed



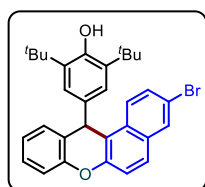
at 0.110 mmol scale of **52p**; pale yellow solid (48.0 mg, 98% yield); $R_f = 0.4$ (5% EtOAc in hexane); $^1\text{H NMR}$ (400 MHz, CDCl_3) δ 8.10 (d, $J = 8.4$ Hz, 1H), 7.84 (d, $J = 8.0$ Hz, 1H), 7.80 (d, $J = 8.9$ Hz, 1H), 7.54 – 7.50 (m, 1H), 7.47 – 7.39 (m, 3H), 7.26 – 7.23 (m, 2H), 7.14 – 7.10 (m, 3H), 5.79 (s, 1H), 5.01 (s, 1H), 1.36 (s, 18H); ^{13}C $\{^1\text{H}\}$ NMR (100 MHz, CDCl_3) δ 152.3, 151.0, 149.8, 136.9, 135.8, 131.9, 130.9, 129.3, 128.7, 128.6, 127.5, 126.6, 126.2, 124.1, 124.0, 123.8, 123.3, 118.1, 117.3, 116.7, 41.74, 41.7, 34.3, 30.3; FT-IR (thin film, neat): 2959, 1582, 1485, 1433, 1245, 738 cm^{-1} ; HRMS (ESI): m/z calcd for $\text{C}_{31}\text{H}_{31}\text{O}_2$ $[\text{M}-\text{H}]^-$: 435.2324; found: 435.2332.

2,6-di-*tert*-butyl-4-(3-methoxy-12H-benzo[a]xanthen-12-yl)phenol (53q): The reaction was



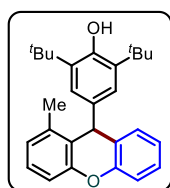
performed at 0.085 mmol scale of **52q**; pale yellow solid (48.0 mg, 96% yield); $R_f = 0.3$ (5% EtOAc in hexane); $^1\text{H NMR}$ (400 MHz, CDCl_3) δ 7.97 – 7.94 (m, 1H), 7.66 (d, $J = 8.0$ Hz, 1H), 7.39 (d, $J = 8.8$ Hz, 2H), 7.26 – 7.19 (m, 2H), 7.17 – 7.14 (m, 2H), 7.09 – 7.04 (m, 3H), 5.70 (s, 1H), 4.95 (s, 1H), 3.90 (s, 3H), 1.31 (s, 18H); ^{13}C $\{^1\text{H}\}$ NMR (100 MHz, CDCl_3) δ 156.4, 152.3, 151.2, 148.4, 136.9, 135.8, 132.0, 129.3, 127.44, 127.4, 127.0, 126.2, 124.8, 123.9, 123.6, 118.8, 118.5, 117.7, 116.6, 107.2, 55.43, 55.4, 41.9, 34.3, 30.3; FT-IR (thin film, neat): 2956, 1611, 1514, 1433, 1247, 752 cm^{-1} ; HRMS (ESI): m/z calcd for $\text{C}_{32}\text{H}_{33}\text{O}_3$ $[\text{M}-\text{H}]^-$: 465.2430; found: 465.2433.

4-(3-bromo-12H-benzo[a]xanthen-12-yl)-2,6-di-*tert*-butylphenol (53r): The reaction was



performed at 0.120 mmol scale of **52r**; yellow white solid (42.0 mg, 85% yield); $R_f = 0.4$ (5% EtOAc in hexane); $^1\text{H NMR}$ (400 MHz, CDCl_3) δ 7.94 (d, $J = 2.0$ Hz, 1H), 7.88 (d, $J = 9.0$ Hz, 1H), 7.66 (d, $J = 9.0$ Hz, 1H), 7.52 (dd, $J = 9.0, 2.0$ Hz, 1H), 7.42 (d, $J = 8.9$ Hz, 1H), 7.38 (d, $J = 7.4$ Hz, 1H), 7.26 – 7.13 (m, 2H), 7.11 – 7.07 (m, 1H), 7.01 (s, 2H), 5.67 (s, 1H), 4.98 (s, 1H), 1.31 (s, 18H); ^{13}C $\{^1\text{H}\}$ NMR (100 MHz, CDCl_3) δ 152.4, 150.7, 149.9, 136.6, 136.0, 132.1, 130.6, 130.5, 129.8, 129.3, 127.8, 127.6, 125.8, 125.1, 124.0, 123.9, 119.3, 117.9, 117.5, 116.7, 41.7, 34.3, 30.3; FT-IR (thin film, neat): 2958, 1627, 1488, 1434, 1249, 753 cm^{-1} ; HRMS (ESI): m/z calcd for $\text{C}_{31}\text{H}_{30}\text{BrO}_2$ $[\text{M}-\text{H}]^-$: 513.1429; found: 513.1427.

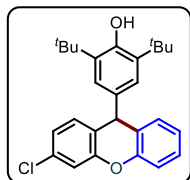
2,6-di-*tert*-butyl-4-(1-methyl-9H-xanthen-9-yl)phenol (53s): The reaction was performed at



0.124 mmol scale of **52s**; pale yellow solid (48.0 mg, 96% yield); m. p. = 88–90 °C; $R_f = 0.4$ (5% EtOAc in hexane); δ 7.31 (dd, $J = 7.6, 1.0$ Hz, 1H), 7.21 – 7.12 (m, 3H), 7.09–7.07 (m, 1H), 7.03 (td, $J = 7.4, 1.2$ Hz, 1H), 6.99 (s, 2H), 6.91 (d, $J = 7.3$ Hz, 1H), 5.14 (s, 1H), 5.01 (s, 1H), 2.28 (s, 3H), 1.36 (s, 18H);

$^{13}\text{C}\{^1\text{H}\}$ NMR (100 MHz, CDCl_3) δ 152.5, 152.3, 151.5, 137.3, 136.2, 135.8, 129.1, 127.5, 127.4, 126.9, 125.1, 124.4, 124.1, 123.3, 116.6, 114.5, 42.83, 42.8, 34.4, 30.4, 19.4; FT-IR (thin film, neat): 2923, 1656, 1462, 1436, 1257, 1155, 749 cm^{-1} ; HRMS (ESI): m/z calcd for $\text{C}_{28}\text{H}_{31}\text{O}_2$ $[\text{M}-\text{H}]^-$: 399.2324; found: 399.2325.

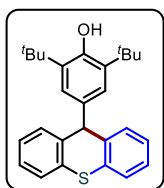
2,6-di-tert-butyl-4-(3-chloro-9H-xanthen-9-yl)phenol (53t): The reaction was performed at



0.118 mmol scale of **52t**; pale yellow solid (46.0 mg, 92 % yield); m. p. = 187–189 °C; R_f = 0.4 (5% EtOAc in hexane); ^1H NMR (400 MHz, CDCl_3) δ 7.24 – 7.20 (m, 1H), 7.16 – 7.09 (m, 3H), 7.05 – 7.00 (m, 2H), 6.99 – 6.97 (m, 1H), 6.94 (s, 2H), 5.12 (s, 1H), 5.10 (s, 1H), 1.38 (s, 18H); $^{13}\text{C}\{^1\text{H}\}$ NMR

(100 MHz, CDCl_3) δ 152.7, 152.0, 151.1, 136.5, 136.1, 132.7, 130.7, 129.7, 127.9, 125.1, 124.9, 124.2, 123.7, 123.5, 116.8, 116.5, 44.1, 34.4, 30.4; FT-IR (thin film, neat): 2921, 1739, 1457, 1274, 929, 753 cm^{-1} ; HRMS (ESI): m/z calcd for $\text{C}_{27}\text{H}_{28}\text{ClO}_2$ $[\text{M}-\text{H}]^-$: 419.1778; found: 419.1787.

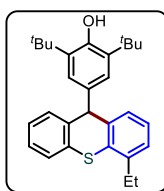
2,6-di-tert-butyl-4-(9H-thioxanthen-9-yl)phenol (55a): The reaction was performed at 0.099



mmol scale of **54a**; yellow gummy solid (32.0 mg, 64% yield); R_f = 0.4 (5% EtOAc in hexane); ^1H NMR (400 MHz, CDCl_3) δ 7.45 – 7.42 (m, 2H), 7.39 – 7.37 (m, 2H), 7.26 – 7.23 (m, 3H), 7.21 – 7.19 (m, 1H), 6.90 (s, 2H), 5.22 (s, 1H), 5.05 (s, 1H), 1.32 (s, 18H); $^{13}\text{C}\{^1\text{H}\}$ NMR (100 MHz, CDCl_3) δ 152.4,

138.1, 135.5, 133.1, 131.5, 129.5, 127.0, 126.7, 126.6, 124.9, 53.2, 53.17, 34.4, 30.3; FT-IR (thin film, neat): 2957, 1588, 1464, 1432, 1232, 741 cm^{-1} ; HRMS (ESI): m/z calcd for $\text{C}_{27}\text{H}_{29}\text{OS}$ $[\text{M}-\text{H}]^-$: 401.1939; found: 401.1956.

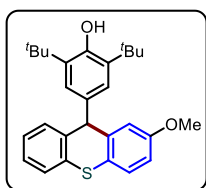
2,6-di-tert-butyl-4-(4-ethyl-9H-thioxanthen-9-yl)phenol (55b): The reaction was performed



at 0.116 mmol scale of **54b**; yellow gummy solid (32.8 mg, 66% yield); R_f = 0.4 (5% EtOAc in hexane); ^1H NMR (400 MHz, CDCl_3) δ 7.45 (dd, J = 7.4, 1.3 Hz, 1H), 7.39 (dd, J = 7.4, 1.4 Hz, 1H), 7.26 – 7.17 (m, 4H), 7.14 – 7.12 (m, 1H), 6.89 (s, 2H), 5.23 (s, 1H), 5.03 (s, 1H), 2.87 – 2.81 (m, 2H), 1.32 (s, 18H),

1.28 (t, J = 7.5 Hz, 3H); $^{13}\text{C}\{^1\text{H}\}$ NMR (100 MHz, CDCl_3) δ 152.4, 141.2, 138.5, 137.8, 135.3, 133.0, 132.2, 131.6, 129.1, 127.3, 127.2, 126.63, 126.6, 126.5, 126.4, 124.9, 53.65, 53.6, 34.4, 30.3, 27.4, 14.7; FT-IR (thin film, neat): 2959, 1588, 1434, 1235, 1120, 739 cm^{-1} ; HRMS (ESI): m/z calcd for $\text{C}_{29}\text{H}_{33}\text{OS}$ $[\text{M}-\text{H}]^-$: 429.2252; found: 429.2260.

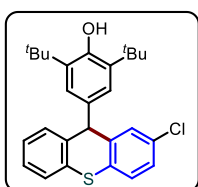
2,6-di-tert-butyl-4-(2-methoxy-9H-thioxanthen-9-yl)phenol (55c): The reaction was performed at 0.115 mmol scale of **54c**; pale yellow solid (42.0 mg, 84% yield); m. p. = 216–218 °C; R_f = 0.3 (5% EtOAc in hexane); ^1H NMR (400 MHz, CDCl_3) δ 7.45 – 7.43 (m, 1H), 7.39 – 7.35 (m, 2H), 7.26 – 7.19 (m, 2H), 6.97 (s, 3H), 6.82 (dd, J = 8.5, 2.7 Hz, 1H), 5.18 (s,



1H), 5.09 (s, 1H), 3.81 (s, 3H), 1.36 (s, 18H), $^{13}\text{C}\{^1\text{H}\}$ NMR (100 MHz, CDCl_3) δ 158.8, 152.5, 139.7, 138.0, 135.5, 133.7, 131.2, 129.3, 127.9, 127.0, 126.7, 126.5, 125.0, 124.2, 115.0, 112.9, 55.6, 55.56, 53.7, 53.65, 34.4, 30.3; FT-IR (thin film, neat): 2957, 1598, 1466, 1434, 1236, 739 cm^{-1} ;

HRMS (ESI): m/z calcd for $\text{C}_{28}\text{H}_{31}\text{O}_2\text{S}$ $[\text{M}-\text{H}]^-$: 431.2045; found: 431.2054.

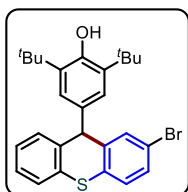
2,6-di-tert-butyl-4-(2-chloro-9H-thioxanthen-9-yl)phenol (55d): The reaction was



performed at 0.115 mmol scale of **54d**; white solid (33.0 mg, 66% yield); R_f = 0.4 (5% EtOAc in hexane); ^1H NMR (400 MHz, CDCl_3) δ 7.49 (dd, J = 7.2, 1.4 Hz, 1H), 7.45 (dd, J = 7.5, 1.7 Hz, 1H), 7.31 – 7.23 (m, 4H), 7.22 – 7.20 (m, 1H), 6.89 (s, 2H), 5.96 (s, 1H), 5.02 (s, 1H), 1.28 (s, 18H); $^{13}\text{C}\{^1\text{H}\}$ NMR

(100 MHz, CDCl_3) δ 152.7, 137.1, 136.5, 135.4, 135.0, 132.5, 132.0, 130.4, 130.3, 130.1, 127.9, 127.8, 127.4, 127.37, 126.9, 124.2, 49.2, 34.4, 30.3; FT-IR (thin film, neat): 2958, 1740, 1432, 1320, 805, 753 cm^{-1} ; HRMS (APCI): m/z calcd for $\text{C}_{27}\text{H}_{28}\text{ClOS}$ $[\text{M}-\text{H}]^-$: 435.1549; found: 435.1542.

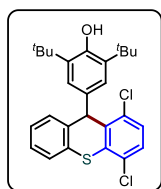
4-(2-bromo-9H-thioxanthen-9-yl)-2,6-di-tert-butylphenol (55e): The reaction was



performed at 0.103 mmol scale of **54e**; pale yellow solid (36.5 mg, 73% yield); R_f = 0.4 (5% EtOAc in hexane); ^1H NMR (400 MHz, CDCl_3) δ 7.52 (d, J = 1.9 Hz, 1H), 7.42 – 7.39 (m, 1H), 7.35 – 7.26 (m, 3H), 7.25 – 7.18 (m, 2H), 6.91 (s, 2H), 5.15 (s, 1H), 5.08 (s, 1H), 1.34 (s, 18H); $^{13}\text{C}\{^1\text{H}\}$ NMR

(100 MHz, CDCl_3) δ 152.7, 140.1, 137.4, 135.7, 132.4, 132.3, 132.2, 131.0, 129.6, 129.5, 128.3, 127.0, 126.93, 126.9, 124.8, 120.2, 53.0, 52.9, 34.4, 30.3; FT-IR (thin film, neat): 2959, 1462, 1436, 1235, 1156, 751 cm^{-1} ; HRMS (ESI): m/z calcd for $\text{C}_{27}\text{H}_{28}\text{BrOS}$ $[\text{M}-\text{H}]^-$: 479.1044; found: 479.1054.

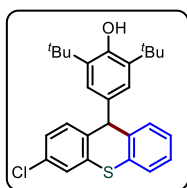
2,6-di-tert-butyl-4-(2,5-dichloro-9H-thioxanthen-9-yl)phenol (55f): The reaction was



performed at 0.136 mmol scale of **54f**; white solid (34.0 mg, 74% yield); m. p. = 178–180 $^\circ\text{C}$; R_f = 0.4 (5% EtOAc in hexane); ^1H NMR (400 MHz, CDCl_3) δ 7.52 – 7.49 (m, 1H), 7.48 – 7.45 (m, 1H), 7.34 – 7.28 (m, 3H), 7.24 – 7.22 (m, 1H), 6.90 (s, 2H), 5.98 (s, 1H), 5.04 (s, 1H), 1.29 (s, 18H); $^{13}\text{C}\{^1\text{H}\}$ NMR (100

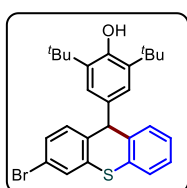
MHz, CDCl_3) δ 152.7, 139.8, 137.4, 135.7, 132.5, 132.3, 131.7, 131.0, 129.5, 129.4, 128.0, 127.0, 126.93, 126.9, 126.8, 124.8, 53.1, 34.4, 30.3; FT-IR (thin film, neat): 2958, 1592, 1459, 1155, 809, 742 cm^{-1} ; HRMS (ESI): m/z calcd for $\text{C}_{27}\text{H}_{27}\text{Cl}_2\text{OS}$ $[\text{M}-\text{H}]^-$: 469.1160; found: 469.1183.

2,6-di-tert-butyl-4-(3-chloro-9H-thioxanthen-9-yl)phenol (55g): The reaction was performed at 0.115 mmol scale of **54g**; yellow gummy solid (29.0 mg, 58% yield); m. p. =



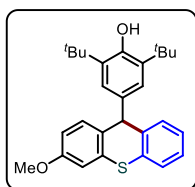
138–140 °C; $R_f = 0.4$ (5% EtOAc in hexane); ^1H NMR (400 MHz, CDCl_3) δ 7.44–7.42 (m, 2H), 7.37–7.35 (m, 1H), 7.30–7.28 (m, 1H), 7.26–7.19 (m, 3H), 6.89 (s, 2H), 5.19 (s, 1H), 5.08 (s, 1H), 1.34 (s, 18H); $^{13}\text{C}\{^1\text{H}\}$ NMR (100 MHz, CDCl_3) δ 152.6, 137.7, 136.7, 135.6, 135.0, 132.31, 132.3, 131.1, 130.4, 129.5, 127.0, 126.9 (2C), 126.7, 126.6, 124.8, 52.6, 52.59, 34.4, 30.3; FT-IR (thin film, neat): 2957, 1580, 1464, 1435, 1235, 746 cm^{-1} ; HRMS (ESI): m/z calcd for $\text{C}_{27}\text{H}_{28}\text{ClOS}$ [$\text{M}-\text{H}$] $^-$: 435.1549; found : 435.1566.

4-(3-bromo-9H-thioxanthen-9-yl)-2,6-di-tert-butylphenol (55h): The reaction was



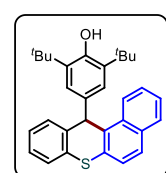
performed at 0.110 mmol scale of **54h**; white solid (35.0 mg, 68% yield); m. p. = 196–198 °C; $R_f = 0.4$ (5% EtOAc in hexane); ^1H NMR (400 MHz, CDCl_3) δ 7.29 (d, $J = 2.0$ Hz, 1H), 7.23–7.19 (m, 1H), 7.11 (dd, $J = 8.1, 1.7$ Hz, 2H), 7.08 (dd, $J = 7.8, 1.6$ Hz, 1H), 7.04–7.01 (m, 1H), 7.00–6.95 (m, 1H), 6.91 (s, 2H), 5.08 (s, 2H), 1.36 (s, 18H); $^{13}\text{C}\{^1\text{H}\}$ NMR (100 MHz, CDCl_3) δ 152.7, 152.1, 151.1, 136.4, 136.1, 131.0, 129.7, 127.9, 126.3, 125.0, 124.9, 124.7, 123.7, 120.4, 119.7, 116.5, 44.2, 44.16, 34.4, 30.4; FT-IR (thin film, neat): 2956, 1595, 1475, 1274, 917, 755 cm^{-1} ; HRMS (ESI): m/z calcd for $\text{C}_{27}\text{H}_{29}\text{BrOS}$ [$\text{M}+\text{H}$] $^+$: 481.1201; found : 481.1217.

2,6-di-tert-butyl-4-(3-methoxy-9H-thioxanthen-9-yl)phenol (55i): The reaction was



performed at 0.114 mmol scale of **54i**; pale yellow solid (36.4 mg, 73% yield); m. p. = 90–92 °C; $R_f = 0.3$ (5% EtOAc in hexane); ^1H NMR (400 MHz, CDCl_3) δ 7.44–7.42 (m, 1H), 7.39–7.37 (m, 1H), 7.28 (d, $J = 8.5$ Hz, 1H), 7.26–7.19 (m, 2H), 7.10 (d, $J = 2.6$ Hz, 1H), 6.93 (s, 2H), 6.81 (dd, $J = 8.4, 2.6$ Hz, 1H), 5.19 (s, 1H), 5.06 (s, 1H), 3.82 (s, 3H), 1.35 (s, 18H); $^{13}\text{C}\{^1\text{H}\}$ NMR (100 MHz, CDCl_3) δ 158.2, 152.4, 138.4, 135.4, 134.1, 132.8, 132.1, 130.3, 130.2, 129.4, 128.5, 126.9, 126.6, 124.8, 113.0, 111.6, 55.6, 55.5, 52.34, 52.3, 34.4, 30.3; FT-IR (thin film, neat): 2956, 1600, 1435, 1246, 1056, 739 cm^{-1} ; HRMS (ESI): m/z calcd for $\text{C}_{28}\text{H}_{32}\text{O}_2\text{S}$ [$\text{M}-\text{H}$] $^-$: 431.2049; found : 435.2045.

4-(12H-benzo[a]thioxanthen-12-yl)-2,6-di-tert-butylphenol (55j): The reaction was



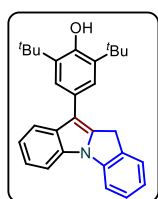
performed at 0.110 mmol scale of **54j**; white solid (35.0 mg, 70% yield); m. p. = 84–86 °C; $R_f = 0.4$ (5% EtOAc in hexane); ^1H NMR (400 MHz, CDCl_3) δ 8.35 (d, $J = 8.6$ Hz, 1H), 7.87–7.85 (m, 1H), 7.73 (d, $J = 8.5$ Hz, 1H), 7.60–7.56 (m, 1H), 7.52 (d, $J = 8.6$ Hz, 1H), 7.49–7.45 (m, 2H), 7.30 (td, $J = 7.4, 1.4$ Hz, 1H), 7.26–7.22 (m, 2H), 6.90 (s, 2H), 6.24 (s, 1H), 4.97 (s, 1H), 1.24 (s, 18H); $^{13}\text{C}\{^1\text{H}\}$ NMR (100 MHz, CDCl_3) δ 152.4, 137.3, 135.3, 132.8, 132.6, 132.3, 132.2, 131.8, 131.0, 130.0, 129.0, 127.2, 127.0, 126.8, 126.75, 126.7, 125.4, 125.2, 124.4, 122.9, 47.0, 34.3, 30.2; FT-IR

(thin film, neat): 2956, 1592, 1435, 1235, 806, 740 cm^{-1} ; HRMS (ESI): m/z calcd for $\text{C}_{31}\text{H}_{32}\text{OS}$ $[\text{M}-\text{H}]^-$: 451.2096; found : 451.2088.

General procedure for the synthesis of 10H-indolo[1,2-a]indole (57a-e):

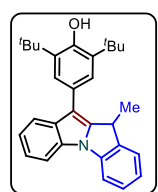
To an oven dried round bottom flask equipped with a stir bar, were charged with 2-indolyl-substituted *p*-QMs (1.0 equiv.) and a stock solution of TfOH (0.2 equiv.) in toluene, and the resulting mixture was stirred at room temperature until the starting material was completely consumed. Then, the excess solvent was removed under reduced pressure to get the crude residue which was further purified by column chromatography on silica gel using a mixture of hexane and ethyl acetate.

2,6-di-*tert*-butyl-4-(10H-indolo[1,2-a]indol-11-yl)phenol (57a): The reaction was performed



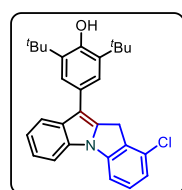
at 0.098 mmol scale of **56a**; Greyish gummy solid (38 mg, 94% yield); $R_f = 0.4$ (5% EtOAc in hexane); ^1H NMR (400 MHz, CDCl_3) δ 7.97 (d, $J = 7.9$ Hz, 1H), 7.85 (d, $J = 8.0$ Hz, 1H), 7.65 (d, $J = 7.8$ Hz, 1H), 7.60 (s, 2H), 7.48 (d, $J = 7.4$ Hz, 1H), 7.42 (t, $J = 7.5$ Hz, 1H), 7.37 – 7.33 (m, 1H), 7.30 – 7.26 (m, 1H), 7.15 (td, $J = 7.5, 0.7$ Hz, 1H), 5.26 (s, 1H), 4.23 (s, 1H), 1.57 (s, 18H); $^{13}\text{C}\{^1\text{H}\}$ NMR (100 MHz, CDCl_3) δ 152.2, 141.5, 138.3, 136.4, 133.5, 131.4, 131.2, 128.0, 126.3, 126.0, 124.3, 122.5, 121.9, 120.8, 120.3, 111.9, 111.0, 110.6, 34.7, 30.6, 29.8; FT-IR (thin film, neat FT-IR (thin film, neat): 3638, 2954, 1604, 1493, 1235, 739 cm^{-1} ; HRMS (ESI): m/z calcd for $\text{C}_{29}\text{H}_{32}\text{NO}$ $[\text{M}+\text{H}]^+$: 410.2484; found : 410.2466.

2,6-di-*tert*-butyl-4-(10-methyl-10H-indolo[1,2-a]indol-11-yl)phenol (57b): The reaction



was performed at 0.094 mmol scale of **56b**; Greyish gummy solid (37 mg, 92% yield); $R_f = 0.4$ (5% EtOAc in hexane); ^1H NMR (400 MHz, CDCl_3) δ 7.89 (d, $J = 7.9$ Hz, 1H), 7.82 (d, $J = 8.2$ Hz, 1H), 7.62 – 7.60 (m, 1H), 7.56 (s, 2H), 7.44 – 7.32 (m, 3H), 7.27 – 7.23 (m, 1H), 7.14 (td, $J = 7.5, 0.6$ Hz, 1H), 5.22 (s, 1H), 4.55 (q, $J = 7.2$ Hz, 1H), 1.57 – 1.55 (m, 21H); $^{13}\text{C}\{^1\text{H}\}$ NMR (100 MHz, CDCl_3) δ 152.3, 143.4, 140.6, 139.8, 136.1, 131.9, 130.8, 128.0, 125.6, 124.9, 124.8, 122.6, 122.1, 120.7, 120.3, 112.5, 110.9, 110.5, 36.3, 34.7, 30.6, 17.6; FT-IR (thin film, neat FT-IR (thin film, neat): 3634, 2955, 1603, 1492, 1312, 740 cm^{-1} ; HRMS (ESI): m/z calcd for $\text{C}_{30}\text{H}_{34}\text{NO}$ $[\text{M}+\text{H}]^+$: 424.2640; found : 424.2620.

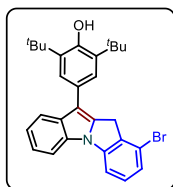
4-(9-chloro-10H-indolo[1,2-a]indol-11-yl)-2,6-di-*tert*-butylphenol (57c): The reaction was



performed at 0.009 mmol scale of **56c**; Greyish gummy solid (36 mg, 90% yield); $R_f = 0.4$ (5% EtOAc in hexane); ^1H NMR (400 MHz, CDCl_3) δ 7.93 (d, $J = 7.9$ Hz, 1H), 7.76 (d, $J = 8.0$ Hz, 1H), 7.59 (d, $J = 1.1$ Hz, 1H), 7.54 (s, 2H), 7.52 – 7.49 (m, 1H), 7.36 – 7.32 (m, 1H), 7.26 (s, 2H), 5.25 (s, 1H), 4.21 (s,

2H), 1.53 (s, 18H); $^{13}\text{C}\{^1\text{H}\}$ NMR (100 MHz, CDCl_3) δ 152.4, 137.7, 136.5, 135.8, 131.5, 131.1, 130.9, 129.2, 125.9, 124.4, 122.2, 122.19, 121.2, 120.5, 115.0, 112.5, 111.6, 110.9, 34.7, 30.6, 29.6; FT-IR (thin film, neat FT-IR (thin film, neat): 3674, 2926, 1743, 1493, 1378, 767 cm^{-1} ; HRMS (ESI): m/z calcd for $\text{C}_{29}\text{H}_{31}\text{ClNO}$ $[\text{M}+\text{H}]^+$: 444.2094; found : 444.2076.

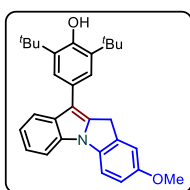
2,6-di-*tert*-butyl-4-(9-bromo-10H-indolo[1,2-*a*]indol-11-yl)phenol (57d): The reaction was



performed at 0.081mmol scale of **56d**; Greyish gummy solid (38 mg, 95% yield); $R_f = 0.4$ (5% EtOAc in hexane); ^1H NMR (400 MHz, CDCl_3) δ 7.94 (d, $J = 7.8$ Hz, 1H), 7.76 (d, $J = 8.0$ Hz, 1H), 7.59 – 7.58 (m, 1H), 7.55 (s, 2H), 7.38 – 7.34 (m, 2H), 7.31 – 7.26 (m, 1H), 7.09 (dd, $J = 7.9, 1.8$ Hz, 1H), 5.26

(s, 1H), 4.15 (s, 2H), 1.55 (s, 18H); $^{13}\text{C}\{^1\text{H}\}$ NMR (100 MHz, CDCl_3) δ 152.4, 142.4, 138.3, 136.4, 133.7, 132.0, 131.6, 131.1, 126.6, 125.8, 124.4, 122.3 (2C), 121.3, 120.4, 112.6, 111.1, 111.0, 34.7, 30.6, 29.3; 3640, 2924, 1599, 1493, 1305, 736 cm^{-1} ; HRMS (ESI): m/z calcd for $\text{C}_{29}\text{H}_{31}\text{BrNO}$ $[\text{M}+\text{H}]^+$: 488.1589; found : 488.1613.

2,6-di-*tert*-butyl-4-(7-methoxy-10H-indolo[1,2-*a*]indol-11-yl)phenol (57e): The reaction



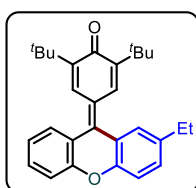
was performed at 0.091 mmol scale of **56e**; Greyish gummy solid (30 mg, 75% yield); $R_f = 0.3$ (5% EtOAc in hexane); ^1H NMR (400 MHz, CDCl_3) δ 7.96 (d, $J = 7.9$ Hz, 1H), 7.77 (d, $J = 8.0$ Hz, 1H), 7.58 (s, 2H), 7.52 (d, $J = 8.5$ Hz, 1H), 7.35 – 7.31 (m, 1H), 7.27 – 7.23 (m, 1H), 7.09 (d, $J = 2.4$ Hz,

1H), 6.93 (dd, $J = 8.5, 2.5$ Hz, 1H), 5.24 (s, 1H), 4.20 (s, 2H), 3.86 (s, 3H), 1.55 (s, 18H); $^{13}\text{C}\{^1\text{H}\}$ NMR (100 MHz, CDCl_3) δ 155.9, 152.1, 138.3, 136.4, 135.5, 135.1, 131.0, 130.9, 126.4, 124.3, 121.8, 120.5, 120.3, 113.1, 112.3, 111.7, 110.64, 110.6, 56.0, 55.96, 34.7, 30.6, 30.1; FT-IR (thin film, neat FT-IR (thin film, neat): 3644, 2922, 1599, 1498, 1247, 737 cm^{-1} ; HRMS (ESI): m/z calcd for $\text{C}_{30}\text{H}_{34}\text{NO}_2$ $[\text{M}+\text{H}]^+$: 440.2590; found : 440.2575.

Procedure for the gram scale synthesis of 53a:

In a 100 mL round bottom flask, *p*-QM **52a** (1.0 g, 2.59 mmol), TsOH (45.7 μL , 0.518 mmol) were taken in 25 mL of CH_2Cl_2 and the resulting reaction mixture was stirred at room temperature for 45 minutes and then, the solvent was evaporated under reduced pressure. The resulting residue was purified through silica gel chromatography using EtOAc/Hexane mixture as an eluent to get the pure **53a** in 0.92 g (92% yield).

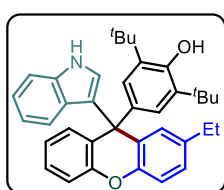
Procedure for the synthesis of 58:



To a solution of **53c** (30 mg, 0.072 mmol) in CH_2Cl_2 (1.5 mL), DDQ (19.7 mg 0.087 mmol) was added and the reaction mixture was stirred at room temperature. After the reaction was complete (based on TLC analysis), reaction mixture was concentrated under reduced pressure. The residue was

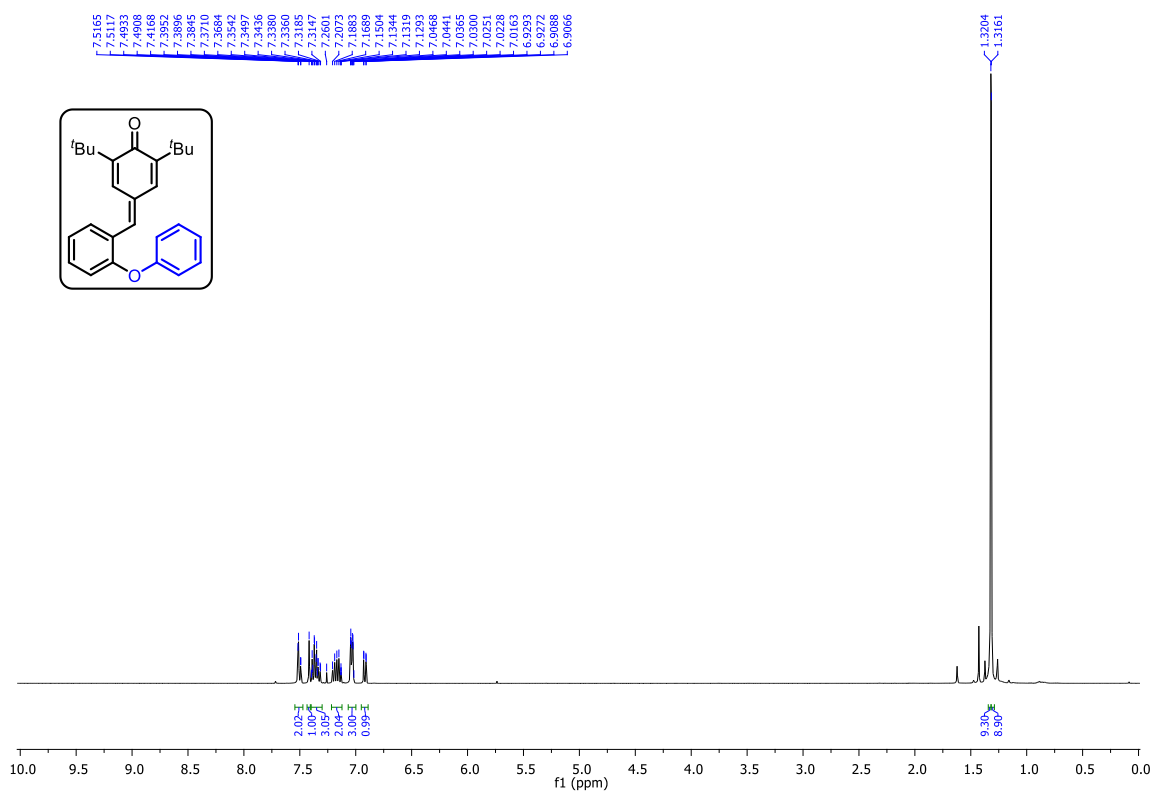
then purified through a silica gel column using EtOAc/Hexane mixture as an eluent to get the pure product **58**. Black gummy solid (32.0 mg, 65% yield); $R_f = 0.4$ (10% EtOAc in hexane); ^1H NMR (400 MHz, CDCl_3) δ 7.80 (dd, $J = 7.8, 2.7$ Hz, 2H), 7.66 (dd, $J = 7.8, 1.4$ Hz, 1H), 7.50 (s, 1H), 7.46 – 7.41 (m, 1H), 7.35 – 7.33 (m, 1H), 7.30 – 7.26 (m, 3H), 2.73 (q, $J = 7.6$ Hz, 2H), 1.34 (s, 9H), 1.32 (s, 9H), 1.30 – 1.28 (m, 3H); $^{13}\text{C}\{^1\text{H}\}$ NMR (100 MHz, CDCl_3) δ 186.7, 154.4, 152.4, 148.0, 147.98, 139.5, 138.2, 130.2 (2C), 130.1, 130.0, 129.3, 128.3, 125.1, 124.0, 123.8, 123.3, 117.0, 116.8, 35.8, 29.8, 29.79, 28.6, 16.11, 16.1; FT-IR (thin film, neat): 2921, 1738, 1663, 1456, 1254, 759 cm^{-1} ; HRMS (ESI): m/z calcd for $\text{C}_{29}\text{H}_{33}\text{O}_2$ $[\text{M}+\text{H}]^+$: 413.2481; found : 413.2471.

Procedure for the synthesis of 59:

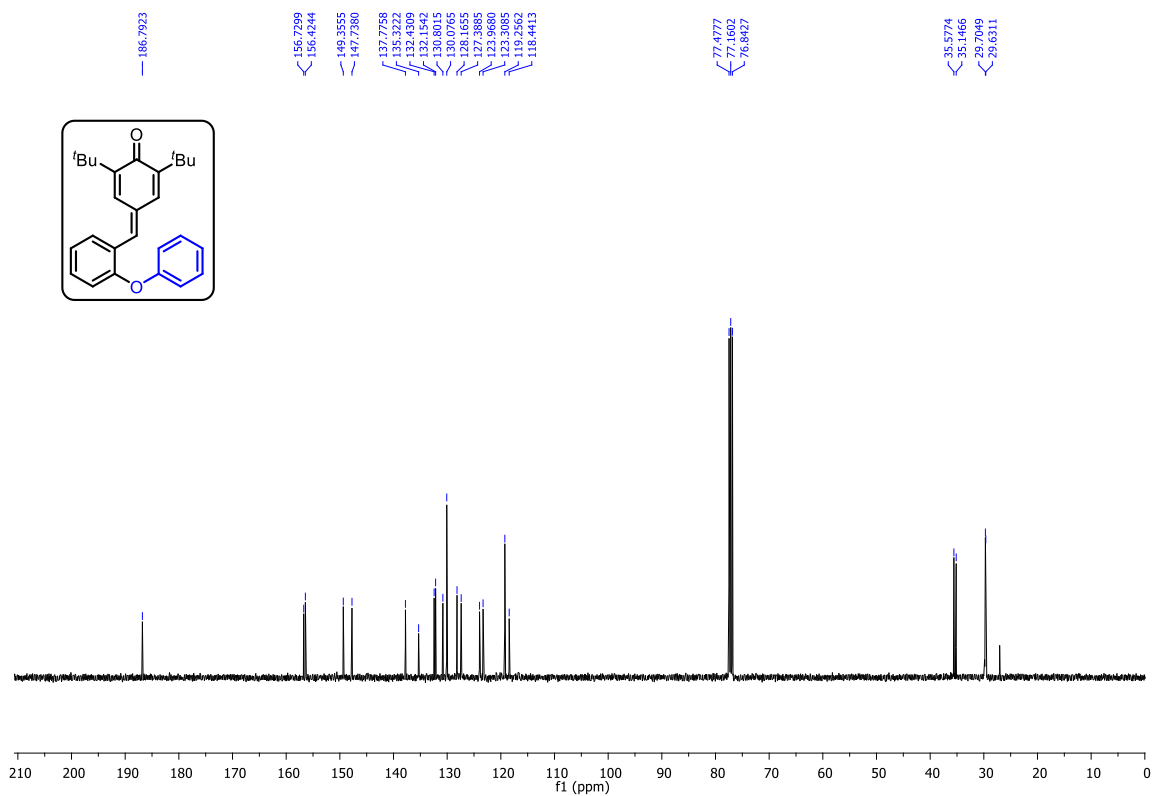


Indole (1.2 equiv.) was added to a solution of **58** (1.0 equiv.) and $\text{Bi}(\text{OTf})_3$ (0.1 equiv.) in 1,2-DCE (2.0 mL) and the resulting reaction mixture was stirred at 60 °C for 6 hours. After completion, reaction mixture was concentrated under reduced pressure. The residue was then purified through silica gel chromatography using EtOAc/Hexane mixture as an eluent to get the pure product **59**. White solid (25 mg, 98% yield); m. p. = 142–144 °C; $R_f = 0.6$ (10% EtOAc in hexane); ^1H NMR (400 MHz, CDCl_3) δ 7.98 (s, 1H), 7.36 (d, $J = 8.2$ Hz, 1H), 7.25 – 7.20 (m, 1H), 7.17 – 7.15 (m, 1H), 7.12 – 7.10 (m, 1H), 7.08 (s, 1H), 7.07 – 7.04 (m, 1H), 6.98 – 6.90 (m, 2H), 6.85 (d, $J = 1.8$ Hz, 1H), 6.83 – 6.77 (m, 4H), 6.49 (d, $J = 2.5$ Hz, 1H), 5.05 (s, 1H), 2.49 – 2.39 (m, 2H), 1.25 (s, 18H), 1.05 (t, $J = 7.6$ Hz, 3H); $^{13}\text{C}\{^1\text{H}\}$ NMR (100 MHz, CDCl_3) δ 152.8, 151.9, 150.7, 138.6, 137.5, 136.5, 134.6, 129.7, 129.3, 128.9, 128.8, 127.6, 127.0, 126.9, 126.2, 125.4, 122.5, 122.46, 122.3, 121.9, 119.3, 116.3, 116.2, 111.0, 48.7, 34.5, 30.4, 28.6, 16.6; FT-IR (thin film, neat): 2925, 1652, 1454, 1251, 1121, 741 cm^{-1} ; HRMS (ESI): m/z calcd for $\text{C}_{32}\text{H}_{35}\text{O}_5$ $[\text{M}-\text{H}]^-$: 528.2903; found : 528.2917.

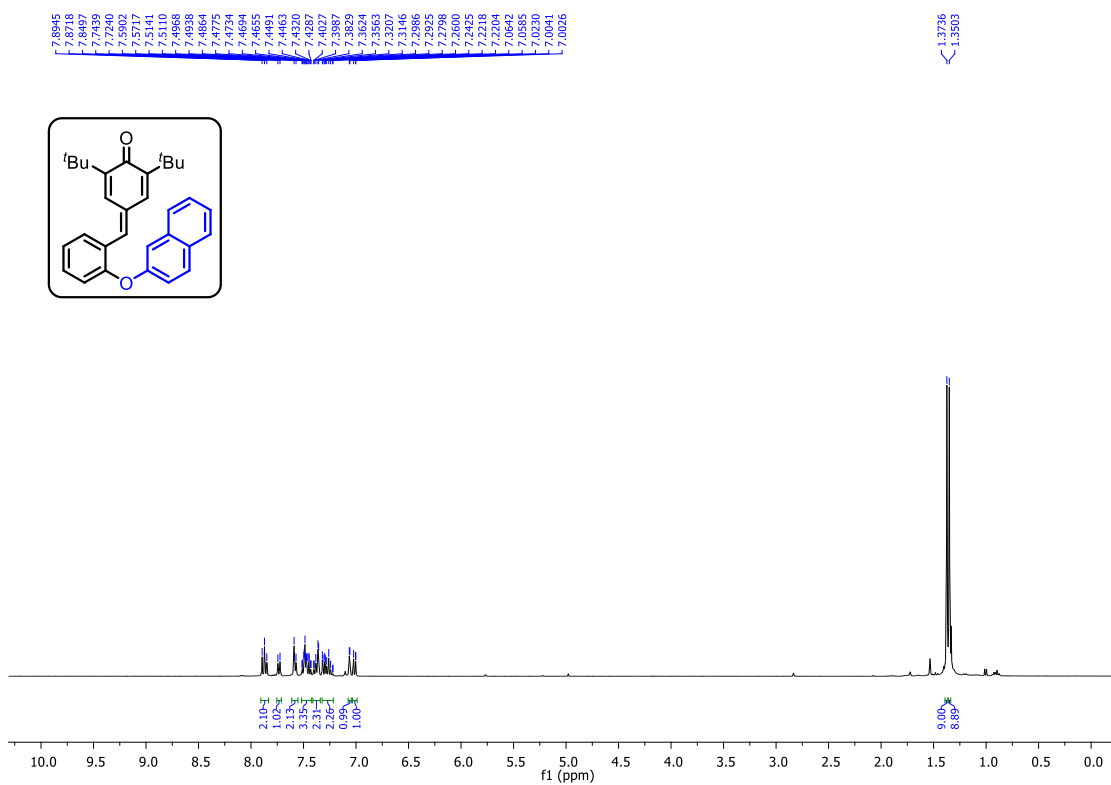
¹H NMR (400 MHz, CDCl₃) spectrum of **52a**



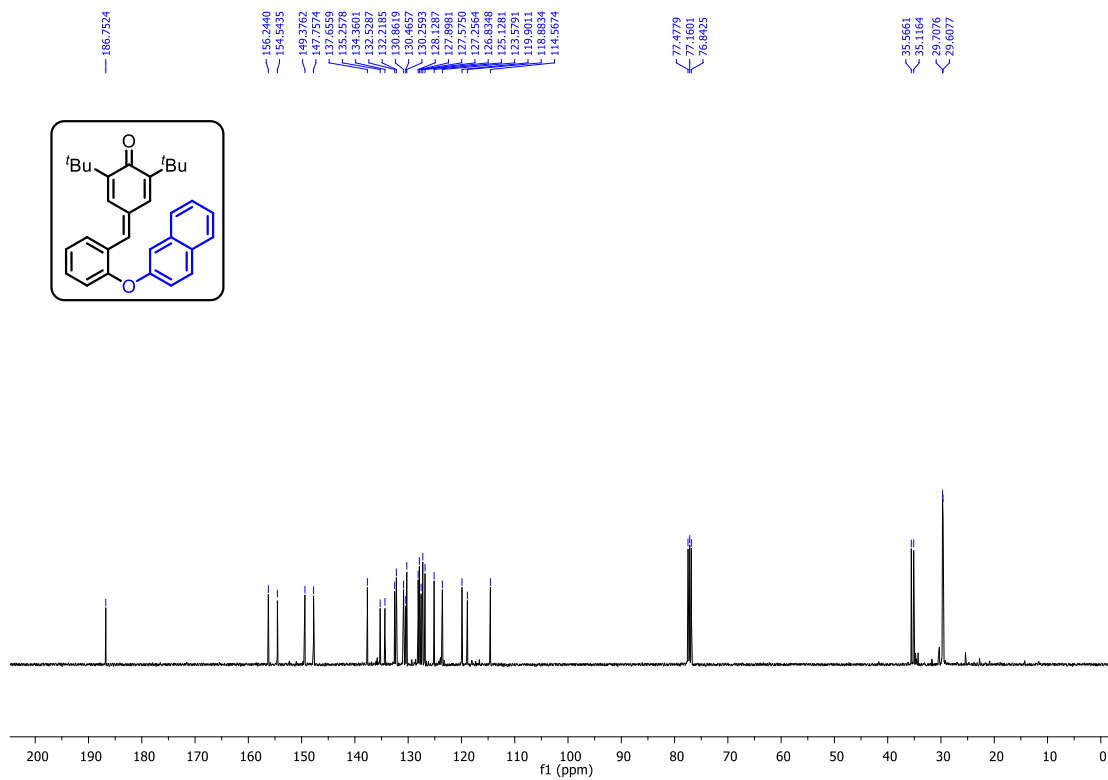
¹³C NMR (100 MHz, CDCl₃) spectrum of **52a**



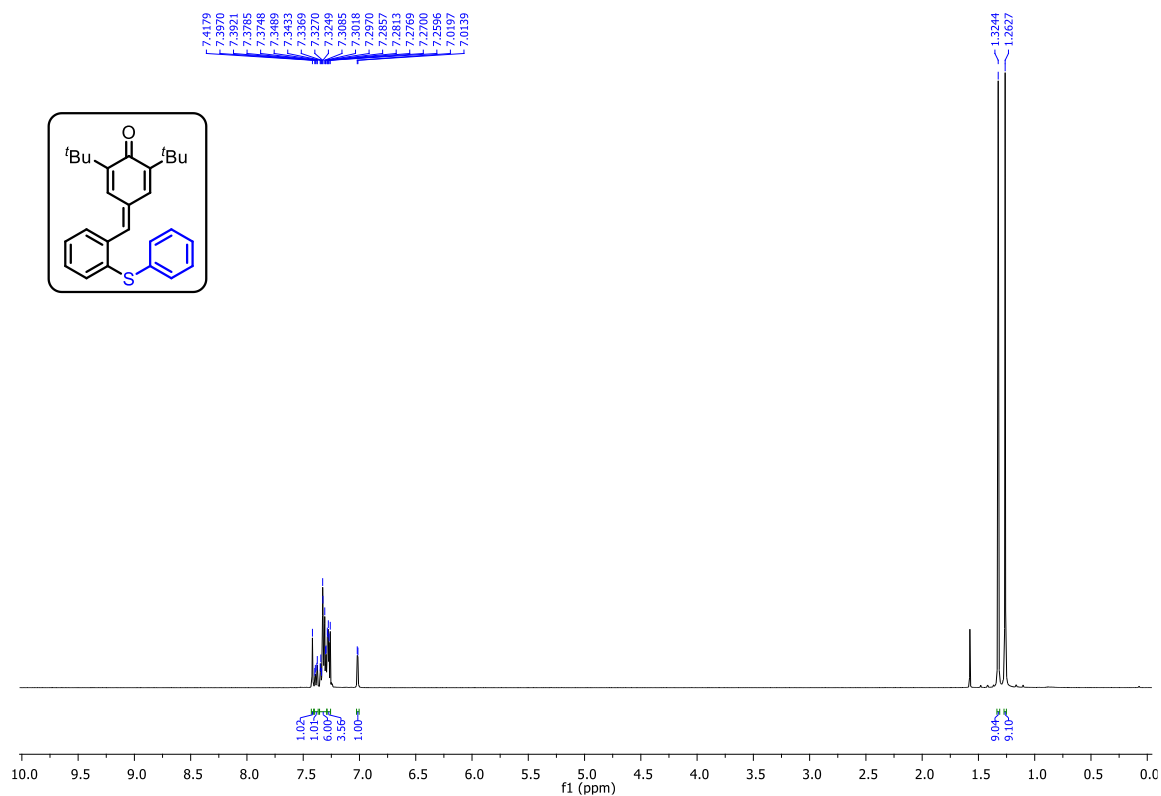
^1H NMR (400 MHz, CDCl_3) spectrum of **52p**



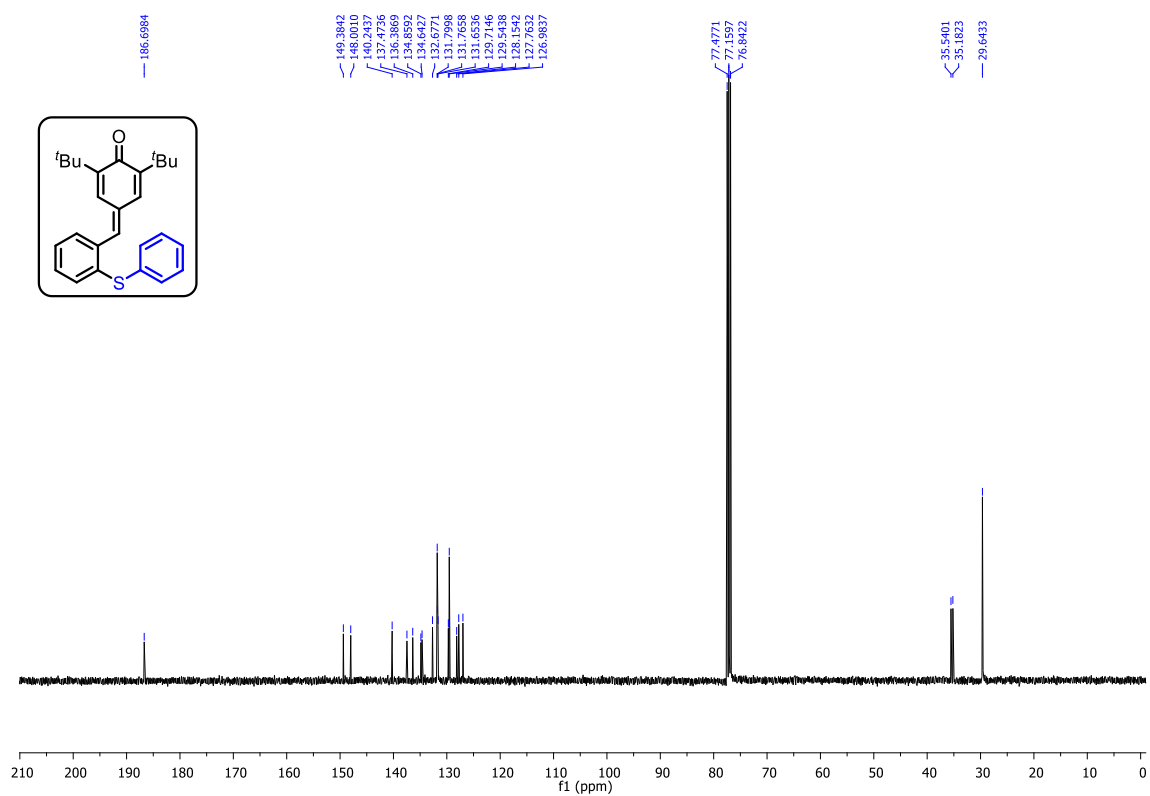
^{13}C NMR (100 MHz, CDCl_3) spectrum of **52p**



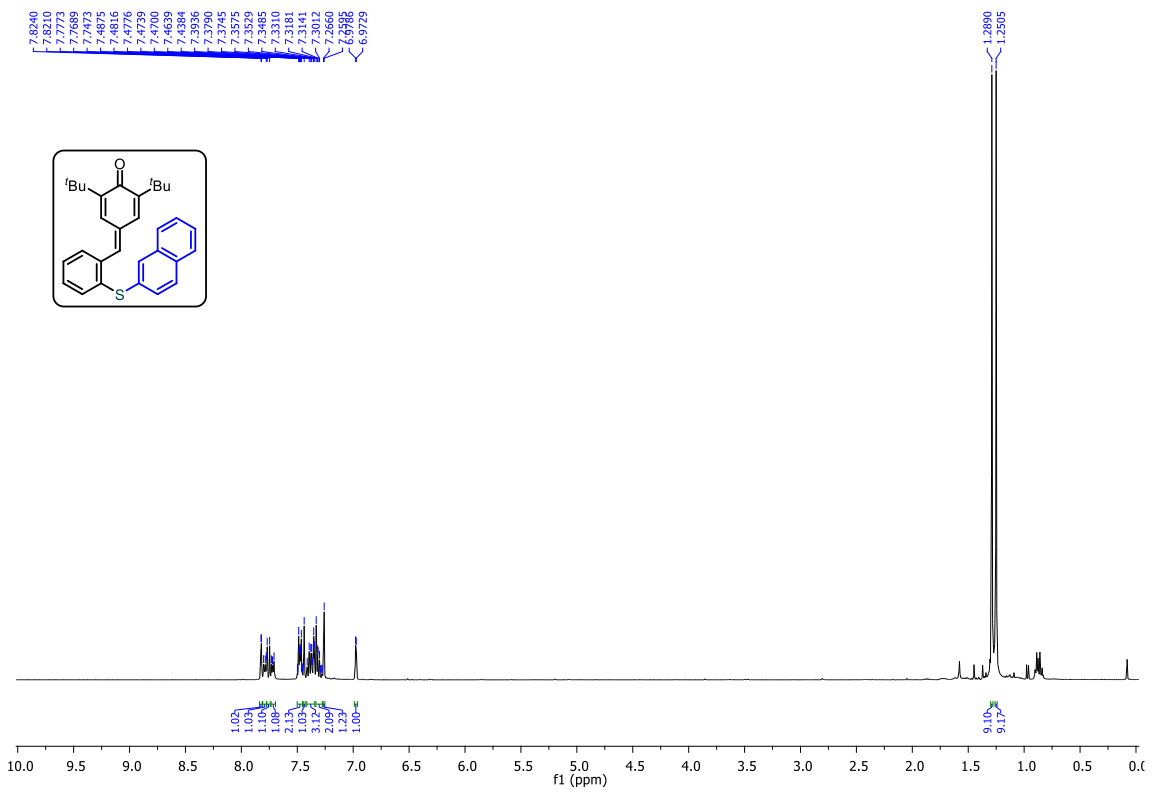
¹H NMR (400 MHz, CDCl₃) spectrum of **53a**



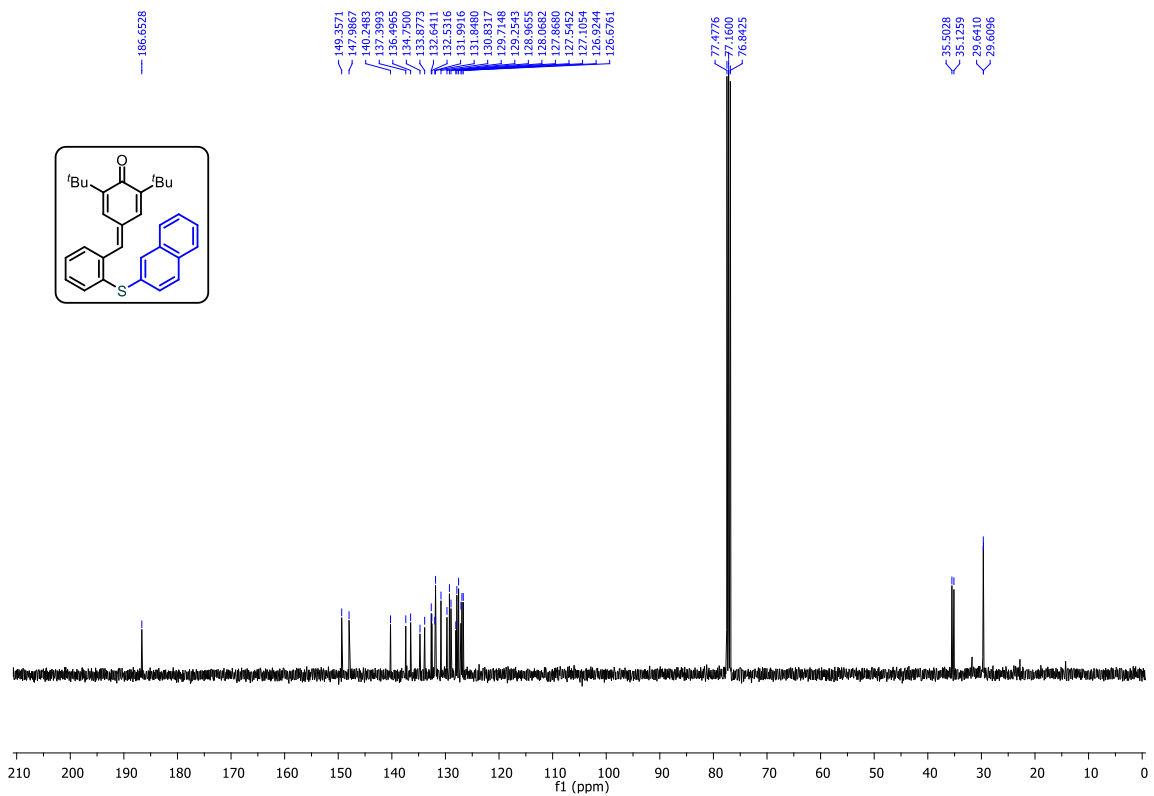
¹³C NMR (100 MHz, CDCl₃) spectrum of **53a**



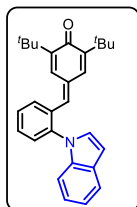
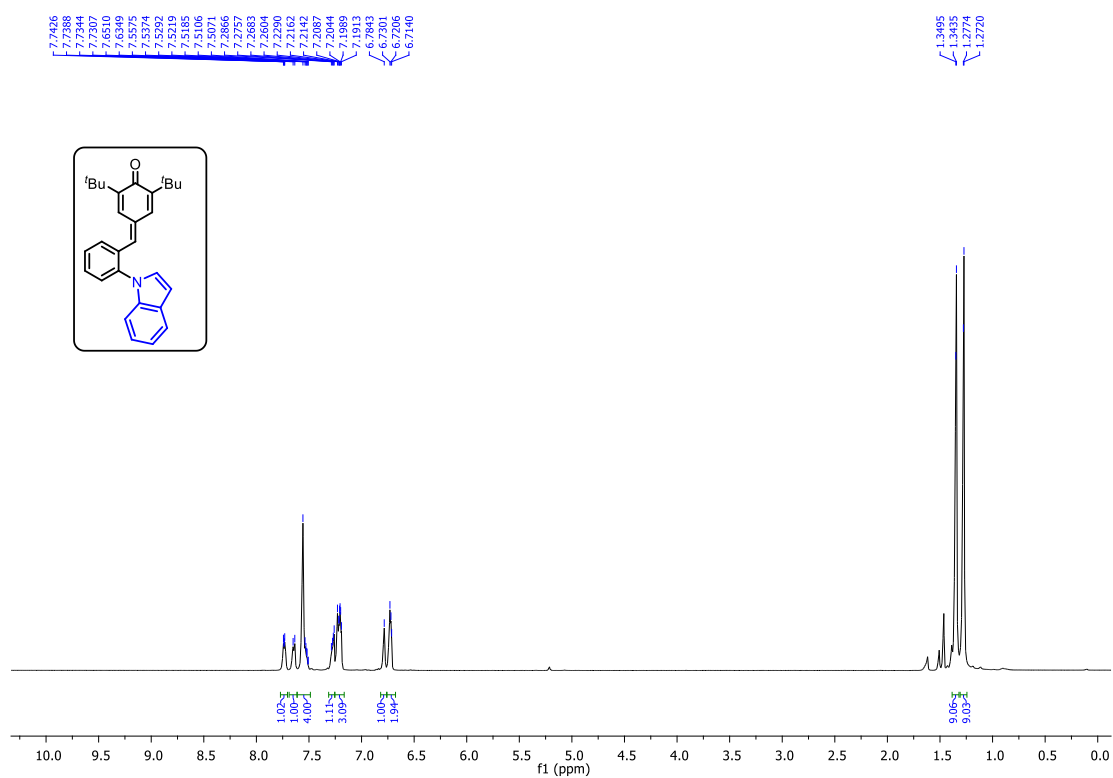
¹H NMR (400 MHz, CDCl₃) spectrum of **53j**



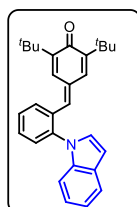
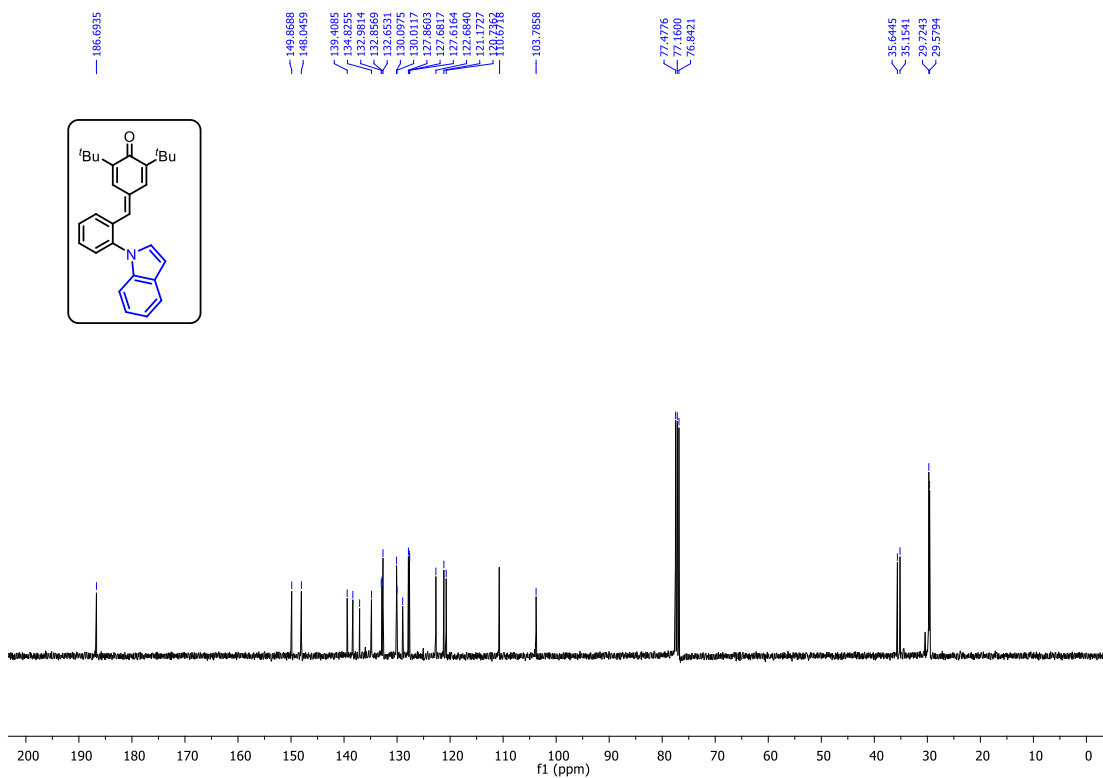
¹³C NMR (100 MHz, CDCl₃) spectrum of **53j**



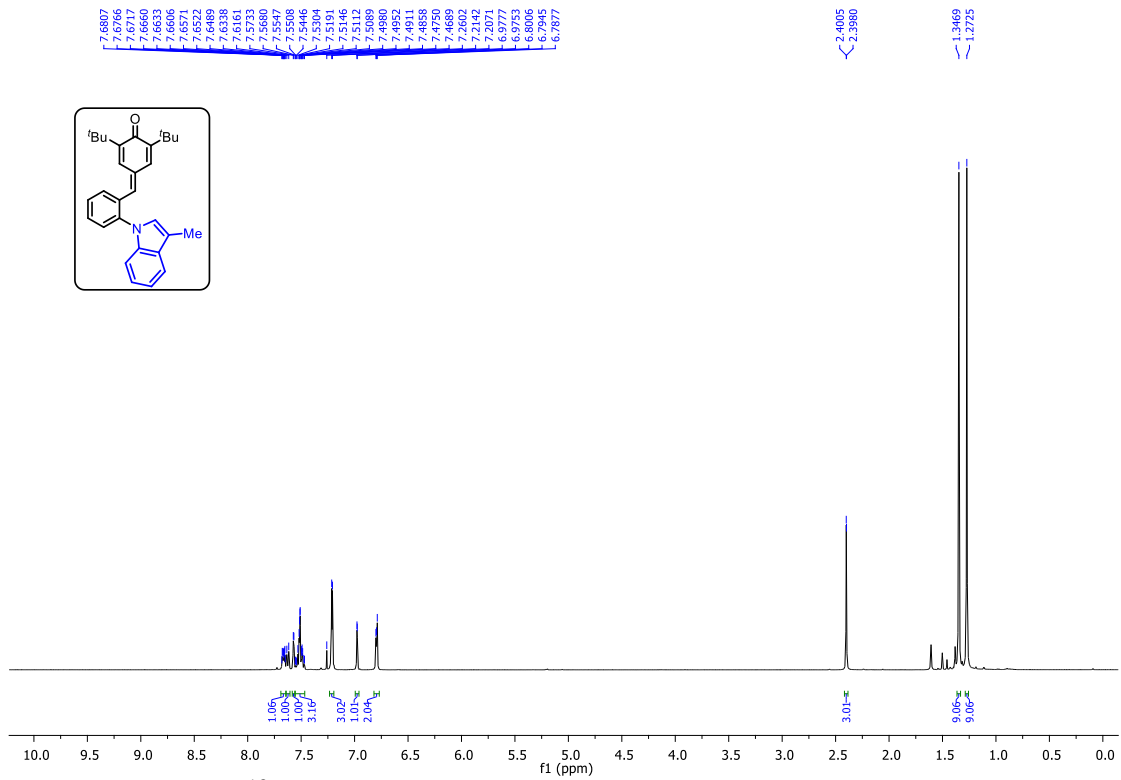
¹H NMR (400 MHz, CDCl₃) spectrum of **56a**



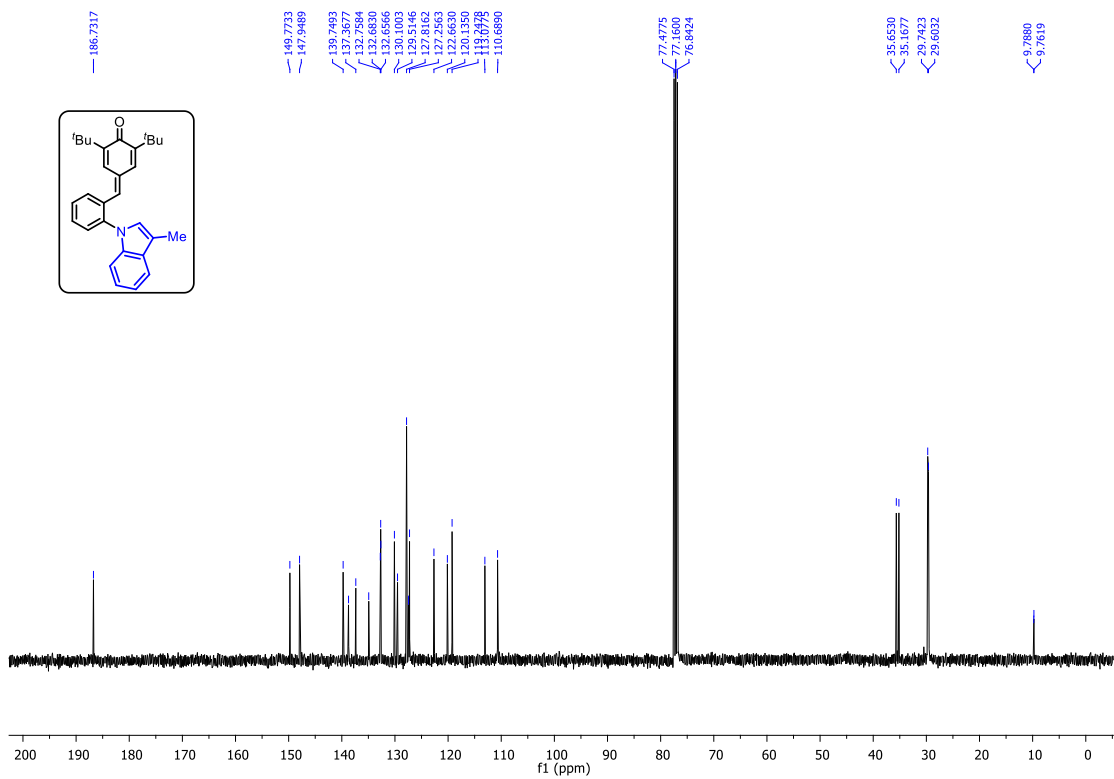
¹³C NMR (100 MHz, CDCl₃) spectrum of **56a**



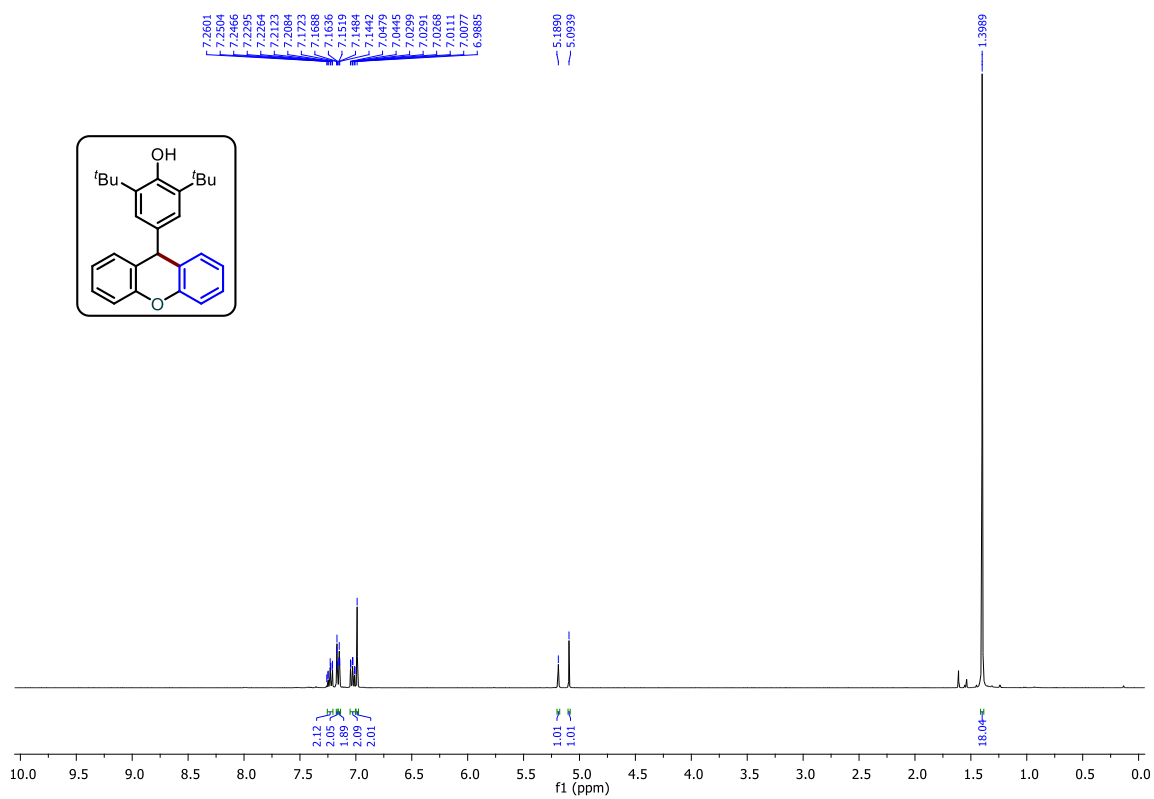
¹H NMR (400 MHz, CDCl₃) spectrum of **56b**



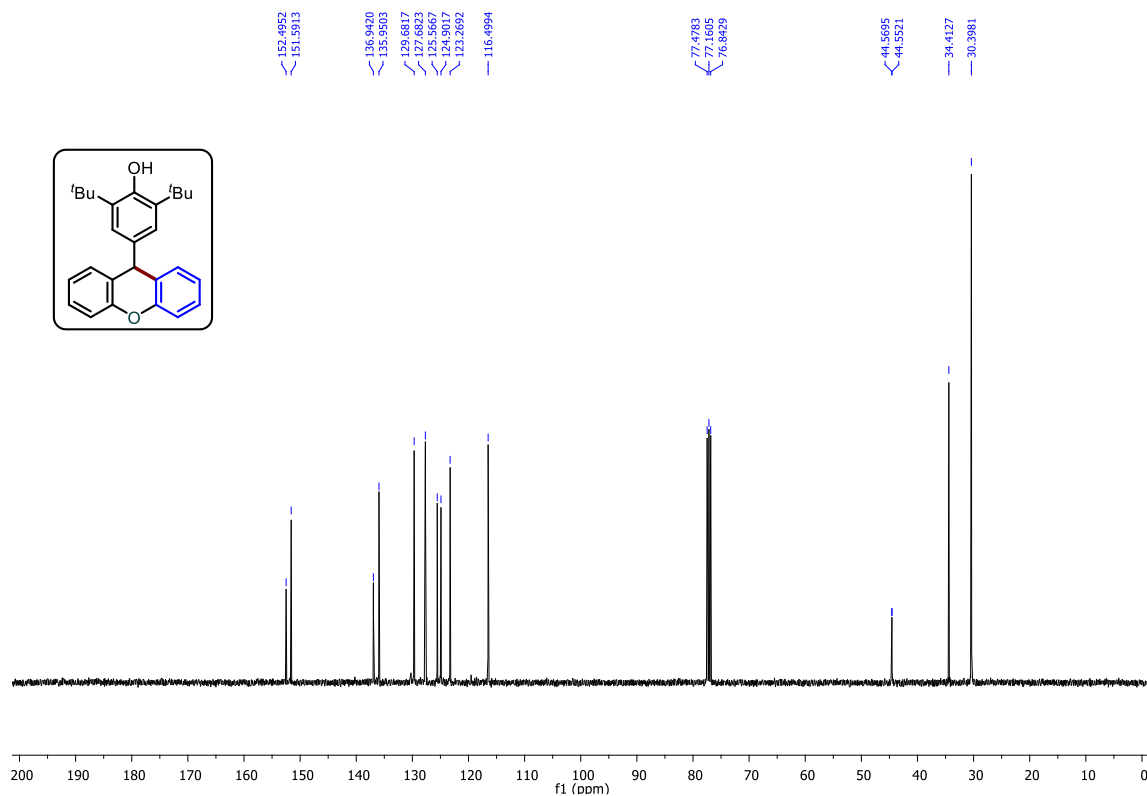
¹³C NMR (100 MHz, CDCl₃) spectrum of **56b**



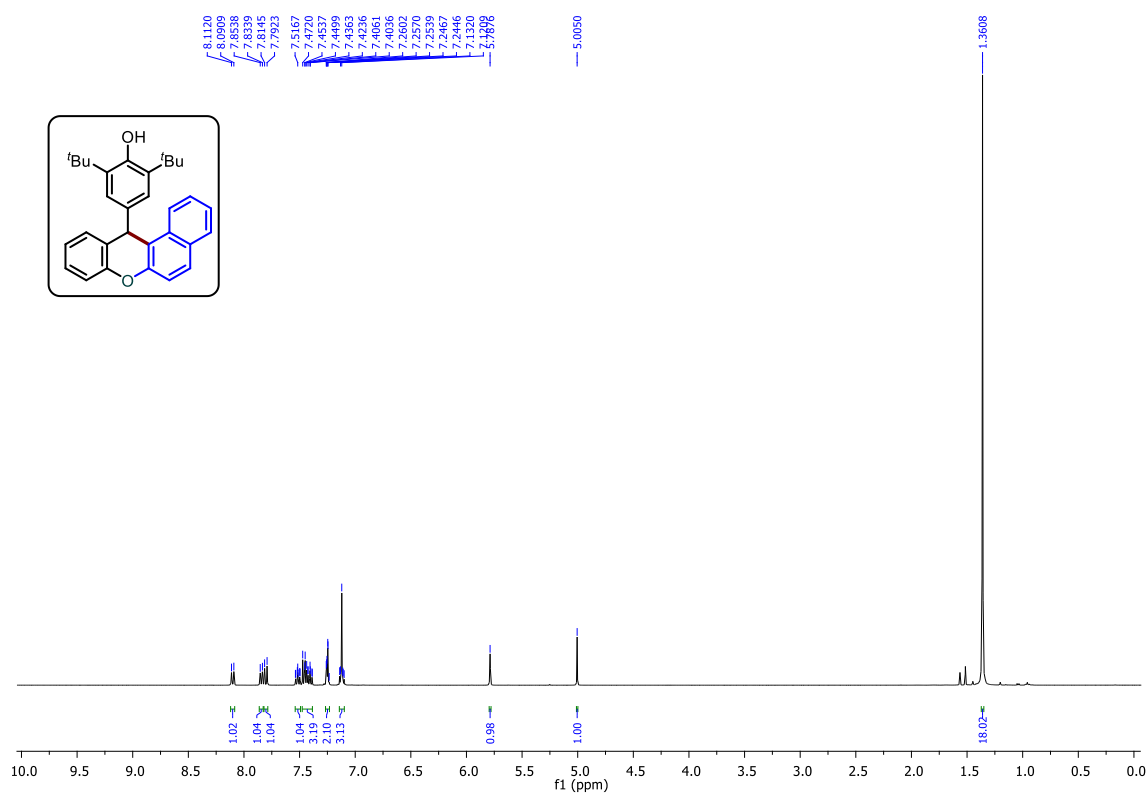
¹H NMR (400 MHz, CDCl₃) spectrum of **53a**



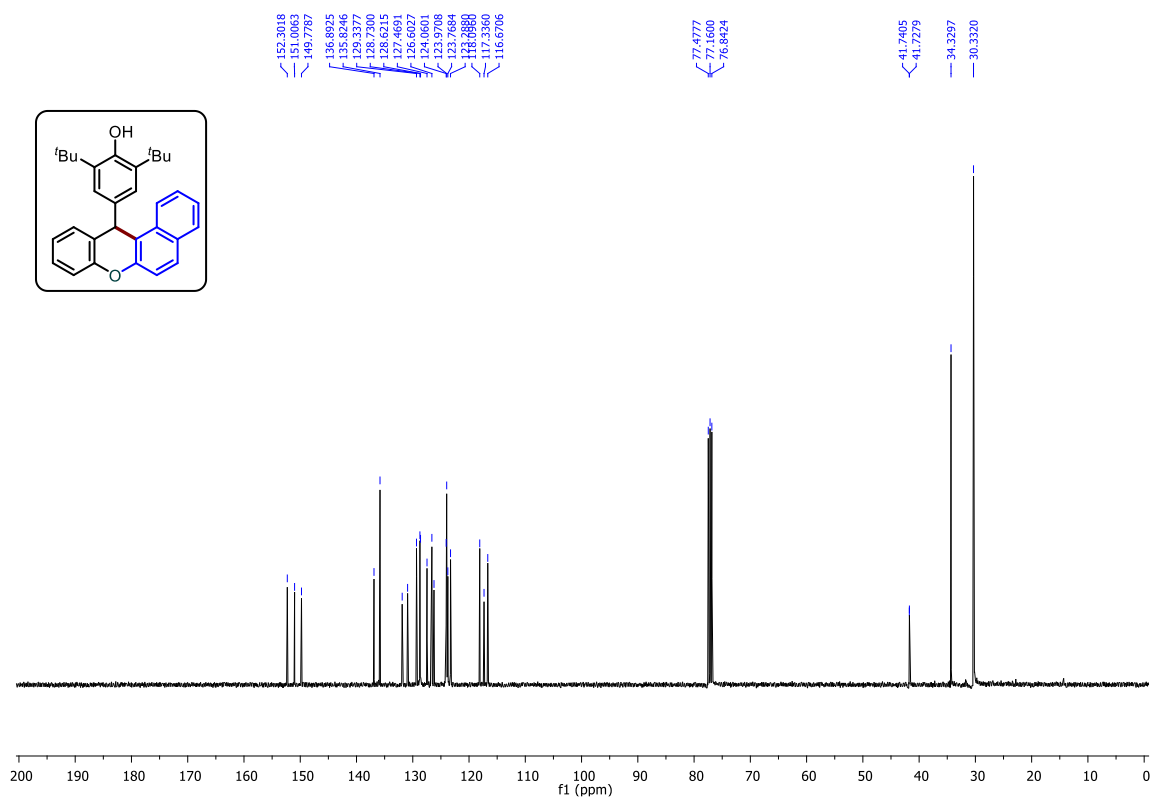
¹³C {¹H} NMR (100 MHz, CDCl₃) spectrum of **53a**



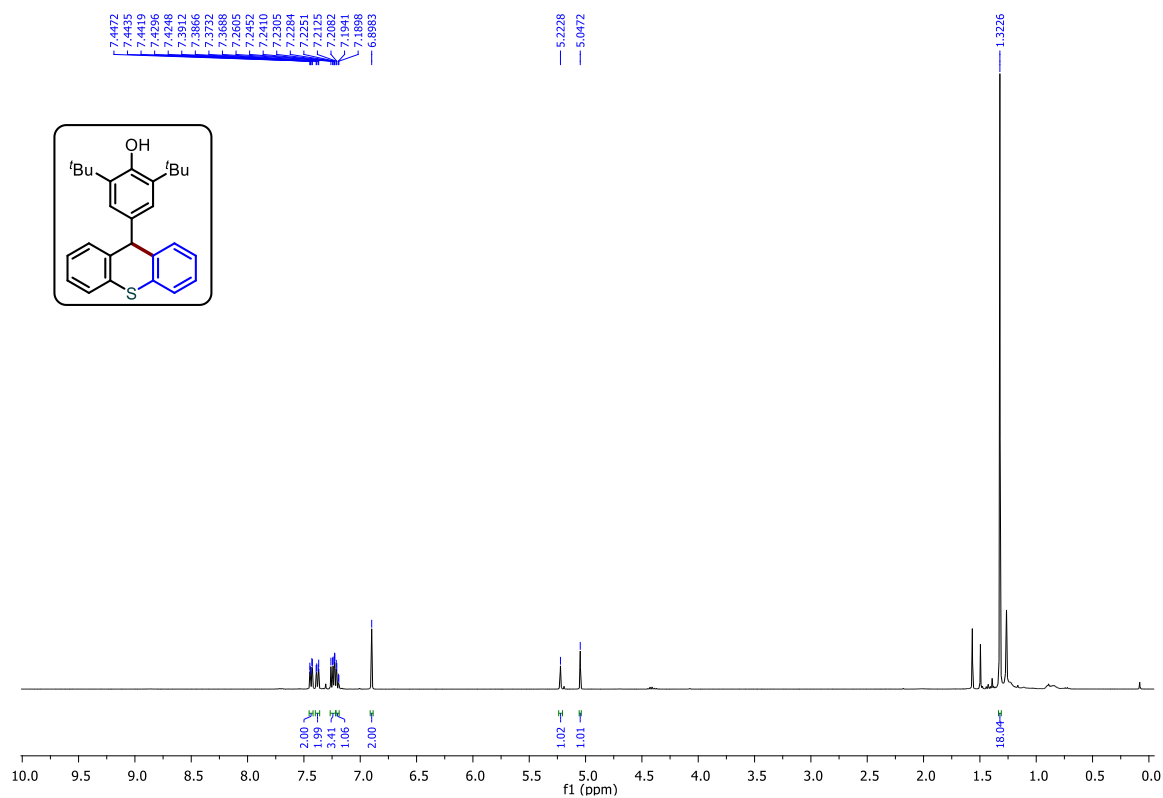
¹H NMR (400 MHz, CDCl₃) spectrum of **53p**



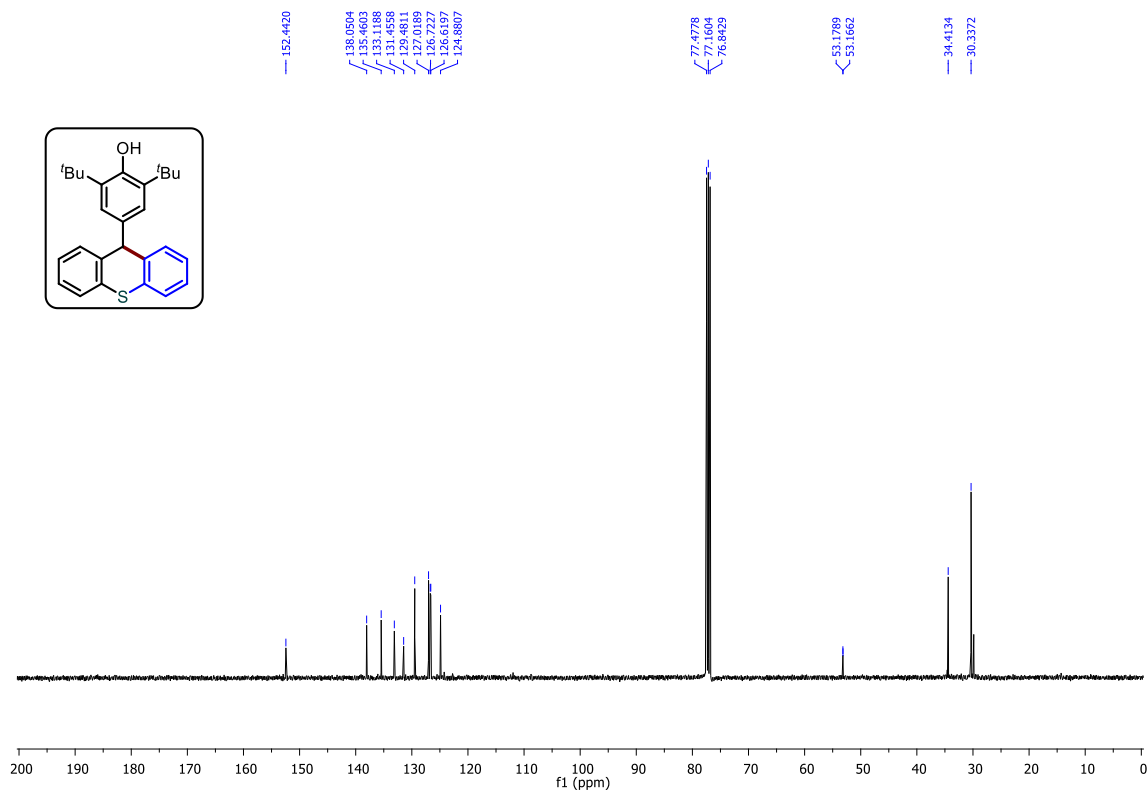
¹³C {¹H} NMR (100 MHz, CDCl₃) spectrum of **53p**



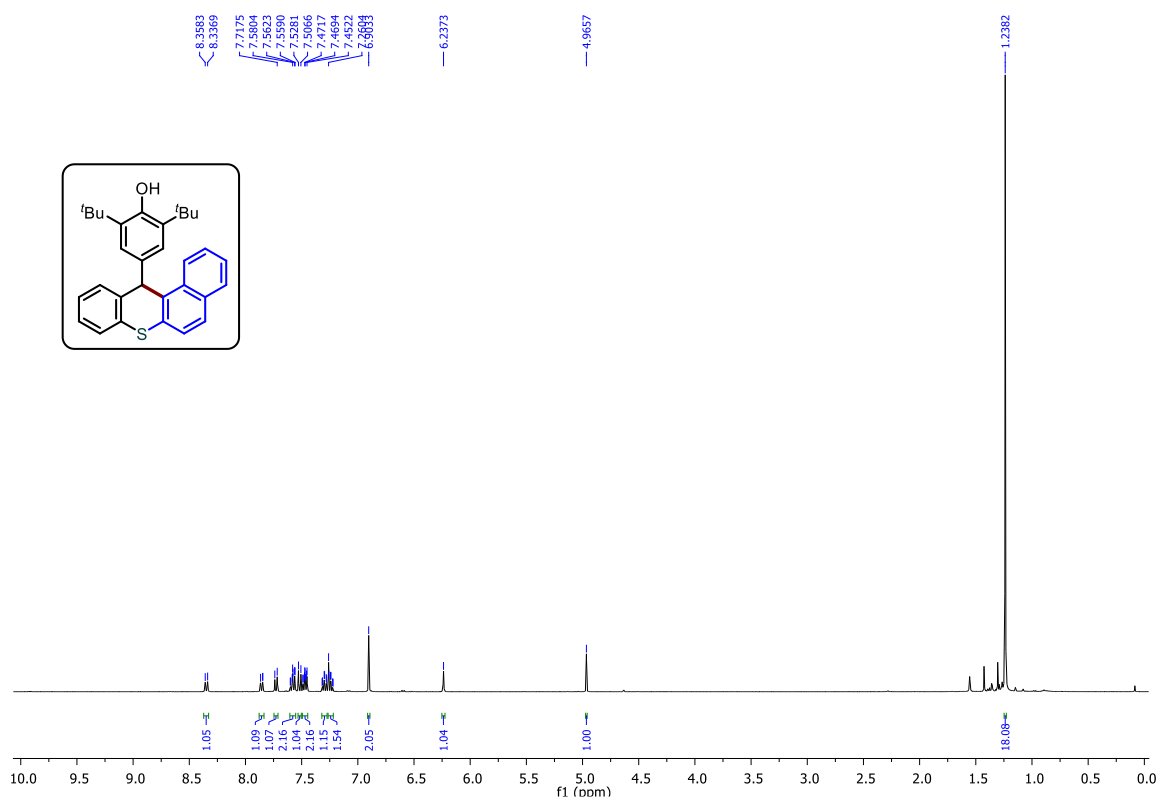
^1H NMR (400 MHz, CDCl_3) spectrum of **55a**



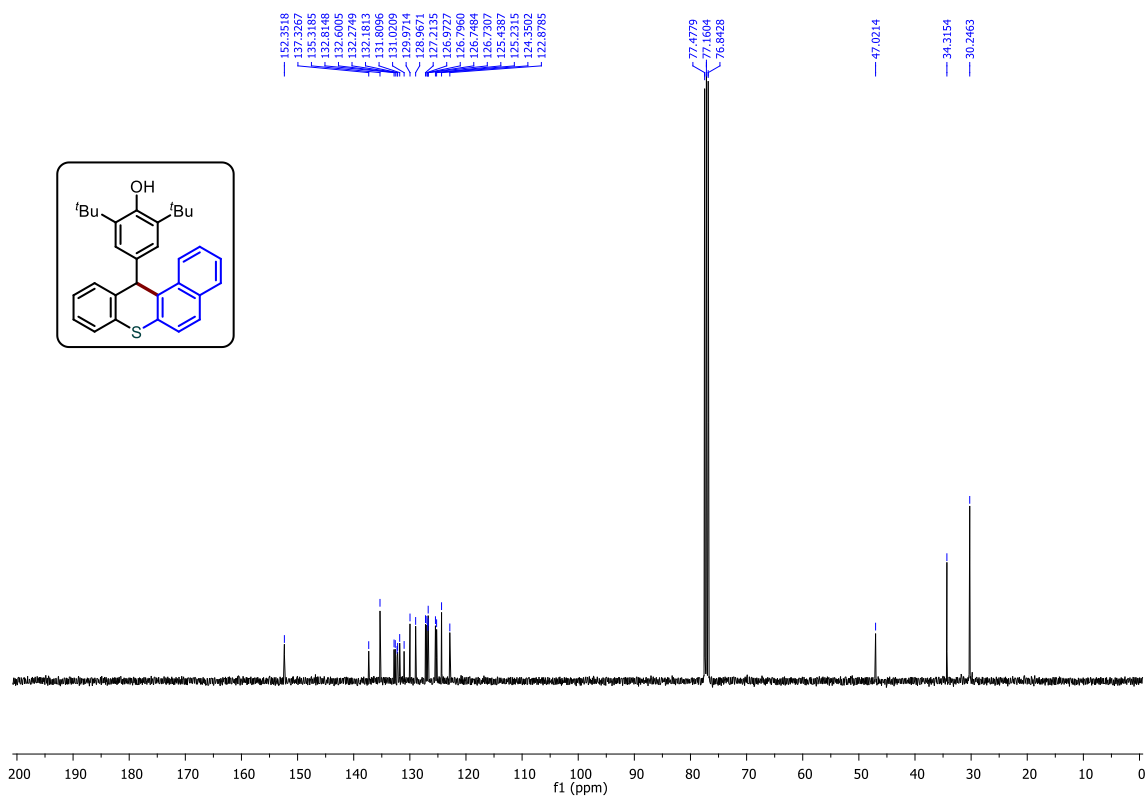
^{13}C { ^1H } NMR (100 MHz, CDCl_3) spectrum of **55a**



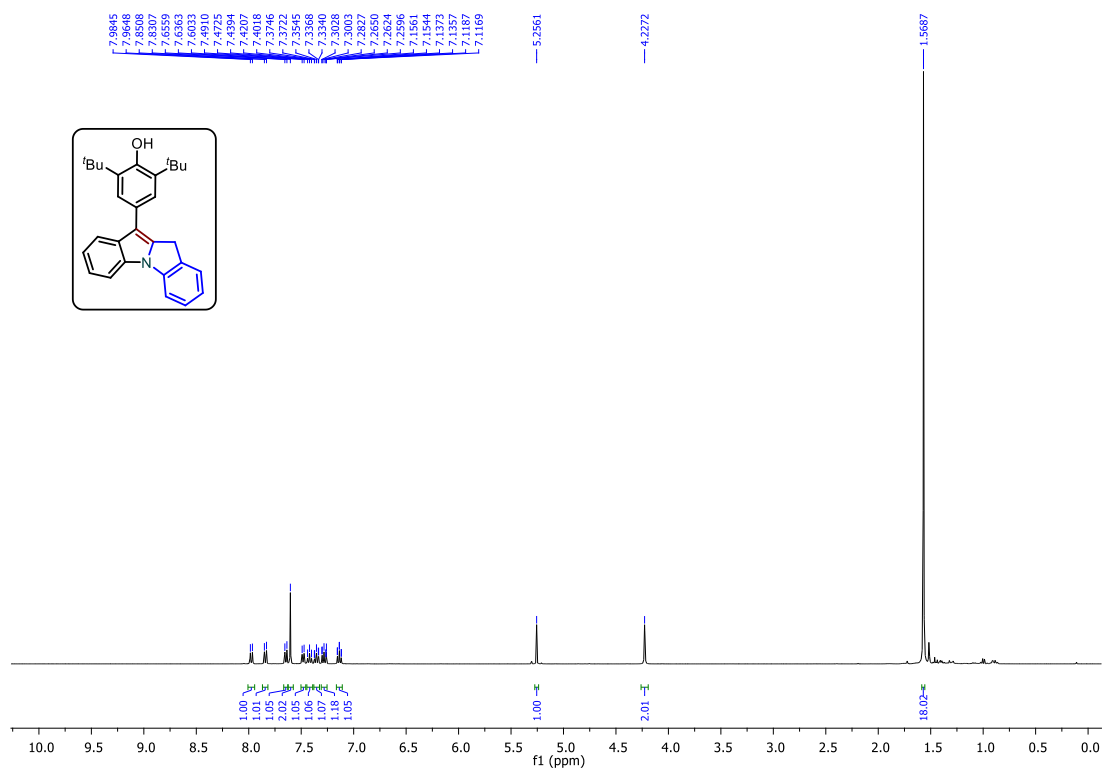
^1H NMR (400 MHz, CDCl_3) spectrum of **55j**



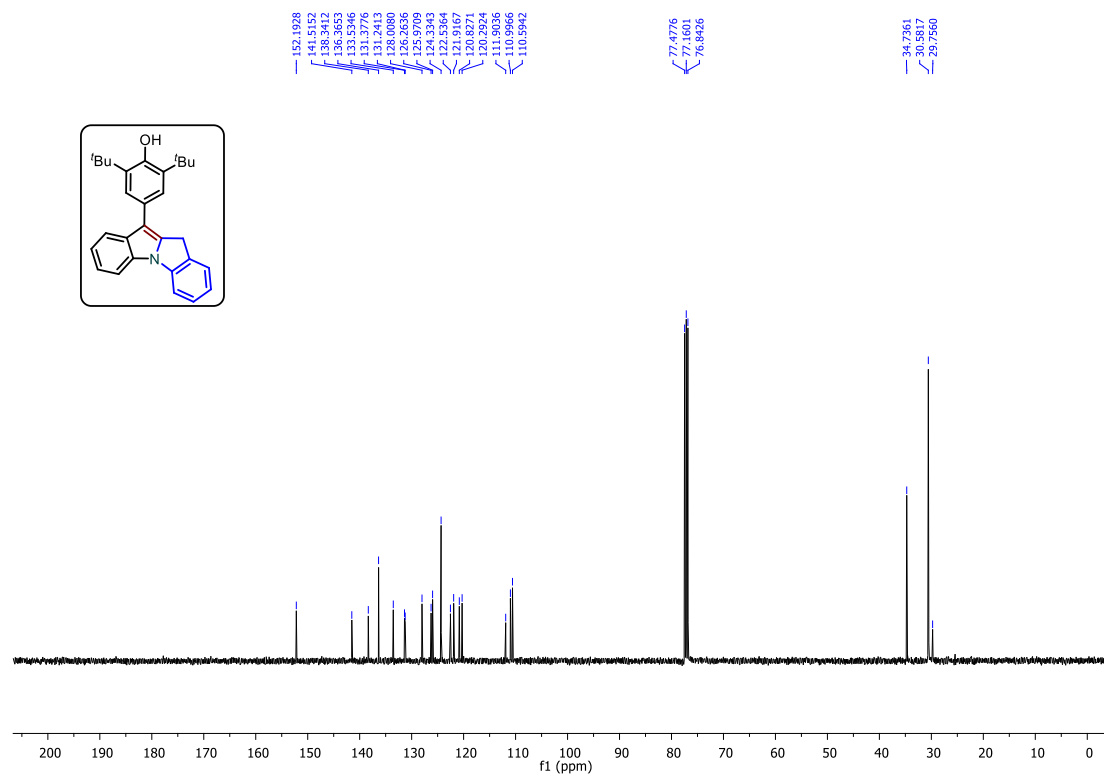
^{13}C { ^1H } NMR (100 MHz, CDCl_3) spectrum of **55j**



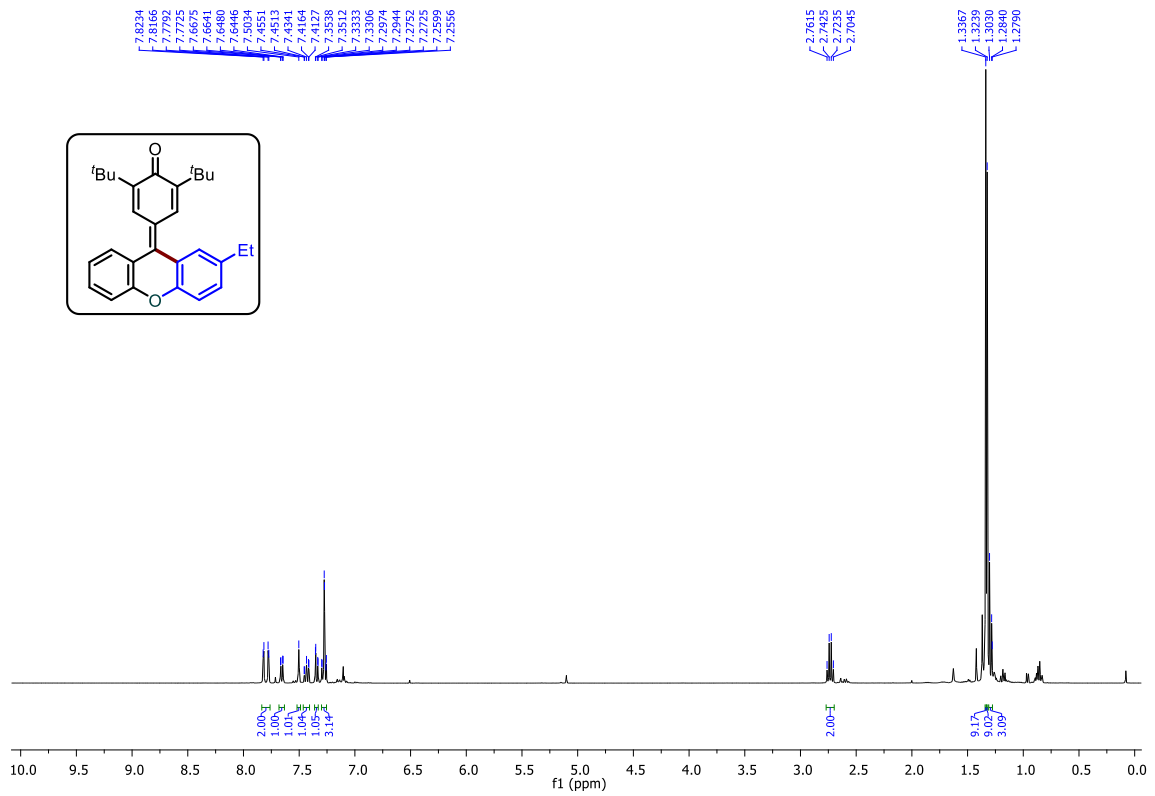
^1H NMR (400 MHz, CDCl_3) spectrum of **57a**



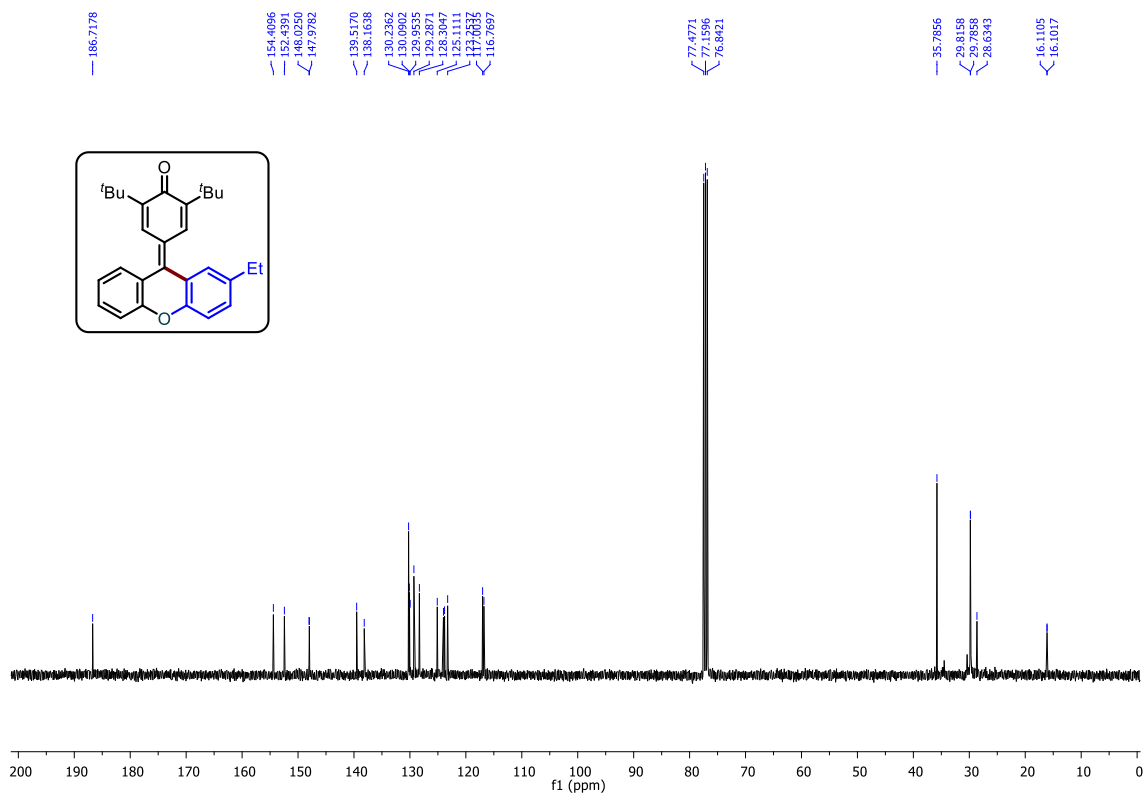
^{13}C { ^1H } NMR (100 MHz, CDCl_3) spectrum of **57a**



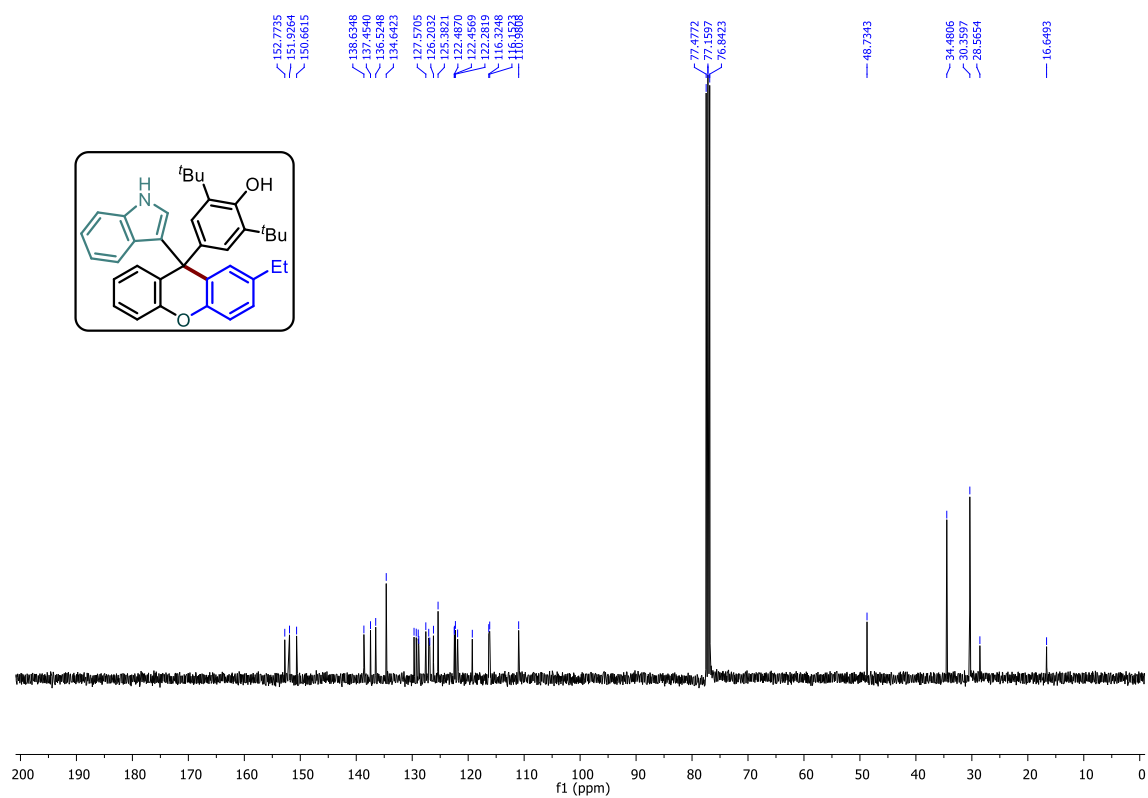
^1H NMR (400 MHz, CDCl_3) spectrum of **58**



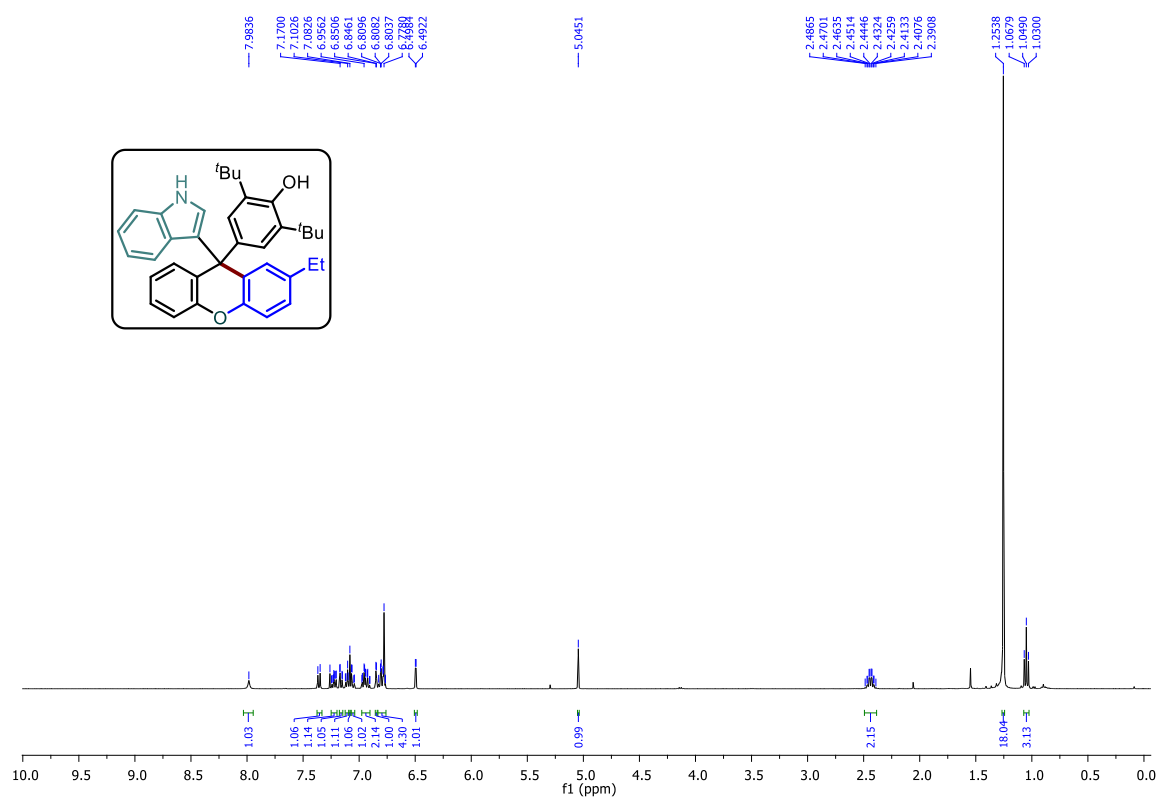
^{13}C $\{^1\text{H}\}$ NMR (100 MHz, CDCl_3) spectrum of **58**



¹H NMR (400 MHz, CDCl₃) spectrum of **59**



¹³C {¹H} NMR (100 MHz, CDCl₃) spectrum of **59**



3.7 References

- 1) For recent reviews: (a) Maia, M.; Resende, D. I. S. P.; Durães, F.; Pinto, M. M. M.; Sousa, E. *Eur. J. Med. Chem.*, **2021**, *210*, 113085. (b) Giri, R.; Goodell, J. R.; Xing, C.; Benoit, A.; Kaur, H.; Hiasa, H.; Ferguson, D. M. *Bioorg. Med. Chem.*, **2010**, *18*, 1456.
- 2) (a) Song, Y.; Yang, Y.; Wu, L.; Dong, N.; Gao, S.; Ji, H.; Du, X.; Liu, B.; Chen, G.; Dembinski, R.; *Molecules.*, **2017**, *22*, 1. (b) Su, J. C.; Wang, S.; Cheng, W.; Huang, X. J.; Li, M. M.; Jiang, R. W.; Li, Y. L.; Wang, L.; Ye, W. C.; Wang, Y. *J. Org. Chem.*, **2018**, *83*, 8522. (c) Luo, X.; Qian, L.; Xiao, Y.; Tang, Y.; Zhao, Y.; Wang, X.; Gu, L.; Lei, Z.; Bao, J.; Wu, J.; He, T.; Hu, F.; Zheng, J.; Li, H.; Zhu, W.; Shao, L.; Dong, X.; Chen, D.; Qian, X.; Yang, Y. *Nat. Commun.*, **2019**, *10*, 1.
- 3) (a) Davis, S.; Weiss, M. J.; Wong, J. R.; Lampidis, T. J.; Chen, L. B.; *J. Biol. Chem.*, **1985**, *260*, 13844. (b) Sun, Z. Y.; Botros, E.; Su, A. D.; Kim, Y.; Wang, E.; Baturay, N. Z.; and Kwon, C. H.; *J. Med. Chem.*, **2000**, *43*, 4160. (c) Chatterjee, M.; Iqbal, J. C.; Kauer, J. P.; Mallamo, S.; Senadhi, S.; Mallya, D. B. C.; Siman, R. *Bioorg. Med. Chem. Lett.*, **1996**, *6*, 1619.
- 4) Yunnikova L.; Voronina, E. *Pharm. Chem. J.*, **1996**, *30*, 695.
- 5) Watanabe, M.; Date, M.; Tsukajaki S, M.; Furukawa, *Chem. Pharm. Bull.*, **1989**, *37*, 36.
- 6) a) Archer, S.; Zayed, A.; Rej, R.; Rugino, T. A. *J. Med. Chem.*, **1983**, *4*, 1240. (b) Showalter, H. D. H.; Angelo, M. M.; Berman, E. M.; Kanter, G. D.; Ortwine, D. F.; Ross-Kesten, S. G.; A Sercel, D.; Turner, W. R.; Werbel, L. M.; Worth, D. F.; Elslager, E. F.; Leopold W. R.; Shillis, J. L. *J. Med. Chem.*, **1988**, *31*, 1527. (c) Wentland, M. P.; Perni, R. B.; Powles, R. G.; Hlavac, A. G.; Mattes, K. C.; Corbett, T. H.; Couhglin, S. A.; Rake, J. B. *Bioorg. Med. Chem. Lett.*, **1994**, *4*, 609.
- 7) Zukić, S.; Oljatic, S.; Nikolic, K.; Veljović, E.; Špirtović-Halilović, S.; Osmanović. A.; Završnik, D.; *J. Biomol. Struct. Dyn.*, **2021**, *39*, 4026.
- 8) Kim, J.; Song, J. H. *Eur. J. Pharmacol.*, **2016**, *779*, 31.
- 9) (a) Hafez, H. N.; Hegab, M. I.; Ahmed-Farag, I. S.; El-Gazzar, A. B. A. *Bioorganic Med. Chem. Lett.*, **2008**, *18*, 4538. (b) Schwarz, V.; Reis, O.; Glaser, T.; Thome, J.; Hiemke, C. Haessler, F. *Pharmacopsychiatry*, **2014**, *47*, 29. (c) Karimi, G.; Vahabzadeh, M.; *Encycl. Toxicol. Third Ed.*, **2014**, *4*, 553.
- 10) (a) Banerjee, A.; Mukherjee, A. K. *Biotech. Histochem.*, 1981, **56**, 83. (b) Dyeing, T.; Unit, T. F.; Kamel M.; Wizinger, R. **1964**, *20*, 491. (c) Katritzky, A. R.; Czerney, P.; Levell, J. R.; *J. Org. Chem.*, **1997**, *62*, 8198.

- 11) Wang, J. Q.; Harvey, R. G. *Tetrahedron.*, **2002**, *58*, 5927.
- 12) Su, W.; Yang, D.; Jin C.; Zhang, B. *Tetrahedron Lett.*, **2008**, *49*, 3391.
- 13) Li, H.; Yang, J.; Liu, Y.; Y Li., *J. Org. Chem.*, **2009**, *74*, 6797.
- 14) Das, S. K.; Singh R.; Panda, G. *European J. Org. Chem.*, **2009**, 4757.
- 15) Singh, R.; Panda, G. *Org. Biomol. Chem.*, **2010**, *8*, 1097.
- 16) Xu, X.; Xu, X.; Li, H.; Xie, X.; Li, Y. *Org. Lett.*, **2010**, *12*, 100.
- 17) Bö, E.; Hillringhaus, T.; Nitsch J.; Klussmann, M. *Org. Biomol. Chem.*, **2011**, *9*, 1744.
- 18) Mao, S.; Hua, Z.; Wu, X.; Yang, Y.; Han J.; Wang, L. *ChemistrySelect.*, **2016**, *1*, 403.
- 19) Zhu, D.; Li, M.; Wu, Z.; Du, Y.; Luo, B.; Huang, P.; Wen, S. *Eur. J. Org. Chem.*, **2019**, *2019*, 4566.
- 20) Verma, S. K.; Prajapati, A.; Saini M. K.; Basak, A. K. *Adv. Synth. Catal.*, **2021**, *363*, 532.
- 21) Yoshida, H.; Watanabe, M.; Fukushima, H.; Ohshita, J.; Kunai, A. *Org. Lett.*, **2004**, *6*, 4049.
- 22) Mei, G. J.; Xu, S. L.; Zheng, W. Q.; Bian, C. Y.; Shi, F. *J. Org. Chem.* **2018**, *83*, 1414.
- 23) Shi, Z.; Chen, S.; Xiao, Q.; Yin, D. *J. Org. Chem.* **2021**, *86*, 3334.
- 24) For a recent review from our research group on *p*-QMs chemistry: Singh, G.; Pandey, R.; Pankhade, Y. A.; Fatma, S.; Anand, R. V.; *Chem. Rec.*, **2021**, *21*, 4150.
- 25) For recent reviews on *para*-quinone methides chemistry: (a) Li, W.; Xu, X.; Zhang, P.; Li, P. *Chem. Asian J.*, **2018**, *17*, 2350. (b) Lima, C. G. S.; Pauli, F. P.; Costa, D. C. S.; de Souza, A. S.; Forezi, L. S. M.; Ferriera, V. F.; de Carvalho da Silva. *Eur. J. Org. Chem.*, **2020**, *18*, 2650. (c) Wang, J. -Y.; Hao, W. -J.; Tu, S. -J.; *Org. Chem. Front.*, **2020**, *7*, 1743.
- 26) (a) Pankhade, Y. A.; Pandey, R.; Fatma, S.; Ahmad F.; Anand, R. V. *J. Org. Chem.*, **2022**, *87*, 3363. (b) Singh, G.; Kumar, S.; Chowdhury, A.; R. V. Anand, *J. Org. Chem.*, **2019**, *84*, 15978. (c) Singh, G.; Goswami, P.; Sharma, S.; Anand, R. V. *J. Org. Chem.*, **2018**, *83*, 10546.
- 27) (a) Chu, W. -D.; Zhang, L. -F.; Bao, X.; Zhao, X. -H.; Zeng, C.; Du, J. -Y.; Zhang, G. -B.; Wang, F. -X.; Ma, X. -Y.; Fan, C. -A. *Angew. Chem. Int. Ed.*, **2013**, *52*, 9229. (b) V. Reddy and R. V. Anand, *Org. Lett.* **2015**, *17*, 3390.
- 28) (a) Cox, E. D.; Cook, J. M.; *Chem. Rev.*, **1995**, *95*, 1797. (b) Bonjoch, J.; Solé, D. *Chem. Rev.*, **2000**, *100*, 3455. (c) O'Connor, S. E.; Maresh, J. J. *Nat. Prod. Rep.*, **2006**, *23*, 532. (d) Chen, G.-S.; Lin X.-T.; Liu, Y.-L. *Synlett.*, **2020**, *31*, 1033. (e) Higuchia, K.; Kawasaki, T. *Nat. Prod., Rep.*, **2007**, *24*, 843.

29) (a) Lin, T.-S.; U. S. PatentNo. US20030228487A1, Dec 11, **2003**. (b) Faust, R.; Garratt, P. J.; Jones, R.; Yeh, L.-K.; Tsotinis, A.; Panoussopoulou, M.; Calogeropoulou, T.; The, M.-T.; Sugden, D. *J. Med. Chem.*, 2000, **43**, 1050-1061. (c) Scopton, A.; Kelly, T. R.; *J. Org. Chem.*, 2005, **70**, 10004. (d) Ikegashira, K.; Oka, T.; Hirashima, S.; Noji, S.; Yamanaka, H.; Hara, Y.; Adachi, T.; Tsuruha, J. I.; Doi, S.; Hase, Y.; Noguchi, T.; Ando, I.; Ogura, N.; Ikeda, S.; Hashimoto, H. *J. Med. Chem.* 2006., **49**, 6950.

4. SmI₂-mediated reductive dimerization of *para*-quinone methides

4.1 Introduction

Electron transfer (ET) reactions play a significant role in organic chemistry. In fact, it has been used by synthetic chemists to explore new techniques for molecules building. Reductive ET to organic molecules is a particularly effective technique for activating substrates by generating radicals, radical anions, anions, and dianions that can be used in bond-cleaving and bond-forming reactions.¹ In pioneering the area of electron transfer reactions, SmI₂, introduced by Kagan & co-workers in 1977, has gained substantial attention as a single electron transfer agent among organic chemists.² It can tune its reactivity among various functional groups using appropriate ligands and additives. Also, the transformations that employed the use of SmI₂ encompass user-friendly and easily operative reaction conditions.³ This phenomenon makes SmI₂ a versatile electron transfer agent amid other reductants. SmI₂ has the unique ability to carry out synthetically relevant reductive processes of functional groups and reductive coupling to make C-C bonds (Figure 1).⁴ In the past 35 years, SmI₂-mediated couplings to form carbon-carbon bonds have found a wide range of applications in developing various molecular scaffolds. These reactions have been employed in intricate cascade sequences to establish molecular architectures and have widened access to difficult carbon-carbon bond disconnections that are not possible to achieve with other reagents.⁵ A few of them are debated below.

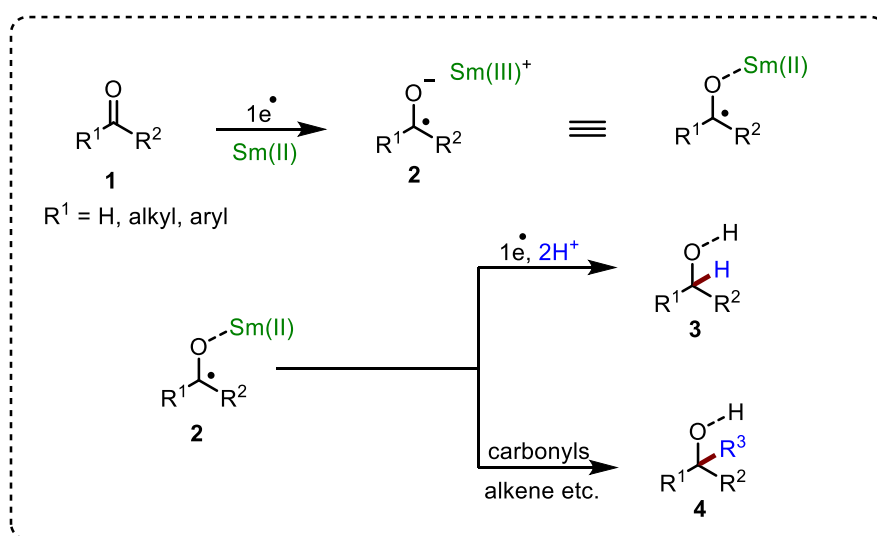
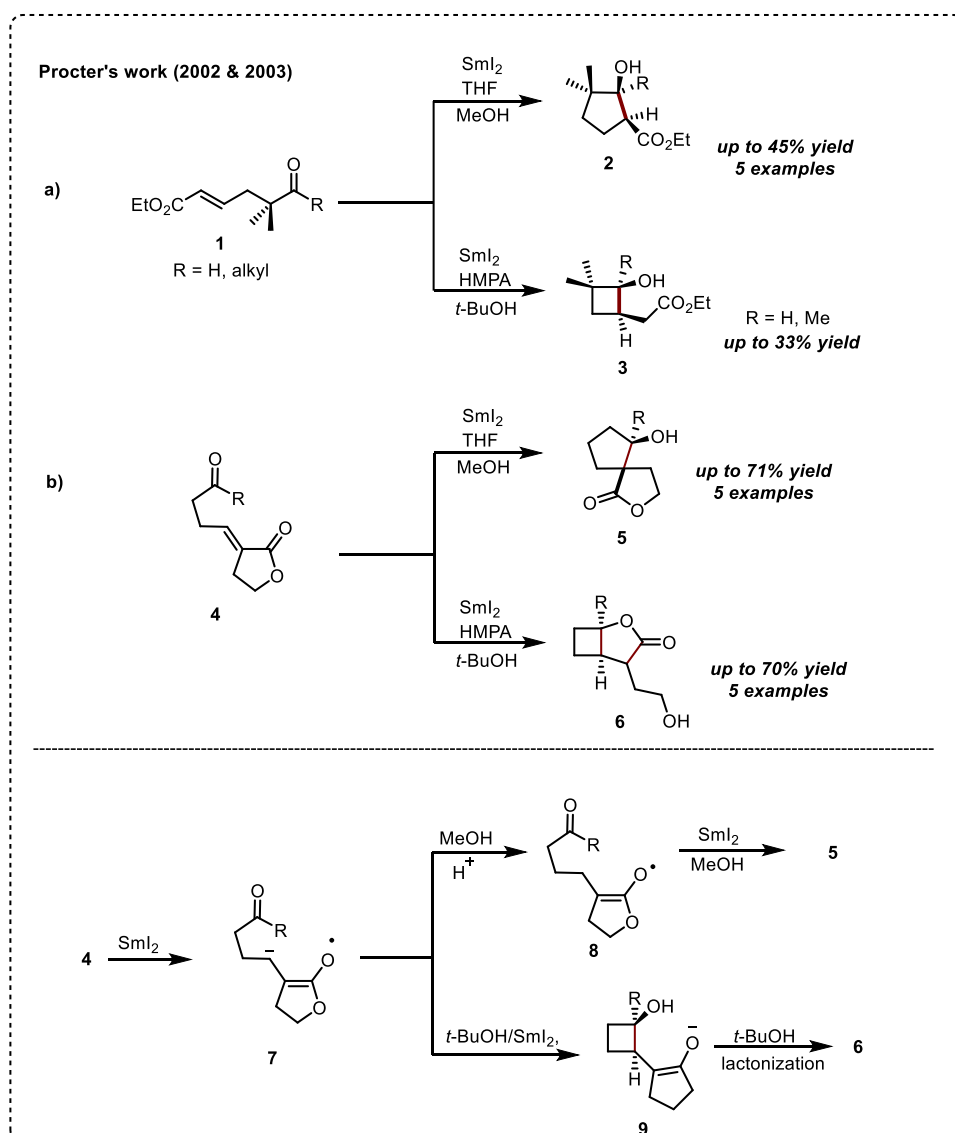


Figure 1. A major mode of activation by SmI₂

4.2 Literature reports on cross-coupling reactions mediated by SmI₂

4.2.1 Cross-coupling of ketyl radical with unactivated olefins

In 2002, Procter and co-workers established a SmI₂-mediated intramolecular carbonyl/olefin cyclizations using protic additives such as MeOH and *t*-BuOH. The use of MeOH as an additive for this transformation resulted in stereoselective cyclization to give *cis* cyclopentanols **2**, while *t*-BuOH as an additive promoted cyclobutanol products **3** via 4-*exo-trig* cyclization. This work was further elaborated using the more reactive α, β -unsaturated cyclic esters **4**. According to the proposed reaction mechanism, initially, SmI₂-mediated one-electron reduction of the lactone occurs to form radical-anion intermediate **7**, which endures rapid protonation in MeOH to give the enolate. The resulting enolate immediately undergoes

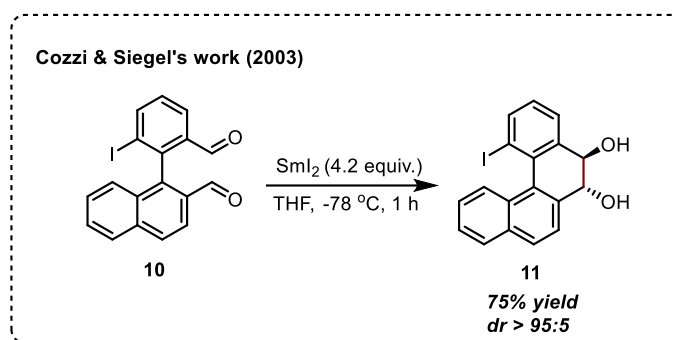


Scheme 1. Intramolecular carbonyl/olefin cyclizations using SmI₂

aldol cyclization in methanol to furnish the desired cyclopentanol product **5**. However, in the case of *t*-BuOH as an additive, protonation was sluggish, due to which the 4-*exo-trig* cyclization predominated to give the cyclobutanol **9**, which subsequently underwent protonation and lactonization to provide the final product **6** (Scheme 1).⁶

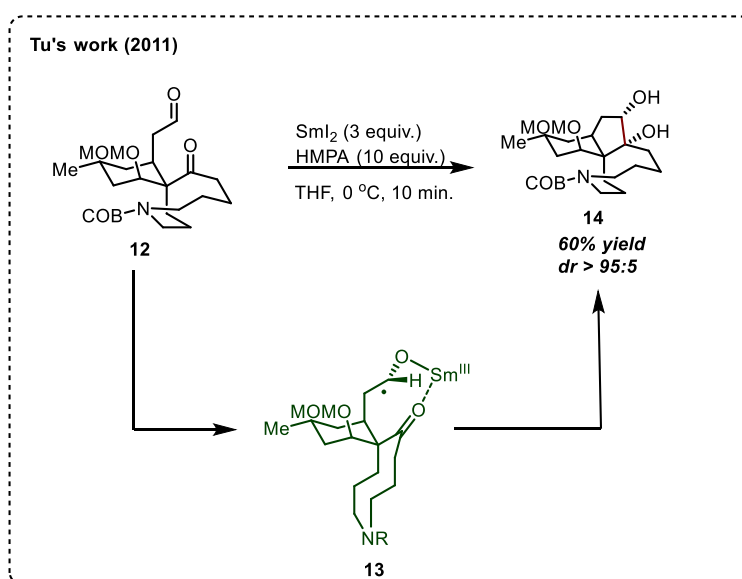
4.2.2 Literature reports on pinacol-pinacolone type couplings

In 2003, Cozzi and Siegel published their findings on the SmI₂-mediated intramolecular aldehyde-aldehyde coupling in the presence of an aryl iodide as a part of their endeavour on the synthesis of conformationally constrained polycyclic structures. The corresponding product **11** was obtained in 75% yield with retention of iodide, which clearly demonstrates the gentle and selective nature of this reagent (Scheme 2).⁷



Scheme 2. Aldehyde-aldehyde cross-coupling

In a similar way, aldehyde-ketone coupling has many applications in the field of natural product synthesis and has become well-established over the past ten years. Tu & co-workers in

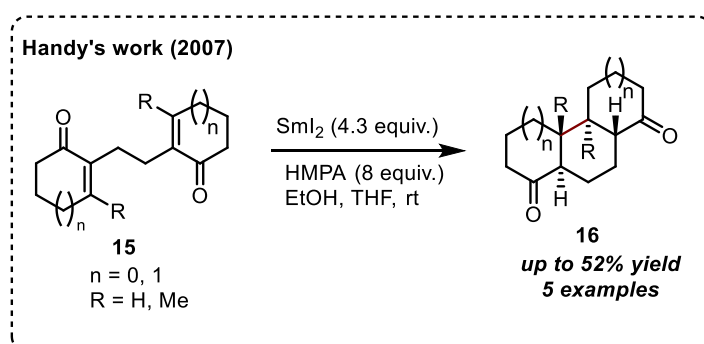


Scheme 3. SmI₂-mediated aldehyde-ketone cross-coupling

2011, established a SmI₂-mediated intramolecular Pinacol coupling between aldehyde and ketone to form a 5-membered ring with *cis*-diastereoselectivity of the resulting 1,2-diol **14** (Scheme 3). Three structurally distinct and related lycopodium alkaloids, (+)-alopecuridine, (+)-sieboldine A, and (+)-lycojapodine A, have been synthesized in enantiomeric forms using this protocol. This chelation-controlled Pinacol cyclization provides a moderate yield of the α -diol **14** with complete diastereo-control. It was hypothesized that the co-ordination of the samarium ketyl governs the selectivity of this reaction to the ketone group. Further, the structure of the diol **14** was confirmed by using single crystal X-ray crystallography (Scheme 3).⁸

4.2.3 Literature reports on reductive dimerization reactions

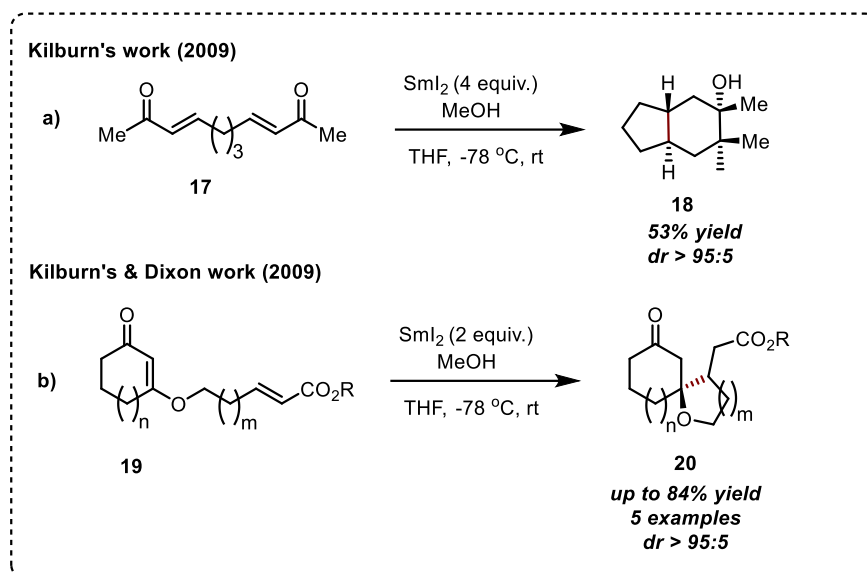
In order to functionalize carbonyl derivatives, reductive dimerization of α , β -unsaturated carbonyl compounds have become an appealing technique. In this context, the use of SmI₂ is advantageous over other methods in terms of mild, non-toxic, and convenient (compare Bu₃SnH/benzene) reaction conditions. In 2007, Handy and co-workers published a comprehensive study on the intramolecular reductive cyclization of cyclic enones (**15**) using the SmI₂/HMPA system with EtOH as a proton source. The other reaction conditions, such as



Scheme 4. Reductive dimerization using SmI₂

proton sources, temperature, and mode of addition mode were found to be less effective. The tricyclic products (**16**) were generated with high stereoselectivity despite the low yields, producing up to four neighbouring stereo-centers in a single transformation (Scheme 4).⁹ Later on, using the SmI₂-MeOH system, Kilburn reported an intramolecular dimerization of unsaturated enone (**17**) in 2009 (a, Scheme 5). After that, the same group extended this study to synthesize *spiro*-cyclic ethers (**20**) from enolates (**19**). The reaction proceeds through a selective reduction of the cyclic β -alkoxyketone, followed by 5/6-*exo-trig* cyclization, which

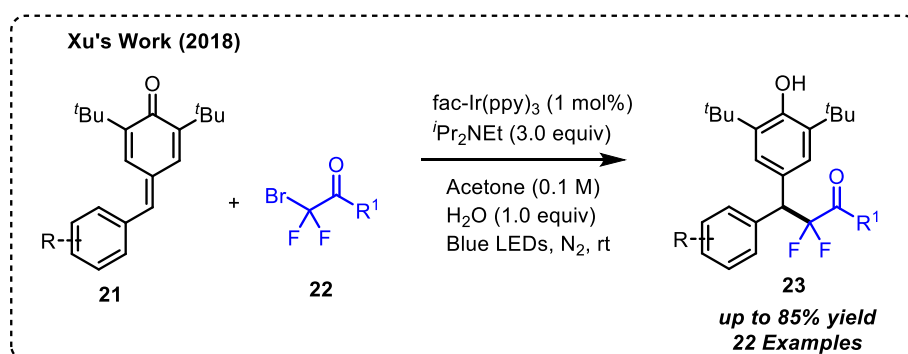
provides an alternative method for the preparation of *spiro*-cyclic ethers (**20**) with high diastereoselectivity (**b**, Scheme 5).¹⁰



Scheme 5. Kilburn & Dixon's approach

4.3 Background

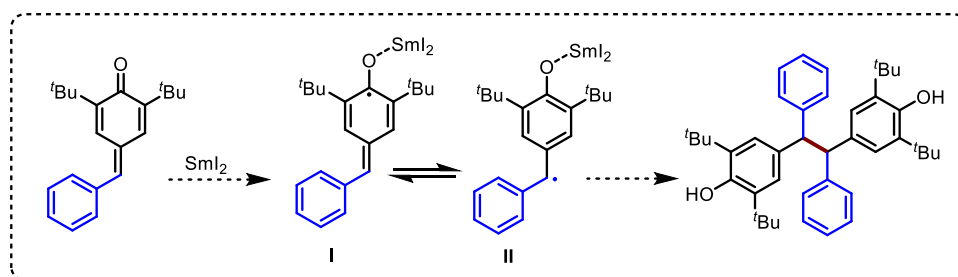
Till now, only a handful of reports are available in the literature for the reductive dimerization reactions using SmI_2 chemistry. In recent years *para*-quinone methides (*p*-QMs) have gained popularity as flexible building blocks in organic synthesis. In particular, the substantial development of the 1,6-Michael addition of *p*-QMs with various nucleophiles has been achieved.¹¹ However, in contrast, the radical-type addition or coupling reaction of *p*-QMs has received less attention. For example, in 2018, Xu and co-workers reported to utilize the radical pathway to generate difluoroalkylated diarylmethanes (**23**). It has been demonstrated that *fac*- $\text{Ir}(\text{ppy})_3$ can act as a photocatalyst when DIPEA, blue light, and water are also present. Under standard conditions, good to exceptional range of product (**23**) yields were realized from



Scheme 6. Synthesis of difluoroalkylated diarylmethanes

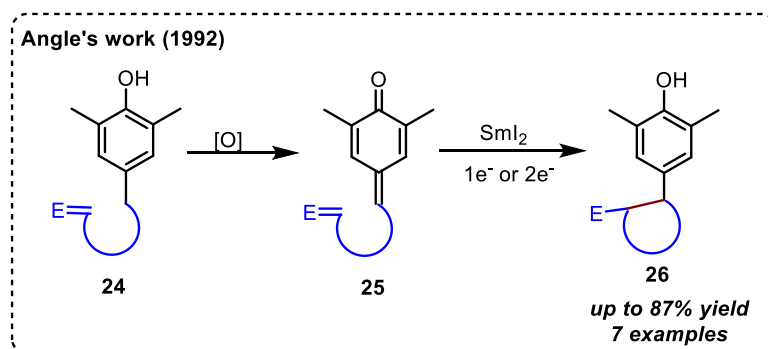
the processing of *p*-QMs (**21**) and ethyl bromodifluoroacetate (**22**) (Scheme 6).¹² Very recently, Lu and co-workers, developed a metal-free, redox-neutral, and highly atom-economical protocol to access 2,2-diarylethylamines *via* visible-light-promoted radical reactions of *para*-quinone methides (*p*-QMs) with *N*-alkyl anilines.¹³

As part of our continuing research in the expanse of *para*-quinone methides, we envisioned that SmI₂-mediated reductive coupling of *para*-quinone methides would potentially lead to a wide range of 1,1,2,2-tetraaryl ethane derivatives in moderate to good yields (Scheme 7).



Scheme 7. Reductive dimerization of *para*-quinone methides

Thorough literature survey revealed that there were a couple of reports available on the reductive dimerization of *p*-QMs. Angle & co-workers, in 1992, utilized quinone methides as synthons **25** for constructing a C-C bond *via* the generation of benzylic radical/anion using



Scheme 8. Reductive cyclization of quinone methides

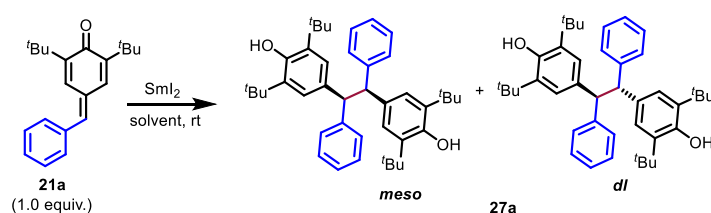
SmI₂ (Scheme 8).¹⁵ The authors have proposed that when they used α , β -unsaturated esters quinone methides, the yield of the cyclized product **26** was relatively lower owing to the formation of dimerized products from the formation of a C-C single bond between benzylic carbons. Based on this observation, they have revealed the initial reduction of quinone methide to radical anion or dianion followed by cyclization. It is unclear from the available data whether the cyclization is happening at the radical stage or if the second one-electron reduction occurs to yield the cyclized product **26**. This report basically involves only intramolecular version

with only one example for intermolecular reductive dimerization of *p*-QMs. In order to understand the mechanism of reductive dimerization of *p*-QMs and also to elaborate the substrate scope in the intermolecular version of this transformation, we have decided to explore this project. While working on this project, another report appeared in the literature from the group of Cai and Tang. They have established a potassium modified carbon-nitride-based heterogeneous photocatalytic system for the decarboxylative radical addition and reductive dimerization of *para*-quinone methides.¹⁴ However, the reaction conditions adapted by them were entirely different from ours.

4.4 Results & discussion

To find out the optimal reaction conditions for the synthesis of 1,1,2,2-tetraaryl ethane derivatives, *p*-QM **21a** was subjected to reductive dimerization under different reaction

Table 1. Optimization study^a

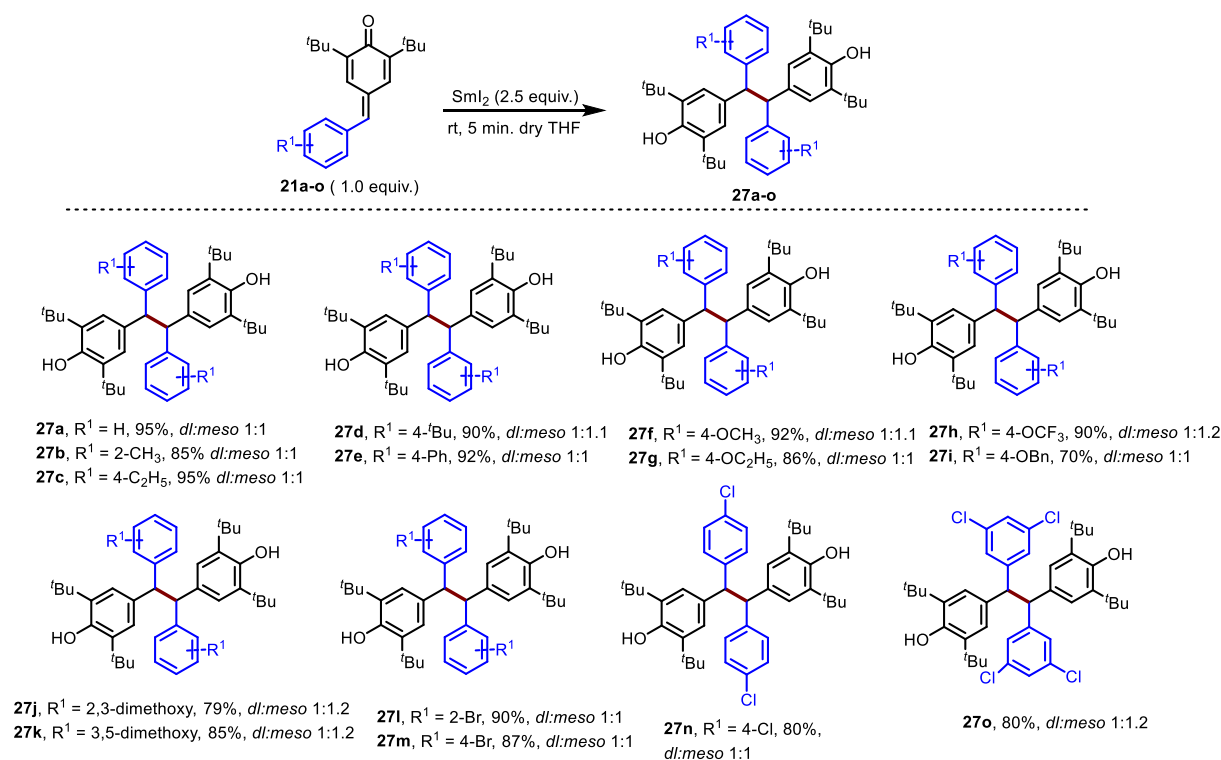


entry	SmI ₂ [equiv.]	Solvent	Time [min.]	Yield (%)
1	0.5	THF	45	50
2	1.0	THF	30	60
3	2.0	THF	15	70
4	2.2	THF	15	78
5	2.5	THF	5	95
6	2.5	1,2 DCE	5	82
7	2.5	MeCN	5	77
8	2.5	DMF	5	92
9	2.5	--	5	86
10	-	THF	720	nr

^aAll reactions were carried out with **21a** (0.136 mmol) in 1.0 mL of anhydrous solvents. Yields reported are isolated yields.

conditions using SmI₂ and, the results are summarized in Table 1. In our initial attempts, we employed SmI₂ (0.5 equiv.) as a single electron source in the THF medium, and within 45 min, some conversion was observed, and the desired 1,1,2,2-tetraaryl ethane derivative **27a** was isolated in 50% yield at room temperature as a 1:1 *meso:dl* mixture (entry 1). On increasing the loading of SmI₂ to 1.0 equiv. at same temperature, some improvement in the conversion of **21a** was observed, and the product **27a** was obtained in 60% isolated yield (entry 2). Further increase in the loading of SmI₂ to 2.0 equiv. resulted in improving the yields of **27a** to 70% with lesser reaction time (entry 3). Surprisingly, when we changed the stoichiometry of SmI₂ to 2.5 equiv., the conversion took place smoothly, and the product **27a** was formed in 95% isolated yield at room temperature within 5 min (entry 5). Other solvents, such as 1,2 DCE and MeCN were found to be a bit less effective for this transformation (entries 6 & 7). The reaction worked relatively well in DMF (entry 8) and the corresponding 1,1,2,2-tetraaryl ethane derivative **27a** was isolated in 92% yield. However, without solvent also, the reaction proceeded; however, in that case, the desired product was obtained only in 86% yield (entry 9). No reaction was observed without SmI₂, which clearly indicates the necessity of SmI₂ to drive this transformation (entry 10). Based on the above-mentioned optimization studies, we

Scheme 9. Substrate scope with different *p*-quinone methides^a

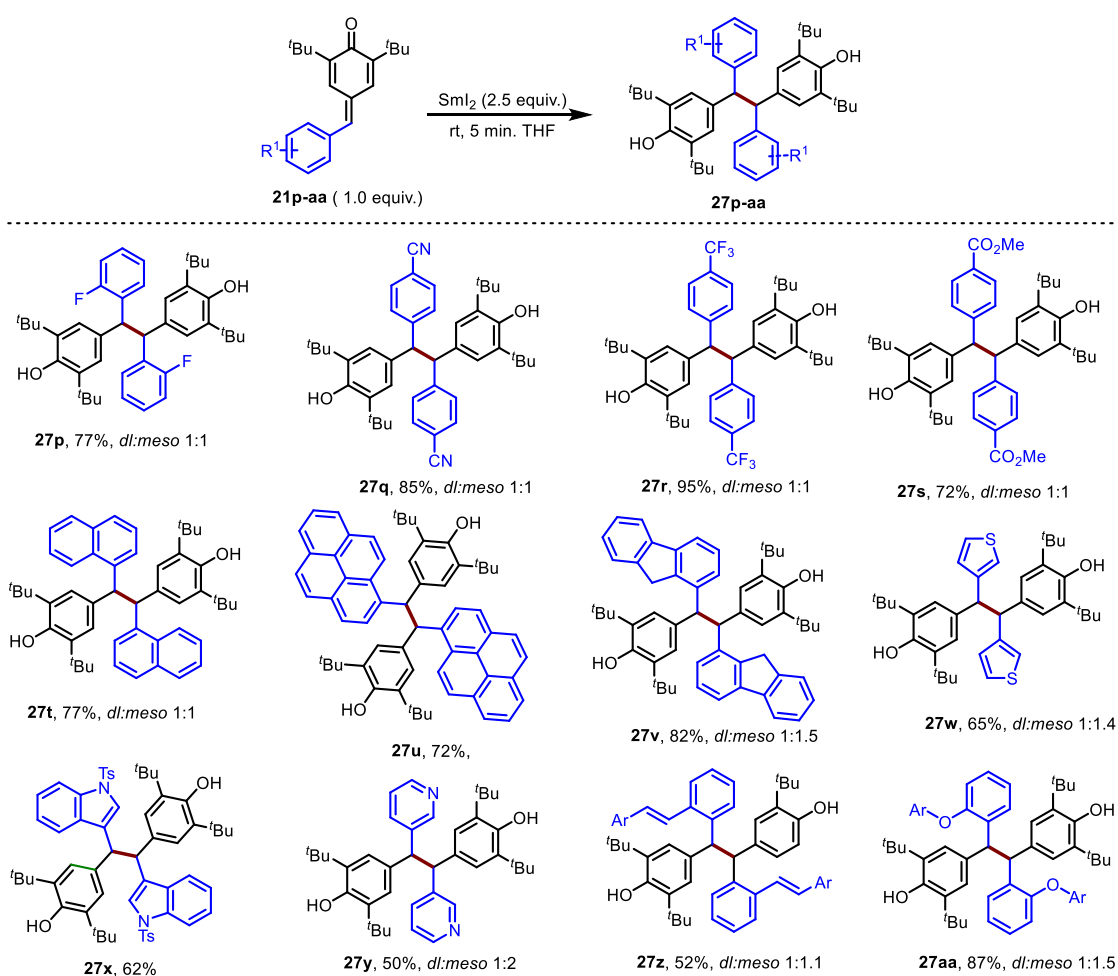


^aAll reactions were carried out with **21a-q** (1.0 equiv.) and SmI₂ (2.5 equiv.) in 1.0 mL of solvent. Yields reported are isolated yields.

discovered that entry 5 in Table 1 was the ideal condition for this conversion. Therefore, for substrate scope investigations, this reaction condition was utilized.

In this context, a wide range of *para*-quinone methides were tested under the optimal condition and, the results are summarized below (Table 2). It is evident from Table 2, the electronic nature of the aryl ring present in *p*-QMs scarcely impacts the substrate scope. Most of the *p*-QMs **21b-k** derived from alkyl and electron-rich aromatic aldehydes reacted efficiently under the optimized conditions to furnish the corresponding reductive dimer products **27b-k** in good to excellent yields (70-95% yields). Delightfully, the present method was found to be robust in cases of *p*-QMs **21l-o**, synthesized from halo-substituted aromatic aldehydes, as these *p*-QMs underwent smooth conversion to their respective 1,1,2,2-tetraaryl ethane derivatives **27l-o** in good yields (80-90% yields). Furthermore, under the envisioned reaction circumstances, the generality of this technique was also examined utilising *p*-QMs **21p-s**,

Scheme 10. Substrate scope with different *p*-quinone methides^a

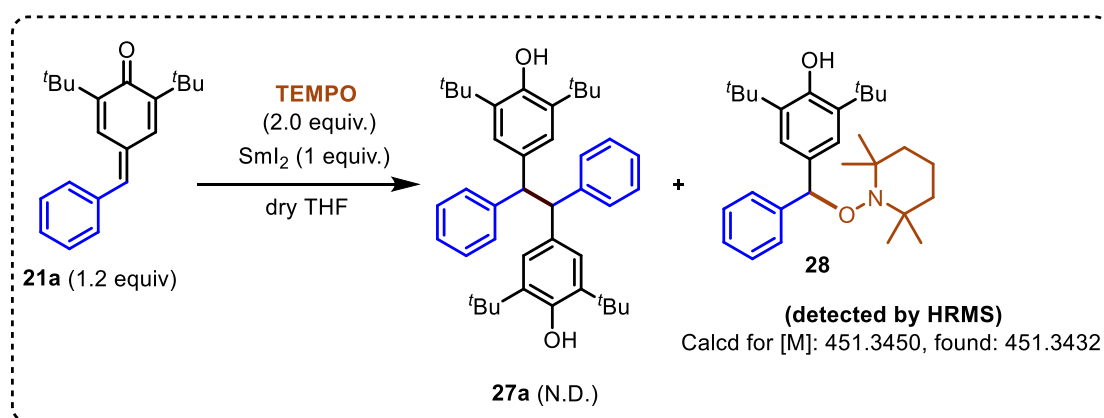


^aAll reactions were carried out with **21t-aa** (1.0 equiv.) and SmI_2 (2.5 equiv.) in 1.0 mL of solvent. Yields reported are isolated yields.

substituted with electron-withdrawing substituents and sensitive functional groups such as nitrile, ester at the aromatic ring. In those cases, the corresponding reductive dimer products **27p–s** were produced in good yields (in the range of 77–95%) [Table 3]. Significantly, even sterically hindered *p*-QMs **21t–v** were also discovered to be appropriate substrates, providing the subsequent products **27t–v** in good yields (72–82%). This approach was also found to be operative for *p*-QMs substituted with heteroarenes **21w–y** and, in all those cases, the respective 1,1,2,2-tetraaryl ethane derivatives (**27w–y**) were isolated in good to excellent yields. 2-Alkenyl phenyl substituted *para*-quinone methide **21z** also reacted well to furnish the corresponding product **27z** in 52% yield. Similarly, 2-arenoxy phenyl substituted *para*-quinone methide **21aa** gave the respective product **27aa** in 87% isolated yield (Table 3).

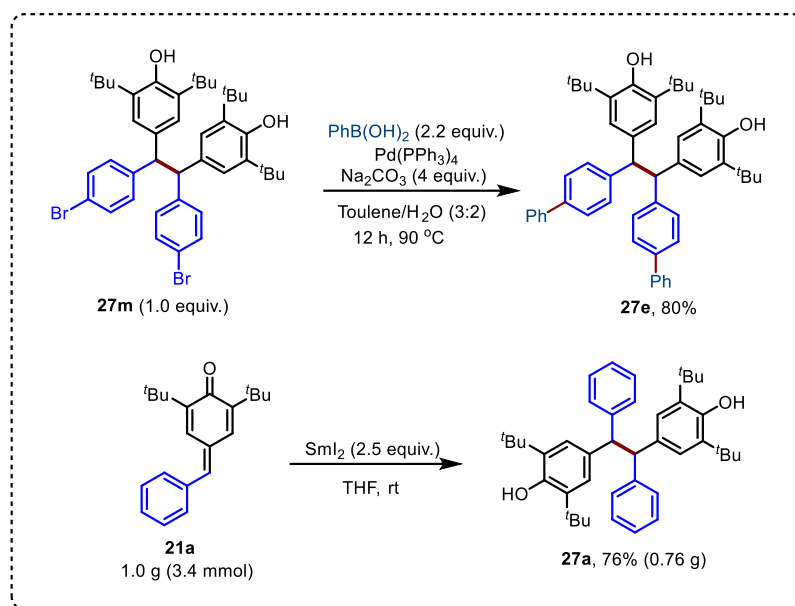
4.5. Control experiments

In order to acquire mechanistic understanding of this reaction, a few control experiments were conducted. Under standard reaction conditions, a radical trapping experiment was carried out using the radical scavenger TEMPO (2,2,6,6-tetramethyl-1-piperidinyloxy). In this case, the formation of **27a** was not observed (Scheme 8), which suggested the involvement of a diarylmethyl radical, the TEMPO adduct could be found by ESI-MS.



Scheme 11. Radical trapping experiment with TEMPO as a radical scavenger

To demonstrate the practical applications of this transformation one of the 1,1,2,2-tetraaryl ethane derivatives (**27m**) was subjected to Suzuki coupling with phenyl boronic acid at 90 °C to produce the C-C coupling product (**27e**) with 80% isolated. A gram scale reaction was also carried out to test the scalability of this transformation (Scheme 9).



Scheme 12. Synthetic elaboration and gram-scale reaction

4.6 Conclusion

In conclusion, we have successfully established a SmI₂ mediated reductive dimerization of *para*-quinone methides to access wide range of 1,1,2,2-tetraaryl ethane derivatives in good to excellent yields. This mild reduction avoids harsh reaction conditions and is particularly suited to substrates with bulky and sensitive functional groups.

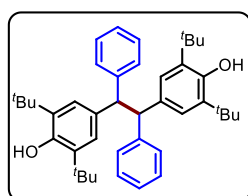
4.7 Experimental section

General information. All reactions were carried out under an argon atmosphere in an oven-dried round bottom flask. All the solvents were distilled before use and stored under an argon atmosphere. Most of the reagents and starting materials were purchased from commercial sources and used as such. *p*-quinone methides were prepared by following a literature procedure.¹⁹ Melting points were recorded on the SMP20 melting point apparatus and are uncorrected. ¹H, ¹³C, and ¹⁹F spectra were recorded in CDCl₃ and DMSO (400, 100, and 376 MHz, respectively) on Bruker FT-NMR spectrometer. Chemical shift (δ) values are reported in parts per million relatives to TMS, and the coupling constants (J) are reported in Hz. High-resolution mass spectra were recorded on Waters Q-TOF Premier-HAB213 spectrometer. FT-IR spectra were recorded on a Perkin-Elmer FTIR spectrometer. Thin-layer chromatography was performed on Merck silica gel 60 F₂₅₄ TLC pellets and visualized by UV irradiation and KMnO₄ stain. Column chromatography was carried out through silica gel (100–200 mesh) using EtOAc/hexane as eluent.

General procedure for the synthesis of 1,1,2,2-tetraaryl ethane derivatives (27a-ab) from para-Quinone Methides (21a-ab):

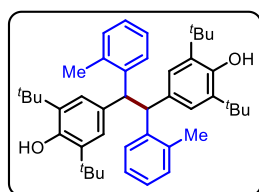
To a clean, oven-dried round bottom flask containing a magnetic stir-bar *para*-quinone methide (40 mg, 1.0 equiv., 0.136 mmol) was added under argon atmosphere. After that dry THF and SmI₂ (2.5 equiv.) was introduced into the reaction flask via syringe. Then resulting reaction mixture was stirred at room temperature. After the reaction was complete (based on TLC analysis), reaction mixture was filtered through silica gel pad using CH₂Cl₂. Excess solvent was then removed under reduced pressure and the residue was then purified through a neutral alumina gel column using EtOAc/Hexane mixture as an eluent to get the pure product.

4,4'-(1,2-diphenylethane-1,2-diyl)bis(2,6-di-*tert*-butylphenol) (27a): The reaction was



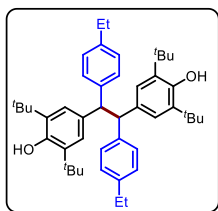
performed at 0.136 mmol scale of **21a**; yellow solid (38.0 mg, 95% yield, *dl:meso* 1:1); m. p. = 208–210 °C; R_f = 0.6 (5% EtOAc in hexane); ¹H NMR (400 MHz, CDCl₃) δ 7.20 (d, *J* = 7.5 Hz, 4H), 7.14 – 7.09 (m, 13H), 7.04 – 7.01 (m, 4H), 6.87 (s, 3H), 6.85 (s, 4H), 4.87 (s, 2H), 4.85 (s, 2H), 4.55 (s, 2H), 4.48 (s, 2H), 1.30 (d, *J* = 3.2 Hz, 72H); ¹³C{¹H} NMR (100 MHz, CDCl₃) δ 151.6, 151.5, 144.6, 144.5, 135.1, 135.0, 134.4, 133.9, 128.8, 128.6, 128.1, 127.9, 125.7, 125.6, 125.5, 125.4, 57.8, 57.7, 34.33, 34.3, 30.5, 30.4; FT-IR (thin film, neat): 3636, 2957, 1642, 1467, 1329, 800 cm⁻¹; HRMS (ESI): *m/z* calcd for C₄₂H₅₃O₂ [M-H]⁻ : 589.4046; found :589.4055.

4,4'-(1,2-di-*o*-tolylethane-1,2-diyl)bis(2,6-di-*tert*-butylphenol) (27b): The reaction was



performed at 0.129 mmol scale of **21b**; yellow solid (34.0 mg, 85% yield, *dl:meso* 1:1); m. p. = 202–204 °C; R_f = 0.4 (5% EtOAc in hexane); ¹H NMR (400 MHz, CDCl₃) δ 7.34 – 7.29 (m, 4H), 7.10 – 6.99 (m, 6H), 6.97 – 6.92 (m, 6H), 6.75 (d, *J* = 3.1 Hz, 8H), 4.85 (d, *J* = 3.0 Hz, 4H), 4.79 (s, 2H), 4.72 (s, 2H), 2.32 (s, 6H), 2.13 (s, 6H), 1.29 (s, 36H), 1.26 (s, 36H); ¹³C{¹H} NMR (100 MHz, CDCl₃) δ 151.5, 151.4, 143.0, 142.0, 136.0, 135.9, 134.9, 134.7 (2C), 133.4 (2C), 130.4, 130.0, 128.4, 126.5, 125.8 (2C), 125.7, 125.5, 125.3, 53.0, 51.8, 34.25, 34.2, 30.6, 30.3, 20.4, 20.1; FT-IR (thin film, neat): 3645, 2962, 1487, 1436, 1235, 743 cm⁻¹; HRMS (ESI): *m/z* calcd for C₄₄H₅₇O₂ [M-H]⁻ : 617.4359; found :617.4364.

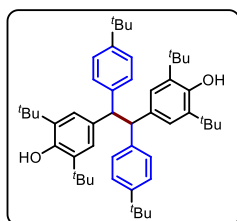
4,4'-(1,2-bis(4-ethylphenyl)ethane-1,2-diyl)bis(2,6-di-*tert*-butylphenol) (27c): The reaction



was performed at 0.124 mmol scale of **21c**; yellow solid (38.0 mg, 95% yield, *dl:meso* 1:1); m. p. = 204–206 °C; R_f = 0.4 (5% EtOAc in hexane);

^1H NMR (400 MHz, CDCl_3) δ 7.14 (d, J = 8.1 Hz, 2H), 7.01 (s, 1H), 6.99 (s, 5H), 6.97 – 6.94 (m, 6H), 6.88 (s, 4H), 6.85 (s, 4H), 4.87 (s, 2H), 4.84 (s, 2H), 4.53 (s, 2H), 4.43 (s, 2H), 2.57 – 2.50 (m, 8H), 1.32 (s, 36H), 1.31 (s, 36H) 1.48 (td, J = 7.5, 0.5 Hz, 12H); $^{13}\text{C}\{^1\text{H}\}$ NMR (100 MHz, CDCl_3) δ 151.5, 151.3, 141.9, 141.7, 141.2, 141.1, 134.92 (2C), 134.9, 134.3, 128.7, 128.3, 127.6, 127.3, 125.6, 125.4, 57.52, 57.5, 34.32, 34.3, 30.5, 30.4, 28.51, 28.5, 15.8, 15.5; FT-IR (thin film, neat): 3648, 2923, 1737, 1459, 1155, 638 cm^{-1} ; HRMS (ESI): m/z calcd for $\text{C}_{46}\text{H}_{61}\text{O}_2$ $[\text{M}-\text{H}]^-$: 645.4672; found :645.4680.

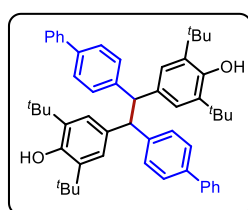
4,4'-(1,2-bis(4-*tert*-butylphenyl)ethane-1,2-diyl)bis(2,6-di-*tert*-butylphenol) (27d): The



reaction was performed at 0.114 mmol scale of **21d**; yellow solid (36.0 mg, 90% yield, *dl:meso* 1:1.1); m. p. = 196–198 °C; R_f = 0.4 (5% EtOAc in hexane); ^1H NMR (400 MHz, CDCl_3) δ 7.14 – 7.12 (m, 9H), 7.09 – 7.07 (m, 4.4H), 7.00 (d, J = 8.3 Hz, 4H), 6.88 (s, 4H), 6.85 (s, 4H), 4.86

(s, 2H), 4.83 (s, 2H), 4.49 (s, 2H), 4.40 (s, 2H), 1.31 (s, 39.6H), 1.30 (s, 36H), 1.24 (s, 37.8H); $^{13}\text{C}\{^1\text{H}\}$ NMR (100 MHz, CDCl_3) δ 151.4, 151.3, 148.1, 147.9, 141.52, 141.5, 134.9, 134.84, 134.8, 134.3, 128.5, 128.1, 125.7, 125.5, 124.8, 124.7, 57.8, 57.6, 34.33, 34.3, 31.54, 31.5, 30.5, 30.4; FT-IR (thin film, neat): 3646, 2957, 1514, 1436, 1154, 739 cm^{-1} ; HRMS (ESI): m/z calcd for $\text{C}_{50}\text{H}_{69}\text{O}_2$ $[\text{M}-\text{H}]^-$: 701.5298; found :701.5294.

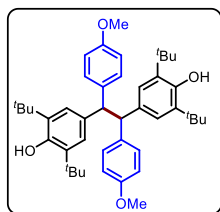
4,4'-(1,2-Di([1,1'-biphenyl]-4-yl)ethane-1,2-diyl)bis(2,6-di-*tert*-butylphenol) (27e): The



reaction was performed at 0.107 mmol scale of **21e**; Yellow solid (37.0 mg, 92% yield, crude *dl:meso* = 1:1 and isolated *dl:meso* = 1:1.2); m.p.

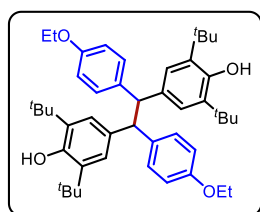
= 229–231 °C; R_f = 0.3 (5% EtOAc in hexane); ^1H NMR (400 MHz, CDCl_3) δ 7.56 – 7.53 (m, 9H), 7.44 – 7.37 (m, 18.1H), 7.35 – 7.31 (m, 7.3H), 7.29 – 7.27 (m, 2H), 7.20 (d, J = 8.2 Hz, 4H), 6.94 (d, J = 2.0 Hz, 8H), 4.92 (s, 2H), 4.90 (s, 2.4H), 4.66 (s, 2.4H), 4.58 (s, 2H), 1.34 (s, 43H), 1.32 (s, 36H); $^{13}\text{C}\{^1\text{H}\}$ NMR (100 MHz, CDCl_3) δ 151.7, 151.5, 143.8, 143.6, 141.4, 141.1, 138.4, 138.3, 135.2, 135.16, 134.4, 133.8, 129.2, 128.9, 128.7, 127.1, 127.0, 126.95, 126.9, 126.7, 125.6, 125.4, 57.43, 57.41, 34.4, 34.3, 30.5, 30.4; FT-IR (thin film, neat): 3640, 2956, 1486, 1235, 1154, 764 cm^{-1} ; HRMS (ESI): m/z calcd for $\text{C}_{54}\text{H}_{62}\text{O}_2$ $[\text{M}-\text{H}]^-$: 741.4672; found : 741.4697.

4,4'-(1,2-bis(4-methoxyphenyl)ethane-1,2-diyl)bis(2,6-di-*tert*-butylphenol) (27f): The



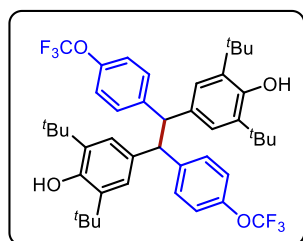
reaction was performed at 0.123 mmol scale of **21f**; yellow solid (37.0 mg, 92% yield, *dl:meso* 1:1.1); m. p. = 206–208 °C; R_f = 0.3 (5% EtOAc in hexane); ^1H NMR (400 MHz, DMSO- d_6) δ 6.39 (d, J = 8.7 Hz, 4H), 6.25 (d, J = 8.6 Hz, 4.2H), 6.06 (s, 4H), 6.04 (s, 4H), 5.78 – 5.75 (m, 9H), 5.62 (s, 2.2H), 5.52 (s, 2H), 3.78 (s, 2H), 3.71 (s, 2.2H), 2.72 (s, 6.6H), 2.71 (s, 6H) 0.37 (d, J = 1.9 Hz, 75.6H); $^{13}\text{C}\{^1\text{H}\}$ NMR (100 MHz, DMSO- d_6) δ 157.5, 157.4, 151.5, 151.3, 137.0, 136.8, 135.0, 134.97, 134.9, 134.3, 129.6, 129.4, 125.5, 125.3, 113.5, 113.3, 57.1, 56.9, 55.3, 55.2, 34.34, 34.3, 30.5, 30.46; FT-IR (thin film, neat): 3642, 2956, 1611, 1511, 1249, 740 cm^{-1} ; HRMS (ESI): m/z calcd for $\text{C}_{44}\text{H}_{57}\text{O}_4$ $[\text{M}-\text{H}]^-$: 649.4257; found : 649.4277.

4,4'-(1,2-Bis(4-ethoxyphenyl)ethane-1,2-diyl)bis(2,6-di-*tert*-butylphenol) (27g): The



reaction was performed at 0.118 mmol scale of **21g**; Yellow solid (35.0 mg, 86% yield, *dl:meso* 1:1); m.p. = 219–221 °C; R_f = 0.3 (5% EtOAc in hexane); ^1H NMR (400 MHz, CDCl_3) δ 7.09 – 7.06 (m, 4H), 6.97 – 6.96 (m, 4H), 6.833 – 6.83 (m, 8H), 6.69 – 6.68 (m, 2H), 6.66 – 6.64 (m, 6H), 4.88 (s, 2H), 4.83 (s, 2H), 4.44 (s, 2.8H), 4.37 (s, 2H), 3.93 (q, J = 7.0 Hz, 8H), 1.37 – 1.35 (m, 12H), 1.31 – 1.30 (m, 72H); $^{13}\text{C}\{^1\text{H}\}$ NMR (100 MHz, CDCl_3) δ 156.8, 156.7, 151.5, 151.3, 136.9, 136.7, 134.94, 134.93, 134.91, 134.4, 129.6, 129.4, 125.5, 125.3, 114.1, 113.9, 63.4, 63.4, 57.1, 56.9, 34.3, 34.26, 30.5, 30.45, 15.0; FT-IR (thin film, neat): 3645, 2957, 1510, 1477, 1245, 738 cm^{-1} ; HRMS (ESI): m/z calcd for $\text{C}_{46}\text{H}_{61}\text{O}_4$ $[\text{M}-\text{H}]^-$: 677.4573; found : 677.4575.

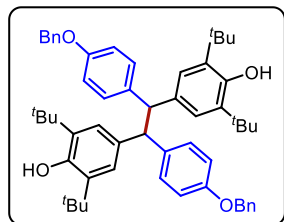
4,4'-(1,2-Bis(4-(trifluoromethoxy)phenyl)ethane-1,2-diyl)bis(2,6-di-*tert*-butylphenol)



(27h): The reaction was performed at 0.106 mmol scale of **21h**; Yellow solid (36.0 mg, 90% yield, crude *dl:meso* = 1:1.2 and isolated *dl:meso* = 1:1.1); m.p. = 175–177 °C; R_f = 0.3 (5% EtOAc in hexane); ^1H NMR (400 MHz, CDCl_3) δ 7.15 (d, J = 8.6 Hz, 4H), 7.08 (d, J = 8.6 Hz, 4.2H), 6.99 (d, J = 7.8 Hz, 9H), 6.84 (s, 4H), 6.80 (s, 4.4H), 4.97 (s, 2.2H), 4.92 (s, 2H), 4.50 (s, 2H), 4.45 (s, 2.2H), 1.30 (d, J = 2.4 Hz, 75.6H); $^{13}\text{C}\{^1\text{H}\}$ NMR (100 MHz, CDCl_3) δ 152.0, 151.8, 147.4 (d, $J_{\text{C-F}}$ = 2.0 Hz), 147.2 (d, $J_{\text{C-F}}$ = 1.8 Hz), 143.2, 142.8, 135.5, 135.4, 133.3, 132.8, 129.9, 129.7, 125.5, 125.4, 120.8, 120.59 (apparent q, $J_{\text{C-F}}$ = 255 Hz), 120.58 (apparent q, $J_{\text{C-F}}$ = 255 Hz), 120.57, 57.2, 57.0, 34.4, 34.3, 30.4, 30.3; ^{19}F NMR (376 MHz, CDCl_3), δ –57.90, –57.93 ppm; FT-IR (thin film, neat): 3645, 2958, 1507,

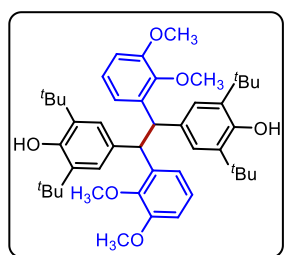
1437, 1257, 686 cm^{-1} ; HRMS (ESI): m/z calcd for $\text{C}_{44}\text{H}_{51}\text{F}_6\text{O}_4$ $[\text{M}-\text{H}]^-$: 757.3692; found : 757.3694.

4,4'-(1,2-Bis(4-(benzyloxy)phenyl)ethane-1,2-diyl)bis(2,6-di-*tert*-butylphenol) (27i): The



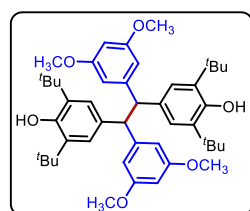
reaction was performed at 0.100 mmol scale of **21i**; Yellow solid (30.0 mg, 70% yield, crude *dl:meso* 1:1 and isolated *dl:meso* 1:1.9); m.p. = 185–187 °C; R_f = 0.3 (5% EtOAc in hexane); ^1H NMR (400 MHz, CDCl_3) δ 7.41 – 7.38 (m, 16H), 7.37 – 7.34 (m, 8H), 7.33 – 7.28 (m, 5.8H), 7.10 – 7.08 (m, 4H), 6.99 – 6.96 (m, 7H), 6.831 – 6.83 (m, 11.6H), 6.78 – 6.76 (m, 4H), 6.75 – 6.72 (m, 7.4H), 4.96 (s, 11.6H), 4.89 (s, 3.8H), 4.84 (s, 2H), 4.45 (s, 2H), 4.38 (s, 3.8H), 1.31 (s, 68.4H), 1.30 (s, 36H); $^{13}\text{C}\{^1\text{H}\}$ NMR (100 MHz, CDCl_3) δ 156.8, 156.7, 151.5, 151.3, 137.4, 137.37, 137.3, 137.1, 135.0, 134.8, 134.3, 129.7, 129.5, 128.6, 128.0, 127.9, 127.7, 127.6, 125.5, 125.3, 114.5, 114.3, 70.1, 70.0, 57.1, 57.0, 34.3, 34.27, 30.5; FT-IR (thin film, neat): 3645, 2926, 1609, 1510, 1249, 739, cm^{-1} ; HRMS (ESI): m/z calcd for $\text{C}_{56}\text{H}_{65}\text{O}_4$ $[\text{M}-\text{H}]^-$: 801.4883; found : 801.4887.

4,4'-(1,2-Bis(2,3-dimethoxyphenyl)ethane-1,2-diyl)bis(2,6-di-*tert*-butylphenol) (27j): The



reaction was performed at 0.113 mmol scale of **21j**; Yellow solid (32.0 mg, 79% yield, *dl:meso* 1:1.2); m.p. = 194–196 °C; R_f = 0.1 (5% EtOAc in hexane); ^1H NMR (400 MHz, CDCl_3) δ 7.10 – 7.08 (m, 2H), 6.93 – 6.85 (m, 10H), 6.83 (s, 4H), 6.61 (t, J = 8.0 Hz, 5H), 5.11 (s, 2H), 5.07 (s, 2.4H), 4.78 (d, J = 3.1 Hz, 4.4H), 3.75 (d, J = 1.6 Hz, 14.4H), 3.51 (s, 6H), 3.30 (s, 6H), 1.28 (s, 43.2H), 1.25 (s, 36H); $^{13}\text{C}\{^1\text{H}\}$ NMR (100 MHz, CDCl_3) δ 152.7, 152.5, 151.4, 151.3, 147.0, 146.7, 138.6, 138.5, 134.8, 134.7, 134.6, 125.7, 123.6, 123.3, 121.8, 121.7, 120.1, 109.7, 109.65, 60.3, 55.9, 55.8, 55.6, 55.55, 48.8, 34.3, 34.2, 30.6, 30.4; FT-IR (thin film, neat): 3647, 2927, 1586, 1475, 1272, 746 cm^{-1} ; HRMS (ESI): m/z calcd for $\text{C}_{46}\text{H}_{61}\text{O}_6$ $[\text{M}-\text{H}]^-$: 709.4468; found : 709.4474.

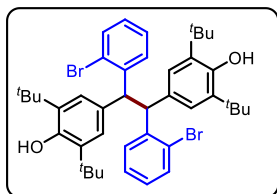
4,4'-(1,2-Bis(3,5-dimethoxyphenyl)ethane-1,2-diyl)bis(2,6-di-*tert*-butylphenol) (27k): The



reaction was performed at 0.113 mmol scale of **21k**; Yellow solid (34.0 mg, 85% yield, crude *dl:meso* 1:1.2 and isolated *dl:meso* 1:1.3); R_f = 0.1 (5% EtOAc in hexane); m.p. = 212–214 °C; ^1H NMR (400 MHz, CDCl_3) δ 6.90 (s, 4), 6.85 (s, 5H), 6.39 (d, J = 2.2 Hz, 5.3H), 6.22 (d, J = 2.2 Hz, 4H), 6.18 – 6.15 (m, 4.7H), 4.93 (s, 2H), 4.85 (s, 2.6H), 4.41 (s, 2.6H), 4.32 (s, 2H), 3.68 (s, 15.6H), 3.63 (s, 12H), 1.32 (s, 36H), 1.29 (s, 46.8H); $^{13}\text{C}\{^1\text{H}\}$ NMR (100 MHz, CDCl_3) δ

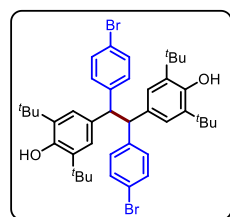
160.4, 160.2, 151.8, 151.5, 146.9, 146.7, 135.1, 135.0, 133.9, 133.6, 125.4, 125.38, 107.1, 106.9, 98.3, 97.9, 58.1, 57.97, 55.3, 55.29, 55.25, 55.22, 34.4, 34.3, 30.5; FT-IR (thin film, neat): 3644, 2926, 1596, 1433, 1154, 767 cm^{-1} ; HRMS (ESI): m/z calcd for $\text{C}_{46}\text{H}_{61}\text{O}_6$ $[\text{M}-\text{H}]^-$: 709.4468; found : 709.4469.

4,4'-(1,2-bis(2-bromophenyl)ethane-1,2-diyl)bis(2,6-di-*tert*-butylphenol) (27l) : The



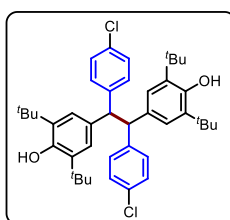
reaction was performed at 0.107 mmol scale of **21l**; yellow solid (36.0 mg, 90% yield, *dl:meso* 1:1); m. p. = 242–244 °C; R_f = 0.4 (5% EtOAc in hexane); ^1H NMR (400 MHz, CDCl_3) δ 7.53 – 7.51 (m, 4H), 7.40 (dd, J = 8.0, 1.2 Hz, 2H), 7.40 (dd, J = 8.0, 1.1 Hz, 2H), 7.21 – 7.18 (m, 2H), 7.17 – 7.14 (m, 2H), 7.00 (s, 4H), 6.97 (s, 4H), 6.88 (td, J = 7.8, 1.5 Hz, 4H), 5.30 (s, 2H), 5.19 (s, 2H), 4.89 (d, J = 1.3 Hz, 4H), 1.30 (s, 36H), 1.31 (s, 36H); $^{13}\text{C}\{^1\text{H}\}$ NMR (100 MHz, CDCl_3) δ 151.9, 151.8, 143.2 (2C), 142.8, 136.1, 136.0, 132.9, 132.6, 132.1, 131.9, 129.5, 128.6, 127.6, 127.4 (2C), 127.1, 125.7, 125.6 (2C), 55.1, 54.0, 34.4, 34.3, 30.5, 30.4; FT-IR (thin film, neat): 3645, 2924, 1738, 1464, 1156, 748 cm^{-1} ; HRMS (ESI): m/z calcd for $\text{C}_{42}\text{H}_{51}\text{Br}_2\text{O}_2$ $[\text{M}-\text{H}]^-$: 745.2256; found :745.2240.

4,4'-(1,2-bis(4-bromophenyl)ethane-1,2-diyl)bis(2,6-di-*tert*-butylphenol) (27m): The



reaction was performed at 0.107 mmol scale of **21m**; yellow solid (35.0 mg, 87% yield, *dl:meso* 1:1); m. p. = 237–239 °C; R_f = 0.4 (5% EtOAc in hexane); ^1H NMR (400 MHz, CDCl_3) δ 7.26 – 7.20 (m, 17.4H), 7.042 – 7.04 (m, 5H), 7.03 – 7.02 (m, 4H), 6.91 – 6.88 (m, 4H), 6.76 (s, 10H), 6.74 (s, 4H), 4.93 (s, 2H), 4.86 (s, 5.4H), 4.43 (s, 5.4H), 4.35 (s, 2H), 1.28 (s, 36H), 1.26 (s, 97.2H); $^{13}\text{C}\{^1\text{H}\}$ NMR (100 MHz, CDCl_3) δ 151.9, 151.7, 143.4, 143.1, 135.4, 135.3, 133.5, 132.8, 131.4, 131.0, 130.4, 130.2, 125.4, 125.2, 119.7, 119.4, 56.9, 56.7, 34.4, 34.3, 30.44, 30.4; FT-IR (thin film, neat): 3647, 2958, 1487, 1437, 1155, 810 cm^{-1} ; HRMS (ESI): m/z calcd for $\text{C}_{42}\text{H}_{51}\text{Br}_2\text{O}_2$ $[\text{M}-\text{H}]^-$: 745.2256; found :445.2249.

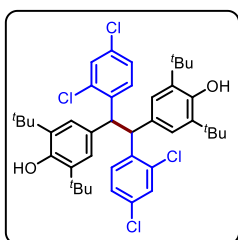
4,4'-(1,2-bis(4-chlorophenyl)ethane-1,2-diyl)bis(2,6-di-*tert*-butylphenol) (27n): The



reaction was performed at 0.122 mmol scale of **21n**; yellow solid (32.0 mg, 80% yield, *dl:meso* 1:1); m. p. = 222–224 °C; R_f = 0.4 (5% EtOAc in hexane); ^1H NMR (400 MHz, CDCl_3) δ 7.11 (s, 8H), 7.10 – 7.08 (m, 4H), 6.99 – 6.97 (m, 4H), 6.79 (s, 4H), 6.78 (s, 4H), 4.96 (s, 2H), 4.89 (s, 2H), 4.47 (s, 2H), 4.40 (s, 2H), 1.30 (d, J = 5.9 Hz, 72H); $^{13}\text{C}\{^1\text{H}\}$ NMR (100 MHz, CDCl_3) δ 151.9, 151.7, 142.9, 142.6, 135.4, 135.3, 133.6, 132.9, 131.5, 131.3, 130.0, 129.8, 128.4, 128.1, 125.4,

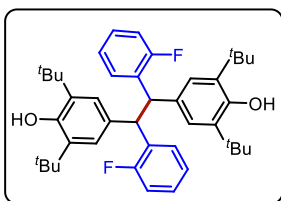
125.2, 57.0, 56.7, 34.4, 34.3, 30.44, 30.4; FT-IR (thin film, neat): 3646, 2921, 1738, 1461, 1153, 723 cm^{-1} ; HRMS (ESI): m/z calcd for $\text{C}_{42}\text{H}_{51}\text{Cl}_2\text{O}_2$ $[\text{M}-\text{H}]^-$: 657.3266; found :657.3265.

4,4'-(1,2-bis(3,5-dichlorophenyl)ethane-1,2-diyl)bis(2,6-di-*tert*-butylphenol) (27o): The



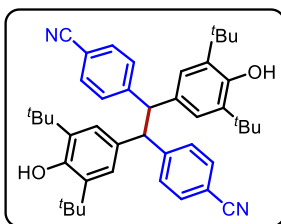
reaction was performed at 0.128 mmol scale of **21o**; yellow solid (32.0 mg, 80% yield, crude *dl:meso* 1:1.2 and isolated *dl:meso* 1:1.5); m. p. = 217–219 °C; R_f = 0.4 (5% EtOAc in hexane); ^1H NMR (400 MHz, CDCl_3) δ 7.41 – 7.38 (m, 5H), 7.25 (d, J = 2.2 Hz, 2H), 7.19 (d, J = 2.2 Hz, 3H), 7.14 (t, J = 2.1 Hz, 3H), 7.11 (t, J = 2.1 Hz, 2H), 6.90 (s, 6H), 6.85 (s, 4H), 5.19 (s, 3H), 5.08 (s, 2H), 4.97 (s, 3H), 4.92 (s, 2H), 1.31 (s, 54H), 1.30 (s, 36H); $^{13}\text{C}\{^1\text{H}\}$ NMR (100 MHz, CDCl_3) δ 152.2, 152.0, 140.3, 139.7, 135.4, 135.3, 134.8, 134.6, 132.2, 131.8, 131.3, 131.1, 130.0, 129.5, 129.0, 128.9, 127.4, 127.2, 125.3, 125.2, 51.60, 51.6, 34.4, 34.3, 30.4, 30.3; FT-IR (thin film, neat): 3647, 2923, 1739, 1587, 1377, 769 cm^{-1} ; HRMS (ESI): m/z calcd for $\text{C}_{42}\text{H}_{49}\text{Cl}_4\text{O}_2$ $[\text{M}-\text{H}]^-$: 725.2487; found :725.2484.

4,4'-(1,2-Bis(2-fluorophenyl)ethane-1,2-diyl)bis(2,6-di-*tert*-butylphenol) (27p): The



reaction was performed at 0.128 mmol scale of **21p**; Yellow solid (31 mg, 77% yield, *dl:meso* 1:1); m.p. = 211–213 °C; R_f = 0.4 (5% EtOAc in hexane); ^1H NMR (400 MHz, CDCl_3) δ 7.47 (td, J = 7.6, 2.1 Hz, 2H), 7.37 (td, J = 7.4, 2.5 Hz, 2H), 7.00 – 6.97 (m, 12H), 6.93 (s, 4H), 6.88 – 6.79 (m, 4H), 5.03 (d, J = 4.9 Hz, 4H), 4.92 (d, J = 3.1 Hz, 4H), 1.32 (s, 72H); $^{13}\text{C}\{^1\text{H}\}$ NMR (100 MHz, CDCl_3) δ 160.6 (d, $J_{\text{C-F}}$ = 242.7 Hz), 160.5 (d, $J_{\text{C-F}}$ = 242.3 Hz), 151.9, 151.8, 135.2, 135.17, 132.9, 132.5, 131.5 (d, $J_{\text{C-F}}$ = 14.3 Hz), 131.1 (d, $J_{\text{C-F}}$ = 14.6 Hz), 129.5, 129.4, 128.93, 128.9, 127.4 (d, $J_{\text{C-F}}$ = 8.3 Hz), 127.1 (d, $J_{\text{C-F}}$ = 8.4 Hz), 125.4, 125.3, 124.0 (d, $J_{\text{C-F}}$ = 3.2 Hz), 123.9 (d, $J_{\text{C-F}}$ = 3.1 Hz), 115.3 (d, $J_{\text{C-F}}$ = 24.8 Hz), 115.1 (d, $J_{\text{C-F}}$ = 23.5 Hz), 48.43, 48.41, 47.8, 47.77, 34.4, 34.3, 30.5, 30.4, ^{19}F NMR (376 MHz, CDCl_3) δ -117.856, -117.86 ppm; FT-IR (thin film, neat): 3644, 2959, 1436, 1229, 1156, 754 cm^{-1} ; HRMS (ESI): m/z calcd for $\text{C}_{42}\text{H}_{51}\text{F}_2\text{O}_2$ $[\text{M}-\text{H}]^-$: 625.3857; found : 625.3868.

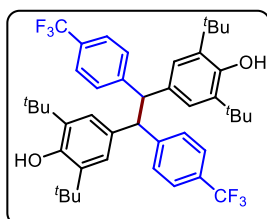
4,4'-(1,2-Bis(3,5-di-*tert*-butyl-4-hydroxyphenyl)ethane-1,2-diyl)dibenzonitrile (2q): (**13-**



ss-15) The reaction was performed at 0.125 mmol **21q**; Yellow solid (34 mg, 85% yield, *dl:meso* 1:1); m.p. = 239–241 °C; R_f = 0.3 (5% EtOAc in hexane); ^1H NMR (400 MHz, CDCl_3) δ 7.46 – 7.42 (m, 8H), 7.27 (s, (s, 2H), 7.26 – 7.25 (m, 2H), 7.16 (d, J = 8.4 Hz, 4H), 6.79 (s, 4H), 6.75 (s, 4H), 5.02 (s, 2H), 4.96 (s, 2H), 4.57 (s, 2H), 4.52 (s, 2H), 1.29 (s, 72H); $^{13}\text{C}\{^1\text{H}\}$

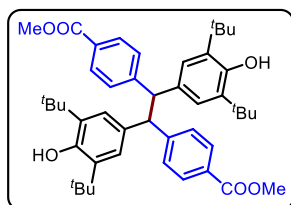
NMR (100 MHz, CDCl₃) δ 152.4, 152.1, 149.6, 149.2, 135.9, 135.7, 132.3, 132.0, 131.9, 131.4, 129.4, 129.2, 125.24, 125.21, 119.1, 119.0, 110.1, 109.6, 57.3, 57.1, 34.4, 34.3, 30.4, 30.3; FT-IR (thin film, neat): 3632, 2956, 2231, 1605, 1440, 1232, 752 cm⁻¹; HRMS (ESI): m/z calcd for C₄₄H₅₁N₂O₂ [M-H]⁻: 639.3951; found : 639.3951.

4,4'-(1,2-Bis(4-(trifluoromethyl)phenyl)ethane-1,2-diyl)bis(2,6-di-*tert*-butylphenol) (2r):



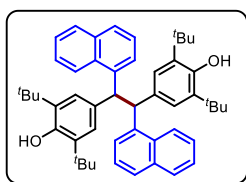
The reaction was performed at 0.110 mmol scale of **21r**; Yellow solid (38.0 mg, 95% yield, crude *dl:meso* = 1:1 and isolated *dl:meso* = 1.1:3); m.p. = 197–199 °C; R_f = 0.4 (5% EtOAc in hexane); ¹H NMR (400 MHz, CDCl₃) δ 7.40 (t, J = 7.7 Hz, 10H), 7.31 (d, J = 8.2 Hz, 5.3H), 7.18 (d, J = 8.1 Hz, 4.3H), 6.83 (s, 4H), 6.78 (s, 4H), 4.98 (s, 2H), 4.93 (s, 2.5H), 4.62 (s, 2.5H), 4.54 (s, 2H), 1.30 (s, 46.8H), 1.28 (s, 36H); ¹³C{¹H} NMR (100 MHz, CDCl₃) δ 152.1, 151.9, 148.3 (apparent q, J_{C-F} = 0.9 Hz), 147.9, 135.6, 135.5, 132.9, 132.2, 129.0, 128.7, 128.2 (d, J_{C-F} = 32.0 Hz), 128.0 (apparent q, J_{C-F} = 32.0 Hz), 125.4 (apparent q, J_{C-F} = 5.4 Hz), 125.3, 125.0 (q, J_{C-F} = 3.7 Hz), 124.4 (d, J_{C-F} = 270.0 Hz), 124.3 (d, J_{C-F} = 270.0 Hz), 57.3, 57.2, 34.4, 34.3, 30.4, 30.3; ¹⁹F NMR (376 MHz, CDCl₃), δ -62.306, -62.310 ppm; FT-IR (thin film, neat): 3645, 2922, 1461, 1324, 768, 636 cm⁻¹; HRMS (ESI): m/z calcd for C₄₄H₅₁F₆O₂ [M-H]⁻: 725.3793; found : 725.3793.

Dimethyl 4,4'-(1,2-bis(3,5-di-*tert*-butyl-4-hydroxyphenyl)ethane-1,2-diyl)dibenzoate (2s):



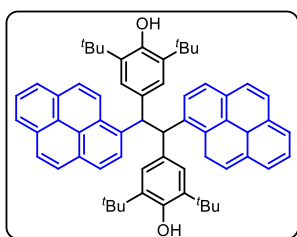
The reaction was performed at 0.113 mmol scale of **21s**; Yellow solid (29.0 mg, 72% yield, crude *dl:meso* = 1:1 and isolated *dl:meso* = 1.1:1); m.p. = 233–235 °C; R_f = 0.3 (5% EtOAc in hexane); ¹H NMR (400 MHz, CDCl₃) δ 7.80 (d, J = 8.3 Hz, 8.4H), 7.23 (d, J = 8.0 Hz, 4.2H), 7.15 (d, J = 8.4 Hz, 4.2H), 6.83 (s, 4H), 6.80 (s, 4.4H), 4.94 (s, 2.2H), 4.91 (s, 2H), 4.61 (s, 2H), 4.56 (s, 2.2H), 3.85 (s, 6.6H), 3.84 (s, 6H), 1.29 (s, 36H), 1.27 (s, 39.6H); ¹³C{¹H} NMR (100 MHz, CDCl₃) δ 167.3, 167.2, 152.0, 151.8, 149.8, 149.4, 135.5, 135.4, 133.1, 132.5, 129.7, 129.4, 128.7, 128.5, 127.8, 127.5, 125.4, 125.3, 57.4, 57.1, 52.1, 52.0, 34.33, 34.3, 30.4, 30.36; FT-IR (thin film, neat): 3643, 2955, 2927, 2876, 1720, 1610, 1436, 1282, 1239, 1185, 1114, 1021, 740, 7111 cm⁻¹; HRMS (ESI): m/z calcd for C₄₆H₅₇O₆ [M-H]⁻: 705.4155; found : 705.4160.

4,4'-(1,2-di(naphthalen-1-yl)ethane-1,2-diyl)bis(2,6-di-*tert*-butylphenol) (27t): The



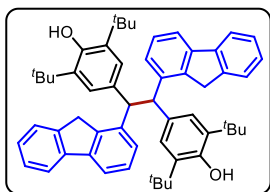
reaction was performed at 0.116 mmol scale of **21t**; yellow solid (31.0 mg, 77% yield, *dl:meso* 1:1.1); m. p. = 205–207 °C; R_f = 0.4 (5% EtOAc in hexane); $^1\text{H NMR}$ (400 MHz, CDCl_3) δ 8.35 (d, J = 8.5 Hz, 2H), 7.75 (d, J = 7.9 Hz, 2H), 7.52 – 7.48 (m, 4H), 7.46 – 7.39 (m, 4H), 7.13 (t, J = 7.8 Hz, 2H), 6.87 (s, 4H), 5.51 (s, 2H), 4.84 (s, 2H), 1.29 (s, 36H); $^{13}\text{C}\{^1\text{H}\}$ NMR (100 MHz, CDCl_3) δ 151.6, 139.6, 135.0, 134.2, 133.7, 132.2, 129.0, 126.4, 125.8, 125.5, 125.4, 125.1, 124.0, 123.9, 52.4, 34.2, 30.6; FT-IR (thin film, neat): 3644, 2957, 1733, 1435, 1232, 778 cm^{-1} ; HRMS (ESI): m/z calcd for $\text{C}_{50}\text{H}_{57}\text{O}_2$ $[\text{M}-\text{H}]^-$: 689.4359; found :689.4356.

4,4'-(1-(5a1,10-dihydropyren-1-yl)-2-(pyren-2-yl)ethane-1,2-diyl)bis(2,6-di-*tert*-butylphenol) (27u): The reaction was performed at 0.096 mmol scale of **21u**; yellow solid



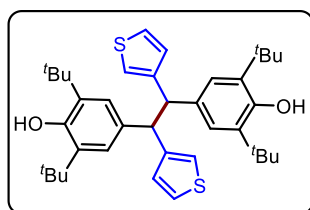
(29.0 mg, 72% yield,); m. p. = 220–222°C; R_f = 0.4 (5% EtOAc in hexane); $^1\text{H NMR}$ (400 MHz, CDCl_3) δ 8.71 (d, J = 9.4 Hz, 2H), 8.16 – 8.12 (m, 5H), 8.10 – 8.05 (m, 3H), 7.94 – 7.91 (m, 2H), 7.87 – 7.85 (m, 2H), 7.78 – 7.73 (m, 4H), 7.06 (s, 4H), 6.06 (s, 2H), 4.89 (s, 2H), 1.33 (s, 36H); $^{13}\text{C}\{^1\text{H}\}$ NMR (100 MHz, CDCl_3) δ 151.7, 137.9, 135.3, 134.3, 131.4, 130.8, 129.3, 129.0, 127.56, 127.5, 126.5, 125.8, 125.7, 125.3, 125.01, 125.0, 124.9, 124.7, 123.4, 53.1, 34.3, 30.6; FT-IR (thin film, neat): 3642, 2955, 1435, 1234, 1151, 843 cm^{-1} ; HRMS (ESI): m/z calcd for $\text{C}_{62}\text{H}_{64}\text{O}_2$ $[\text{M}-\text{H}]^-$: 840.4906; found :840.4916.

4,4'-(1,2-Di(9H-fluoren-1-yl)ethane-1,2-diyl)bis(2,6-di-*tert*-butylphenol): (27v) The



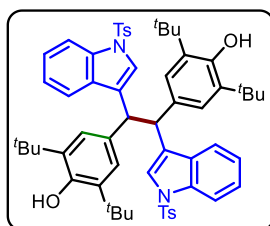
reaction was performed at 0.105 mmol scale of **21v**; Yellow solid (33.0 mg, 83% yield, crude *dl:meso* = 1:1.5 and isolated *dl:meso* = 1:1.2); m.p. = 241–243 °C; R_f = 0.3 (5% EtOAc in hexane); $^1\text{H NMR}$ (400 MHz, CDCl_3) δ 7.70 (d, J = 7.5 Hz, 2H), 7.64 (d, J = 7.5 Hz, 2.3H), 7.57 (d, J = 7.9 Hz, 2H), 7.53 (d, J = 7.9 Hz, 2.4H), 7.49 (d, J = 7.4 Hz, 2H), 7.46 (d, J = 7.4 Hz, 2.4H), 7.42 (s, 2.3H), 7.48 – 7.46 (m, 6H); 7.27 – 7.25 (m, 4.5H), 7.23 – 7.21 (m, 2.4H), 6.96 (d, J = 7.9 Hz, 8H), 4.89 (s, 2.4H), 4.87 (s, 2H), 4.70 (s, 2H), 4.63 (s, 2H), 3.76 (s, 8H), 1.33 (s, 43.2H), 1.26 (s, 36H); $^{13}\text{C}\{^1\text{H}\}$ NMR (100 MHz, CDCl_3) δ 151.6, 151.5, 143.6, 143.4, 143.3, 143.2, 143.0, 142.0, 141.9, 139.4, 139.2, 135.1, 135.09, 134.7, 134.1, 127.3, 127.2, 126.7, 126.6, 126.2, 126.15, 125.6, 125.5, 125.4, 125.0, 124.97, 119.63, 119.6, 119.5, 119.4, 58.0, 57.8, 37.0, 36.9, 34.33, 34.3, 30.5, 30.4; FT-IR (thin film, neat): 3646, 2922, 1457, 1234, 880, 764, cm^{-1} ; HRMS (ESI): m/z calcd for $\text{C}_{56}\text{H}_{61}\text{O}_2$ $[\text{M}-\text{H}]^-$: 765.4672; found : 765.4675.

4,4'-(1,2-Di(thiophen-3-yl)ethane-1,2-diyl)bis(2,6-di-*tert*-butylphenol) (27w): The reaction



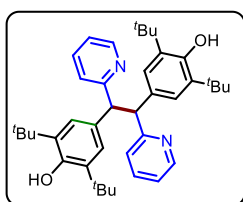
was performed at 0.133 mmol scale of **21w**; Yellow solid (26.0 mg, 65% yield, crude *dl:meso* = 1:1.4 and isolated *dl:meso* = 1.5:1); m.p. = 200–202 °C; R_f = 0.5 (5% EtOAc in hexane); $^1\text{H NMR}$ (400 MHz, CDCl_3) δ 7.13 (dd, J = 5.0, 3.2 Hz, 3H), 7.06 (dd, J = 5.0, 3.0 Hz, 2H), 6.92 (dd, J = 5.0, 1.0 Hz, 3H), 6.88 – 6.87 (m, 7H), 6.79 (s, 6H), 6.75 (dd, J = 5.0, 1.0 Hz, 2H), 6.66 (dd, J = 2.8, 0.9 Hz, 2H), 4.96 (s, 2H), 4.87 (s, 3H), 4.55 (s, 3H), 4.51 (s, 2H), 1.34 (s, 36H), 1.30 (s, 54H); $^{13}\text{C}\{^1\text{H}\}$ NMR (100 MHz, CDCl_3) δ 151.9, 151.6, 145.4, 145.0, 135.2, 135.1, 134.0, 133.8, 128.4, 128.1, 125.3, 125.2, 124.7, 124.3, 121.4, 120.9, 53.8, 53.7, 34.4, 34.3, 30.5; FT-IR (thin film, neat): 3646, 2960, 2878, 2331, 1437, 1364, 1318, 1235, 1156, 1122, 888, 771, 739, 671 cm^{-1} ; HRMS (ESI): m/z calcd for $\text{C}_{38}\text{H}_{49}\text{O}_2\text{S}_2$ $[\text{M}-\text{H}]^-$: 601.3174; found : 601.3195.

4,4'-(1,2-bis(1-tosyl-1H-indol-3-yl)ethane-1,2-diyl)bis(2,6-di-*tert*-butylphenol) (27x): The



reaction was performed at 0.082 mmol scale of **21x**; yellow solid (25.0 mg, 62% yield.); m. p. = 208–210 °C; R_f = 0.3 (5% EtOAc in hexane); $^1\text{H NMR}$ (400 MHz, CDCl_3) δ 7.94 (d, J = 8.1 Hz, 2H), 7.55 (d, J = 7.7 Hz, 2H), 7.40 (s, 2H), 7.27 – 7.24 (m, 8H), 6.97 (d, J = 8.2 Hz, 4H), 6.74 (s, 4H), 4.87 (s, 2H), .62(s, 2H); $^{13}\text{C}\{^1\text{H}\}$ NMR (100 MHz, CDCl_3) δ 152.0, 144.8, 135.2, 135.1, 134.9, 131.8, 131.2, 129.9, 127.1, 126.3, 126.1, 124.9, 123.5, 122.2, 120.2, 113.6, 49.0, 34.2, 30.5, 21.6; FT-IR (thin film, neat): 3626, 2964, 2329, 1447, 1174, 747 cm^{-1} ; HRMS (ESI): m/z calcd for $\text{C}_{60}\text{H}_{68}\text{N}_2\text{NaO}_6\text{S}_2$ $[\text{M}+\text{Na}]^+$: 999.4416; found : 999.4423.

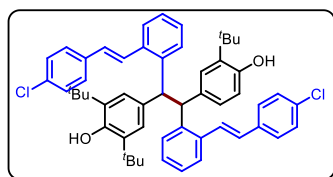
4,4'-(1,2-Di(2,6-pyridin-2-yl)ethane-1,2-diyl)bis(2,6-di-*tert*-butylphenol) (27y): The



reaction was performed at 0.135 mmol scale of **21y**; Yellow solid (31 mg, 75% yield, *dl:meso* = 1:2); m.p. = 207–209 °C; R_f = 0.1 (10% EtOAc in hexane); $^1\text{H NMR}$ (400 MHz, CDCl_3) 8.32 – 8.29 (m, 4H), 7.42 (d, J = 7.9 Hz, 2H), 7.11 – 7.08 (m, 2H), 6.81 (s, 4H), 4.99 (s, 2H), 4.50 (s, 2H), 1.29 (s, 36H); $^{13}\text{C}\{^1\text{H}\}$ NMR (100 MHz, CDCl_3) δ 152.3, 150.0, 146.9, 139.6, 136.1, 135.9, 131.8, 125.4, 123.2, 54.8, 34.4, 30.4; FT-IR (thin film, neat): 3624, 2955, 1463, 1260, 1122, 773 cm^{-1} ; HRMS (ESI): m/z calcd for $\text{C}_{40}\text{H}_{53}\text{N}_2\text{O}_2$ $[\text{M}-\text{H}]^-$: 593.4107; found : 593.4100.

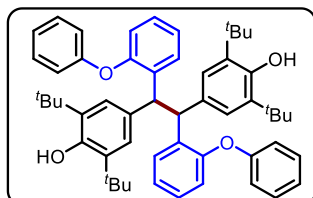
(2-(4-chlorostyryl)benzylidene)-1,2-diphenylethane bis(2,6-di-*tert*-butylphenol) (27z):

The reaction was performed at 0.092 mmol scale of **21z**; yellow solid (21 mg, 52% yield,



dl:meso 1:1.1); m. p. = 208–210 °C; R_f = 0.4 (5% EtOAc in hexane); $^1\text{H NMR}$ (400 MHz, CDCl_3) δ 7.49 (s, 1H) 7.45 (s, 1H) 20 7.43 – 7.40 (m, 2H), 7.38 – 7.33 (m, 9H), 7.32 – 7.30 (m, 7H), 7.26 – 7.23 (m, 9H), 7.10 – 7.05 (m, 8H), 6.84 (s, 1H), 6.80 (s, 1H), 6.76 (s, 5H), 6.71 (s, 1H), 6.67 (s, 5H), 4.97 (s, 2H), 4.89 (s, 2.2H), 4.86 (s, 2.2H), 4.83 (s, 2H), 1.27 (s, 36H) 1.27 (s, 39.6H); $^{13}\text{C}\{^1\text{H}\}$ NMR (100 MHz, CDCl_3) δ 151.7, 151.6, 141.2, 136.58, 136.57, 136.4, 135.2, 135.0, 133.3, 133.2, 133.0, 128.9, 128.8, 128.6, 128.2, 127.8, 127.5, 125.9, 53.1, 34.3, 34.2, 30.6, 30.3; FT-IR (thin film, neat): 3639, 2923, 1700, 1489, 1365, 749 cm^{-1} ; HRMS (ESI): m/z calcd for $\text{C}_{54}\text{H}_{55}\text{Cl}_2\text{O}_2$ $[\text{M}-\text{H}]^-$: 805.3579; found : 805.3589.

4,4'-(1,2-bis(2-(argiooxy)phenyl)ethane-1,2-diyl)bis(2,6-di-*tert*-butylphenol) (27aa): The

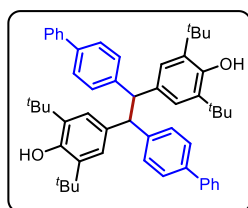


reaction was performed at 0.115 mmol scale of **21aa**; yellow solid (35.0 mg, 87% yield, *dl:meso* 1:1.5); m. p. = 201–203 °C; R_f = 0.4 (5% EtOAc in hexane); $^1\text{H NMR}$ (400 MHz, CDCl_3) δ 7.53 (d, J = 7.4 Hz, 2H), 7.48 – 7.46 (m, 3H), 7.22 – 7.13 (m, 11H), 7.05 – 6.99 (m, 6H), 6.97 – 6.95 (m, 8H), 6.92 (s, 6H), 6.76 (d, J = 7.9 Hz, 2H), 6.72 (s, 4H), 6.69 (d, J = 8.2 Hz, 4H), 6.65 – 6.63 (m, 3H), 6.61 – 6.59 (m, 6H), 5.25 (s, 3H), 5.14 (s, 2H), 4.83 (s, 3H), 4.74 (s, 2H), 1.24 (s, 54H), 1.19 (s, 36H); $^{13}\text{C}\{^1\text{H}\}$ NMR (100 MHz, CDCl_3) δ 158.4, 154.2, 151.5, 136.5, 134.7 (2C), 133.6, 129.4, 126.5, 125.7, 123.5, 122.2, 119.5, 118.2, 50.0, 34.3, 34.1, 30.4; FT-IR (thin film, neat): 3643, 2955, 1583, 1484, 1231, 749 cm^{-1} ; HRMS (ESI): m/z calcd for $\text{C}_{54}\text{H}_{61}\text{O}_4$ $[\text{M}-\text{H}]^-$: 773.4570; found : 773.4555.

General procedure for Suzuki coupling of 21m

Nitrogen gas was expelled solution of sodium carbonate solution (0.106 mmol, 2 equiv.) and toluene (2:3) for 15 min. After that phenyl boronic acid (0.064 mmol, 1.2 equiv.), $\text{Pd}(\text{PPh}_3)_4$ (0.003 mmol, 5 mol%), and 4,4'-((1R,2R)-1,2-bis(4-bromophenyl)ethane-1,2-diyl)bis(2,6-di-*tert*-butylphenol) (0.053 mmol, 1.0 equiv.) were added to the reaction flask. The resulting reaction mixture was agitated at 100 °C for 12 hours. After completion of the reaction the reaction mixture was diluted with ethyl acetate and water. The organic layer was separated, and dried over anhydrous sodium sulfate, filtered, and concentrated under reduced pressure. The residue was purified through neutral alumina column chromatography using hexane/

EtOAc to obtain pure 4,4'-(1,2-Di([1,1'-biphenyl]-4-yl)ethane-1,2-diyl)bis(2,6-di-*tert*-butylphenol) derivative.

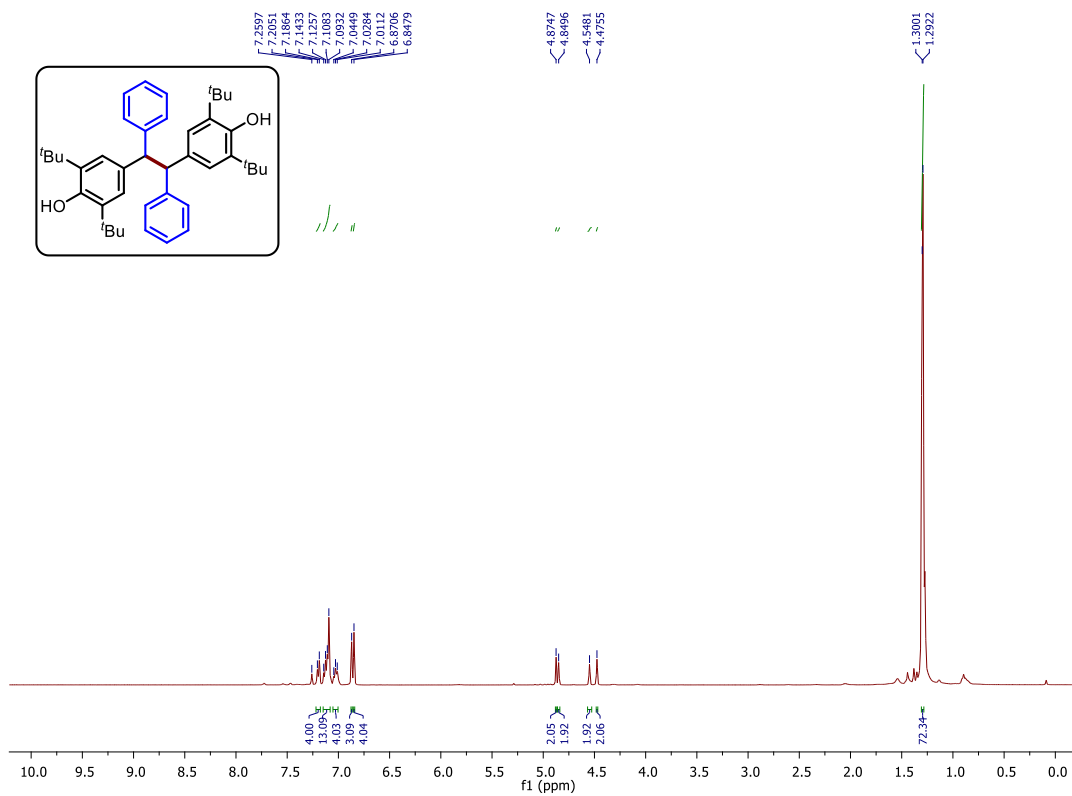


Yellow solid (32.0 mg, 80% yield, crude *dl:meso* = 1:1.5 and isolated *dl:meso* = 1:1.5); m.p. = 229–231 °C; R_f = 0.3 (5% EtOAc in hexane); ^1H NMR (400 MHz, CDCl_3) δ 7.54 – 7.51 (m, 15H), 7.42 – 7.36 (m, 30H), 7.33 – 7.29 (m, 13H), 7.284 – 7.28 (m, 3H), 7.19 – 7.17 (m, 4H), 6.92 – 6.916 (m, 12H), 4.91 (s, 2H), 4.86 (s, 5H), 4.64 (s, 5H), 4.56 (s, 2H), 1.32 (s, 90H), 1.30 (s, 36H); $^{13}\text{C}\{^1\text{H}\}$ NMR (100 MHz, CDCl_3) δ 151.7, 151.5, 143.8, 143.6, 141.4, 141.1, 138.4, 138.3, 135.2 (2C), 134.4, 133.8, 129.2, 128.9, 128.7 (2C), 127.1, 127.0 (2C), 126.95, 126.9, 126.7, 125.6, 125.4, 57.43, 57.40, 34.4, 34.3, 30.5, 30.4; ; FT-IR (thin film, neat): 3640, 2956, 1486, 1235, 1154, 764 cm^{-1} ; HRMS (ESI): m/z calcd for $\text{C}_{54}\text{H}_{62}\text{O}_2$ $[\text{M}-\text{H}]^-$: 741.4672; found : 741.4697.

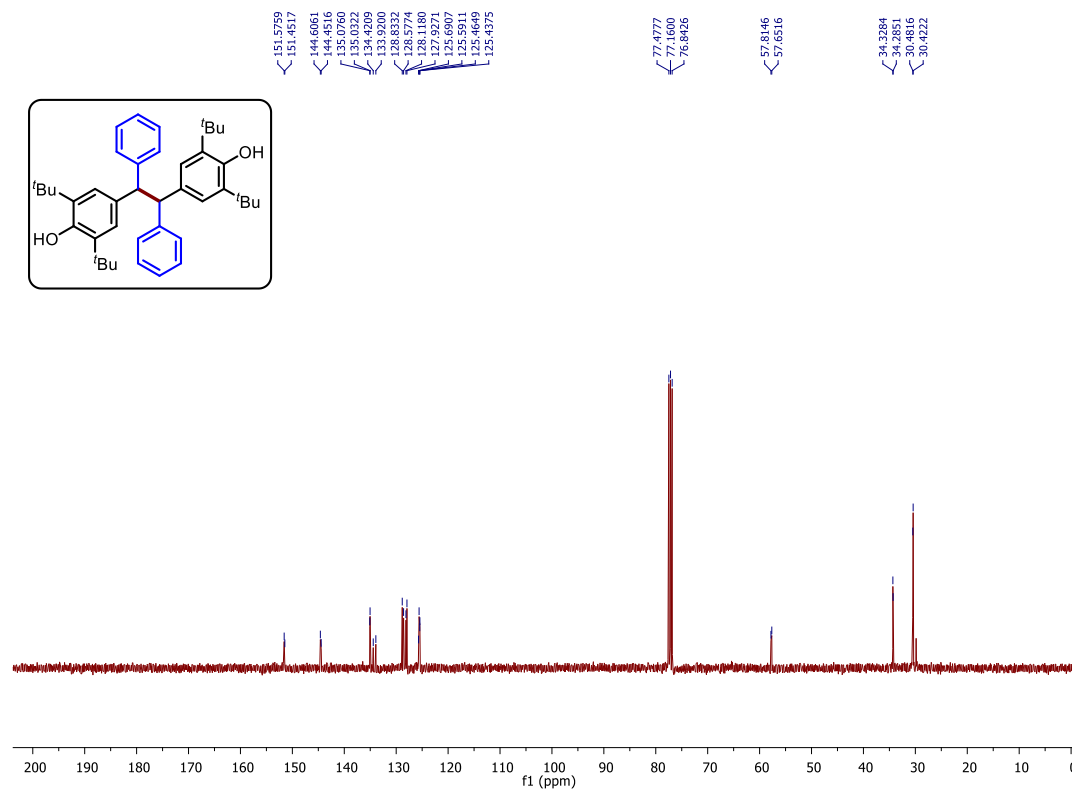
General procedure for for gram-scale synthesis of 27a

To a clean, oven-dried round bottom flask, 100 mL containing a magnetic stir-bar *para*-quinone methide (1g, 3.40 mmol) was added under argon atmosphere. After that dry THF 10 mL and SmI_2 (2.5 equiv.) was introduced into the reaction flask via syringe. Then resulting reaction mixture was stirred at room temperature for about 30 min. After the reaction was complete (based on TLC analysis), reaction mixture was filtered through silica gel pad using CH_2Cl_2 . Excess solvent was then removed under reduced pressure and the residue was then purified through a neutral alumina gel column using EtOAc/Hexane mixture as an eluent to get the pure product.

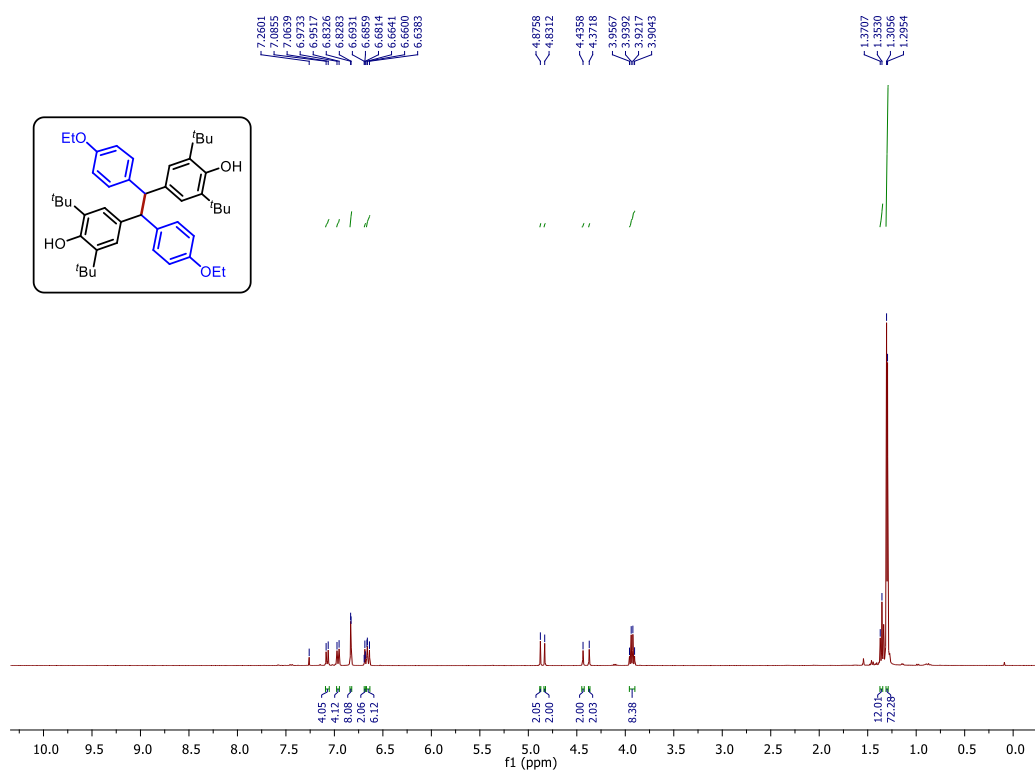
^1H NMR (400 MHz, CDCl_3) Spectrum of **27a**



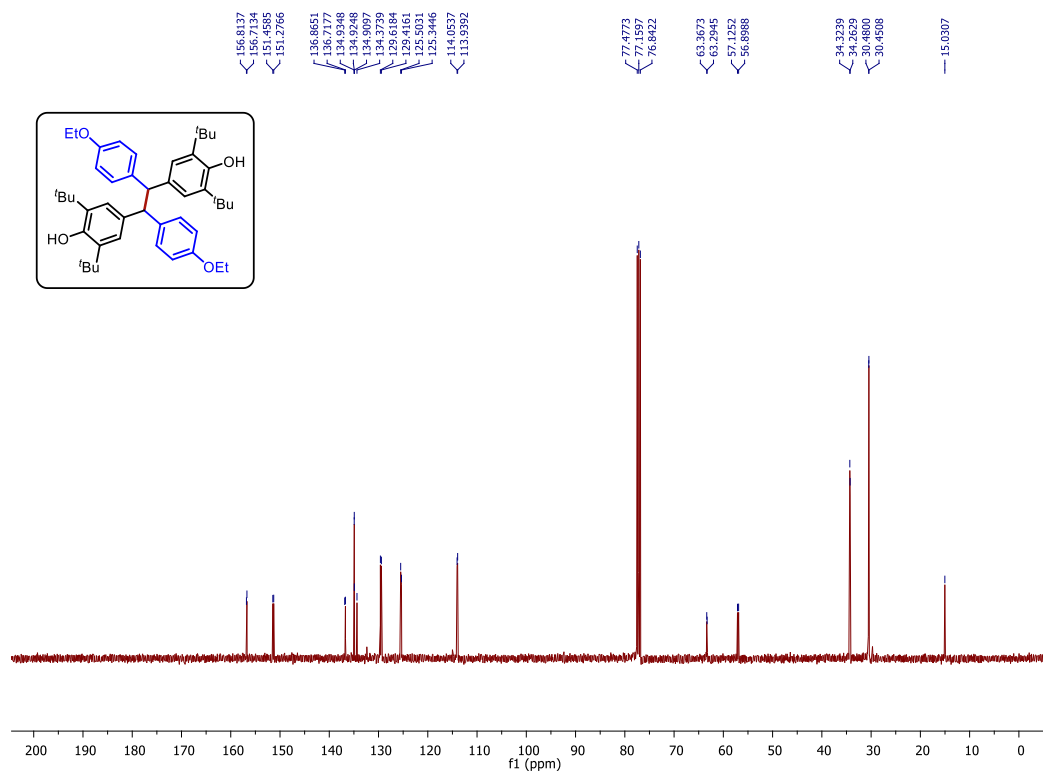
^{13}C { ^1H } NMR (100 MHz, CDCl_3) Spectrum of **27a**



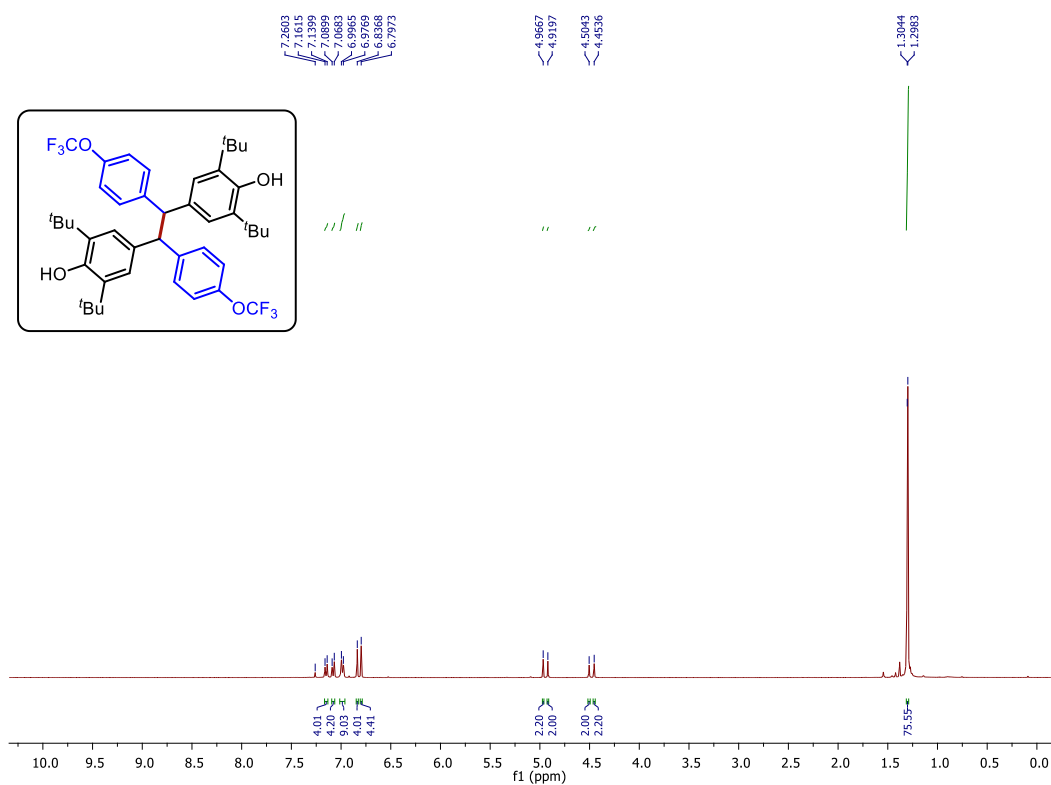
^1H NMR (400 MHz, CDCl_3) Spectrum of **27g**



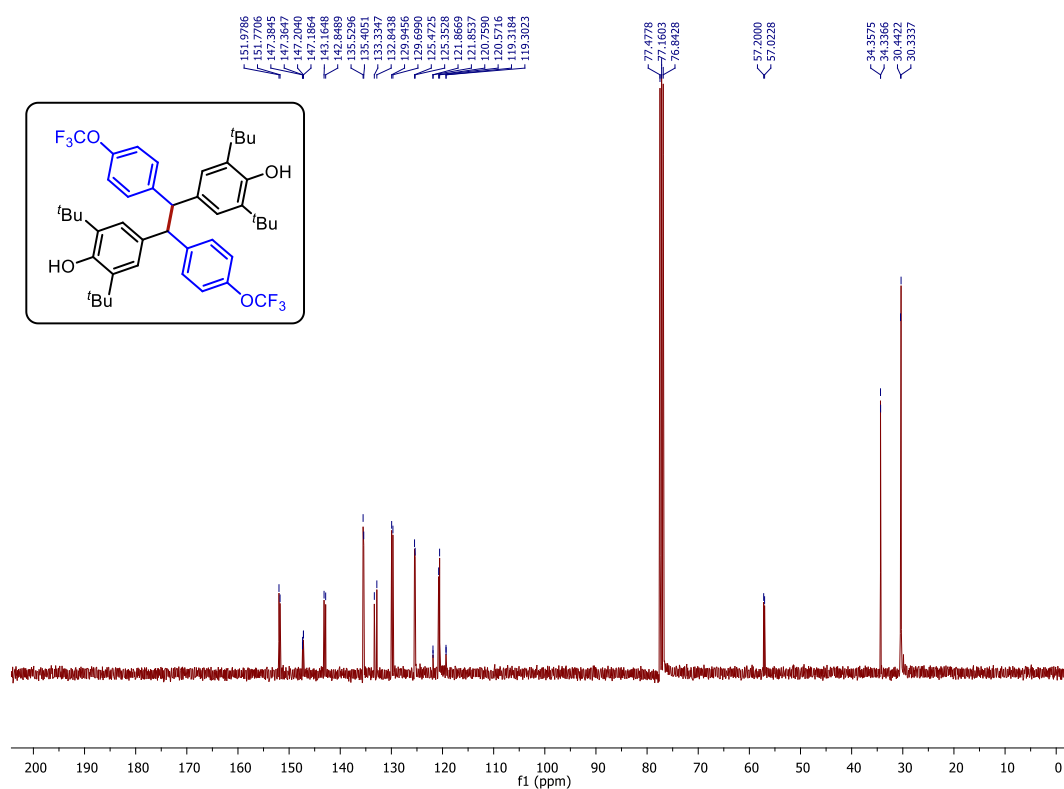
^{13}C { ^1H } NMR (100 MHz, CDCl_3) Spectrum of **27g**



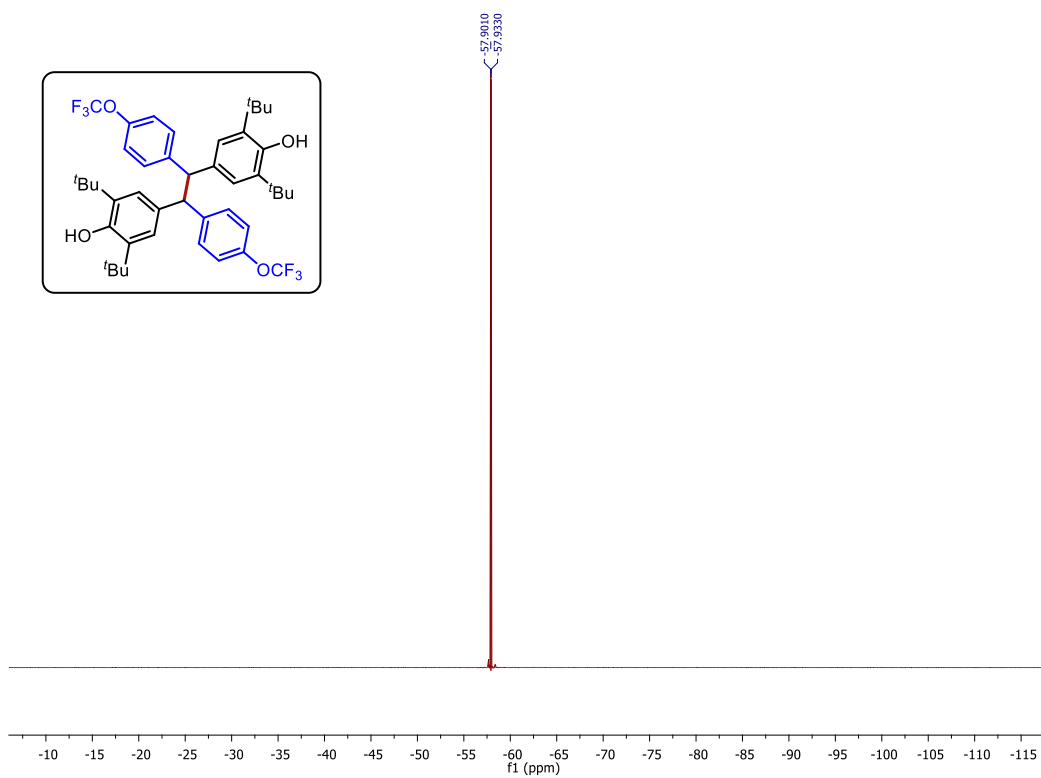
¹H NMR (400 MHz, CDCl₃) Spectrum of **27h**



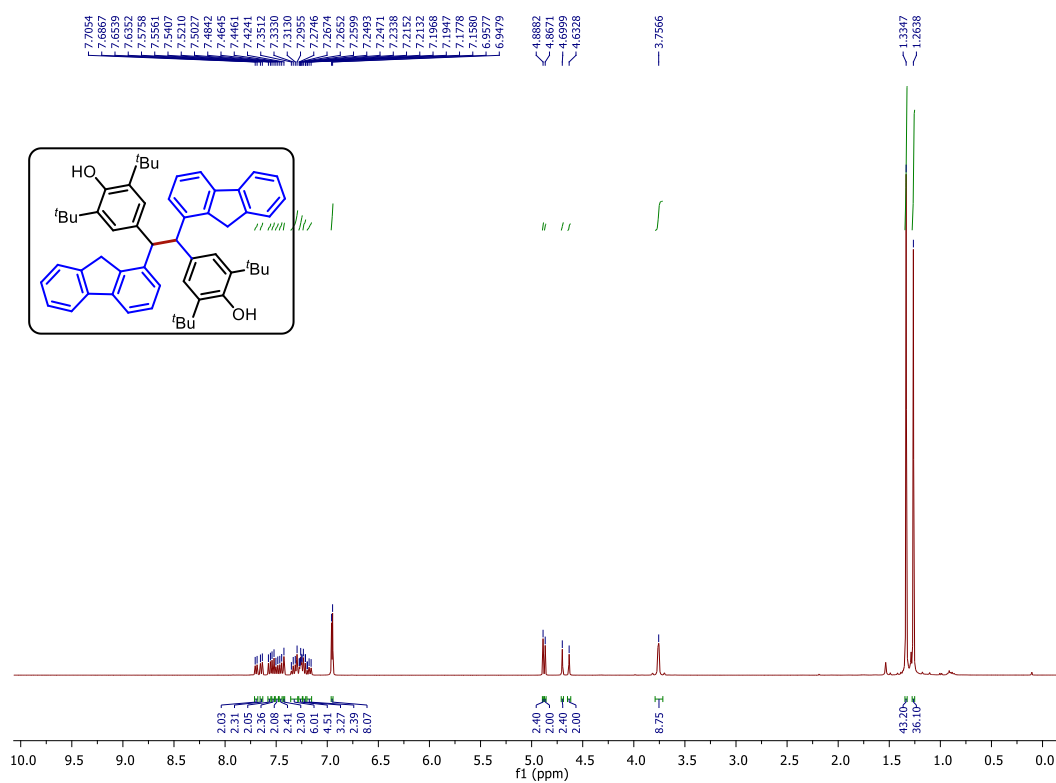
¹³C {¹H} NMR (100 MHz, CDCl₃) Spectrum of **27h**



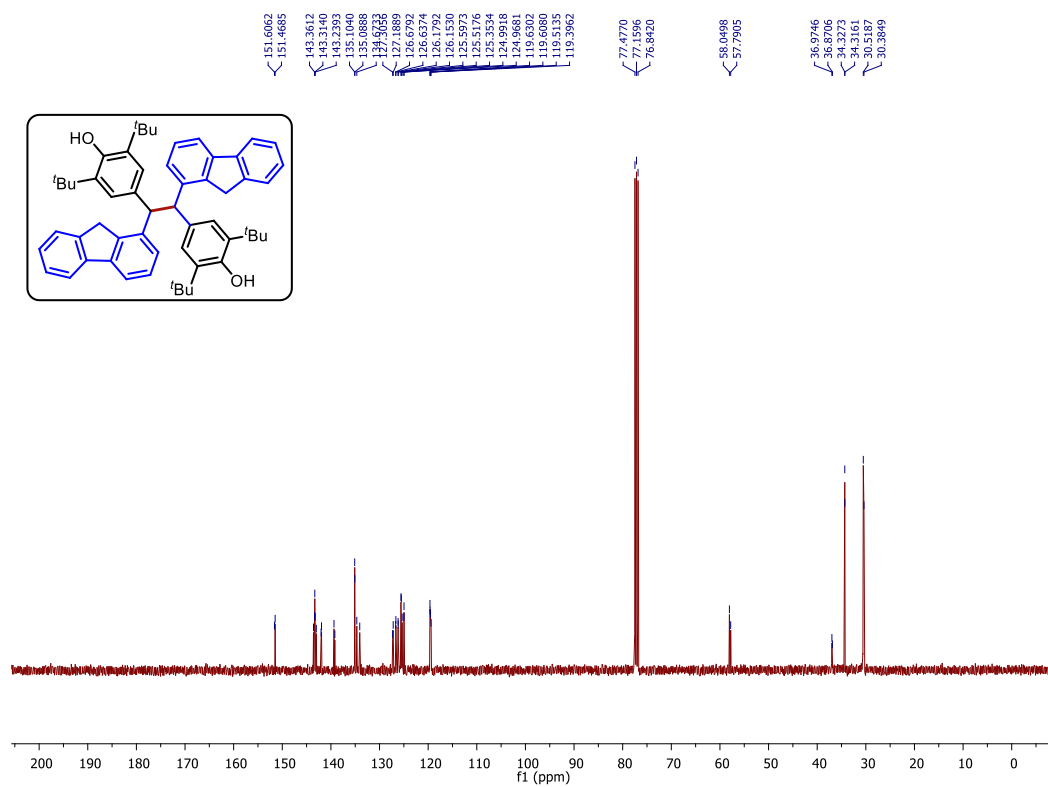
^{19}F $\{^1\text{H}\}$ NMR (376 MHz, CDCl_3) Spectrum of **27h**



^1H NMR (400 MHz, CDCl_3) Spectrum of **27w**



^{13}C { ^1H } NMR (100 MHz, CDCl_3) Spectrum of **27w**



4.8 References:

1. For recent review (a). Szostak, M.; Fazakerley, N. J.; Parmar, D.; Procter, D. *J. Chem. Rev.* **2014**, *114*, 5959. (b) Maity, S. *Eur. J. Org. Chem.* **2021**, 5312. (c) Heravi, M. M.; Nazari, A. *RSC. Adv.*, **2022**, *12*, 9944. (d) Zhang, N.; Samanta, S. R.; Rosen, B. M.; Percec, V. *Chem. Rev.* **2014**, *114*, 5848.
2. (a). Namy, J. L.; Girard, P.; Kagan, H. B. *Nouv. J. Chim.* **1977**, *1*, 5. (b). Girard, P.; Namy, J. L.; Kagan, H. B. *J. Am. Chem. Soc.* **1980**, *102*, 2693.
3. Procter, D. J.; Flowers, R. A., II; Skrydstrup, T. *Organic Synthesis Using Samarium Diiodide: A Practical Guide*; RSC Publishing: Cambridge, 2010.
4. (a) Trost, B. M.; Fleming, I. *Comprehensive Organic Synthesis*; Pergamon Press: New York, 1991. (b) Gansäuer, A.; Blum, H. *Chem. Rev.* **2000**, *100*, 2771. (c) Gansäuer, A.; Lauterbach, T.; Narayan, S. *Angew. Chem., Int. Ed.* **2003**, *42*, 5556. (d) Justicia, J.; Álvarez de Cienfuegos, L.; Campana, A. G.; Miguel, D.; Jakoby, V.; Gansäuer, A.; Cuerva, J. M. *Chem. Soc. Rev.* **2011**, *40*, 3525. (e) Renaud, P.; Sibi, M. *Radicals in Organic Synthesis*; Wiley-VCH: New York, 2001.
5. (a) Corey, E. J.; Zheng, G. Z. Catalytic reactions of samarium (II) iodide. *Tetrahedron Lett.* **1997**, *38*, 2045. (b) Steel, P. G. *J. Chem. Soc., Perkin Trans. 1* **2001**, 2727.
6. (a) Soderquist, J. A. *Aldrichimica Acta* **1991**, *24*, 15. (b) Molander, G. A. *Chem. Rev.* **1992**, *92*, 29. (c) Molander, G. A. *Org. React.* **1994**, *46*, 211. (d) Molander, G. A.; Harris, C. R. *Chem. Rev.* **1996**, *96*, 307. (e) Molander, G. A.; Harris, C. R. *Tetrahedron* **1998**, *54*, 3321. (f) Imamoto, T. *Lanthanides in Organic Synthesis*; Academic Press: London, 1994. (g) Skrydstrup, T. *Angew. Chem., Int. Ed. Engl.* **1997**, *36*, 345. (h) Krief, A.; Laval, A. M. *Chem. Rev.* **1999**, *99*, 745.
7. (a) Hutton, T. K.; Muir, K.; Procter, D. J. *Org. Lett.* **2002**, *4*, 2345. (b) Hutton, T. K.; Muir, K. W.; Procter, D. J. *Org. Lett.* **2003**, *5*, 4811.
8. Cozzi, F.; Annunziata, R.; Banaglia, M.; Cinquini, M.; Raimondi, L.; Baldrbridge, K. K.; Siegel, J. S. *Org. Biomol. Chem.* **2003**, *1*, 157.
9. (a) Zhang, X. M.; Tu, Y. Q.; Zhang, F. M.; Shao, H.; Meng, X. *Angew. Chem., Int. Ed.* **2011**, *50*, 3916. (b) Zhang, X. M.; Shao, H.; Tu, Y. Q.; Zhang, F. M.; Wang, S. H. *J. Org. Chem.* **2012**, *77*, 8174.
10. Handy, S. T.; Omune, D. *Tetrahedron*, **2007**, *63*, 1366.
11. (a) Powell, J. R.; Dixon, S.; Light, M. E.; Kilburn, J. D. *Tetrahedron Lett.* **2009**, *50*, 3564. (b) Meng, J.; Light, M. E.; Kilburn, J. D.; Dixon, S. *Tetrahedron Lett.* **2011**, *52*, 928.

12. For recent reviews on *para*-quinone methides chemistry: (a) Li, W.; Xu, X.; Zhang, P.; Li, P. *Chem. Asian J.* **2018**, *17*, 2350. (b) Lima, C. G. S.; Pauli, F. P.; Costa, D. C. S.; de Souza, A. S.; Forezi, L. S. M.; Ferriera, V. F.; de Carvalho da Silva. *Eur. J. Org. Chem.* **2020**, *18*, 2650. (c) Wang, J. -Y.; Hao, W. -J.; Tu, S. -J.; Jiang, B. *Org. Chem. Front.* **2020**, *7*, 1743. (d) Singh, G.; Pandey, R.; Pankhade, Y. A.; Fatma, S.; Anand, R. V. *Chem. Rec.* **2021**, *21*, 4150.
13. For selected recent examples: Pankhade, Y. A.; Pandey, R.; Fatma, S.; Ahmad, F.; Anand, R. V. *J. Org. Chem.* **2022**, *87*, 3363–3377. (b) Jadhav, A. S.; Pankhade, Y. A.; Anand, R. V. *J. Org. Chem.* **2018**, *83*, 8615–8626. (c) Singh, G.; Goswami, P.; Sharma, S.; Anand, R. V. *J. Org. Chem.* **2018**, *83*, 10546–10554. (d) For a recent review on *p*-QM chemistry from our group: Singh, G.; Pandey, R.; Pankhade, Y. A.; Fatma, S.; Anand, R. V. *Chem. Rec.* **2021**, *21*, 4150–4173.
14. Zhao, Y-N.; Luo, Y-C.; Wang, Z-Y.; Xu, P-F. *Chem. Commun.*, **2018**, *54*, 3993.
15. Wu, Q-L.; Guo, Jing.; Huang, G-B.; Chan, Albert S. C.; Weng, Jiang.; Lu, Gui. *Org. Biomol. Chem.*, **2020**, *18*, 860.
16. Yang, Q.; Pan, G.; Wei, J.; Wang, W.; Tang, Y.; Cai, Y. *ACS Sustainable Chem. Eng.* **2021**, *9*, 5, 2367.
17. Angle, S. R.; Rainier, J. D. *J. Org. Chem.* **1992**, *57*, 6883.

CURRICULUM VITAE

Ms. Sonam Sharma

Ph.D. Research Scholar,

Department of Chemical Science, Indian Institute
of Science Education and Research Mohali

Email: sharmaasonam273@gmail.com

Mob: +91-9877398840



Experimental Organic Chemistry Skill:

First-hand expertise in project design and lab setup for synthetic organic chemistry. Excellent understanding of the synthesis of *N*-heterocyclic carbene (NHC) and Bis-(amino) cyclopropenylidene (BAC) precursors and how to use them in organocatalysis. Thorough understanding of organic and organometallic chemistry, experience in managing reactions in a Schlenk line, microwave reactor, and continuous-flow microreactor. Furthermore, I have also gained hands-on experience in the area of chiral phosphoric acid (CPA) catalyzed transformations and photo-redox reactions. Excellent practical skills in handling air/moisture sensitive reagents/reactions and gram/milligram scale reactions. Good knowledge of multi-step synthesis. Experience in modern chromatographic and spectroscopic (IR, UV, NMR, and HRMS) techniques. Proficiency in handling HPLC and Biotage-Isolera One flash column chromatography.

Research Expertise: Synthetic Organic Chemistry, Organocatalysis, Photocatalysis.

Education and Research Training

- **2017 –: Ph. D. in Synthetic Organic Chemistry**, Department of Chemical Sciences, Indian Institute of Science Education and Research (IISER) Mohali, 140306, Punjab, India.
 - **Thesis Title:** *“Exploring the vinylogous conjugate-addition and radical reactions of para-quinone methides”*
 - **Ph.D. Thesis Supervisor:** Prof. R. Vijaya Anand
- **2013 – 2015: M.Sc in Chemistry**, Department of Chemistry, Guru Nanak Dev University Amritsar, 143005, Punjab, India with CPI **8.04**.

- **2010 – 2013: Bachelor of Science**, Guru Nanak Dev University Amritsar, 143005, Punjab, India with 65%.

Awards/Scholarships and Grants

- Awarded **Senior Research Fellowship** and **Junior Research Fellowship** (MHRD Fellowship) from Indian Institute of Science Education and Research (IISER) Mohali from August 2017 to July 2022.
- Awarded **INSPIRE Fellowship** from the Department of Science and Technology (DST), Government of India from 2010 to 2015.
- Qualified Graduate Aptitude Test in Engineering (GATE) held in February 2016.
- Qualified intermediate examination with 38th state rank.

List of Publications

- 1) **Sharma, S.**;# Singh, G.;# Anand R. V. “Enaminones with *p*-Quinone Methides: Access to Chromenone and Chromene Derivatives. *Eur. J. Org. Chem*, **2022**, doi.org/10.1002/ejoc.202200792 # These authors contributed equally.
- 2) **Sharma, S.**; Anand, R. V. TfOH acid-mediated one-pot synthesis of *O*, *S*, and *N*-based heterocycles from 2-hetero atom functionalized para-quinone methides. (Manuscript under preparation).
- 3) **Sharma, S.**; Anand, R. V. SmI₂-mediated reductive coupling of para-quinone methides.(Manuscript under preparation).
- 4) Singh, G.;# **Sharma, S.**;# Anand R. V. A One-Pot Approach for the Synthesis of Tetrahydroindolo[2,3-*b*]carbazoles through 1,6-Conjugate Addition of 2-indolylmethanol to para-Quinone Methides # These authors contributed equally. (Manuscript Submitted).
- 5) Goswami, P.; **Sharma, S.**; Singh, G.; Anand, R. V. Bis(amino)cyclopropenylidene catalyzed Rauhut-Currier reaction between α,β -unsaturated carbonyl compounds and para-quinone methides. *J. Org. Chem.* **2018**, 83, 4213.
- 6) Singh, G.; Goswami, P.; **Sharma, S.**; Anand, R. V. A One-pot Approach to 2,3-Diarylbenzo[*b*]furans Through *N*-Heterocyclic Carbene Catalyzed 1,6-Conjugate

Addition Followed by Acid Mediated Dehydrative Cyclization. J. Org. Chem. **2018**, *83*, 10546.

- 7) Rekha, **Sharma, S.**; Singh, G, Anand, R. V. *Tropylium Salt-promoted Vinylogous Aza-Michael Addition of Carbamates to para-Quinone Methides: Elaboration to Diastereomerically Pure α,α' -Diarylmethyl Carbamates.* *ACS Org. Inorg. Au* **2022**, *2*, 186.
- 8) Rekha, **Sharma, S.**; Anand, R. V. *HBF₄-Catalyzed 3,6-Bis-diarylmethylation of Carbazoles with para-Quinone Methides.* *Eur. J. Org. Chem*, **2022**, doi.org/10.1002/ejoc.202201323.

Conferences/Symposia

- Participated in the 24th *National Conference on Liquid Crystals* held at the Department of Chemical Sciences, Indian Institute of Science Education and Research (IISER) Mohali, S. A. S. Nagar, India (11-13th October, 2017).
- Participated in the *Recent Advances In Organic And Bioorganic Chemistry* (RAOBC) held at the Department of Chemical Sciences, Indian Institute of Science Education and Research (IISER) Mohali, S. A. S. Nagar, India (22-24th March, 2019).
- Participated in the *1st Cricc Chemistry Symposium* (CCS 2019) held at the Department of Chemical Sciences, Indian Institute of Science Education and Research (IISER) Mohali, S. A. S. Nagar, India (2nd & 3rd November, 2019).
- Presented a poster on “Reactions of Enaminones with *para*-Quinone Methides: Access to 4H-Chromene and 4H-Chromen-4-one Derivatives” **Sharma S.**; Anand, R. V. in the *Symposium On Recent Advances In Self-Assembled Materials and Supramolecular Chemistry* held at Department of Chemistry, Guru Nanak Dev University, Amritsar, India
- Presented a poster on “Reactions of Enaminones with *para*-Quinone Methides: Access to 4H-Chromene and 4H-Chromen-4-one Derivatives” **Sharma S.**; Anand, R. V. in the 29th CRSI- National Symposium in Chemistry & CRSI-ACS Symposium Series in chemistry held at the Department of Chemical Sciences, Indian Institute of Science Education and Research (IISER) Mohali, S. A. S. Nagar, India (7-9th July, 2022).

- Presented a poster on “Reactions of Enaminones with *para*-Quinone Methides: Access to 4H-Chromene and 4H-Chromen-4-one Derivatives” **Sharma S.**; Anand, R. V. in the *Symposium On Recent Advances in Bioorganic and Medicinal Chemistry (RABMC)* held at NIPER, SAS Nagar Mohali (19th November, 2022).